EQUIVALENT CIRCUIT MODELLING OF BIPOLAR TRANSISTORS

by

Monica Dowson

A thesis submitted to the University of Leicester

for the degree of Doctor of Philosophy

March 1982

ACKNOWLEDGEMENTS

The author gratefully acknowledges the advice and encouragement given by her supervisor, Dr. O.P.D. Cutteridge; the helpful discussions with and the provision of data by Mr. P.J. Rankin and Mr. K.W. Moulding of Philips Research Laboratories; and the understanding of her husband, who provided encouragement, food and drink at all the appropriate times.

EQUIVALENT CIRCUIT MODELLING OF BIPOLAR TRANSISTORS

Monica Dowson

ABSTRACT

Existing equivalent circuit models of bipolar transistors are reviewed together with techniques for the evaluation of suitable values of the model elements. A method enabling the optimisation of the element values of any particular model in order to match the measured S parameters of a device that is to be modelled is described. This method uses a modified Gauss Newton algorithm to minimise an objective function defined as the sum of the squares of the weighted errors between the required S parameters and those of the model.

Details are then given of a new modelling algorithm for the development of accurate equivalent circuit models which was developed from this original optimisation method. The new modelling algorithm requires some S parameter measurements of the device to be modelled over an appropriate range of frequencies, together with a potentially suitable model. The initial model elements are optimised and then, if necessary, suitable topological changes, involving the addition or deletion of both elements and nodes, are made until a model having the required accuracy or complexity is obtained.

A number of examples are given of small-signal equivalent circuit models of bipolar transistors developed using the algorithm. These particular transistors were operating at frequencies up to 1 GHz . A further example is given of the use of the modelling algorithm in the development of a bias dependent small-signal model of two similar bipolar transistors operating at frequencies up to 2 GHz . Additional S parameter data for the same two transistors is also used to demonstrate that the algorithm can be used successfully for the development of non-linear models.

CONTENTS

CHAPTER 1

INTRODUCTION

Since the invention of the transistor in 1948, models have been sought which simulate the behaviour of the device. The work undertaken by the author and described here, has been concerned entirely with modelling bipolar transistors, the construction and applications of which are discussed in Chapter 2.

Models of a transistor can be either in terms of mathematical relationships or in the form of equivalent circuits. Equivalent circuit models are popular for several reasons: circuit designers tend to feel more at ease with a circuit diagram rather than a set of numbers or mathematical relationships; transistor and integrated circuit designers prefer a model that reflects the construction of the device enabling modifications to the construction to be mapped onto the model; and there are many circuit analysis packages now available that use equivalent circuit models of transistors and other devices to incorporate in larger circuits to be analysed.

The author has been fortunate in receiving data on a number of bipolar transistors from Philips Research Laboratories for which they were interested in obtaining equivalent circuit models. In addition to proving that the electronics industry is interested in the modelling of transistors, this also provided a definite direction for the research. The requirement was for small-signal (implying linear) models for transistors designed to operate at frequencies in ranges between 0.5 MHz and 2 GHz. Maclean[1] has also expressed an interest in this type of problem.

Although the techniques described here were originally devised for the generation of linear models of bipolar transistors, the techniques involved are equally applicable to other modelling problems. In the final problem here, which was a bias dependent model, the author obtained models for the non-linear operation of a bipolar transistor. Mathews and Ajose[2] have

used one optimisation technique to model both bipolar and field effect transistors.

1.1. Background

In recent years, there has been a great deal of research interest at Leicester in network synthesis and optimisation. Theses on passive network synthesis have been presented by di Mambro[3,4], Wright[5], Krzeczkowski[6], Hegazi[7] and Savage[8] , whilst Dowson[9], Henderson[10] and Dimmer[11] have presented theses more concerned with the optimisation processes. This expertise has been of direct benefit to the author.

The techniques used for the analysis of passive networks, particularly those developed by di Mambro[3,4] and di Mambro and Cutteridge[12] , were considered for the author's application as described in Chapter 3; these were, however, only used for a short time until the analysis routine written by the author, also described in Chapter 3, was developed. The technique of coefficient matching which all these earlier network synthesis programs used was not considered suitable for the problems being studied by the author.

In addition to the local experience in the analysis of networks, there was also a considerable knowledge of optimisation techniques available. In particular the technique developed by Henderson[10], to which the author[9] also made some contributions, were of great importance. This optimisation technique involved the use of a two-part algorithm and was designed to solve difficult optimisation problems. It was discovered that for the type of problems to be solved by the author one part, the Gauss Newton section, with adaptations to suit the problem type, was an ideal technique. Details of the optimisation problem and the techniques used are given in Chapter 4.

1.2. Aims of the Research

As already mentioned, some data was provided by Philips Research Laboratories on some devices for which they were interested in obtaining equivalent circuit models. The data was provided in three stages.

The first set of data[13] was for a lateral p-n-p transistor. This was an integrated circuit transistor and was described[13] as "a notoriously difficult device to model" and "one of current interest to us [Philips Research Laboratories]". In addition to the data, a first stage model of the device was provided. The requirement by Philips Research Laboratories was that a more accurate model of the device be developed.

This requirement, as discussed in Section 2.5, is quite common. Frequently, standard models of devices do not give adequate correlation with the measured characteristics of the devices. Thus, the aim of this research was to develop techniques whereby models of devices could be verified, and if necessary, improved models be produced. These improved models could be produced merely by optimising the element values of the original models. If this is still not adequate then it becomes necessary to optimise the topology of the models together with the element values until the required accuracy or complexity is obtained.

These aims necessitated the development of analysis and optimisation techniques which were then combined together to form an overall modelling strategy. The development of an improved model for the lateral p-n-p transistor is described in Chapter 5 and the modelling technique devised from this experiment is detailed in Section 5.6.

This new technique was then tested on the second set of data provided by Philips Research Laboratories[14]. This data was for another integrated circuit transistor, this time a vertical n-p-n transistor, with data for each of the common emitter, common base and common collector configurations.

Finally, a set of data[15,16] was provided for two similar n-p-n tran-

sistors at different bias conditions. Measured data was available at two voltages and at six different currents for the first type and at two voltages and at seven different currents for the second type. Slatter[17] had published a model for a limited bias range based on physical aspects of these devices. The author's aim was to improve on this model by obtaining more accurate bias dependent models covering a wider bias range using as few bias dependent elements as possible consistent with the use of simple relationships for those elements. This problem is described in detail in Chapter 7.

1.3. Achievements

As will be seen later the author has produced a method by which equivalent circuit models of bipolar transistors can be verified against a set of s parameter measurements of the devices and if they are inadequate the element values of the models can be optimised. Then, if necessary, the topology of the model can be modified until the required accuracy or complexity is obtained.

In order to achieve this, the author has produced a computer program to analyse a network in terms of its s parameters and combined this with an optimisation routine together with a new modelling strategy.

Using this technique a number of models have been produced using data supplied by Philips Research Laboratories. The first of these was a model for a lateral p-n-p transistor which operated in the frequency range 0.5 MHz to 10 MHz. The maximum absolute errors in the s parameters of the final model were 0.1 dB in the modulus and 1.2° in the phase with r.m.s. (root mean square) errors of 0.04 dB and 0.4°. This final model consisted of 6 nodes with 12 elements and included one current source only.

The next device modelled was a vertical n-p-n transistor model which

operated in the frequency range 0.1 GHz to 1 GHz. Separate models were produced for each of the common emitter, common collector and common base configurations. These gave maximum absolute errors of 1.5 dB and 4° and r.m.s. errors of 0.3 dB and 3° . An attempt was made to produce a single general model applicable for any of the configurations. This became a task of tremendous volume and was only partially successful giving r.m.s. errors of 1.3 dB and 12.9° . Whilst the author believes that this type of task is possible, it requires a large, fast computer with extremely efficient code in order to generate sufficiently accurate models.

Finally, a bias dependent model was produced for two similar bipolar transistors operating at frequencies of 0.1 GHz to 2 GHz . The same model was produced for both transistors and was valid for the linear operation of the devices at voltages of 0.5 V and 3 V and for emitter currents in the range 0.5 mA to 4 mA for the first and 0.5 mA to 8 mA for the second of the two transistors. Simple expressions for the bias dependent elements were developed and good agreement with the measured characteristics of the transistors was achieved. Accurate models were also developed for the non-linear operation of the transistors.

Thus, this modelling technique has been extensively tested and although these tests have been with s parameter data for bipolar transistors, the author is of the opinion that the techniques could be applied to many electronic modelling problems.

1.4. Computing Facilities Used.

The majority of the computing work has been done on the CDC Cyber 73 at the University of Leicester and the CDC 7600 at the University of Manchester (UMRCC). These machines are compatible and programs are easily transportable between the two. The main feature of these machines is the word length which is 60 bits. This means that high precision can

be easily obtained. The UMRCC CDC 7600 is approximately 12 times more 'powerful' than the Leicester Cyber 73, thus for larger jobs where the Leicester time limit of 33 minutes of c.p.u. time proved an encumbrance, the UMRCC facilities were used. In general, the time problem depends on the amount of s parameter data available and the complexity of the models involved. The p-n-p transistor model described in Chapter 5 was produced on the Cyber 73 but the n-p-n transistor models described in Chapter 6 required the CDC 7600, whilst the majority of the computing for the bias dependent model in Chapter 7 was done on the Cyber 73.

Graphical output was generally obtained using the Cyber 73 together with the GHOST library of graphical subroutines. The model circuit diagrams were produced on the University of Leicester PDP-11/44 using an interactive circuit layout program written by the author and which used the GINO library. Flow charts were also produced using the PDP-11/44, using the interactive program FLOW[18].

All the computer programs were written in FORTRAN IV.

CHAPTER 2

MODELLING THE BIPOLAR TRANSISTOR

A special report on the transistor in Electronics[19] describes the stages leading to the announcement in 1948 by Bardeen, Brattain and Shockley that they had invented the transistor. This first transistor was a point contact device. Shockley then went on to develop the junction transistor. These three inventors were awarded the Nobel Prize in 1956 for their work.

Since the invention of the transistor, models describing their behaviour have been sought. Both circuit and device designers need models that will simulate the performance of the transistor over a wide range of operation. Device designers generally require models which are based on the physical structure of the device in order that the effects of changes in the construction or geometry of the device can be predicted. On the other hand, circuit designers are more concerned with the accuracy of the model and are less interested whether the elements in the model have a physical equivalent in the manufactured device.

Equivalent circuit models of transistors can be used in conjunction with computer aided design techniques to assist in the design and analysis of discrete or integrated circuits without the time and expense of manufacturing the circuits. Getreu[20] lists a number of such uses of models, from performing analyses of waveforms and frequency responses of circuits to predicting the performance of an integrated circuit at high frequencies without the parasitics a breadboard would introduce.

This chapter starts with a brief description of the bipolar transistor and its applications. Then some of the popular models are described beginning with the classical hybrid pi model and going on to more complicated models such as the Ebers Moll model and its variants.

2.1. The Bipolar Transistor

A bipolar transistor consists of an emitter, base and collector and may be either an n-p-n or p-n-p type. Block diagrams of both types are given in Figure 2.1 together with their circuit symbols. Navon[21] defines the modes of operation of the bipolar transistor as follows.

1. Active mode - the emitter junction is forward biased and the collector reverse biased.

2. Saturated mode - both the emitter and collector junctions are forward biased.

3. Cutoff mode - both the emitter and collector junctions are reverse biased.

4. Inverse mode - the collector junction is forward biased and the emitter is reverse biased.

In the active mode the transistor may be used as an amplifier. A schematic of the active region biasing arrangements for an n-p-n transistor in common base configuration is given in Figure 2.2. Figure 2.3 shows an amplifier circuit described in Reference (22) where the biasing is achieved by using a single battery together with the voltage divider network consisting of resistors R_3 and R_4. In the diagram R_1 is the source resistance and R_2 is the load resistance.

Navon[21] states that in a linear amplifier circuit such as this, the signal transmission can be quite fast, of the order of 10^{-9} seconds, and this rapid response can be used to achieve signal amplification at frequencies up to several gigahertz. In addition to the common base configuration, common emitter and common collector amplifiers can also be used. The common emitter amplifier is probably the most used in practice because, as stated in Reference (22), it is

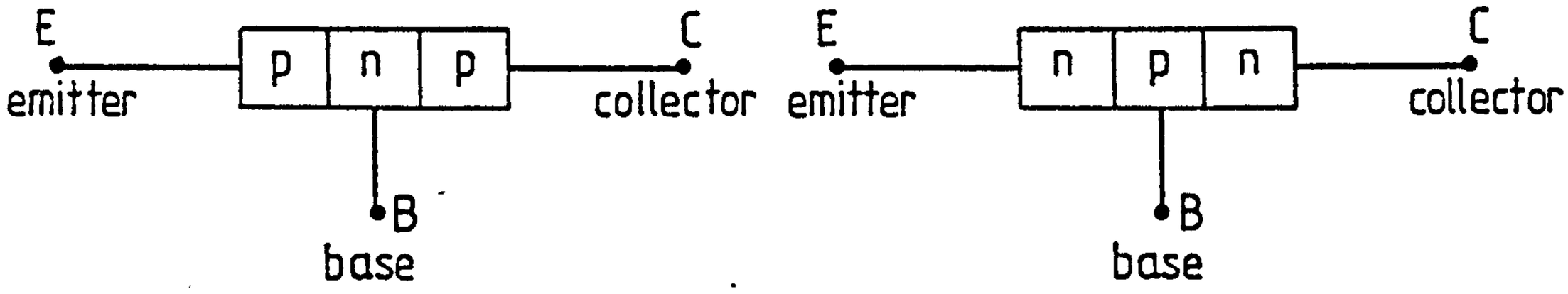

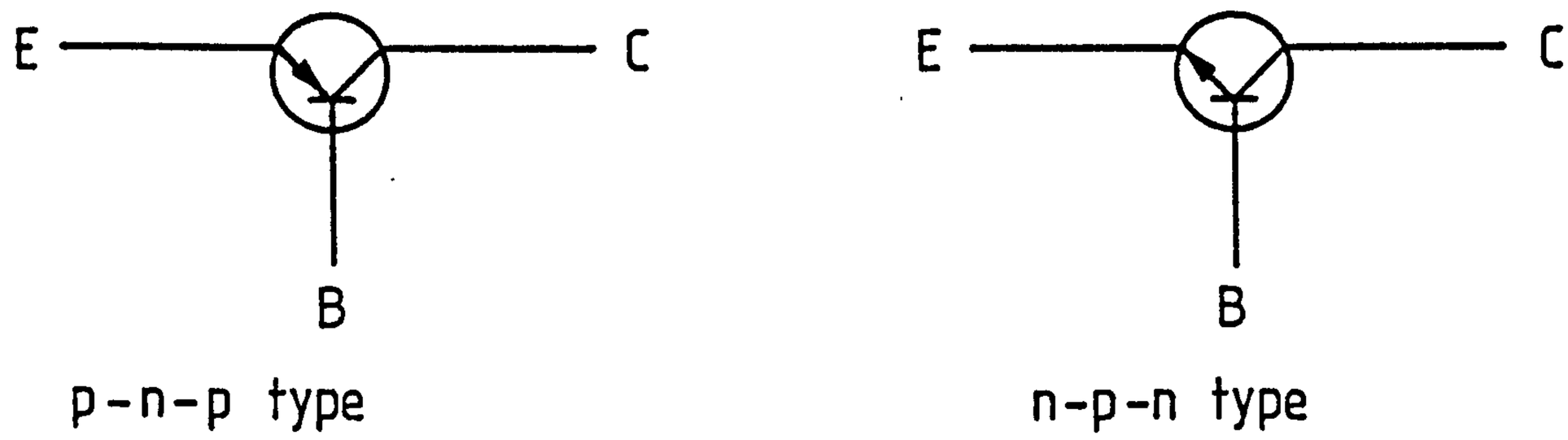

Figure 2.1. The Structure and Circuit Symbols for Bipolar Transistors

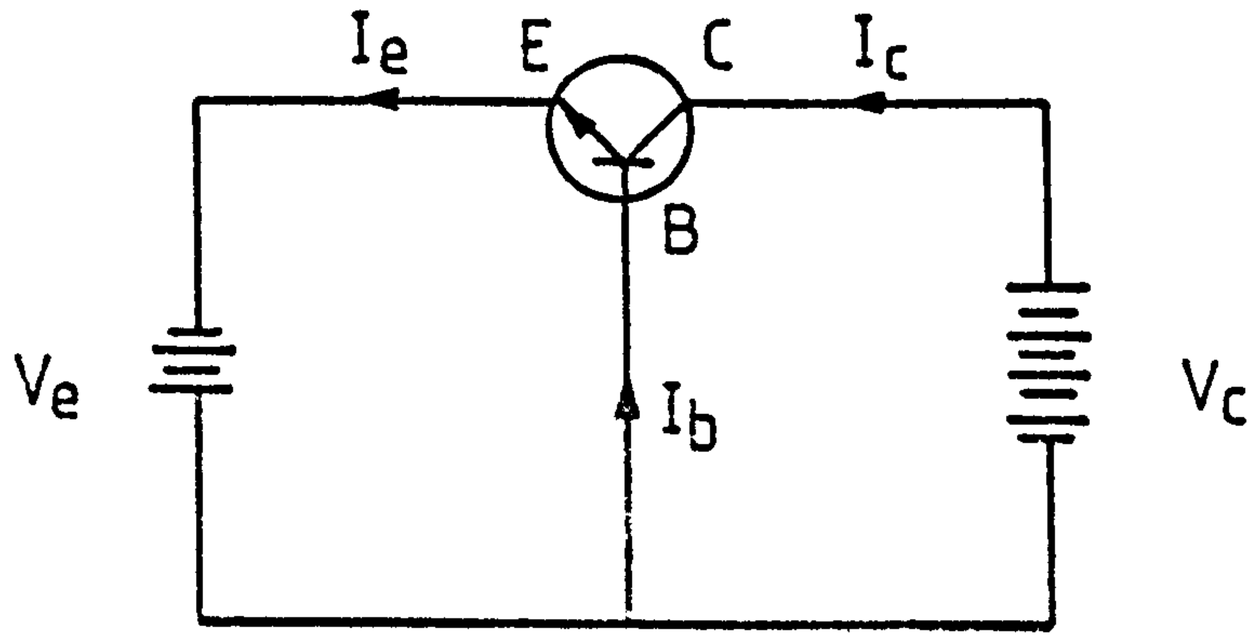

Figure 2.2. Typical Bias Arrangement for an N-P-N Transistor Biased in the Active Region

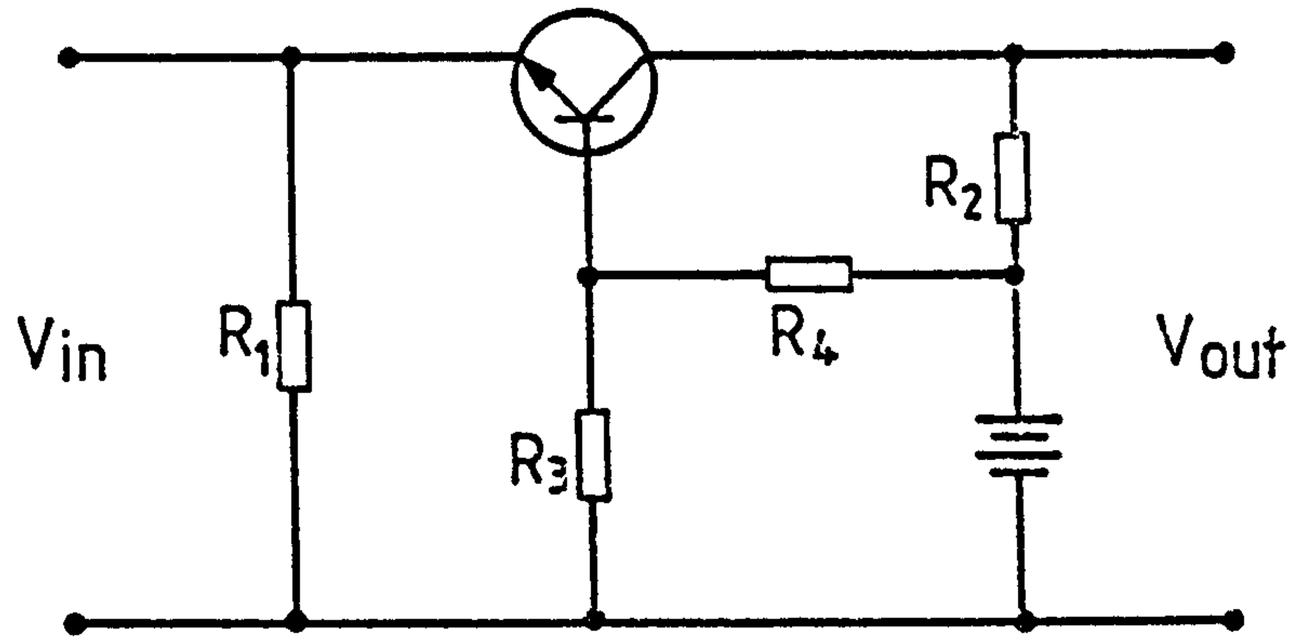

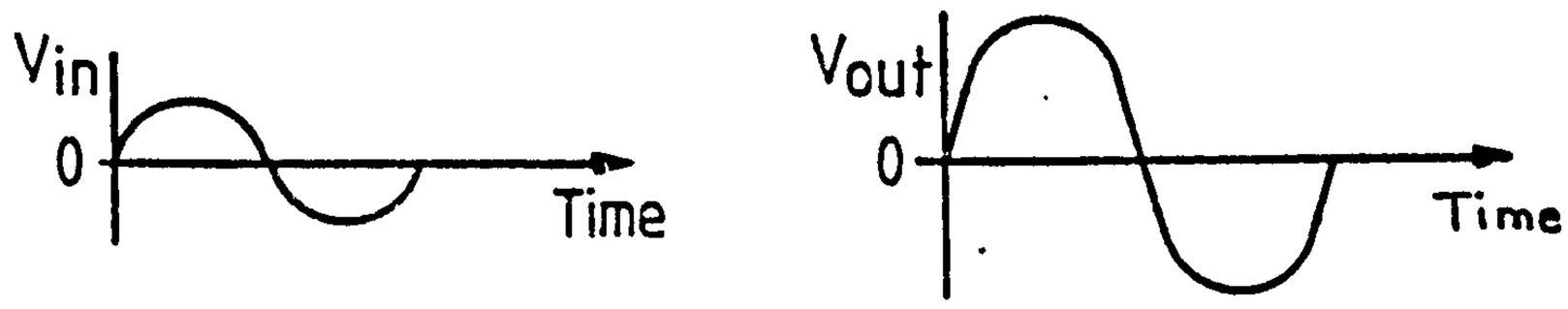

Figure 2.3. A Simple Common Base Amplifier

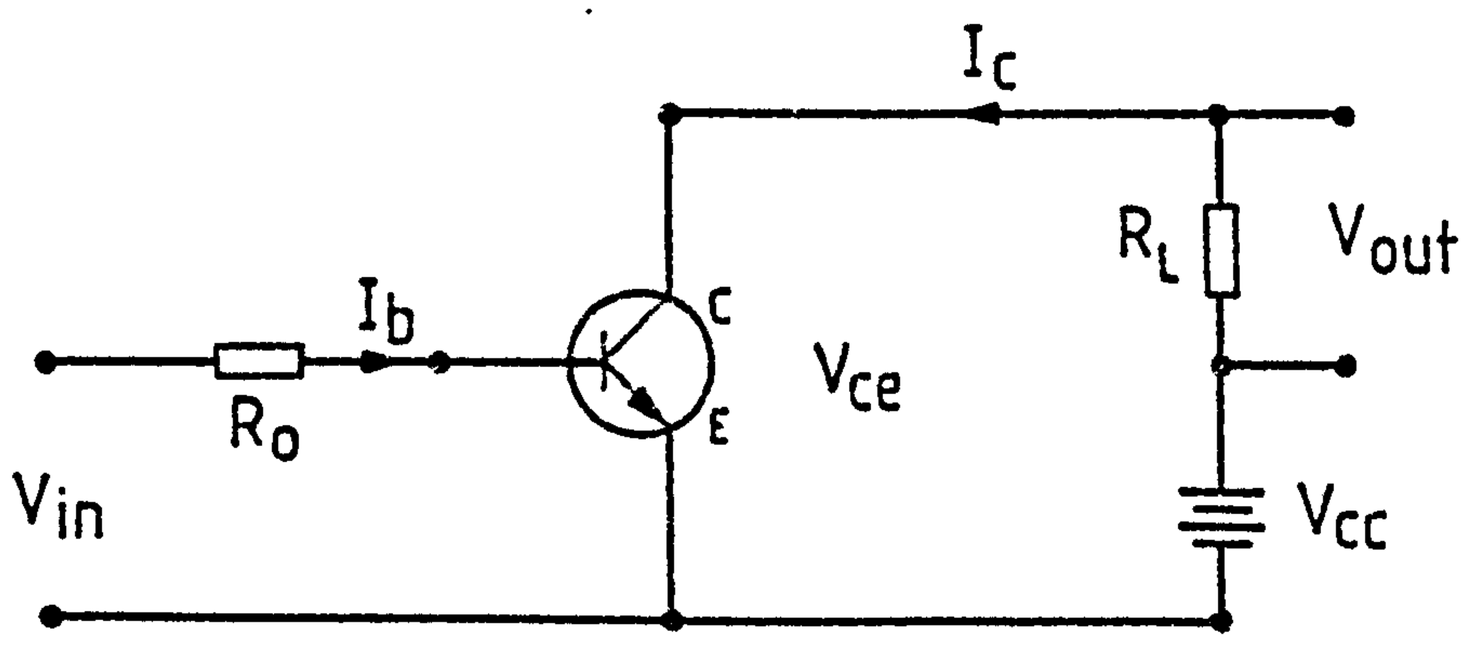

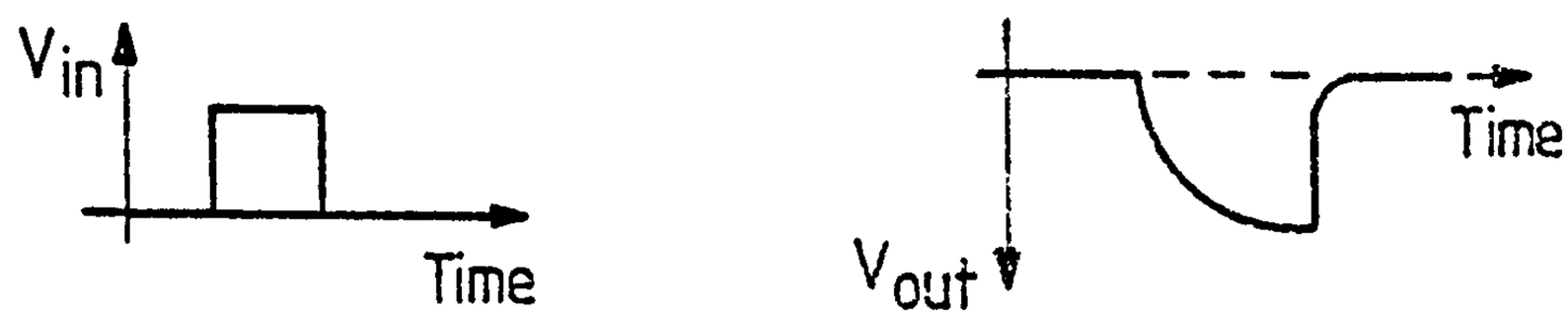

Figure 2.4. An N-P-N Transistor Used in Switching Mode

the only configuration to provide current, voltage and power gain.

In the saturated and cutoff modes the bipolar transistor can be used as a switch. When used in switching mode, the transistor is normally connected in common emitter mode as in the simple switch shown in Figure 2.4. The two parts of the switch are the emitter and collector terminals and a small signal, V_{in}, applied to the base terminal can cause the normally non-conducting transistor to convert to the conducting state thus producing a voltage V_{out} across the load R_L. Navon[21] states that in this configuration the current gain, defined as the ratio of the collector current increase to the base current which causes this increase, can be higher than 50.

If the transistor was symmetrically designed then the operation of the transistor in the inverse mode would be identical with the active mode but with the collector and emitter interchanged. However, in practice the emitter is more heavily doped and the collector cross-sectional area is greater than that of the emitter. Thus the p-n-p transistor should be more accurately described as a p^+-n-p type.

A more accurate diagram of the construction of a planar n-p-n transistor than that given in Figure 2.1 is now shown in Figure 2.5. This diagram will aid the identification of some of the physical elements in the models described in the following sections of this chapter and is also relevant to the modelling of the integrated circuit transistors described in later chapters.

A full description of the theory and manufacturing processes involved in the construction of these devices is given by Hamilton and Howard[23]. Briefly, an integrated circuit n-p-n transistor such as that shown in Figure 2.5, is built up layer by layer on a p-type substrate. The n^+ buried layer serves to reduce the series collector resistance of the transistor. The n-type collector is grown by means of epitaxial growth and is part of the same single crystal structure as the substrate. The p^+ channels

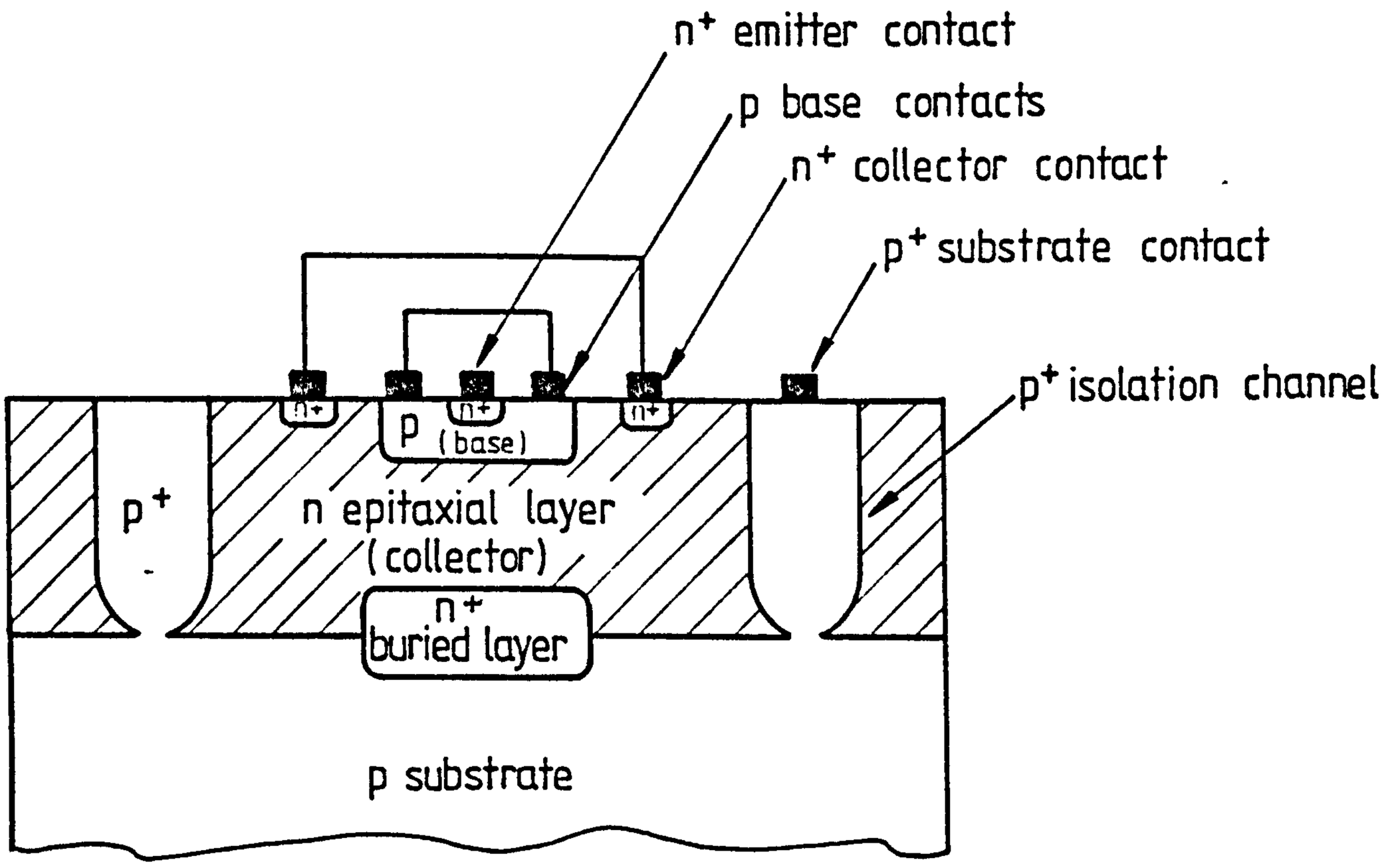

Figure 2.5 Construction of an Integrated Circuit N-P-N Transistor

isolate the device from the rest of the integrated circuit. The p-type base and n-type emitter are formed by a diffusion process and this is followed by metalisation of the contacts.

2.2. Hybrid Pi Model

The hybrid pi model is the most popular linear model of a bipolar transistor. Its appeal lies in its simplicity, its accuracy over a wide frequency range and the ease of parameter determination.

2.2.1. Basic Hybrid Pi Model

The basic seven element, common emitter hybrid pi model is described by Chua and Lin[24] and Brown[25,26] and is shown here in Figure 2.6. By comparing the model with Figure 2.5 which showed the construction of a transistor, it is possible to see the relevance of most of the elements.

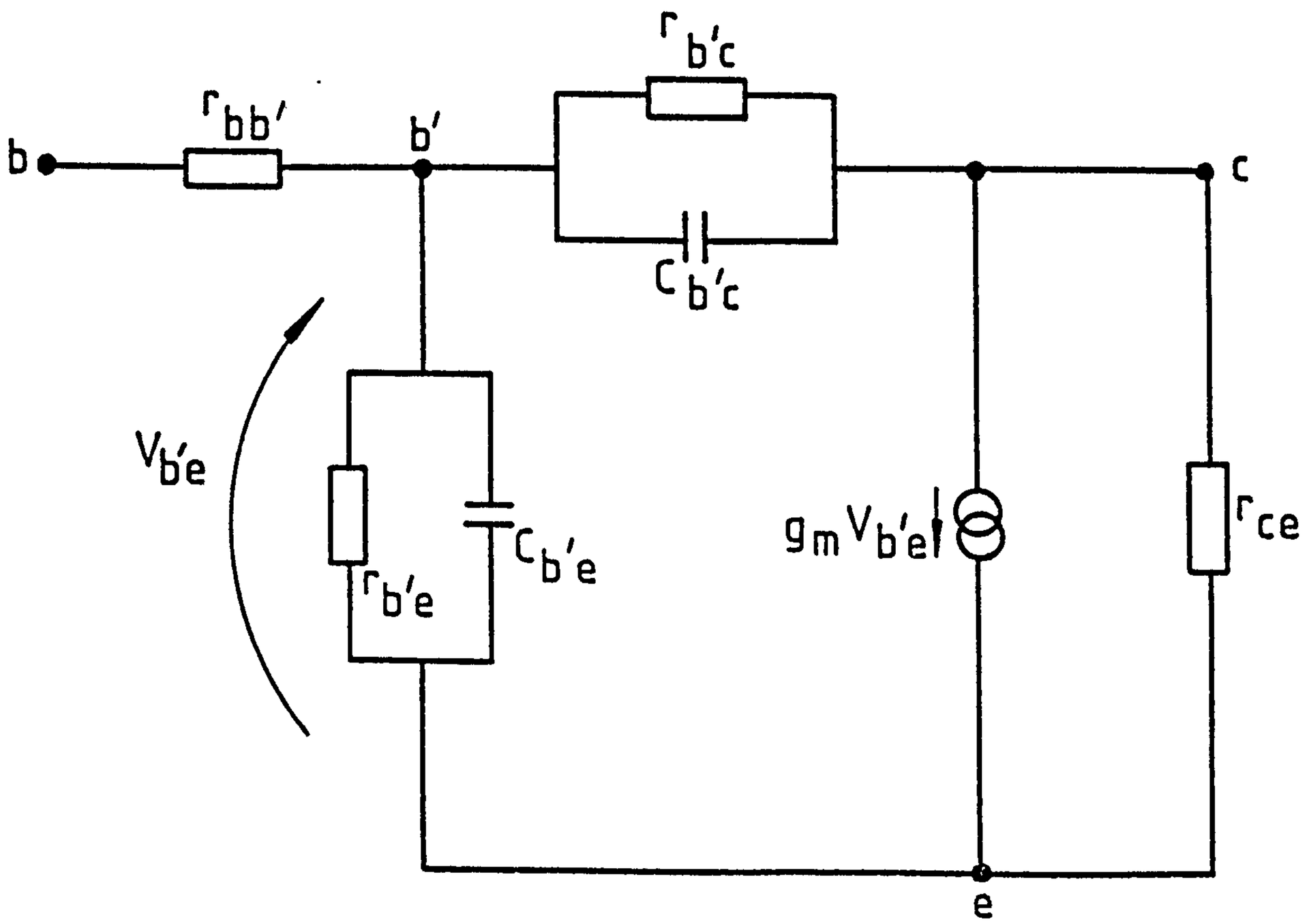

Figure 2.6 Common Emitter Hybrid Pi Transistor Model

Of particular interest is $r_{bb'}$, which Chua and Lin[24] term the base spreading resistance, stating that this is practically constant for a given transistor and is typically between $5\,\Omega$ and $100\,\Omega$. Gray and Searle[27] describe how this element is inserted to allow for the transverse voltage drops in the base region caused by the drift of base region majority carriers flowing into the active region between the emitter and collector. The inclusion of capacitors $C_{b'e}$ and $C_{b'c}$ to account for the space charge layer capacitances is also described by Gray and Searle[27].

Brown[26] describes how measurements of the y parameters (short-circuit admittance parameters) can be used together with other selected measurements to determine the values of the elements in the model for any particular case.

It is generally agreed that the basic hybrid pi model is a good linear model for frequencies up to a few megahertz.

2.2.2. Modified Hybrid Pi Model

As the frequency increases, the agreement between the basic hybrid pi model and the performance of the transistor deteriorates.

Brayden[28] describes a modified hybrid pi model in which the collector-base depletion capacitance is split, taking part of it to b instead of b'. A phase shift term is also included in the mutual conductance g_m and, as at higher frequencies $r_{b'c}$ and r_{ce} are swamped by the capacitance around them, these are eliminated from the model. It is also generally agreed that interlead and case capacitances are also significant. The new element C_{be} inserted by Brayden[28] will thus also include some interlead capacitance. Gray and Searle[27] state that while the interlead capacitances in an integrated circuit component are smaller than for the same component in discrete form, the junction

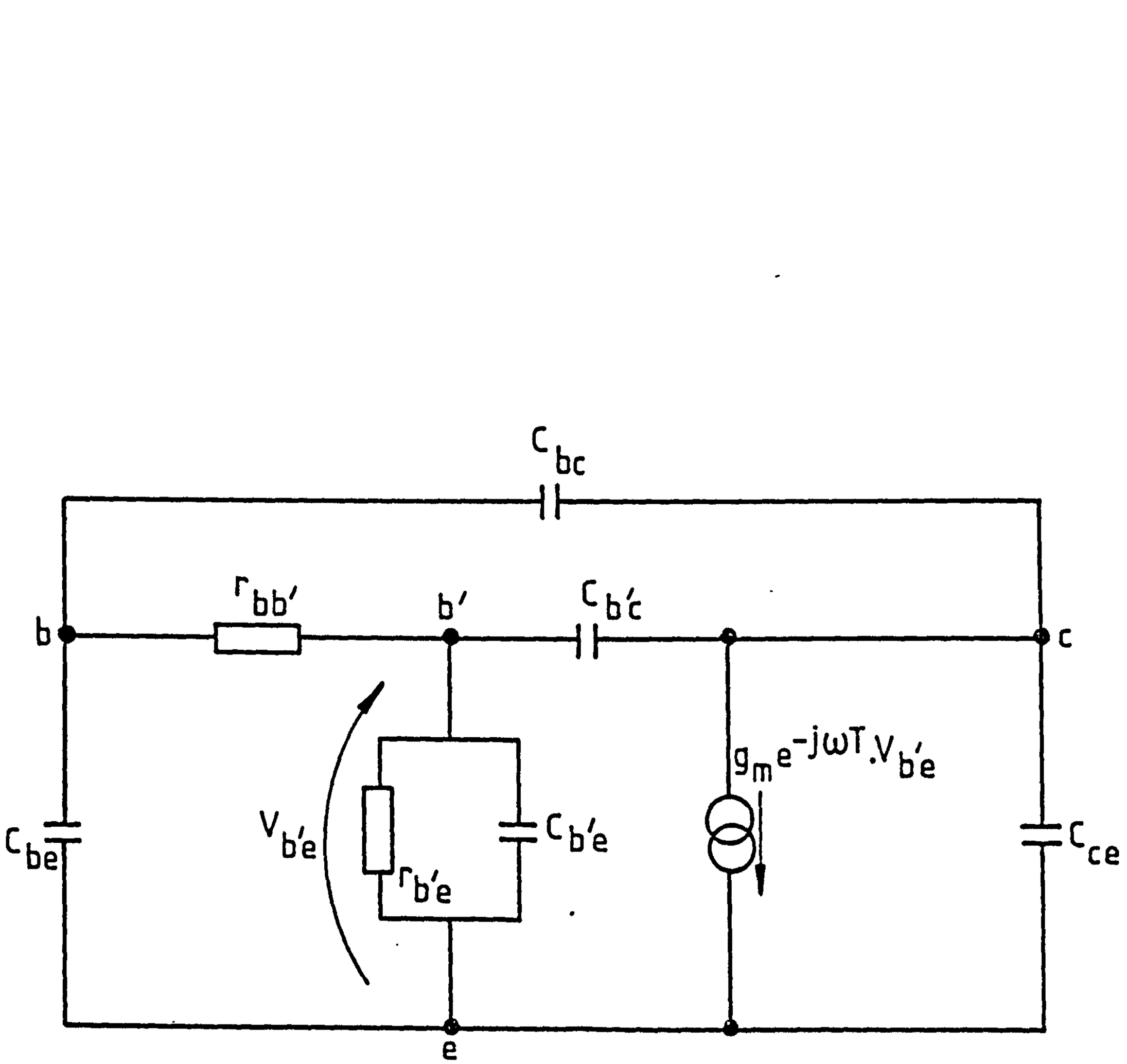

Figure 2.7 Modified Hybrid Pi Model

capacitances must still be accounted for.

The above thus leads to the modified hybrid pi model shown in Figure 2.7 which Brown[25,26] states should be accurate at frequencies higher than 300 MHz, especially if some emitter lead inductance is also included.

As with the basic hybrid pi model, Brown[26] also describes the measurements which must be made to determine the element values for this model.

2.3. Ebers Moll Model

The Ebers Moll model is probably the most popular non-linear model for bipolar transistors. This model was first published by Ebers and Moll[27] in 1954 and there have been numerous variations on this original model published since then. This model is included here because, even though the work in this thesis was concerned mainly with small-signal linear models, the final problem involved a transistor which entered the non-linear region. Also, the non-linear modelling problem and the Ebers Moll model are too important to be ignored. Here the notation used by Getreu[20] is used to differentiate between the stages in the development of the models.

2.3.1. Basic Ebers Moll Model - EM1

A diagram of the basic Ebers Moll model, is given in Figure 2.8. The basic model is a d.c. model that describes the behaviour of the transistor in all modes of its operation. The model is described by its reference currents I_F and I_R, the currents through the diodes. Getreu[20] describes this model as follows.

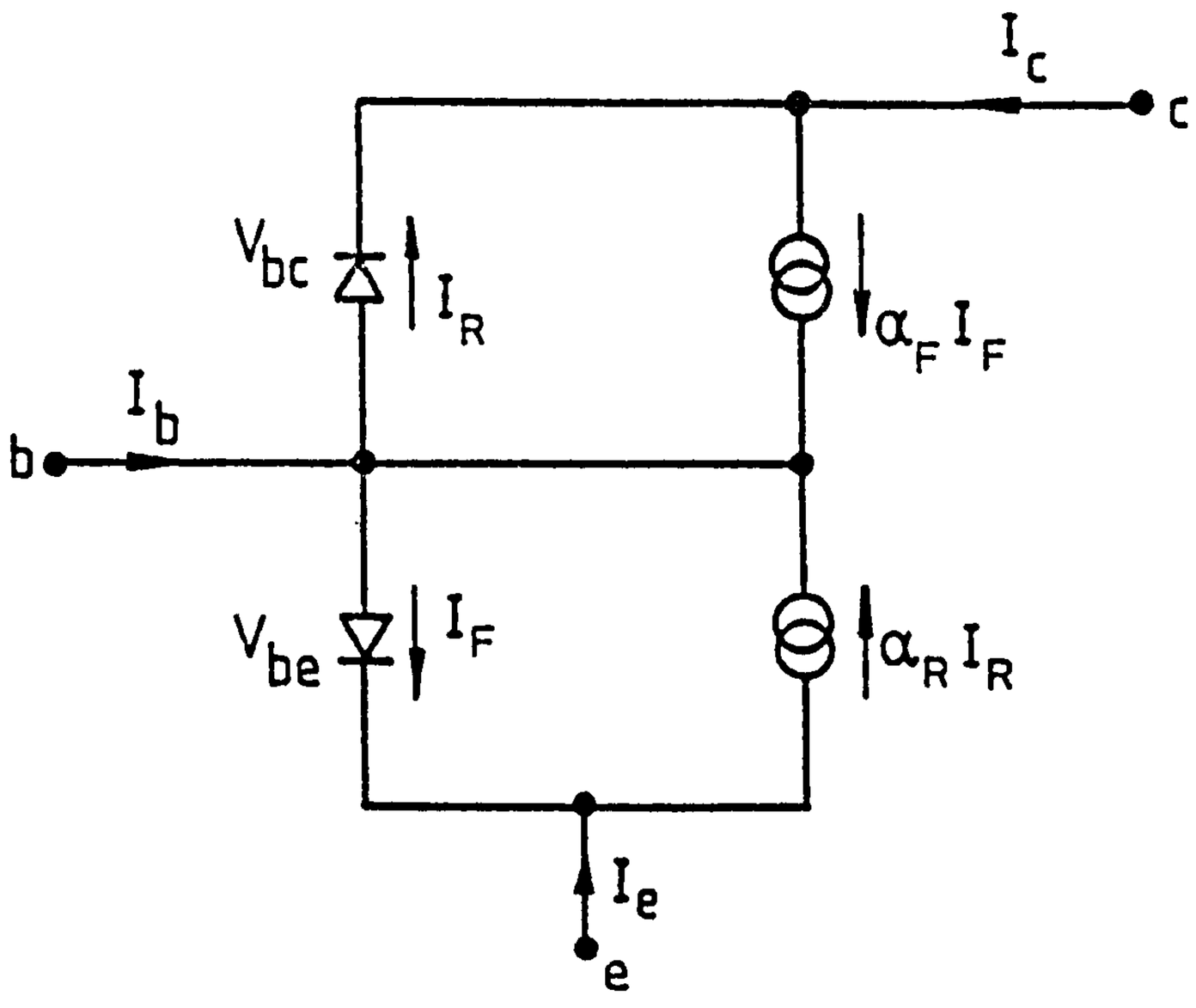

Figure 2.8 Basic Ebers Moll Model - EM1

The diodes represent the base-emitter and base-collector junctions of the transistor. I_F is the current that would flow across the base-emitter junction for a given base-emitter voltage V_{be}, if the collector region were replaced by an ohmic contact without disturbing the base. I_{es} is the saturation current of this junction. Thus, for a given value of V_{be}

$$I_F = I_{es} \left(e^{\frac{q\, V_{be}}{kT}} - 1 \right) \qquad (2.1)$$

where q = electron charge

k = Boltzmann's constant

T = Absolute temperature

Similarly, if the emitter were replaced by an ohmic contact without disturbing the base and I_{cs} is the saturation current of the collector-base junction

$$I_R = I_{cs}\left(e^{\frac{q\,V_{bc}}{kT}} - 1\right) \qquad (2.2)$$

Coupling between the junctions of the transistor is provided by the base region and is modelled by the two current dependent current sources.

Thus

$$I_c = \alpha_F I_F - I_R \qquad (2.3)$$

where α_F is the large signal forward current gain of a common base transistor and is related to the large signal forward current gain (β_F) of a common emitter transistor by the expression

$$\beta_F = \frac{\alpha_F}{1 - \alpha_F} \quad . \qquad (2.4)$$

Similarly the base terminal current can be written

$$I_b = (1 - \alpha_F) I_F + (1 - \alpha_R) I_R \qquad (2.5)$$

where α_R is the large signal reverse current gain of a common base transistor and similarly to equation (2.4)

$$\beta_R = \frac{\alpha_R}{1 - \alpha_R} \quad . \qquad (2.6)$$

The derivation of these equations is given by Ebers and Moll[29].

Getreu[20] shows how the linearised version of this model for operation in the forward active region reduces to the d.c. portion of the small-signal hybrid pi model.

2.3.2. Extended Ebers Moll Model - EM2

The EM1 model is a basic d.c. model of a bipolar transistor. The next stage in the development of the model is to take into account the charge storage effects and to improve the d.c. representation.

In the EM2 model described fully by Getreu[20] and shown here in Figure 2.9, the basic EM1 model has been transformed. Expressions for the currents I_1, I_2 and I_3 are derived by Getreu. Around this EM1 model a number of elements have been added. The three resistors $r_{bb'}$, $r_{cc'}$, and $r_{ee'}$ are added to improve the d.c. characterisation. These resistors represent the ohmic resistance of the active region of the transistor to its base, collector and emitter respectively. The charge storage effects are modelled by (i) two junction capacitors, C_{Jc} and C_{Je}, which model the incremental fixed charges stored in the transistor's space-charge layers for incremental changes in the associated junction voltages, (ii) two diffusion capacitors, C_{Dc} and C_{De}, which model the charge associated with the mobile carriers in the transistor, and (iii) the substrate capacitor, C_{sub}, which is important in integrated circuit transistors.

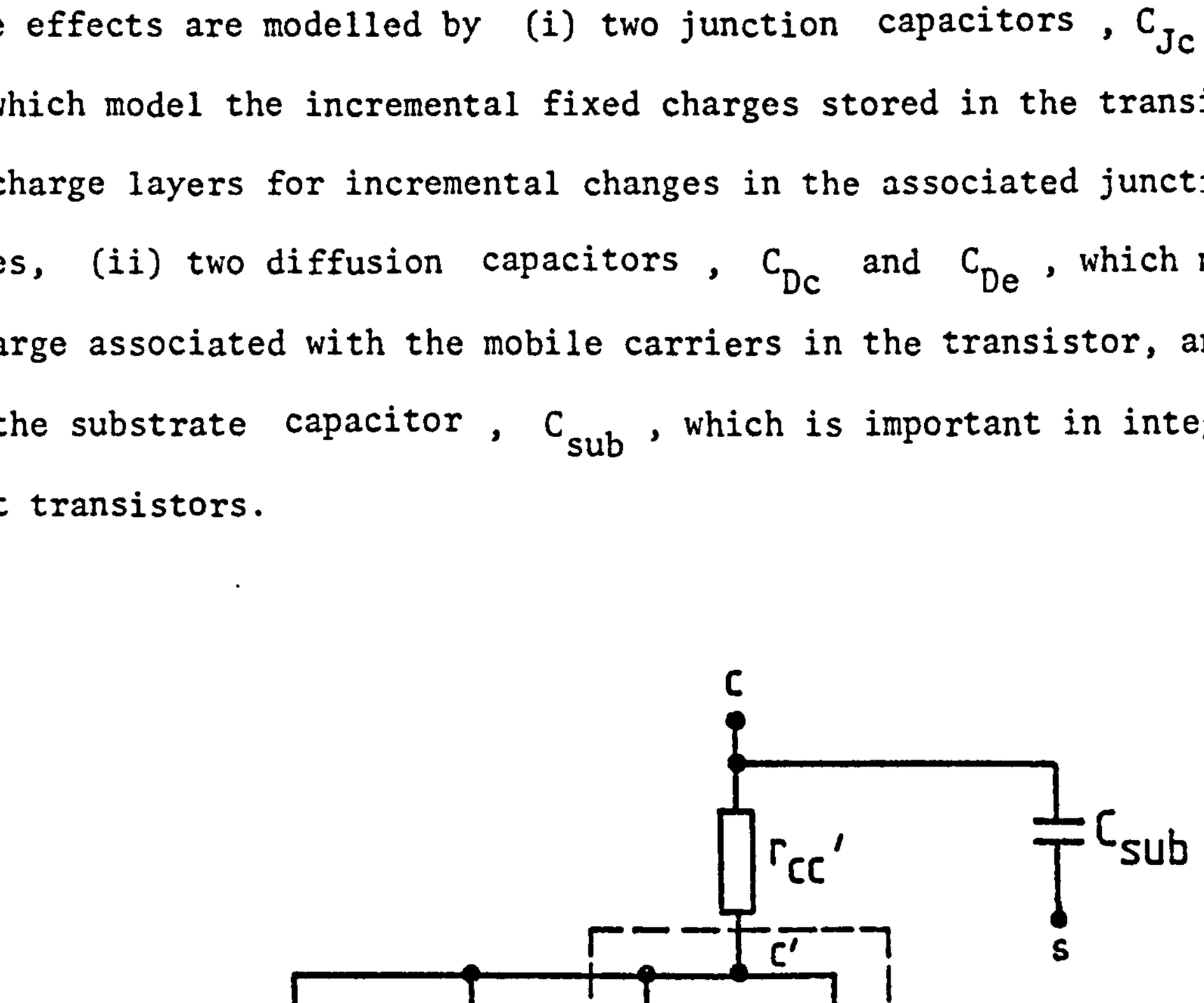

Figure 2.9 Ebers Moll Model - EM2

As with the EM1 model, Getreu[20] demonstrates that this model reduces to the linear hybrid pi model in the forward active region.

2.4. Other Non-Linear Models

In addition to the Ebers Moll models described in Section 2.3, Getreu[20] goes on to describe a further refinement of the Ebers Moll model which he calls the EM3 model. This model includes a further two diodes and a junction capacitor and models the base-width modulation and variation of current gain β with current and voltage, and some temperature effects.

Another model described by Getreu[20] is the Gummel Poon model which he states is almost entirely concerned with improvements to the d.c. characteristics of the EM3 model but is still basically equivalent to the EM3 model.

Other popular models include the Linvill[30] lumped model which, while adhering closely to the physics of the device, introduces the new network parameters of storance, diffusance and combinance, and the Beaufoy Sparkes[31] model which is favoured by Brown[26]. He describes this model as lying between the Ebers Moll and Linvill models with only two new network elements namely storance and charge controlled current generators.

Hamilton et al.[32] in their comparison of models conclude that the Ebers Moll, Linvill and Beaufoy Sparkes models are all similar in their degree of approximation and give similar results for transient problems.

There are many variations on the models described here, Ruch[33] gives a list of references concerned with high-injection effects and Agajanian[34] presents a total of 486 references in his bibliography on semiconductor device modelling although not all of these are concerned with bipolar transistors.

2.5. Choice of Models

For each of the models described in this chapter, at least one set of measurements enabling the evaluation of the element values is published. For example, Orlik[35] describes a set of electrical measurements that can be made to determine the parameter values of a Gummel Poon model while Roulston[36] describes how the parameters of a similar model may be determined directly from fabrication data. Another method of determining the element values for any particular model is to optimise the values of the elements to give the best fit to a set of measured data. Probably the first description of this method was by Bassett[37].

It is obvious from the discussion in Section 2.4 that there is not a universally accepted single model for the bipolar transistor. A number of physical effects have been incorporated into models with varying degrees of complexity but while Getreu[20] states that the simplest existing model adequate for the analysis to be undertaken should be used, Ruch[33] suggests that time and effort spent on modelling even a complex model has definite advantages, in particular that it saves the wasted time and expense of evaluating many models or of using unsuitable models.

The author feels that model verification is an important aspect of modelling, an opinion confirmed by Ruch[33], and one which is often overlooked. Similarly, there is virtually no guidance as to what action should be taken if the model chosen is inadequate.

Thus, the author's aim was to present here a method by which models could be verified and if necessary, better models could be evolved to the complexity and accuracy required. It was also hoped that by so doing, the knowledge of the further effects that must be incorporated in order to produce acceptable models could be extended.

The work by Bassett[37] on optimising the element values of models indicated a method by which models could be verified. The optimisation techniques developed by the author to achieve the aims stated are described in the later chapters of this thesis.

CHAPTER 3

TRANSISTOR PARAMETER MEASUREMENTS AND ANALYSIS OF MODELS

In order to obtain element values of models of transistors and to check their validity, a set of measurements characterising the transistor to be modelled must be available. It was mentioned in the previous chapter that there are prescribed measurements that may be made to enable the calculation of element values for specific models.

Similarly, the validation and optimisation of a model require that functions that can be measured for the transistor can also be calculated for the model in order to make the necessary comparisons. Suitable measurements are the short-circuit admittance, or y, parameters and the scattering, or s, parameters. These parameters are described later in this chapter and are related to each other by a set of equations also given later. The y parameters of a network can be obtained by nodal analysis as shown in Section 3.1.1.

Earlier work on network synthesis at Leicester has used coefficient matching techniques to generate passive networks. In these cases the network to be synthesized was represented by network polynomials such as those given by Lucal[38], investigated by Hegazi[7] and Savage[8] and shown in equations (3.1).

$$y_{11} = \frac{36p^4 + 2058p^3 + 6552p^2 + 4638p + 36}{36p^3 + 216p^2 + 396p + 216}$$

$$-y_{12} = \frac{36p^4 + 36p^3 + 72p^2 + 36p + 36}{36p^3 + 216p^2 + 396p + 216} \qquad (3.1)$$

$$y_{22} = \frac{36^4 + 533p^3 + 1572p^2 + 1183p + 36}{36p^3 + 216p^2 + 396p + 216}$$

where y_{11}, y_{12} and y_{22} are the short circuit admittance parameters and p is the complex frequency variable.

Cutteridge and di Mambro[12] developed a method to calculate the coefficients of p for a passive two-port network using the nodal admittance matrix thus enabling network synthesis by coefficient matching to be performed. In addition to his work with passive networks, di Mambro[39] later developed an analysis routine to calculate the network polynomial coefficients for networks containing active elements.

As it would be possible to convert measured s or y parameters in the frequency domain into complex rational functions, for example in a similar manner to that suggested by Enden and Groenendaal[40] , it would therefore be possible to perform coefficient matching on a transistor model.

Coefficient matching techniques for network synthesis were first suggested by Calahan[41] and this approach has been favoured for many years. Savage[8] states that the advantages of this method include good convergence properties since the coefficients and derivatives are multi-linear functions of the network elements with the consequent easy and accurate formulation of the derivatives. Also, using coefficient matching the minimum size of the network required to effectively synthesize the functions is well defined and, as stated by Savage, it is clearly apparent when a realization has been achieved.

However, there is the disadvantage that the formulation of the rational functions in p , known as the approximation stage, is bound to introduce errors before any matching is even begun. It would also be necessary to decide somehow on the orders of the polynomials in p . One way would be to choose orders giving less than a specified error at the approximation stage.

This seems to be over-complicated and error-prone, thus the author rejected coefficient matching as a suitable technique for this application, choosing direct matching of the measured parameters in the frequency domain. This is not without precedent: Bassett[37], one of the first to use optimisation methods for transistor modelling, chose to match the y parameters

directly and most others have followed this example.

3.1. Y Parameters

The y parameters, or short-circuit admittance parameters, are a means of describing a two-port network as a 'black box' network, i.e. one whose interior is inaccessible. They are defined in terms of the port small-signal voltages and currents, which are shown in Figure 3.1, and are the complex functions y_{11}, y_{12}, y_{21} and y_{22} where

$$\begin{aligned} I_1 &= y_{11}V_1 + y_{12}V_2 \\ I_2 &= y_{21}V_1 + y_{22}V_2 \end{aligned} \tag{3.2}$$

at any particular bias point and frequency.

By examination of equations (3.2) it can be seen that the parameters may be defined and measured by short-circuiting the input or output port and taking the relevant admittance, thus

$$\begin{aligned} y_{11} &= \frac{I_1}{V_1} \quad \text{when} \quad V_2 = 0 \\ y_{12} &= \frac{I_1}{V_2} \quad \text{when} \quad V_1 = 0 \\ y_{21} &= \frac{I_2}{V_1} \quad \text{when} \quad V_2 = 0 \\ y_{22} &= \frac{I_2}{V_2} \quad \text{when} \quad V_1 = 0 \end{aligned} \tag{3.3}$$

hence their description as the short-circuit admittance parameters.

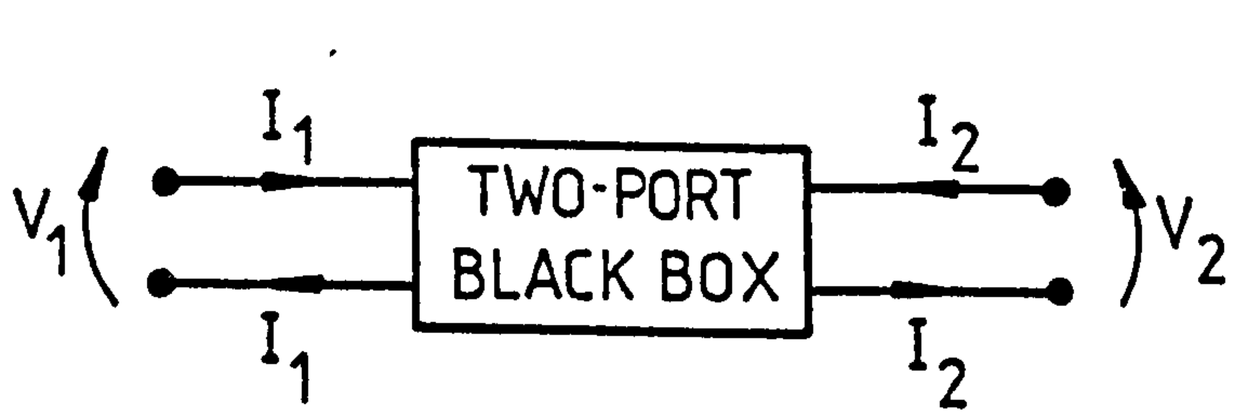

Figure 3.1 Two-Port 'Black Box'

3.1.1. Nodal Analysis

Nodal analysis is a method by which the y parameters of a two-port network can be calculated.

Consider an m-terminal passive network where, conventionally, nodes 1 and 2 are the input and output nodes respectively, and denote, say, node m as a reference node. Spence[42] describes how applying Kirchhoff's Current Law to each node in turn we can obtain the equations which in matrix form give

$$\underline{I} = [Y_{ind}]\underline{V} \tag{3.4}$$

where Y_{ind} is the indefinite admittance matrix

$\underline{I}$ is the vector of currents entering each node from external sources

and $\underline{V}$ is the vector of voltages at each node with reference to node m.

For a two-port network, since the internal nodes are inaccessible, there cannot be any current injected into these internal nodes from external sources, thus only I_1 and I_2 are non-zero.

Spence also shows how Y_{ind}, the indefinite admittance matrix, may be formed by inspection of the network. Thus, each diagonal element Y_{ii} $(i = 1,m)$ is formed by the sum of the admittances incident at node i and each off-diagonal element Y_{ij} $(i = 1,m;\ j = 1,m;\ i \neq j)$ is formed by the negative of the sum of all the admittances connected directly between nodes i and j, where in general terms the admittance Y between any two nodes is given by

$$Y = pC + G + \frac{1}{pL} \tag{3.5}$$

where p is the complex frequency variable

C is the capacitance in Farads between the two nodes

G is the conductance in Siemens between the two nodes

and L is the inductance in Henrys between the two nodes.

It can be seen that for a passive network the indefinite admittance matrix will always be symmetric.

This analysis can now be extended to include a voltage controlled current source having mutual conductance g_m . Again referring to Spence[42] the terms in the indefinite admittance matrix due to the controlled source can be formed by inspection. If the controlling voltage is between nodes k and ℓ (voltage high at k) and the controlled current flows from node i into node j then the additional terms in Y_{ind} are

$$\begin{aligned} &+ g_m \text{ to element } Y_{ik} \text{ of } Y_{ind} \\ &- g_m \text{ to element } Y_{i\ell} \text{ of } Y_{ind} \\ &- g_m \text{ to element } Y_{jk} \text{ of } Y_{ind} \\ &+ g_m \text{ to element } Y_{j\ell} \text{ of } Y_{ind} \,. \end{aligned} \tag{3.6}$$

If a time constant τ is also required, as in the model referred to in Section 2.2.2, then the terms become $\pm g_m e^{p\tau}$. Thus we are able to form the indefinite admittance matrix of an active network.

The $n \times n$ nodal admittance matrix, where $n = m - 1$, is obtained by deletion of the mth row and column of Y_{ind} where node m is the reference node and is usually the earth node. At any particular value of p , the nodal admittance matrix may be reduced using pivotal condensation as described by Aitken[43] to obtain the y parameters as defined in equations (3.2). This procedure is described in detail in Section 3.1.3.

An alternative approach developed by di Mambro[4] and Cutteridge and di Mambro[12] making use of the network polynomials is described in Section 3.1.2.

3.1.2. Generation of the Network Polynomial Coefficients from the Nodal Admittance Matrix

As described in the previous section, for a two-port network containing a total of $n+1$ nodes, in which nodes 1 and 2 are the input and output respectively, plus the earth node which is designated the reference node, the nodal equations may be written

$$\sum_{j=1}^{n} Y_{ij}V_j = I_i \quad , \quad i = 1,n \tag{3.7}$$

where $[Y]$ is the $n \times n$ nodal admittance matrix and $I_i = 0$, $i = 3,n$.

Cutteridge and di Mambro[12] describe how the y parameters can be written

$$\begin{aligned} y_{11} &= \frac{\Delta_{22}}{\Delta_{1122}} \\ y_{12} &= \frac{\Delta_{21}}{\Delta_{1122}} \\ y_{21} &= \frac{\Delta_{12}}{\Delta_{1122}} \\ y_{22} &= \frac{\Delta_{11}}{\Delta_{1122}} \end{aligned} \tag{3.8}$$

where Δ is defined as the determinant of $[Y]$

and Δ_{ij} and Δ_{iijj} are the unsigned minors of Δ .

They then describe how, for a purely resistive network, the y parameters can be obtained using Gaussian elimination and state that since Δ_{1122} is given by the product of the diagonal elements produced in rows 3 to n inclusive, Δ_{11}, Δ_{12}, Δ_{21} and Δ_{22} can be obtained with only slightly more work than the calculation of Δ_{1122} alone.

Extending the analyses to networks containing reactive elements, it can be seen that all the determinants involved are polynomials in the complex frequency variable, p , and if inductances are present these include a division by some power of p . Cutteridge and di Mambro state the upper

limits of the powers of p in the numerator and denominator for RC, RL and RLC networks. In their method any inverse powers of p are removed by multiplying through by p as appropriate. Then, if m is the highest order of the polynomials produced, $m+1$ values are assigned to p, say p_i, $i = 0,m$, giving

$$\begin{bmatrix} 1 & p_o & p_o^2 & - & - & - & - & p_o^m \\ 1 & p_1 & p_1^2 & - & - & - & - & p_1^m \\ \vdots & & & & & & & \\ \vdots & & & & & & & \\ \vdots & & & & & & & \\ \vdots & & & & & & & \\ 1 & p_m & p_m^2 & - & - & - & - & p_m^m \end{bmatrix} \begin{bmatrix} a_o \\ a_1 \\ \vdots \\ \vdots \\ \vdots \\ \vdots \\ a_m \end{bmatrix} = \begin{bmatrix} \Delta(p_o) \\ \Delta(p_1) \\ \vdots \\ \vdots \\ \vdots \\ \vdots \\ \Delta(p_m) \end{bmatrix} \qquad (3.9)$$

where $\Delta(p)$ is the value of a cofactor evaluated at a particular value of p and a_i, $i = 0,m$, are the coefficients of the corresponding polynomial.

The $(m+1) \times (m+1)$ matrix on the left hand side of equation (3.9) is the Vandermonde matrix and this Cutteridge and di Mambro invert using an algorithm given by Traub[44] thus enabling calculation of the polynomial coefficients.

Cutteridge and di Mambro[12,45] also describe how the partial derivatives of the polynomial coefficients with respect to the network elements may be efficiently computed.

di Mambro[4] further developed this technique to allow for the presence of active elements without a time constant. A later, development, version of a computer program written by di Mambro[39] which allowed voltage controlled current sources with time constants was received by the author. Time constants, τ, introduce exponential terms $\pm e^{p\tau}$ into the nodal admittance matrix. di Mambro overcame this problem by approximating these terms using

the first two terms of the series

$$e^x = 1 + \frac{x}{1!} + \frac{x^2}{2!} + \frac{x^3}{3!} \ldots \qquad (3.10)$$

thus replacing $e^{p\tau}$ by $1 + p\tau$.

The author used this version of di Mambro's program in the early stages of research, calculating the y parameters at any particular frequency from the network polynomials. Unfortunately, this being a development version there were some errors present, one of these occurring when inductors were included. However, even on correcting this fault, the method was still not satisfactory. In particular, the approximation $1 + p\tau$ for the terms involving time constants was considered too inaccurate. Also, it was felt that a more direct method using pivotal condensation, as described in the next section, would be more suitable.

The results obtained using di Mambro's method and the method described in the next section are compared in Section 3.1.4.

3.1.3. Calculation of the y Parameters using Pivotal Condensation

If all the values of the elements present in a network are inserted into the nodal admittance matrix together with the value of the complex frequency p at which the y parameters are required, then the Gaussian elimination procedure described in the previous section can be performed in a systematic procedure known as pivotal condensation which is described by Aitken[43].

In pivotal condensation, since the currents I_3 to I_{n+1} of the n+1 node two-port 'black box' are zero, the $n \times n$ nodal admittance matrix $[Y]$ is reduced to an $(n-1) \times (n-1)$ matrix using the formula

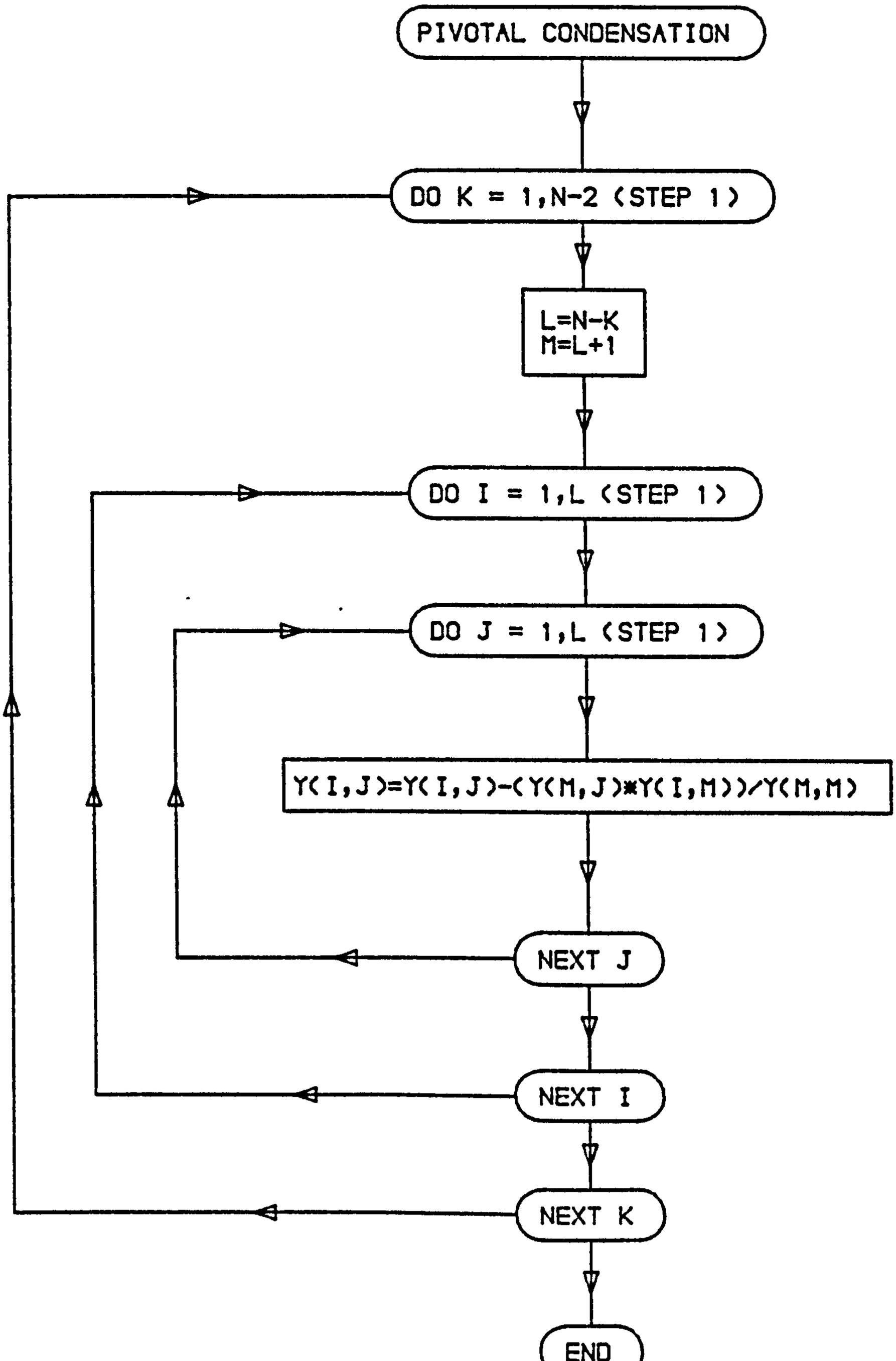

Figure 3.2 Flow Chart for Pivotal Condensation Procedure

$$Y'_{ij} = Y_{ij} - \frac{Y_{nj} \cdot Y_{in}}{Y_{nn}} \qquad \begin{matrix} i = 1, n-1 , \\ j = 1, n-1 \end{matrix} \qquad (3.11)$$

where [Y'] is the new matrix of size (n - 1) x (n - 1).

This procedure can then be repeated on [Y'] and so on until a 2 x 2 matrix is obtained thus giving the *y* parameters.

The flow chart in Figure 3.2 gives the computational procedure for the calculation of the *y* parameters from the nodal admittance matrix using this technique.

In the FORTRAN subroutine written by the author, since the *y* parameters for any particular network would be required at a number of frequencies, it was decided to set up two-dimensional arrays G, L and C to contain the contributions of conductance, inductance and capacitance respectively, to the nodal admittance matrix. Then at any given frequency an element in the nodal admittance matrix [Y] was given by

$$Y_{ij} = G_{ij} + pC_{ij} + \frac{1}{pL_{ij}} \pm g_m e^{p\tau} \qquad (3.12)$$

where $g_m e^{p\tau}$ was the term due to a current source, which was included as appropriate.

As complex arithmetic is available in FORTRAN on modern computersthere was no difficulty in the complex arithmetic due to p which is given by

$$p = j2\pi f \qquad (3.13)$$

where f = frequency in Hertz.

3.1.4. Accuracy of Calculations

When calculating the *y* parameters using pivotal condensation it is possible, just as with Gaussian elimination, to choose the pivotal element in order to preserve the maximum accuracy. However, as pointed out by Spence[42], the nodal admittance matrix should always have non-zero elements

on the diagonal, unless a node is not connected in which case it should be eliminated anyway, therefore the matrix is generally well-conditioned.

Fairbrother and Basset[46] also consider the effect of the frequency on the calculation. They observe that, in particular, at very low or high frequencies or at resonant frequencies, some elements in the matrix can become very large compared with other elements in the matrix and that this can lead to inaccuracies of calculation. However, they felt that even this was an infrequent occurrence and took no special precautions.

In the subroutine written by di Mambro[39], because of the in-built method of setting up the frequency components used in the calculation of the network polynomial coefficients, it was found that the calculations were grossly inaccurate in the MHz frequency range required by the author. To overcome this it was necessary to scale the values by multiplying the frequency values by 10^{-9} and the reactive component and time constant values by 10^{9}.

Bearing in mind the above points the author decided first of all, that in order to preserve the maximum accuracy in the pivotal condensation, that section should be performed in double precision arithmetic. Remembering that the computers in use had a 60 bit word length this, it was felt, should provide adequate protection. Additionally, it was decided to apply the factors of 10^{9} and 10^{-9} in the same way as was necessary with di Mambro's method, partly for reasons of consistency but also to avoid the presence of both very large and very small values in the arithmetic.

Checks were then made using the circuit shown in Figure 3.3 at frequencies of 0.5 MHz, 10 MHz and 100 MHz and with time constants τ on the current generator of 0, -0.01 ns and +0.01 ns .[†] This circuit, which appeared to be prone to loss of accuracy, was analysed manually to obtain as accurate

---

[†] The notation used here is that a negative value of τ indicates a time delay.

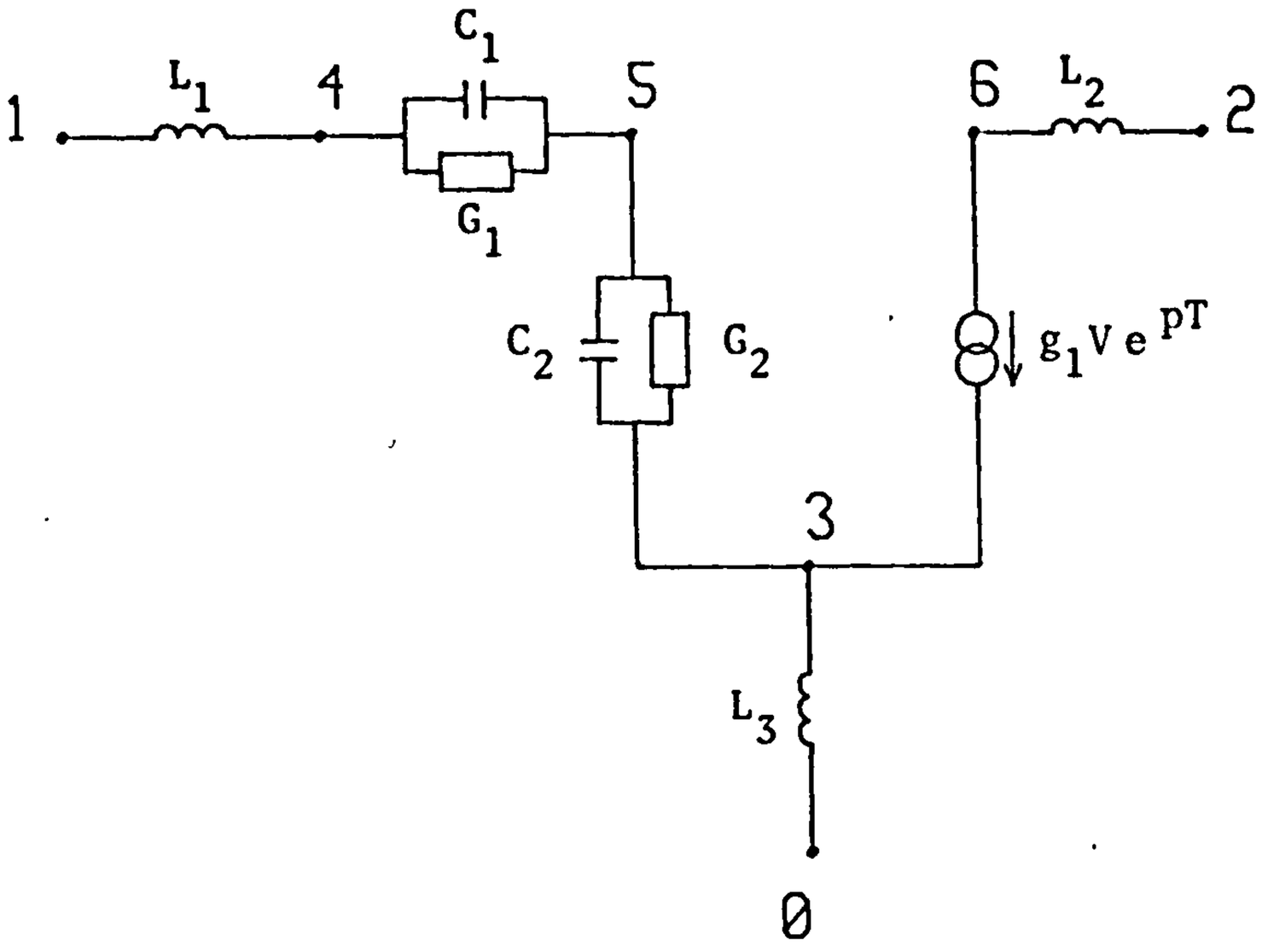

Node 1 - Input

Node 2 - Output

Node 0 - Ground

L_1 = L (1-4) = 4.15E+00 nH

L_2 = L (2-6) = 2.38E+01 nH

L_3 = L (3-0) = 5.71E+00 nH

C_1 = C (4-5) = 3.16E-02 nF

C_2 = C (5-3) = 8.89E-02 nF

G_1 = G (4-5) = 2.85E-02 S

G_2 = G (5-3) = 5.96E-03 S

g_1 = g (6-3) = 6.84E-01 S

T = 0 , -0.01 ns , +0.01 ns

V across nodes $\begin{matrix}5\\3\end{matrix}$

p = $j2\pi f$

f = 0.5 MHz , 10 MHz , 100 MHz

Figure 3.3 Circuit for Testing Analysis Methods

values of the y parameters as possible. The definite nodal admittance matrix of this circuit, using $\omega = 2\pi f$, is given in equation (3.14).

$$\begin{bmatrix}
\frac{1}{j\omega L_1} & 0 & 0 & -\frac{1}{j\omega L_1} & 0 & 0 \\
0 & \frac{1}{j\omega L_2} & 0 & 0 & 0 & -\frac{1}{j\omega L_2} \\
0 & 0 & \frac{1}{j\omega L_3}+G_2+j\omega C_2+g_1 e^{j\omega\tau} & 0 & -(G_2+j\omega C_2+g_1 e^{j\omega\tau}) & 0 \\
-\frac{1}{j\omega L_1} & 0 & 0 & \frac{1}{j\omega L_1}+G_1+j\omega C_1 & -G_1-j\omega C_1 & 0 \\
0 & 0 & -G_2-j\omega C_2 & -G_1-j\omega C_1 & j\omega(C_1+C_2)+G_1G_2 & 0 \\
0 & -\frac{1}{j\omega L_2} & -g_1 e^{j\omega\tau} & 0 & g_1 e^{j\omega\tau} & \frac{1}{j\omega L_2}
\end{bmatrix} \qquad (3.14)$$

Using the notation of Section 3.1.2 and cancelling terms where appropriate we get

$$\Delta_{11} = 0$$

$$\Delta_{12} = \frac{C_1 R}{\omega^2 L_1 L_2 L_3} + \frac{G_1 I}{\omega^3 L_1 L_2 L_3} + j\left\{ -\frac{G_1 R}{\omega^3 L_1 L_2 L_3} + \frac{C_1 I}{\omega^2 L_1 L_2 L_3} \right\}$$

$$\Delta_{21} = 0$$

$$\Delta_{22} = -\frac{(G_1 C_2 + G_2 C_1)}{\omega^2 L_1 L_2 L_3} - j\left\{ \frac{C_1 C_2}{\omega\, L_1 L_2 L_3} - \frac{G_1 G_2}{\omega^3 L_1 L_2 L_3} \right\} \qquad (3.15)$$

$$\Delta_{11,22} = -\frac{L_3 G_1 (G_2 + R) + C_1 + C_2 + G_1 G_2 L_1 - \omega^2 (L_1 + L_3) C_1 C_2}{\omega^2 L_1 L_2 L_3} + \frac{C_1 I}{\omega\, L_1 L_2}$$

$$+ j\left\{ \frac{(G_1+G_2)}{\omega^2 L_1 L_2} - \frac{(G_1 C_2 + C_1 (G_2+R)) + \frac{(C_2 G_1 + C_1 G_2)}{L_3}}{\omega\, L_2} - \frac{G_1 I}{\omega^2 L_1 L_2} \right\}$$

where R = Real part of $g_1 e^{j\omega\tau}$

I = Imaginary part of $g_1 e^{j\omega\tau}$

$\omega = 2\pi f$

and f = frequency.

Thus the y parameters of this circuit are given by

$$y_{11} = \frac{\Delta_{22}}{\Delta_{1122}}$$

$$y_{12} = -\frac{\Delta_{21}}{\Delta_{1122}} = 0 \qquad (3.16)$$

$$y_{21} = -\frac{\Delta_{12}}{\Delta_{1122}}$$

$$y_{22} = \frac{\Delta_{11}}{\Delta_{1122}} = 0$$

The values of y_{11} and y_{21} were evaluated from these expressions using double precision accuracy on the Cyber 73 at the required values of f and τ. The results to 14 significant figures are given in Table 3.1. Comparisons were then made between the values obtained using the variations on the two methods of analysis described. The number of significant figures that corresponded with those in Table 3.1 are given in Table 3.2. Starting with a value of $\tau = 0$ only, the methods compared were:

P - di Mambro's method

P9 - as in P but with factors of 10^9 and 10^{-9} applied to frequencies, reactive component values and time constants as appropriate

M - pivotal condensation using double precision arithmetic

M9 - as in M but with factors applied as in P9

M9S - as in M9 but using single precision arithmetic.

τ ns	Frequency MHz	y_{11} (x 10^{+3})	y_{21} (x 10^{+1})
0	0.5	4.9283017247867 + j 0.14328266924797	5.6561340451695 - j 0.10073439776783
	10.0	5.7866154724525 + j 0.25448883448201	4.9938834648201 - j 1.7618422669097
	100.0	13.014283365634 + j 4.4134390099870	0.70223789723946 -j 1.5185771544468
- 0.01	0.5	4.9283001544095 + j 0.14328265159357	5.6561290769242 - j 0.10091202616116
	10,0	5.7858636997144 + j 2.5448319403397	4,9922841139509 - j 1.7645829386237
	100.0	12.978650202236 + j 4.4509017282193	0.69678813251413 -j 1.5181879061931
+ 0.01	0.5	4.9283032951644 + j 0.14328268695170	5.6561390078396 - j 0.10055676910543
	10.0	5.7873673832388 + j 2.5449451747643	4.9954816704218 - j 1.7591001008490
	100.0	13.050008474251 + j 4.3758376821048	0.70770470993690 -j 1.5189706828740

Table 3.1 Values of y parameters to 14 significant figures

τ ns	Method	0.5 MHz				10 MHz				100 MHz			
		y_{11}		y_{21}		y_{11}		y_{21}		y_{11}		y_{21}	
		R	I	R	I	R	I	R	I	R	I	R	I
0	P9	13	14	13	14	14	14	14	14	14	14	14	14
	M	14	11	14	14	14	12	14	14	14	14	13	14
	M9	14	11	14	14	14	12	14	14	14	14	14	14
	M9S	13	9	13	14	13	11	13	14	14	13	13	14
- 0.01	P9	13	10	9	10	8	7	7	7	6	4	5	5
	M9	14	10	14	14	14	11	14	14	14	13	14	14
+ 0.01	P9	13	10	9	10	8	7	7	7	5	4	5	5
	M9	14	11	14	14	14	11	14	14	14	13	14	14

Table 3.2 Number of Correct Significant Figures in Computed Values

The results using method P are not shown in Table 3.2 because the errors were so large that none of the values corresponded even to one significant figure and many values were an order of magnitude in error.

As can be seen from Table 3.2, with $\tau = 0$ method P9 was the most accurate closely followed by methods M9 and M. Whilst the 10^9 factors had a major effect on method P, there was only a very slight improvement when they were applied to method M. However, the differences between the single and double length arithmetic versions of methods M9 and M9S were more marked although M9S might still be considered accurate enough for most purposes.

Taking the two most accurate methods, P9 and M9, for further comparisons with time constants τ of -0.01 ns and +0.01 ns, it can be seen from Table 3.2 that at 0.5 MHz method P9 has lost some accuracy and that, as might be expected, this loss of accuracy rises as the frequency increases so that by a frequency of 100 MHz the results are becoming unacceptable. Meanwhile, method M9 has suffered negligible loss of accuracy and is unaffected by the magnitude of the frequency. Thus, although method P9

is slightly more accurate when no time constants are applied to any current generators, method M9 is significantly superior when time constants are applied.

In all cases the computed values for y_{12} and y_{22} had absolute errors of less than 10^{-20}.

3.1.5. Further Considerations on the Choice of Algorithm

In addition to the accuracy of calculations, when choosing a computer algorithm, consideration should also be given to the speed of calculation and the storage space required by the algorithm.

For the given analyses, method M9 took 90% of the computation time taken by method P9, while M9S took 50% of the time taken by M9.

The storage space required by M9 was 70% of that required by P9, while M9S required 80% of that required by M9.

Thus, method M9, in addition to being more suitable from accuracy considerations, was also better than P9 in terms of speed and storage space. If the accuracy of method M9S is considered sufficient then the obvious savings in calculation time and storage space make it the best choice. Taking a cautious approach the author elected to use method M9.

3.2. S Parameters

In Section 3.1 it was described how the y parameters of a two-port network could be measured by short-circuiting the input and output ports in turn and measuring the appropriate admittances. However, at frequencies above 100 MHz it becomes increasingly difficult to measure the y parameters because of the difficulty in obtaining good short circuits and because short circuits often cause oscillation.

The s, or scattering, parameters are similar to the y parameters in

that they describe the inputs and outputs of a two-port black box, but have the advantage that they are easily measured up to the GHz frequency range. Weinert[47] describes how the s parameters are defined in terms of the incident and reflected parameters (a_1, b_1) and (a_2, b_2) which are shown in Figure 3.4 and are defined in equations (3.17).

$$
\begin{aligned}
a_1 &= \frac{1}{2}\left(\frac{V_1}{\sqrt{Z_o}} + \sqrt{Z_o}\, I_1\right) \\
b_1 &= \frac{1}{2}\left(\frac{V_1}{\sqrt{Z_o}} - \sqrt{Z_o}\, I_1\right) \\
a_2 &= \frac{1}{2}\left(\frac{V_2}{\sqrt{Z_o}} + \sqrt{Z_o}\, I_2\right) \\
b_2 &= \frac{1}{2}\left(\frac{V_2}{\sqrt{Z_o}} - \sqrt{Z_o}\, I_2\right)
\end{aligned}
\qquad (3.17)
$$

The s parameters are then given by

$$
\begin{aligned}
b_1 &= s_{11}a_1 + s_{12}a_2 \\
b_2 &= s_{21}a_1 + s_{22}a_2 \quad .
\end{aligned}
\qquad (3.18)
$$

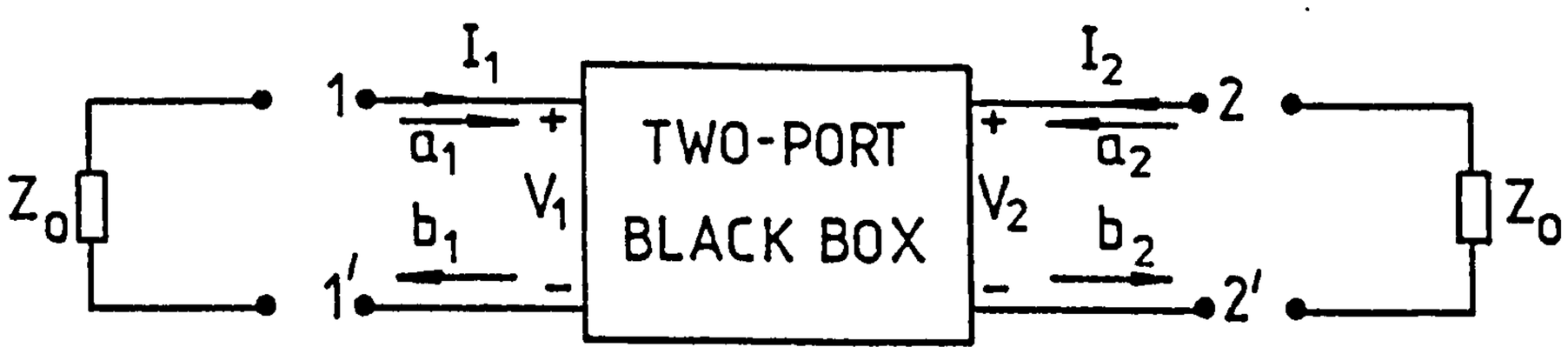

Fig.3.4 Incident and Reflected Parameters Used to Define the s Parameters

3.2.1. Measurement of the s Parameters

Just as the y parameters can be defined and measured by short-circuiting the input or output port and taking the appropriate admittance measurement, so the s parameters may be defined and measured by setting the incident parameters a_1 or a_2 to zero and taking the appropriate ratio. Therefore we can express the S parameters as:

$$
\begin{aligned}
s_{11} &= \frac{b_1}{a_1} \quad \text{when} \quad a_2 = 0 \\
s_{12} &= \frac{b_1}{a_2} \quad \text{when} \quad a_1 = 0 \\
s_{21} &= \frac{b_2}{a_1} \quad \text{when} \quad a_2 = 0 \\
s_{22} &= \frac{b_2}{a_2} \quad \text{when} \quad a_1 = 0
\end{aligned}
\tag{3.19}
$$

The s parameters can therefore be expressed as ratios of the reflected and incident voltages at the input and output ports when one port is matched.

In the introduction of reference (48) it is explained how the matching of the input or output port necessary to set a_1 or a_2 respectively to zero may be achieved by using 50Ω transmission lines to connect the device under test and then terminating the transmission line in its characteristic impedance, Z_o in Figure 3.4. A measurement jig is described by Hewlett Packard[49], incorporating the 50Ω transmission lines and 50Ω loads in such a way that the device under test is easily reversed thereby enabling the measurement of the reverse parameters s_{22} and s_{12} in the same set-up as the forward parameters s_{11} and s_{21}. The jig is used in conjunction with a Hewlett Packard 8405A vector voltmeter which is used to measure the required voltages and phase angles.

Thus the s parameters may be easily measured over a range of frequencies for any particular device.

3.2.2. Calculation of the s Parameters

The s parameters of a model may be obtained by first calculating the y parameters of the model using one of the methods described earlier in this chapter and then applying the conversion formulae given in reference (49) and reproduced as equations (3.20) below.

$$
\begin{aligned}
s_{11} &= \frac{(1 - y_{11})(1 + y_{22}) + y_{12}y_{21}}{d_y} \\
s_{12} &= -\frac{2y_{12}}{d_y} \\
s_{21} &= -\frac{2y_{21}}{d_y} \\
s_{22} &= \frac{(1 + y_{11})(1 - y_{22}) + y_{12}y_{21}}{d_y}
\end{aligned}
\qquad (3.20)
$$

where $d_y = (1 + y_{11})(1 + y_{22}) - y_{12}y_{21}$

For conversion from the s parameters to the y parameters equations (3.21) may be used.

$$
\begin{aligned}
y_{11} &= \frac{(1 - s_{11})(1 + s_{22}) + s_{12}s_{21}}{d_s} \\
y_{12} &= -\frac{2s_{12}}{d_s} \\
y_{21} &= -\frac{2s_{21}}{d_s} \\
y_{22} &= \frac{(1 + s_{11})(1 - s_{22}) + s_{12}s_{21}}{d_s}
\end{aligned}
\qquad (3.21)
$$

where $d_s = (1 + s_{11})(1 + s_{22}) - s_{12}s_{21}$

The y parameters given in equations (3.20) and (3.21) are all normalised to Z_o, therefore if y'_{ij} is one of the actual parameters, conversion is performed using

$$y'_{ij} = \frac{y_{ij}}{Z_o}, \quad i = 1,2; \; j = 1,2. \qquad (3.22)$$

CHAPTER 4

NUMERICAL OPTIMISATION

Numerical optimisation is a widely studied subject area with a vast range of applications, not just in electronics modelling but encompassing modelling, design and manufacturing problems in many disciplines. At its most basic, optimisation can be described as a means by which the best value of some variable may be obtained. The definition of 'best' depends on the application but usually some error function is defined which indicates the difference between the ideal value of a parameter which is dependent on one or more variables and the value of that parameter currently available. The optimisation problem thus becomes one of minimising the error function. In most problems there are a number of criteria, therefore the sum of squares function

$$F(\underline{x}) = \sum_{i=1}^{m} (f_i(\underline{x}))^2 \qquad (4.1)$$

where $f_i(\underline{x})$, i = 1,m, are the individual error functions dependent on a vector of variables $\underline{x}$, is often used as a single overall error indicator. The sum of squares function is also useful in the solution of nonlinear simultaneous equations. If the equations are

$$f_i(\underline{x}) = 0 \ , \ i = 1,m \qquad (4.2)$$

then it can be seen that a zero minimum of the sum of squares function would give a solution of the equations.

There are numerous other formulations that are suitable for an overall error function. Another popular one is the minimax function which takes the value

$$F(\underline{x}) = \max|f_i(\underline{x})| \quad , \quad i = 1,m \qquad (4.3)$$

where $f_i(\underline{x})$, i = 1,m are individual error functions. The general term for the single function to be minimised is the objective function.

The optimum value of all sum of squares problems as defined in equation (4.1) is when $F(\underline{x}) = 0$, although a zero minimum may not necessarily exist. If any set of values of $\underline{x}$ is found such that $F(\underline{x}) = 0$ then a global minimum has been found since $F(\underline{x})$ cannot be negative for real values of the individual error functions $f_i(\underline{x})$. However, whether or not a zero minimum of $F(\underline{x})$ exists, the global minimum is defined to be at the vector of values $\underline{x}^*$ where

$$F(\underline{x}^*) \leq F(\underline{x}) \tag{4.4}$$

for all other values of $\underline{x}$.

In any particular region R there might be a non-zero minimum at $\underline{x}'$ where

$$F(\underline{x}') \leq F(\underline{x})$$

for all values of $\underline{x}$ within R but where

$$F(x^*) < F(x') \quad . \tag{4.5}$$

The vector $\underline{x}'$ in this case is termed a local minimum.

Global optimisation is a very difficult and time consuming operation, not least because of the uncertainty of knowing whether the lowest minimum found so far is the lowest minimum overall. Dixon, Gomulka and Szegö[50] in their survey of global optimisation methods observe that the situation with regard to solving global optimisation problems is very poor. The most popular methods are random methods, including multistart methods where local minimisation is performed many times from different randomly-selected starting points, and those based on Branin's trajectory method, reviewed by Dixon et al.[50]. At Leicester University, Price[51,52] has worked on global optimisation techniques with some success.

The distinction should also be made between constrained and unconstrained optimisation. Unconstrained optimisation is when the solution values may occur at any values between $-\infty$ and $+\infty$. In many real optimisation problems, however, there are restrictions on the acceptable solution

values and so constraints must be imposed. In practice many constrained optimisation problems can be treated as unconstrained by the application of transformations to the variables such as those described by Box[53]. One of the simplest transformations, which is used in the author's work as described later, is to work in the domain of the logarithms of the variables, thus constraining the variables to take positive values only. Also, Lootsma[54] has reviewed a number of methods whereby more complex constraints can be imposed by suitable definition of the objective function to which unconstrained optimisation methods may then be applied.

It can be seen, therefore, that most design problems are in fact constrained local minimisation problems.

In the case of the modelling of a bipolar transistor in terms of the standard elements of resistance, capacitance and inductance together with voltage controlled current sources, the global minimum could be likened to the approximation to $\cos x$ by the series

$$\cos x = 1 - \frac{x^2}{2!} + \frac{x^4}{4!} - \frac{x^6}{6!} + \ldots \quad (x < \infty) \quad . \tag{4.6}$$

A reasonable approximation to $\cos x$ requires at least the first n terms of the series, where n is given by

$$x^m < m! \tag{4.7}$$

where $m = 2(n - 1)$.

Thereafter each further term improves the accuracy of the approximation but it could be argued that only an infinite number of terms will give the true value.

Similarly, in a model of a bipolar transistor, some elements, for example a voltage controlled current source, are necessary to obtain any reasonable model whilst the inclusion of other elements is desirable in order to obtain higher accuracy, but it would require an infinite number of elements to get a true match. Therefore, in this context a good model should contain

only those elements that have a major effect, together with those that make a significant contribution to the accuracy of the model. Thus, if a model is built up element by element, as each new significant element is added to the model a new local minimum is found.

The modelling strategy developed by the author is dealt with in Chapter 5. The remainder of this chapter is concerned firstly with optimisation methods that have been used in similar applications to those of the author and secondly with the optimisation method actually used by the author.

4.1. Available Methods

Numerical methods of optimisation can be divided into three main categories.

(i) Methods using function values only.

(ii) Methods using derivatives.

(iii) Methods designed for minimising sum of squares functions.

Brief details of some of the algorithms in each category follow, together with an indication of applications where they have been found useful.

4.1.1. Algorithms Using Function Values Only

In this first category are random and pattern searches. Random methods were discussed briefly at the beginning of this chapter. Pattern searches are more systematic. A simple pattern search was used by Knudsen[55] to determine model parameters for MOS transistor models. The attractions of this method are its simplicity and its suitability for small computers. The disadvantage, as noted by Knudsen, is its tendency to get trapped in narrow, curved valleys in the function. The simplex method of Nelder and Mead[56], also studied by Price[57] assisted by the author[58], forms a regular polyhedron (or simplex) in n-dimensional space. On examination of the

function values at the vertices of the simplex, it is then expanded, contracted or reflected about a vertex, the process being repeated until a suitable minimum is located. A simplex algorithm was used by Mathews and Ajose[2] to obtain optimum values of elements in particular models of microwave FETs and bipolar transistors by matching S parameter data of the devices. Durbin, Montaron and Heydemann[59] used a combination of simple pattern and random searches together with a simplex algorithm in the d.c. optimisation of electrical circuits, although they noted that their method was limited due to the large computing time required. The global search algorithm of Price[51,52] combines a random search with a simplex technique by initially evaluating the objective function at N random points thereafter selecting each new point to be evaluated using a randomly selected simplex of points from the N best points currently available. This algorithm was used by the author[60] to obtain suitable starting values for a trial model of a p-n-p transistor as described in the next chapter.

4.1.2. Algorithms Using Derivatives

The classic optimisation methods are those of steepest descent and Newton Raphson which use first and second derivatives respectively.

In the method of steepest descent, the gradient vector $\underline{g}$ of the objective function is used as a search direction, hence from any position given by the vector $\underline{x}^k$ with associated gradient vector $\underline{g}^k$, an improved position $\underline{x}^{k+1}$ should be obtained, using k to indicate the iteration, by

$$\underline{x}^{k+1} = \underline{x}^k - \lambda^k \underline{g}^k \qquad (4.8)$$

where λ^k is chosen by linear search to minimise the objective function. It is generally agreed that this method has bad convergence properties, however, a variation on the method was used by Agnew[61] who, for the optimisation of filter circuits, used only active residuals at any particular stage to generate the smallest step length necessary to produce a specified

"reasonable" reduction in a minimax error function. Mention should also be made here of the gradient descent method of Cutteridge[62] (with later improvements by Henderson[10] and Dowson[9]), which included the Hessian matrix of second partial derivatives to generate a "curve of steepest descent", which was used at the initial stage in a two-part algorithm for the solution of, amongst other applications, a particularly difficult problem encountered in producing a d.c. Ebers Moll model of a bipolar transistor.

Algorithms using conjugate gradients are more popular and effective methods using first derivatives. The most well-known of these is by Fletcher and Reeves[63]. In this method, using the superscripts k to denote the iteration number and T to denote the transpose of a vector, the sequence of points in the iterative scheme is given by

$$\begin{aligned} \underline{x}^{k+1} &= \underline{x}^{k} - \lambda^{k}\underline{y}^{k+1} \\ \underline{y}^{k+1} &= \underline{g}^{k} - \beta^{k}\underline{y}^{k} \end{aligned} \tag{4.9}$$

where λ^{k} is the linear search parameter minimising the objective function

$\underline{g}^{k}$ is the gradient vector

$\underline{y}^{k}$ is the vector of conjugate directions

and β^{k} is given by

$$\beta^{k} = 0 \quad \text{for} \quad k = 0\,,\ (n+1)\,,\ 2(n+1)$$

$$\beta^{k} = \frac{\left(\underline{g}^{k}\right)^{T}\left(\underline{g}^{k}\right)}{\left(\underline{g}^{k-1}\right)^{T}\left(\underline{g}^{k-1}\right)} \quad \text{otherwise} \,. \tag{4.10}$$

On a quadratic function this method locates the minimum in at most n iterations, where n is the number of variables in $\underline{x}$. The method was used by both Krzeczkowski[6] and Savage[8] for the initial stages in the synthesis of lumped linear three-terminal networks.

The Newton Raphson method is based on the Taylor series expansion

$$F(\underline{x} + \underline{\delta}) = F(\underline{x}) + \underline{\delta}^{T}\,\underline{g} + \ldots \tag{4.11}$$

where $\underline{g}$ is the gradient vector of F.

Ignoring higher order terms, differentiating and equating the first derivatives to zero, i.e. the equation for a minimum of F, gives

$$0 = \underline{g} + H\underline{\delta} \tag{4.12}$$

where H is the Hessian matrix of second partial derivatives of F. It is usual, as with the steepest descent algorithm, to include a linear search along the direction given by $\underline{\delta}$, thus the Newton Raphson iteration becomes

$$\underline{x}^{k+1} = \underline{x}^{k} - \lambda^{k}(H^{k})^{-1}\, g^{k} \tag{4.13}$$

where λ^{k} is chosen to minimise the objective function.

The Newton Raphson algorithm thus requires the evaluation of the Hessian matrix at each iteration. Variable metric algorithms are a class of algorithms which attempt to approximate equation (4.13) using the first derivatives only. Among these algorithms are those of Davidon[64] and the later, very successful algorithm by Fletcher and Powell[65]. Variable metric algorithms may be classified as quasi-Newton if they satisfy the criteria that S°, the initial approximation to the inverse Hessian matrix, is positive definite and that

$$S^{k+1}\, \underline{\delta}^{k} = \underline{h}^{k} \tag{4.14}$$

where $\underline{\delta}^{k} = \underline{x}^{k+1} - \underline{x}^{k}$

$$\underline{h}^{k} = \underline{g}^{k+1} - \underline{g}^{k} \quad ,$$

thus giving the Newton Raphson iteration for a quadratic function.

A variable metric algorithm was used by Lanca and Nichols[66] for the design of networks to time-domain specifications and the method of Fletcher and Powell was used by Orlik[35] to obtain some of the element values in Gummel Poon models of integrated circuit transistors.

4.1.3. Algorithms Designed for Minimising Sum of Squares Functions

When minimising sum of squares functions

$$F(\underline{x}) = \sum_{i=1}^{m} \left(f_i(\underline{x})\right)^2 \qquad (4.15)$$

where $f_i(\underline{x}), i = 1,m$, are the component functions dependent on the vector of n variables $\underline{x}$, then, in addition to the values of the objective function and its derivatives, there are also available the values of the component functions and their derivatives.

If we say that we are attempting to obtain

$$f_i(\underline{x}) = 0 \ , \ i = 1,m \qquad (4.16)$$

then taking the Taylor series expansion of each component function gives

$$f_i\ (\underline{x} + \underline{\delta}) = f_i(\underline{x}) + \sum_{j=1}^{n} \frac{\partial f_i(\underline{x})}{\partial x_j} \delta_j + \ldots, \ i = 1,m \qquad (4.17)$$

which, ignoring higher order terms, gives

$$\underline{f}(\underline{x} + \underline{\delta}) = \underline{f}(\underline{x}) + J\underline{\delta} \qquad (4.18)$$

where J is the Jacobian matrix of first derivatives.

Equating this to zero as required from equation (4.16) we get

$$0 = \underline{f}(\underline{x}) + J\underline{\delta} \ . \qquad (4.19)$$

If $m = n$ and J is non-singular then

$$\underline{\delta} = - J^{-1}\ \underline{f}(\underline{x}) \ . \qquad (4.20)$$

If $m > n$ then we can use

$$\underline{\delta} = - (J^T J)^{-1}\ J^T \underline{f}(\underline{x}) \ . \qquad (4.21)$$

Dimmer[11] describes how equation (4.21) is derived by finding the least squares solution of equation (4.19).

Thus, introducing a linear search parameter λ we get the Gauss Newton iteration

$$\underline{x}^{k+1} = \underline{x}^{k} - \lambda^{k} ((J^{k})^{T} J^{k})^{-1} (J^{k})^{T} \underline{f}(\underline{x}^{k}) \quad . \qquad (4.22)$$

Dimmer[11] shows that provided a point at which $(J^{k})^{T} \underline{f}(\underline{x}^{k}) = \underline{0}$ has not been reached and $(J^{k})^{T} J^{k}$ is non-singular, then there will be a value of $\lambda > 0$ which will reduce the objective function. Dimmer also emphasises the differences between the Gauss Newton and Newton Raphson methods and notes a superiority of performance by the Gauss Newton method over the Newton Raphson method on sum of squares problems.

The Gauss Newton method has been used extensively at Leicester University on optimisation problems arising from the synthesis of electrical networks.

Most other methods designed for minimising sum of squares functions are based on the Gauss Newton method and are concerned either with avoiding singularity of the matrix to be inverted as with the Levenberg[67] Marquardt[68] method or with the use of approximations for the Jacobian matrix thus requiring the calculation of the component function values only as in the method by Broyden[69] .

4.2. Some Details of the Optimisation Algorithm Chosen

It can be seen from section 4.1 that just as no single model of the bipolar transistor has found universal favour, so no single optimisation algorithm has become the standard even for applications of a similar nature.

It was mentioned in section 4.1.1 that the author used the global search of Price to obtain the starting values for one of the trial problems; however it was the author's intention to, initially, use the two-part algorithm of Cutteridge and Henderson[62,10] for the major part of the model optimisation. At this early stage the reason for this choice was largely

because of familiarity with the algorithm together with first-hand observation of its efficacy.

The two parts of this algorithm consisted of a gradient descent section, mentioned in section 4.1.2, and a modified Gauss Newton section. The author soon discovered that the gradient descent section was not in fact needed in her particular application since the Gauss Newton section proved quite adequate for the optimisation involved. Furthermore, benefits of this second section from the modelling point of view also became apparent. Therefore, this Gauss Newton algorithm was the major optimisation method used by the author and included several modifications due to Henderson[10].

One of the modifications was to limit the change in any value x_i in one iteration to some predetermined limit. This was achieved in the linear search used to choose the value of λ^k. The linear search included a preliminary search using trial values of λ^k calculated from the Fibonacci series λ_o^k, $2\lambda_o^k$, $3\lambda_o^k$, $5\lambda_o^k$ ... where λ_o^k was a given starting value. The aim of this preliminary search was to attempt to bracket a minimum. Should this not be achieved, the preliminary search continued until the preset maximum change in value was reached in each variable.

If a bracket was obtained in the preliminary search then the minimum was located more accurately using a quadratic interpolation algorithm which was safeguarded against the occurrence of non-unimodal functions and against slowness of convergence onto the minimum through taking new points for evaluation too close to the current three points used in the quadratic interpolation.

Henderson also categorised the possible terminations of the algorithm. The first of these, which was not really relevant in the author's application, concerned conditions when it was not advisable to attempt using the algorithm. The second concerned successful termination which was based on the absolute values of the correction terms $\underline{\delta}$ calculated by Gauss Newton. The third category described criteria for failure due to the J^TJ matrix being or

almost being singular. The fourth and final category predicted ultimate failure of the algorithm. There were three criteria in this category: (i) if the number of iterations exceeded a certain number, (ii) if $\delta^k_{max} > 100\ \delta^o_{max}$, where $\delta^k_{max} = \max |\underline{\delta}|$ at iteration k, and (iii) if $\delta^k_{max} > \delta^{k-1}_{max}$ on 10 successive iterations with the increase $(\delta^k_{max} - \delta^{k-1}_{max})$ larger at each successive iteration, i.e. the rate of increase accelerating.

The author, like Dimmer[11], is of the opinion that termination prediction, especially of ultimate failure, is an important aspect of any optimisation algorithm. When the optimisation problem is one of developing models it is most important that unsuccessful models be detected and discarded as early as possible. We thus have a further justification for the author's use of this algorithm.

CHAPTER 5

DEVELOPMENT OF THE MODELLING ALGORITHM

Philips Research Laboratories (PRL) who provided data for the author specified certain conditions for their models. One of these was that the s parameters be fitted directly. The reasons given for this request were that (i) these were the quantities actually measured, and (ii) operation on the equivalent sets of y parameters obtained applying the standard transformation formulae would alter the weightings of the fit. PRL also provided models which they thought would provide a suitable starting point for a model optimisation exercise.

Thus, this chapter first describes how the component parts of the three previous chapters were combined together to form a single method designed, initially, to calculate the optimum element values for any particular model to fit the s parameter measurements of any particular device subject to the conditions set by PRL. Details are then given of the possible ways in which models may be improved and of the methods chosen by the author.

At each stage examples are given of the results obtained for the first model developed for PRL, that of a lateral p-n-p transistor. The results of this exercise were published jointly by Cutteridge and Dowson[60]. It should be noted that although the major criteria for the final modelling algorithm were developed during this first exercise, the process of refining and confirming the techniques continued throughout the period of research and some suggestions for further improvements are included in Chapter 8.

5.1. Details of the First Modelling Exercise

The first set of data provided by PRL was for a lateral p-n-p transistor connected in common emitter configuration and consisted of the set of s parameter measurements given in Table 5.1. The data in its original form is included in Appendix 1.

Z_o = 50ohm	S_{11}		S_{12}		S_{21}		S_{22}	
Frequency MHz	Modulus dB	Phase degrees	Modulus dB	Phase degrees	Modulus dB	Phase degrees	Modulus dB	Phase degrees
0.5	-0.10	-1.40	---*	---*	-12,50	178.10	0,00	-0.20
2.0	-0.20	-5,40	-64.70	88.70	-12.50	169.90	0.00	-0.30
5.0	-0.40	-11.20	-57.20	84.00	-12.80	155.00	0.00	-0.50
10.0	-1.20	-19.40	-52.00	76.30	-14.00	132.90	0.00	-0.90

* A measurement of s_{12} at 0.5 MHz was not available

Table 5.1 Measured s Parameters of a Lateral P-N-P Transistor

It can be seen that the measurements for each of the s parameters are in terms of modulus in dB and phase in degrees and are given at four frequencies in the range 0.5 MHz to 10 MHz except for s_{12} for which a measurement at 0.5 MHz was not available. The accuracies of these measurements were given as "about ± 0.5 dB" for the modulus and "phase angles near 0° are certain to ± 0.5°, and near 180° to about ± 2°".

In addition to these measurements, PRL provided a simple model which they suggested would be a good starting point for the derivation of a model. This model, which is shown in Figure 5.1, consisted of four nodes (including the node 0) and five elements of which two elements were voltage controlled current sources. It was suggested that these generators should take specific values with zero time constants. These values are given in the diagram. It was felt that this model was too basic and so a further three elements were added by the author. The global search technique of Price[51,52] was then used to minimise the single overall error function described in Section 5.2.1. in order to obtain suitable starting values for the unknown element values. This model, which is shown in Figure 5.2, was then used as the initial trial model for the lateral p-n-p transistor.

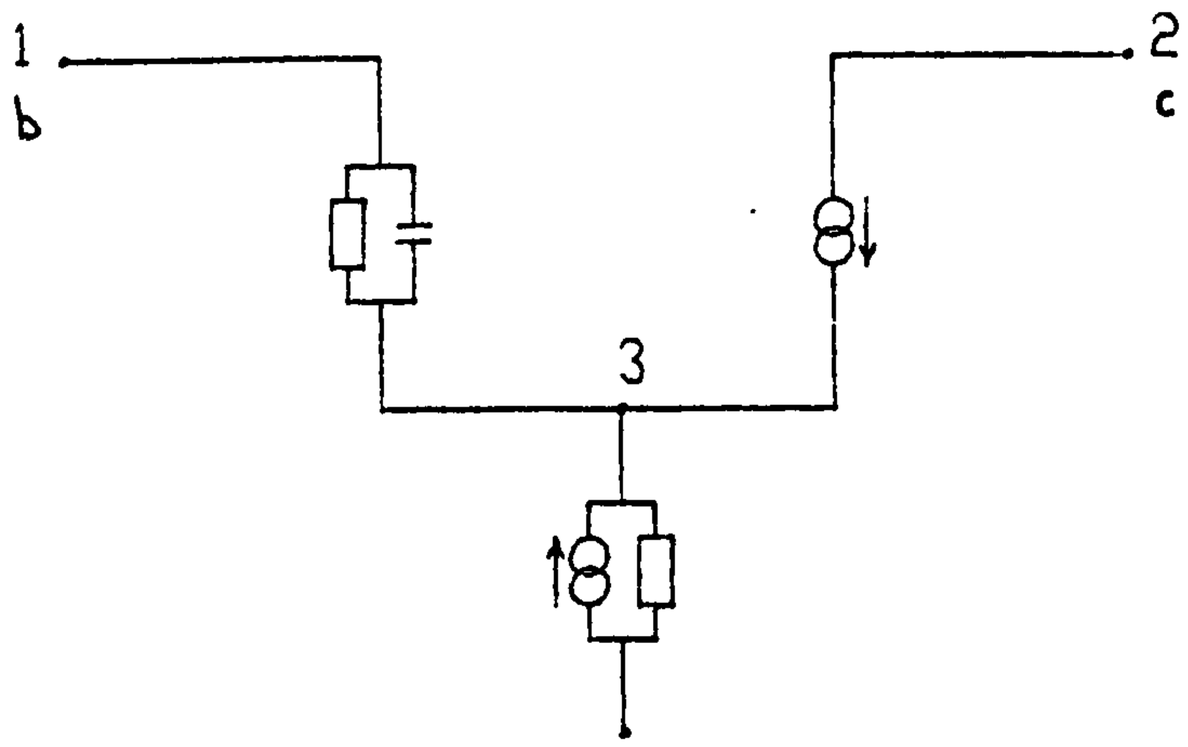

No. of nodes = 4
No. of elements = 5

g (2-3) = 3.53E-03 S
(T = 0)
(V across nodes $\frac{1}{3}$)
g (0-3) = 2.07E-05 S
(T = 0)
(V across nodes $\frac{1}{3}$)

Node 1 - Base
Node 2 - Collector
Node 0 - Substrate and Emitter

Figure 5.1 Simple Model of Lateral P-N-P Transistor

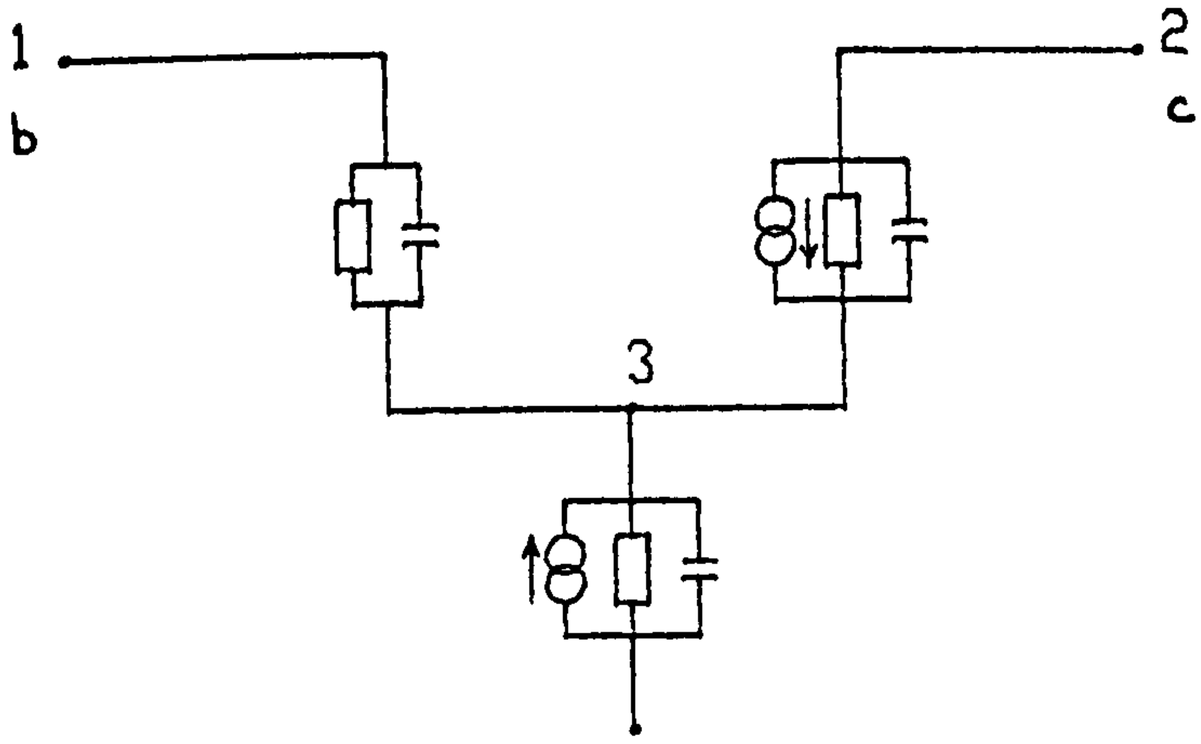

No. of nodes = 4
No. of elements = 8

g (2-3) = 3.53E-03 S
(T = 0)
(V across nodes $\frac{1}{3}$)
g (0-3) = 2.07E-05 S
(T = 0)
(V across nodes $\frac{1}{3}$)
G (1-3) = 6.12E-10 S
C (1-3) = 8.68E-02 nF
G (2-3) = 5.22E-05 S
C (2-3) = 5.06E-04 nF
G (0-3) = 6.77E-03 S
C (0-3) = 3.71E-06 nF

Node 1 - Base
Node 2 - Collector
Node 0 - Substrate and Emitter

Figure 5.2 Initial Model of Lateral P-N-P Transistor

5.2. Construction of an Algorithm to Optimise Model Element Values

Given a set of measured s parameters as shown in Table 5.1 and a trial model as shown in Figure 5.2, the first requirement by the optimisation algorithm was for an error function to be constructed to give an indication of how good the model was. Since the author had chosen the Gauss Newton algorithm described in Section 4.2, the first partial derivatives of the objective function were also required. The element values of the model were obviously the variables, but it was necessary to decide whether any constraints should be applied to these. Finally, it has already been stated that, in the author's view, an acceptable first stage model would be obtained when a local minimum had been found by the optimisation algorithm. Therefore, the exit criteria of the Gauss Newton algorithm are also discussed.

5.2.1. Construction of the Error Function

Techniques for the calculation of the s parameters of a model were discussed in Chapter 3. The method first used by the author, and used for the examples given in this chapter, was to calculate the y parameters using the method of diMambro described in Section 3.1.2. and to then use the conversion formulae given in Section 3.2.2. to obtain the s parameters. The calculation of the y parameters was later done by the method of pivotal condensation as described in Section 3.1.3, and all the examples in the following chapters used that method.

PRL had requested that the s parameters be fitted directly and it was decided that individual error functions should be calculated at each of the given frequency values for each of the s parameters. There was a choice of whether the individual error functions should be in terms of the real and imaginary parts of the s parameters or whether the modulus and phase should be matched. One advantage seen in favour of matching the former was that by weighting equally the errors in the real and imaginary

parts of the s parameters the problems of choosing the appropriate weights for errors in the modulus in decibels and in the phase in degrees could be avoided. However, it was felt that it would be preferable to consider the errors in terms of decibels and degrees and that by allowing the weightings on these to be stated individually for the different frequencies and for each of the s parameters it would give an engineer the opportunity to emphasise the most important region of operation of the model in question. The weightings chosen by the author, based on discussions with PRL, were such that an error of 1 dB in the modulus was equivalent to a 10° error in the phase. It was felt that absolute errors were more appropriate than relative errors, particularly in the case of the phase errors where the paradox exists that a small absolute error in a phase angle close to 0° gives a large relative error while a similar absolute error in a phase angle close to 360° gives a totally different relative error. A slightly different problem occurs for the modulus when it is stated in decibels. Since the decibel is basically a logarithmic unit, a large negative value means that there is negligible gain and many engineers would feel that an error of 1 dB in a modulus of -5 dB was less significant than an error of 1 dB in 5 dB . In view of the stated errors in the measurements by PRL, it was decided that the weighted absolute errors would be suitable for both types of individual error functions.

The overall error function to be minimised was then made up of the sum of the squares of the weighted individual errors in the modulus and phase of each of the s parameters at each of the frequencies for which measurements were given.

In the early stages, for ease of programming, values of -77.40 dB and 89.60° were given for the modulus and phase of s_{12} at 0.5 MHz , these values being chosen by eye from plots of s_{12} against frequency. Thus the initial problem was one of minimising a sum of squares function made up of 32 individual functions in 8 unknowns (the elements in Figure 5.2.).

5.2.2. Generation of the Jacobian Matrix

When analytic first derivatives are not available as was the case here, then numerical estimates of the Jacobian matrix can be used. The author first experimented using central differences so that to evaluate $\partial f_i(\underline{x})/\partial x_j$ a displacement vector $\delta\underline{x}$ is defined such that $\delta x_k = d.x_j, k=j$ and $\delta x_k = 0, k \neq j$, where d is some small value, then

$$\frac{\partial f_i(\underline{x})}{\partial x_j} \simeq \frac{f_i(\underline{x} + \partial\underline{x}) - f_i(\underline{x} - \partial\underline{x})}{2\,\delta x_j} \quad . \tag{5.1}$$

By progressively reducing the value of d and recalculating using equation (5.1), the accuracy of the value of $\partial f_i(\underline{x})/\partial x_j$ can be checked. To do this during an optimisation run produces prohibitive computing times. However, some results were obtained which proved that the value of δx_j recommended by Henderson[10] gave sufficient accuracy. This value was given by

$$2\,\delta x_j = 10^{-7}\ (1 + |x_j|) \ , \tag{5.2}$$

which was based on the reasoning of Gill and Murray[70], who suggest a fixed small value governed by the word length of the computer in use, assuming $|x_j|$ to be of the order unity, but which also allowed for the possibility of large values of $|x_j|$.

One further point raised by this choice is that the minimum value of $2.\delta x_j$ will be 10^{-7} . Since in many models of bipolar transistors there will be elements which have values smaller than this as seen in the example in Figure 5.2, this provides a further reason for the use of the factors applied to the element and frequency values described in Chapter 3.

The use of central differences requires two function evaluations for each element of the Jacobian matrix. The number of function evaluations can be reduced if forward differences are used since the current function values should already be available. Although the use of forward differences reduces the accuracy of the estimates of the Jacobian matrix, Brown and

Dennis[71] found them to be adequate in methods for sum of squares function minimisation.

5.2.3. Application of Constraints

Although it is not strictly necessary for model elements to only take physically feasible values, most engineers find models more acceptable if they can visualise the component elements. An interesting exception was one of the initial models provided by PRL, who were most insistent that model elements should have some physical significance, which included a negative-valued capacitor. It therefore seemed reasonable to the author that model elements of capacitance, resistance and inductance should be constrained to take positive values only.

With regard to voltage controlled current sources represented by $g\,Ve^{j\omega\tau}$ where V is the controlling voltage and τ is the time constant, then a negative value of g would merely indicate that the current was flowing in the opposite direction to that with a positive value. However, it could generally be assumed that the model is sufficiently correct that the value of g could be restricted to positive values only. The time constant τ would normally be expected to take a small negative value indicating a time delay. However it was found that there were many instances where a small positive value was the optimum value for a particular stage in the development of a model. The author decided to allow the time constant to take both negative and positive values since it could be that a positive value at any particular stage merely compensated for elements which were not yet present in the model. Certainly there were cases where a positive time constant at an early stage became negative as the model development progressed. So that the same constraints could be applied to all the variables, it was decided that the value to be optimised should be $(1 + \tau)$ns. Since the value of τ should never be more negative than -1 ns then $(1 + \tau)$ should always be positive.

Thus, since all the variables were constrained to take positive values only, a logarithmic transformation could be applied. Although other transformations, such as a square transformation, could be applied in this situation, the logarithmic transformation has been used with some success at Leicester University and Krzeczkowski[6] found that the natural scaling exhibited by the use of this transformation aided the convergence of his optimisation algorithms.

5.2.4. Exit Criteria

In Section 4.2 some details were given of the various termination modes of the Gauss Newton algorithm categorised by Henderson. Obviously the one aimed for was the successful termination characterised by all the individual corrections $\underline{\delta}$ to the element values becoming negligible. If this occurred then one could say that the elements were all necessary as part of the present model and that the optimum element values had been obtained for that particular model. The successful termination criterion was set at when $|\delta_i| < 10^{-8}$,i = 1,n , where $\underline{\delta}$ is the vector of corrections in the logarithmic domain.

If one of the failure termination modes occurred then it could be that the model was not suitable and that it should be modified. It would then become necessary to study the model, the element values and the reasons for failure of the optimisation algorithm in order to determine what action should be taken.

5.3. Example of Results

Applying the algorithm described in Section 5.2 to the model shown in Figure 5.2, the algorithm failed to converge. The reason for failure was that there were too many successive increases in the rate of increase of the maximum modulus correction. This failure mode, which we will refer to

as failure mode 1, was in fact the most common mode encountered in all the examples. At this stage, failure mode 1 had to occur on 10 successive iterations before the optimisation algorithm terminated and in this example the maximum modulus correction was being applied to element G_{1-3}, the conductor between nodes 1 and 3. At termination this element had reduced in value from 6.12×10^{-10} S to 9.91×10^{-11} S while the correction term in the logarithmic domain had changed from -8.01×10^{4} to -4.95×10^{5}. Meanwhile, all the other element values were virtually unchanged. Taking this progression to its limit, because of the logarithmic transformation this would make G_{1-3} zero, i.e. open-circuit. The author therefore removed that element from the model and restarted the optimisation algorithm. Again the algorithm failed in failure mode 1. This time the element causing the failure was C_{3-0} which was increasing in value. It was decided that this element should also be removed open-circuit. On restarting the algorithm, one of the current generators, both of which had been allowed to vary, caused a further failure mode 1. The value of g_{0-3} was tending to zero. As there were two generators in the model it was felt that removing one of them would not make the model invalid. However, there was still the question of whether the generator should be connected with the current flowing in the opposite direction. On attempting to optimise the element values with the generator reversed, its value still tended to zero, therefore it too was removed from the model. On applying the optimisation algorithm to this model, convergence was obtained.

The new model is shown in Figure 5.3. It can be seen that the optimised values of the remaining elements are quite similar to their original values, the largest change of about 20% being in C_{2-3}. At this stage the overall error function had been reduced from 384.2 to 114.9. The individual errors are shown later in Table 5.2 and it can be seen that the maximum absolute errors have been reduced from 0.55 dB to 0.43 dB in the modulus and from 11.02° to 6.52° in the phase.

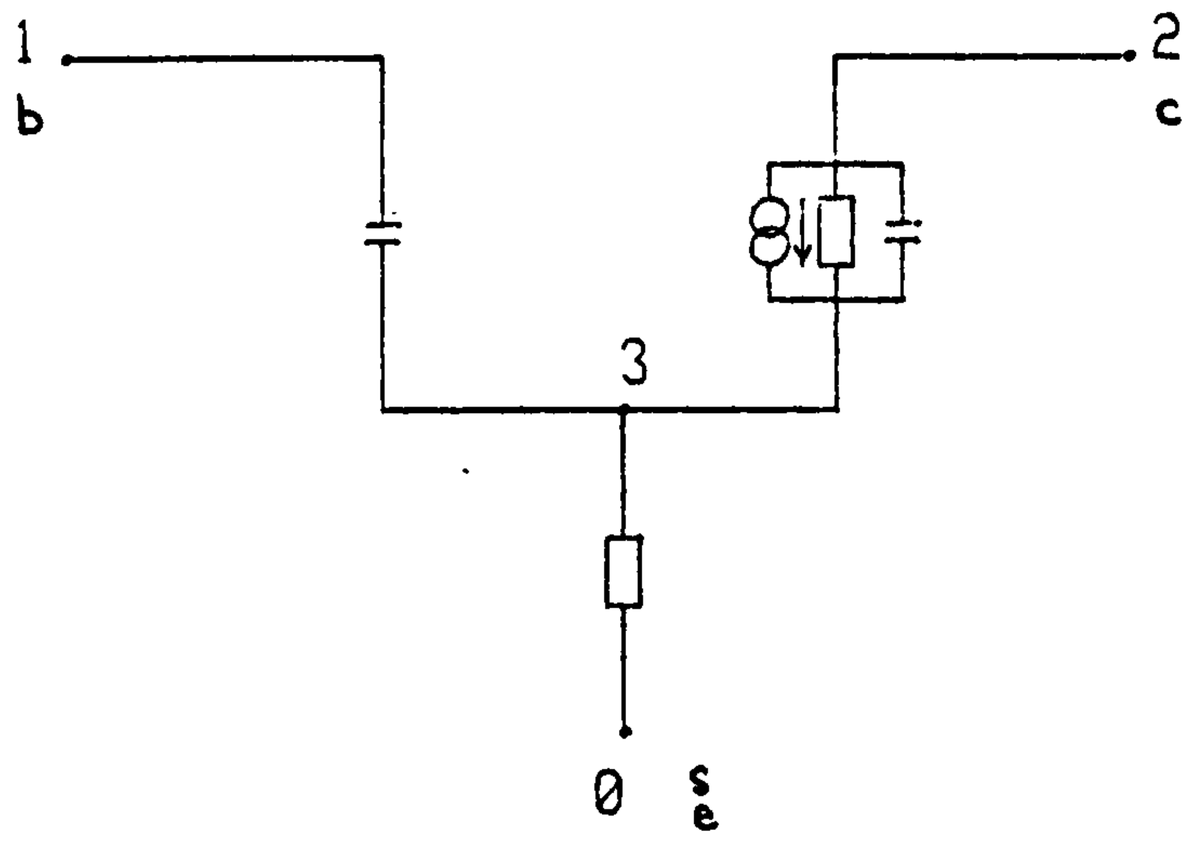

F = 1.15E+02

No. of nodes = 4
No. of elements = 5

g (2-3) = 3.94E-03 S
(T = 0)
(V across nodes $\frac{1}{3}$)
C (1-3) = 1.05E-01 nF
G (2-3) = 4.67E-05 S
C (2-3) = 3.90E-04 nF
G (0-3) = 6.63E-03 S

Node 1 - Base
Node 2 - Collector
Node 0 - Substrate and Emitter

Figure 5.3 First Model at a Local Minimum

The question of why a model containing fewer elements should be better than one with more elements could be asked. The author's explanation of this would be that firstly, a model containing more elements would only be better than one with fewer elements if the extra elements were of the right types and values and in the correct positions, and secondly, the original element values in this example had been optimised and two of the elements had optimum values of zero, while a third had an optimum value of infinity.

5.4. Improvement of Models

Having found a model which gave a minimum value of the objective function, it then became necessary to consider how the model could be improved. It would not be expected that the removal of any elements from a model giving a local minimum of the objective function would make an improvement, therefore the addition of elements must be the only course of

action. There are many strategies that could be employed for the addition of elements, some of these will be considered now.

If we assume that we want the model to be as simple as possible then we should avoid adding extra nodes. Therefore we should first of all concentrate on adding elements within the existing structure. Other restrictions might be that although we could attempt to replace any current generator that has been removed, we should not insert any additional generators, and that we should not insert inductors other than at the terminals since the most likely physical reason for the presence of inductance would be lead inductance.

It might be that the engineer would like there to be present only those elements for which some physical explanation for their presence could be given. Certainly, this is a popular strategy and one which Nabawi and Nicols[72] refer to as "intuitive modelling". However, it is possible that the engineer's preconceived concepts of a suitable topology for a model could preclude the development of another acceptable and more accurate model. This factor contributed to the failure by Hegazi[7] to discover the six node realisation to the set of equations by Lucal given in Chapter 3, which was later found by Savage[8].

For the first modelling exercise, the author used an intuitive approach and experimented by attempting to add one element at a time to the model at an arbitrary value based on the values of elements of the same type already present. Each attempt involved restarting the optimisation algorithm and checking the result. If the algorithm converged and the overall error function was reduced, then the new element was left in the model and another new element was tried. If the algorithm failed to converge it was generally because failure mode 1 occurred. Usually, this was caused by the corrections to the new element value. If this was the case or if one of the other failure modes occurred it was assumed that the new element would not make a suitable addition. There was one case, which can

be seen in the example in the next section, where failure mode 1 was caused by one of the existing elements in the model. In this case the new element was left in and the element causing the failure was removed and the optimisation algorithm then terminated successfully.

The entire sequence of successful additions to the first model are described in the next section.

5.5. Example of Results

After failing to replace singly each of the elements removed from the initial model, it was decided to attempt to add elements of conductance and capacitance between nodes 1 and 0 and nodes 2 and 0. These were all successful apart from the conductor between nodes 2 and 0. The order in which they were added is shown in Figure 5.4. It can be seen that the values of the existing elements changed by only a relatively small amount between each addition. The new elements of capacitance and conductance were inserted at values of 1pF and 10^{-4} S respectively prior to optimisation. These values too, were reasonably close to the optimum values calculated and the Gauss Newton algorithm took between 11 and 13 iterations to converge onto the local minima. The value of the overall error function F is given at each stage and it can be seen that it was reduced from 114.9 to 56.50 by the addition of these three new elements. It should be pointed out that the function being minimised at this stage included the individual errors calculated against the extrapolated values for S_{12} at 0.5 MHz. The function values quoted do not include these individual errors as the weightings were later adjusted to exclude them from the objective function.

Next, it was decided to attempt to insert inductors at each of the external nodes. The two successful attempts are shown in Figure 5.5. The first of these was originally inserted at a value of 4nH and was optimised

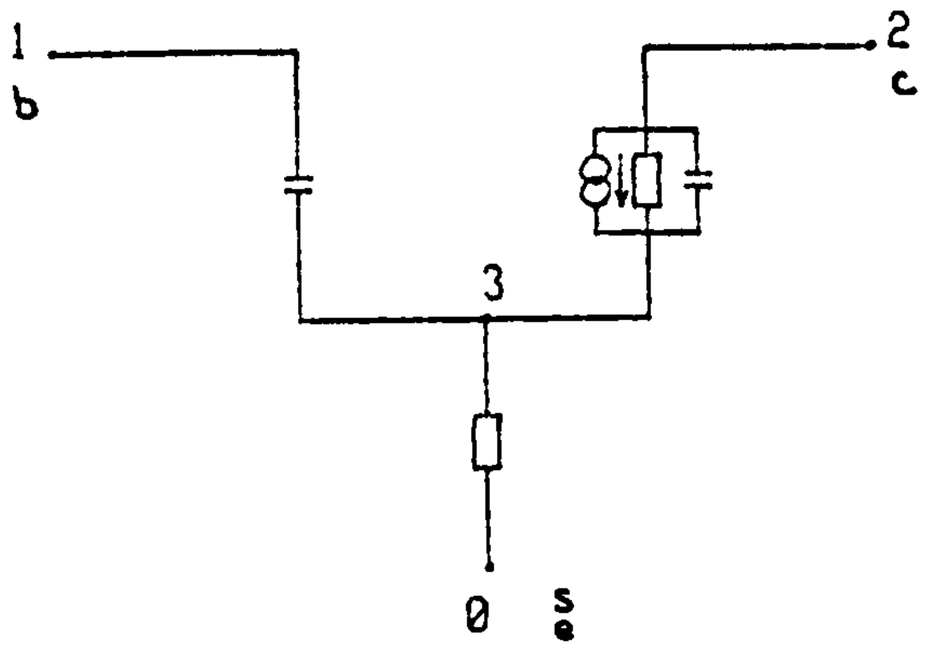

F = 1.15E+02

No. of nodes = 4
No. of elements = 5

g (2-3) = 3.94E-03 S
(T = 3)
(V across nodes 1 3)
C (1-3) = 1.05E-01 nF
G (2-3) = 4.67E-05 S
C (2-3) = 3.90E-04 nF
G (0-3) = 6.63E-03 S

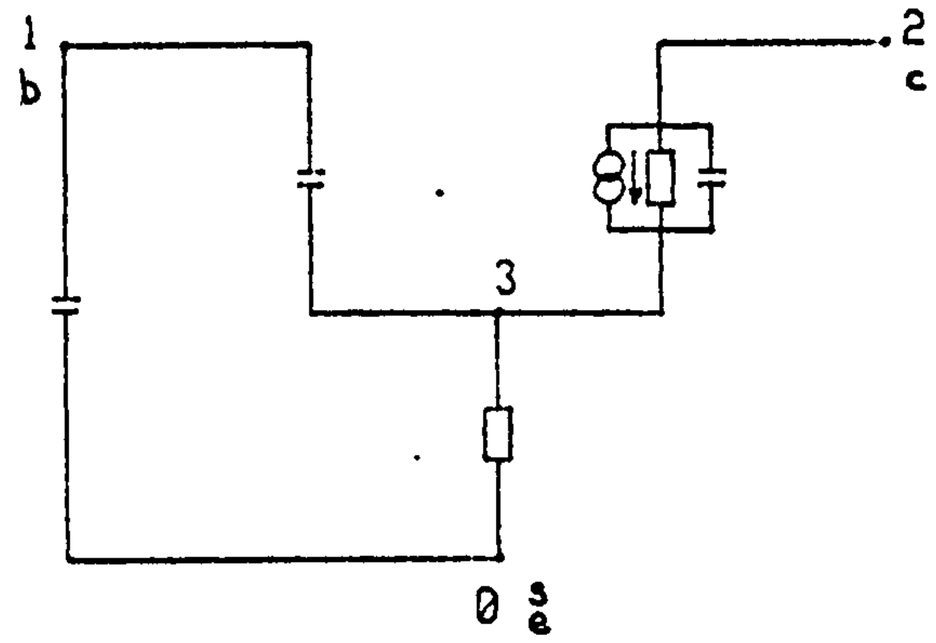

F = 6.68E+01

No. of nodes = 4
No. of elements = 6

g (2-3) = 6.35E-03 S
(T = 0)
(V across nodes 1 3)
C (1-3) = 1.09E-01 nF
G (2-3) = 4.50E-05 S
C (2-3) = 4.04E-04 nF
G (0-3) = 4.01E-03 S
C (1-0) = 2.75E-02 nF

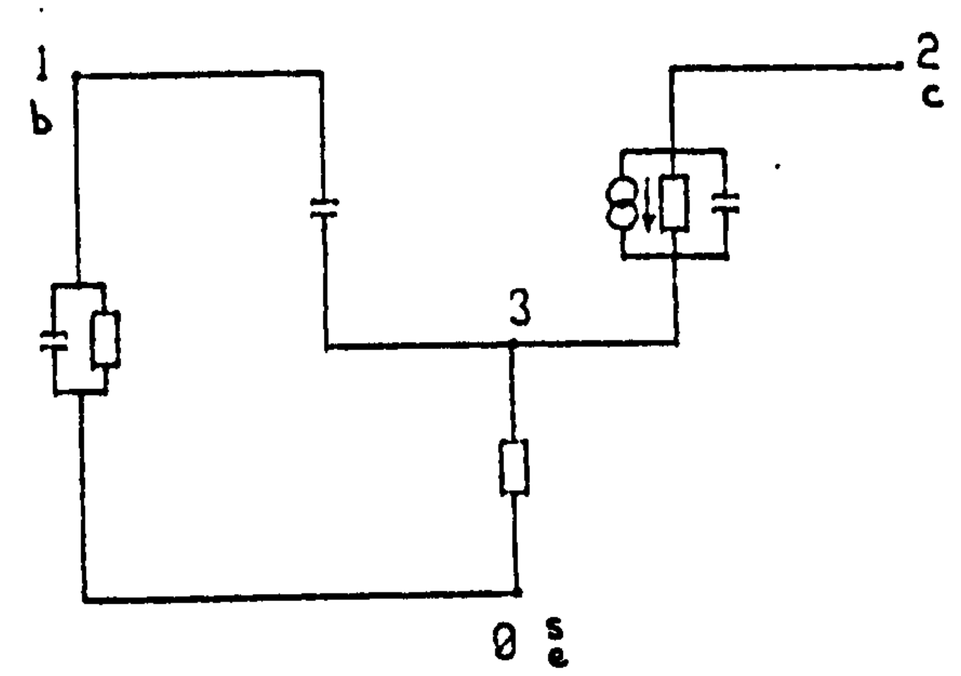

F = 5.96E+01

No. of nodes = 4
No. of elements = 7

g (2-3) = 1.06E-02 S
(T = 0)
(V across nodes 1 3)
C (1-3) = 1.47E-01 nF
G (2-3) = 4.28E-05 S
C (2-3) = 4.02E-04 nF
G (0-3) = 3.23E-03 S
C (1-0) = 3.30E-02 nF
G (1-0) = 2.11E-04 S

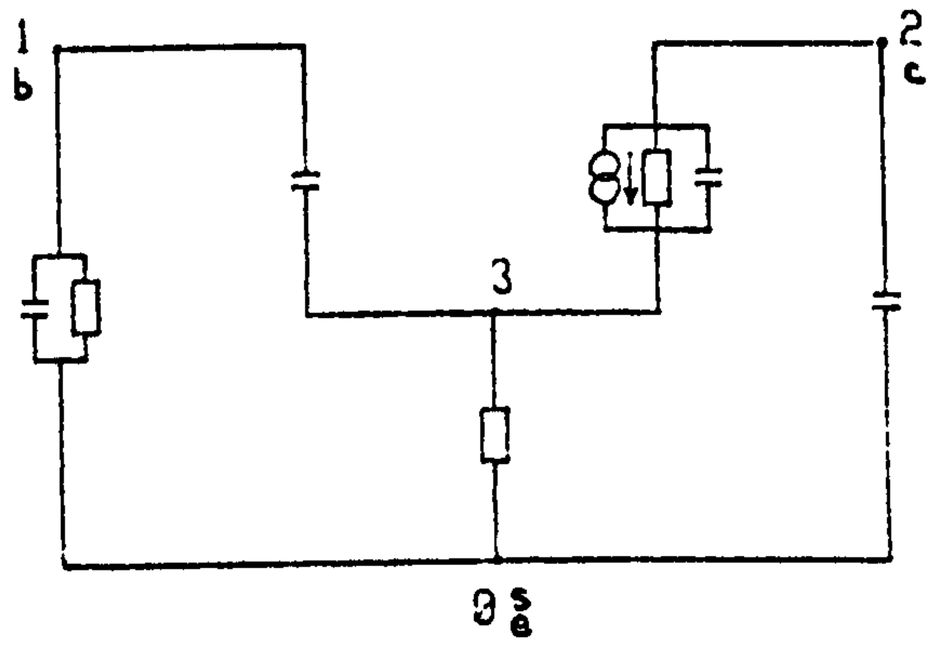

F = 5.65E+01

No. of nodes = 4
No. of elements = 8

g (2-3) = 8.55E-03 S
(T = 0)
(V across nodes 1 3)
C (1-3) = 1.25E-01 nF
G (2-3) = 4.36E-05 S
C (2-3) = 4.10E-04 nF
G (0-3) = 3.48E-03 S
C (1-0) = 3.10E-02 nF
G (1-0) = 1.97E-04 S
C (2-0) = 1.95E-03 nF

Node 1 - Base
Node 2 - Collector
Node 0 - Substrate and Emitter

Figure 5.4 Addition of Elements Between Nodes 1 and 0 and Nodes 2 and 0

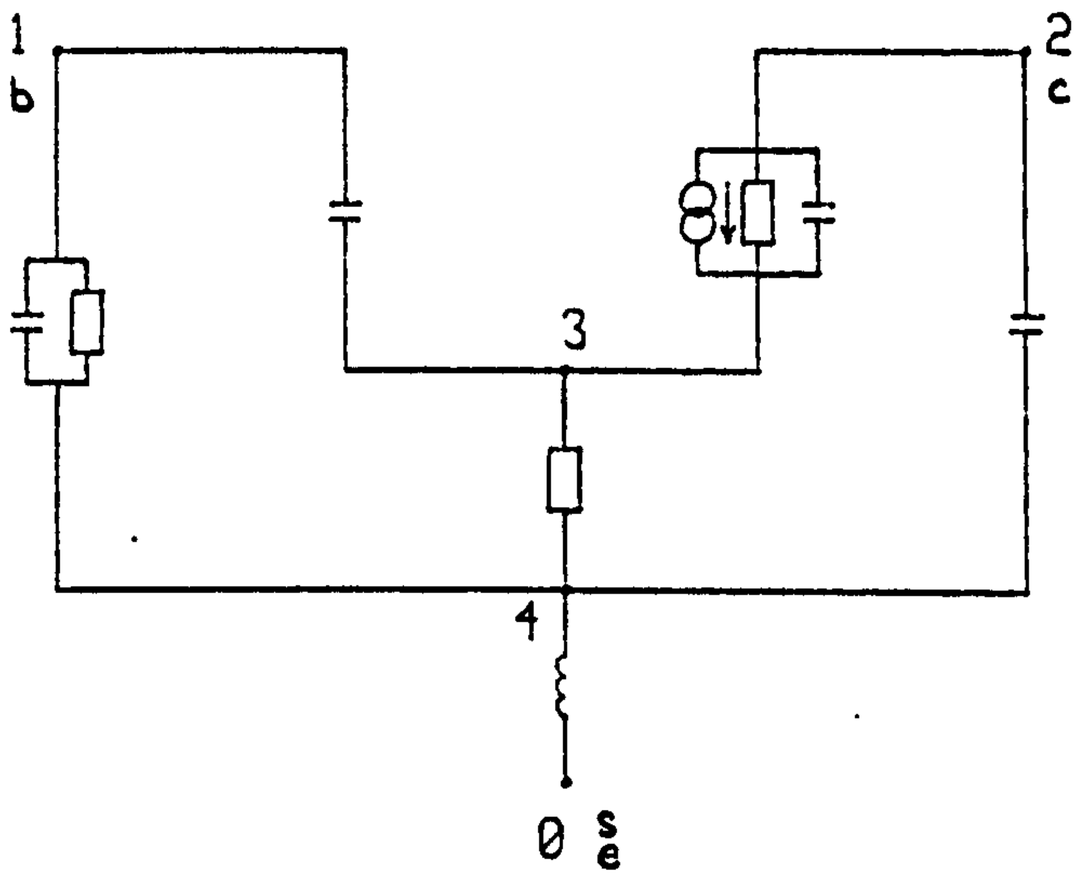

F = 1.85E+01

No. of nodes = 5
No. of elements = 9

g (2-3) = 1.16E-02 S
(T = 0)
(V across nodes $\frac{1}{3}$)
C (1-3) = 1.53E-01 nF
G (2-3) = 4.39E-05 S
C (2-3) = 4.19E-04 nF
G (4-3) = 3.14E-03 S
C (1-4) = 3.42E-02 nF
G (1-4) = 2.27E-04 S
C (2-4) = 4.50E-03 nF
L (4-0) = 1.27E+01 nH

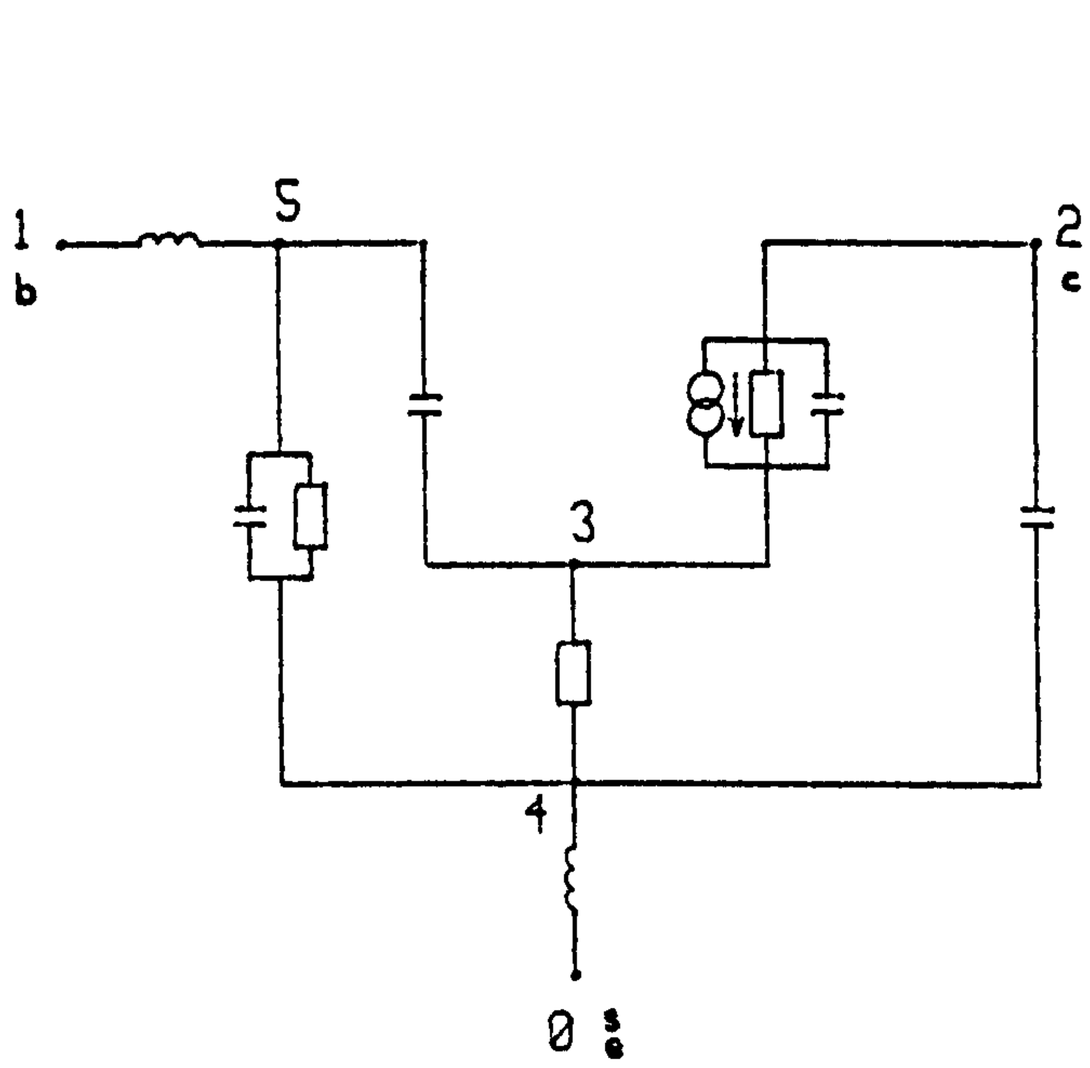

F = 2.25E+01

No. of nodes = 6
No. of elements = 10

g (2-3) = 8.79E-03 S
(T = 0)
(V across nodes $\frac{5}{3}$)
C (5-3) = 1.31E-01 nF
G (2-3) = 4.19E-05 S
C (2-3) = 4.04E-04 nF
G (4-3) = 3.33E-03 S
C (5-4) = 2.67E-02 nF
G (5-4) = 1.25E-04 S
C (2-4) = 2.40E-03 nF
L (4-0) = 6.45E+01 nH
L (5-1) = 3.52E+02 nH

Node 1 - Base
Node 2 - Collector
Node 0 - Substrate and Emitter

Note: The values given here were later found to be in error due to a fault in the analysis routine in use at the time

Figure 5.5 Addition of Inductors

to a value of 12.7 nH. The second was inserted at a value of 50 nH and was optimised to 352 nH. In each case, the existing elements changed by factors of up to about two, but when the second inductor was added the first inductor changed by a factor of over five. However, both of these cases converged within 11 iterations of the Gauss Newton algorithm. The overall error function had now been reduced to 22.45. At this point, the error in diMambro's analysis routine, referred to earlier, was detected. After correction of the error the second model in Figure 5.5 was re-optimised and in addition to changes in the element values, the value of the overall error function for this model was reduced to 12.27.

Then several different additions were attempted including G_{1-3}, C_{3-4}, G_{2-4} (where, for example, G_{1-3} signifies an element of conductance between nodes 1 and 3) but each of these failed. On attempting to add C_{1-4} the failure mode 1 was due to the corrections to element C_{5-4} . C_{5-4} was therefore removed and on convergence the overall error function had been reduced to 9.70. This model is shown in Figure 5.6 and it might have been considered that sufficient improvements had been made. However, one last attempt was made to replace the current generator that had been removed from the initial model. This last attempt was successful although the current was flowing in the opposite direction to that in the initial model. The values of many of the elements also changed quite considerably as can be seen from Figure 5.6. However, convergence of the Gauss Newton algorithm was achieved without difficulty and the overall error function was reduced to 6.13.

The individual errors of this model are shown in Table 5.2 and most of these are considerably smaller than the stated measurement errors.

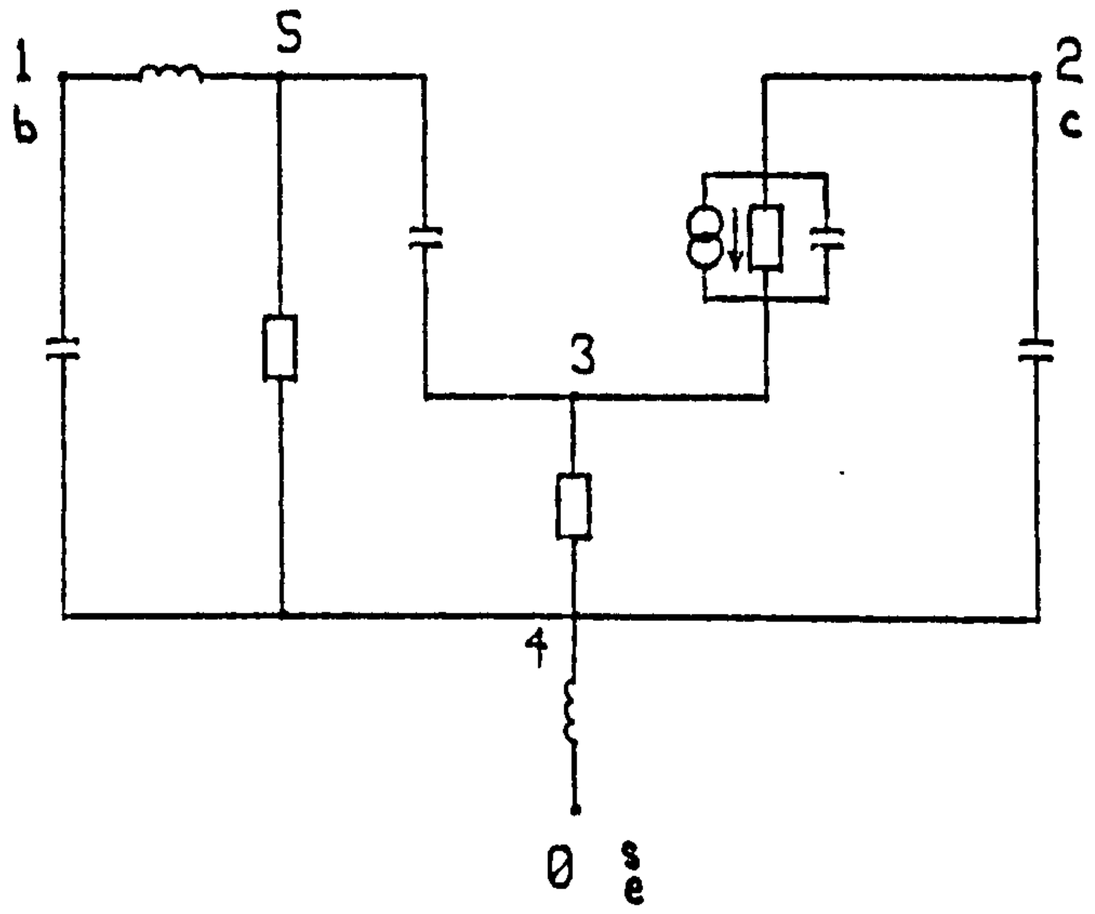

F = 9.70E+00

No. of nodes = 6
No. of elements = 10

g (2-3) = 7.95E-03 S
(T = 0)
(V across nodes $^{5}_{3}$)
C (5-3) = 1.18E-01 nF
G (2-3) = 4.47E-05 S
C (2-3) = 4.20E-01 nF
G (4-3) = 3.48E-03 S
G (5-4) = 1.29E-04 S
C (2-4) = 2.50E-03 nF
L (4-0) = 8.58E+01 nH
L (5-1) = 5.89E+02 nH
C (1-4) = 2.80E-02 nF

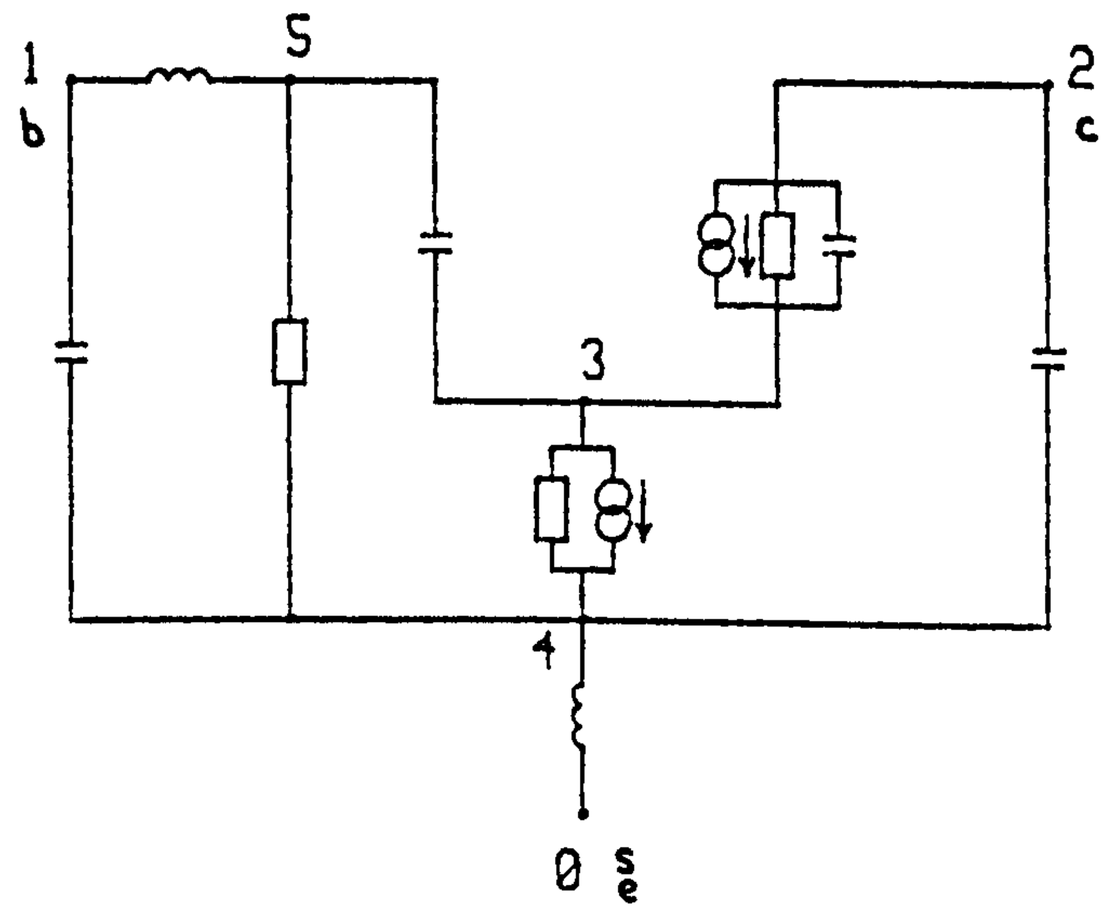

F = 6.13E+00

No. of nodes = 6
No. of elements = 11

g (2-3) = 1.20E-04 S
(T = 0)
(V across nodes $^{5}_{3}$)
C (5-3) = 1.96E-03 nF
G (2-3) = 4.43E-05 S
C (2-3) = 6.19E-01 nF
G (4-3) = 2.74E-03 S
G (5-4) = 1.15E-04 S
C (2-4) = 2.64E-03 nF
L (4-0) = 1.59E+02 nH
L (5-1) = 1.93E+03 nH
C (1-4) = 3.73E-02 nF
g (3-4) = 2.72E-03 S
(T = 0)
(V across nodes $^{1}_{3}$)

Node 1 - Base
Node 2 - Collector
Node 0 - Substrate and Emitter

Figure 5.6 Further Improvements

		S_{11}		S_{12}		S_{21}		S_{22}	
Model	Frequency MHz	Modulus dB	Phase degrees	Modulus dB	Phase degrees	Modulus dB	Phase degrees	Modulus dB	Phase degrees
Fig. 5.2	0.5	-0.10	-0.37	0.00*	0.00*	0.27	0.17	0.03	-0.19
	2.0	-0.14	-1.33	0.55	-0.17	0.34	-1.89	0.03	-0.26
	5.0	-0.02	-1.60	0.20	-3.41	0.46	-5.12	0.03	-0.41
	10.0	0.05	-3.31	-0.36	-9.66	0.46	-11.02	0.03	-0.71
Fig. 5.3	0.5	-0.09	-0.21	0.00*	0.00*	-0.30	0.52	0.03	-0.19
	2.0	-0.11	-0.71	0.08	2.19	-0.19	-0.49	0.03	-0.27
	5.0	0.10	-0.36	-0.05	1.97	0.07	-2.00	0.03	-0.42
	10.0	0.38	-2.21	-0.04	-1.48	0.43	-6.52	0.03	-0.74
Fig. 5.6 (Final Model)	0.5	0.00	-0.21	0.00*	0.00*	-0.05	0.67	0.00	-0.14
	2.0	-0.04	-0.66	0.10	1.03	0.01	0.13	0.00	-0.07
	5.0	0.04	0.09	-0.13	0.04	0.07	0.06	0.00	0.07
	10.0	0.00	0.08	0.02	-0.19	-0.03	-0.05	0.00	0.24

* A measurement of S_{12} at 0.5 MHz was not available

Table 5.2 Errors in the S Parameters of Models of a Lateral P-N-P Transistor

5.6. Description of the Final Modelling Algorithm

Having developed a model in a trial and error manner it was felt that a more automatic algorithm could be developed. The Gauss Newton algorithm gave, it was felt, a very reliable indication of whether any particular model was suitable or not, but it was extremely time consuming to do one batch computer run for each possible stage in the development of a model. Unfortunately, the program was too large and slow to permit on-line execution.

The author's modelling algorithm was required to continuously attempt model improvements, rejecting those that were unsuitable and retaining the successful ones. In addition it was felt that the attempted improvements should cover as many possible placements as was practicable. As the computer program would have to be run in batch mode, user interaction would not be possible. However, it was felt that each intermediate stage should be stored so that it was possible for the user to choose a model from any particular stage, and perhaps modify it, before manually restarting the modelling process. This way, the model development would not be inhibited by the user's prejudices, although the user could still exercise some control over the

process. New criteria were introduced to indicate more quickly whether a model would be suitable or not and techniques for the addition of elements and nodes to a model were also developed. Some details of the final modelling algorithm were published by the author[73] in 1981.

The final modelling algorithm can be divided into three separate stages. The first stage consists of taking the initial model and attemping to find a local minimum of the objective function, if necessary removing elements from the model until a minimum is obtained. The second stage involves the addition of new elements within the existing number of nodes since we assume that we want as few nodes as possible. The third stage is for the addition of a new node. Stages two and three can be repeated alternately until the required accuracy or complexity is obtained. These three stages will now be described in more detail.

5.6.1. Stage 1 - Obtaining the First Local Minimum

In attempting to find the first local minimum, the Gauss Newton algorithm is applied to the initial model. The criterion for successful termination is identical to that described in Chapter 4.

The criteria for failure are more stringent than those described in Chapter 4, in particular, the two most common reasons for failure are detected sooner. Failure mode 1 is now deemed to be fatal if the rate of increase in the maximum modulus correction has increased on 5 successive iterations and the mode we could now call failure mode 2, is deemed fatal if the number of iterations by the Gauss Newton algorithm exceeds 50 without obtaining convergence.

Whichever failure mode occurs the next step is to examine the vector of corrections $\underline{\delta}$ (which is in the logarithmic domain) to determine which elements it might be best to remove from the model. Throughout all the earlier experimentation it was found that removal of the elements having the

maximum modulus corrections aided convergence. Thus the basic aim is to remove from the model the element giving the maximum modulus correction and to then restart the Gauss Newton algorithm, generally continuing from the element values current at the time of the failure.

If the element being removed is a resistor and its corresponding correction is positive (or similarly a conductor having a negative correction) then it is assumed that the element is tending to an open-circuit and so the element is removed open-circuit. Conversely, the removal of a resistor having a negative correction (or conductor having a positive correction) is achieved by a short-circuit. This latter case necessitates the removal of a node and involves the removal of any other elements which are connected in parallel with the offending element.

The situation with regard to the removal of elements of inductance and capacitance is not so straightforward. It was decided that, as any inductor would normally occur only at one of the external nodes, elements of this type should always be removed as a short-circuit. Again this necessitates the deletion of a node although it is less likely that there will be other elements in parallel with an inductor than with a resistor. It was also decided that, in order to reduce the possibility of premature collapse of a model, elements of capacitance should be removed open-circuit provided that at least one other element is in parallel with it. If there is no other element in parallel with a capacitor that is being removed then it is replaced by a resistor. The initial value of this resistor was set quite arbitrarily at $1 K\Omega$. The setting of the initial values of new elements is discussed in more detail in Section 5.6.2.

There are a number of cases when short-circuiting an element is deemed to have failed. These are

(i) if any of the external nodes are connected together

(ii) if any current generator is short-circuited

(iii) if the controlling voltage of any current generator is short-circuited.

Furthermore, it was decided that it would not be permitted for a current generator to be removed automatically since the presence of current generators is normally critical to a model, particularly as most models contain only one current generator. It was felt that if there was a situation where removal of a current generator was the only remaining option, then it should be done manually.

The method described above for the removal of elements is summarised in the flow chart in Figure 5.7.

The overall scheme for Stage 1 is shown in Figure 5.8. Although the basic scheme is to remove only the element causing the maximum modulus correction and to then restart the Gauss Newton algorithm, it was found that when there were a number of elements causing large modulus corrections, the removal of several elements at one time could save on the number of failure/removal cycles. The criterion devised for multiple element removal was that all those elements whose modulus correction $|\delta_i| > 10^{j+2}$, where j is the average of the positive powers of 10 of all the corrections $\underline{\delta}$ (in the logarithmic domain), should be removed. If none of the corrections satisfy this criterion then only the element having the maximum modulus correction is removed.

If, following the removal scheme already described, none of the prescribed elements are successfully removed, then an attempt is made to remove the element having the second highest modulus correction. If this is successful then the remaining elements are given their values at the time of entry to Stage 1 and the process restarted, otherwise Stage 1 is abandoned. If this should happen then the best course of action is for the user to first check the initial model for errors and to then try a different model, perhaps based on the initial model but containing some additional elements.

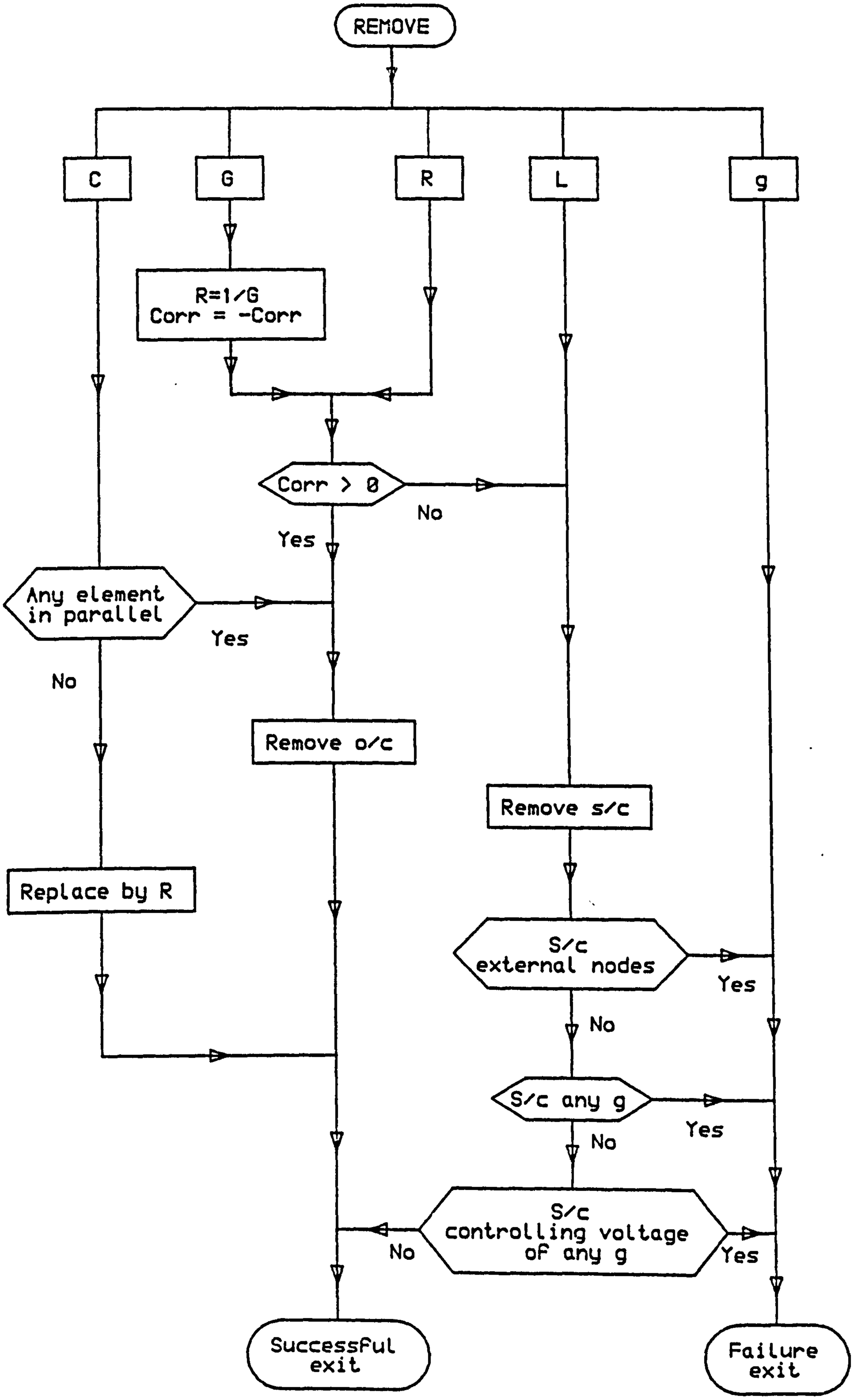

Figure 5.7 Scheme for Removal of Elements

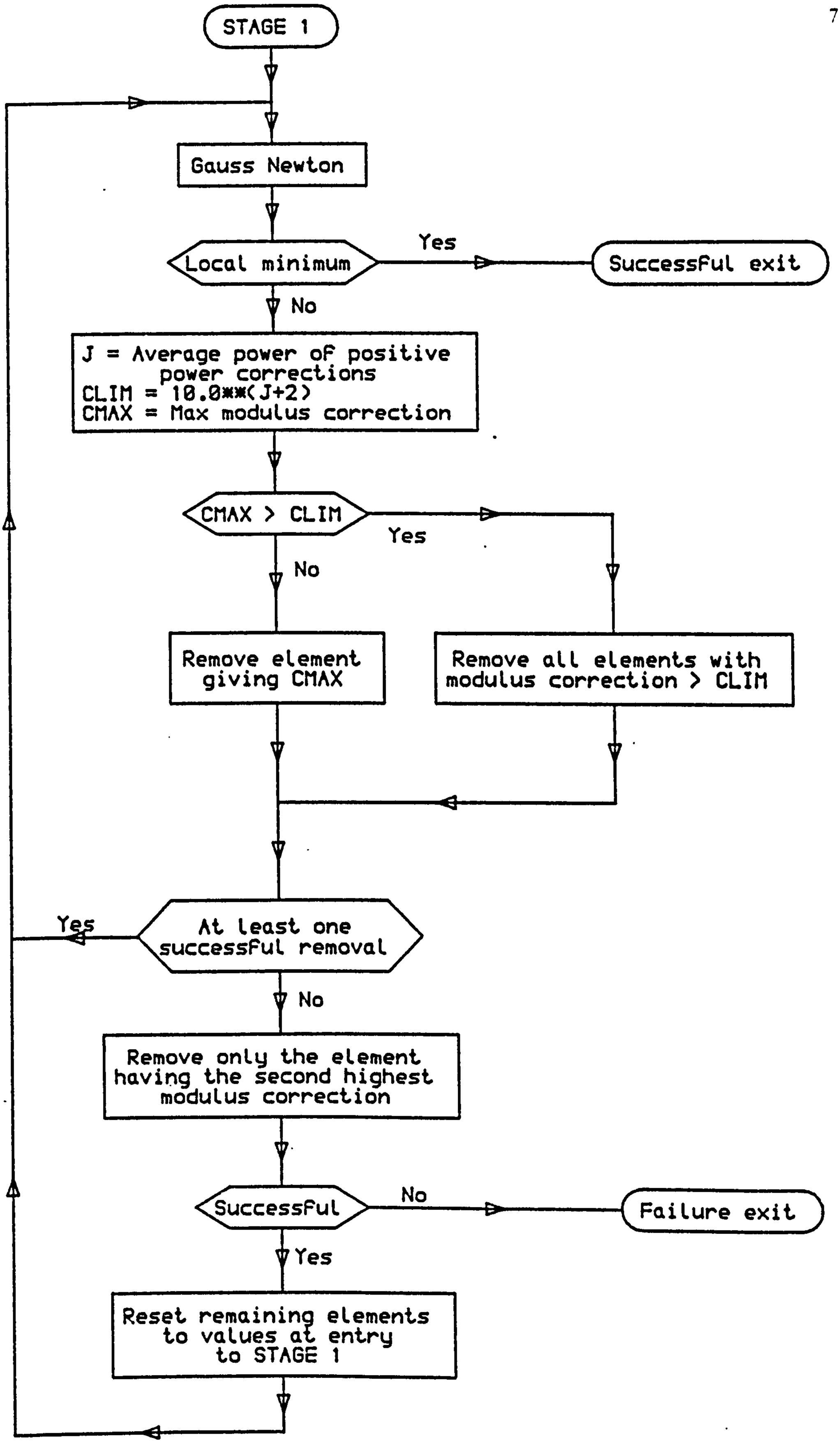

Figure 5.8 Scheme for Stage 1

5.6.2. Stage 2 - Element Addition

Having obtained a model giving a local minimum of the objective function, F_{min}, the second stage may now be entered. The aim of this stage is to add extra elements into the model without increasing the number of nodes. The author decided that only elements of capacitance and resistance should be added at this stage. Elements of inductance are expected to occur only at the external modes and are unlikely to be successfully inserted in parallel with another element even at an external node. Therefore, it was decided that inductors should only be added with a new node at Stage 3. The author also felt that users were likely to have strong ideas about the number of voltage controlled current sources that should be present in a model, and their positions. This factor, coupled with the problems of choosing suitable positions and controlling voltages of current sources to be inserted, led to the decision that they should not be added automatically. The user always has the ability to modify a model at any particular stage and then restart the modelling process.

The problems associated with intuitive modelling have already been discussed. The author felt that in Stage 2, all possible placements of elements of capacitance and resistance should be attempted. Cutteridge[74] had developed expressions for the optimum values for the placement of virtual elements which were applicable to network synthesis using coefficient matching techniques and which had been utilised by Krzeczkowski[6]. Savage[8] however, eventually rejected the use of this technique in favour of one based on the Gauss Newton corrections of virtual elements. The author independently developed a similar scheme for the addition of elements to a model. This scheme is shown in Figure 5.9.

In this scheme, taking each type of new element in turn, attempts are systematically made to insert the new element between each pair of nodes where an element of that type does not already exist. If the addition

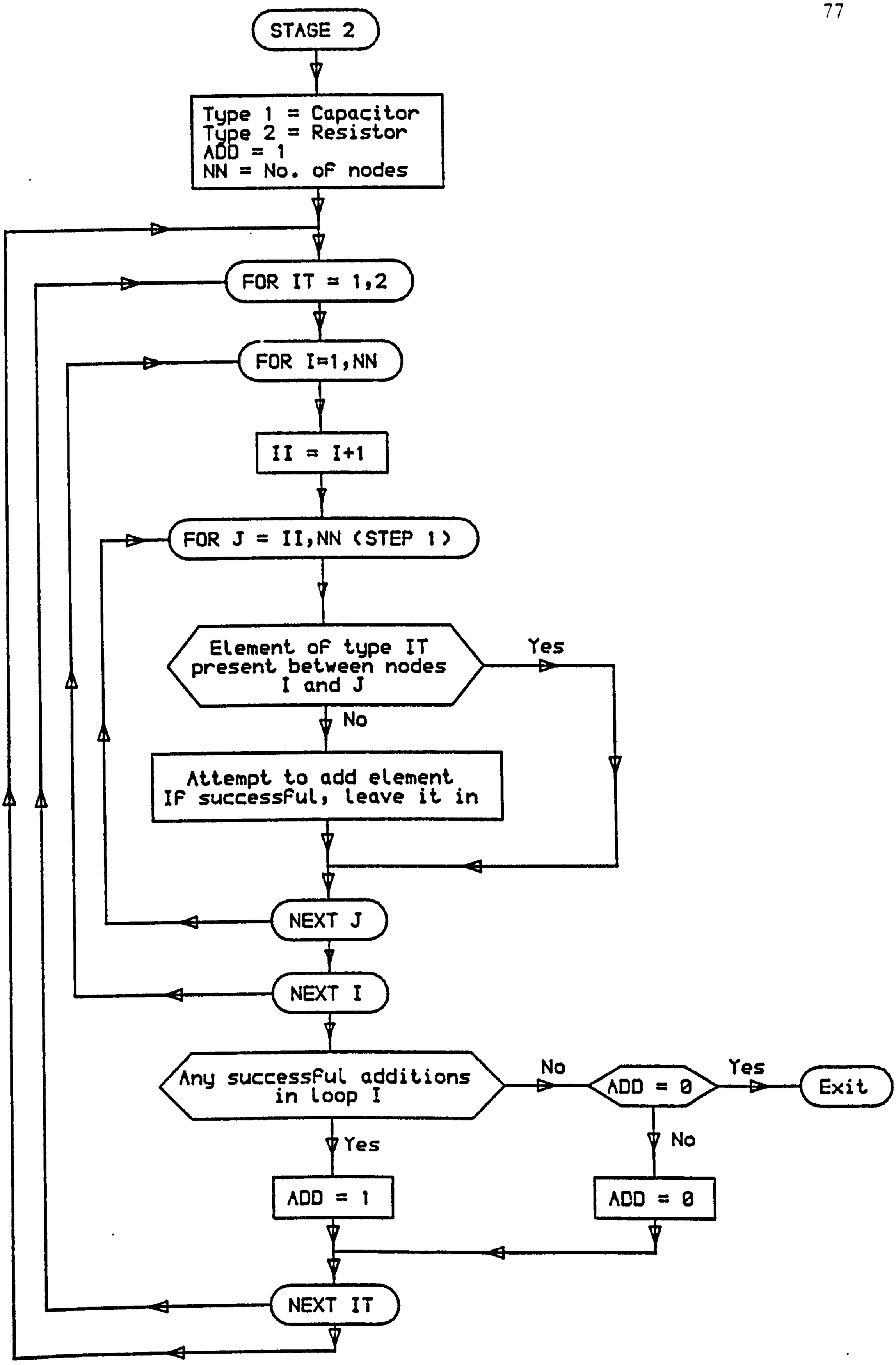

Figure 5.9 Scheme for Stage 2

is successful, the criteria for which will be given later, then the element remains in place, otherwise the model retains its former topology. These placements are attempted repeatedly until neither a capacitor nor a resistor has been added in one complete cycle. The reason for these repeated attempts is that it was found that even if a particular element has failed to be added at one stage, it might be successful at a later stage when the model topology has changed slightly. Indeed, in Section 5.7 there is an example where an element was deleted from a model at one stage and then re-inserted later.

An alternative strategy might have been to evaluate each of the possible placements and to only add the best of these, followed by further cycles of evaluation and addition of the best until no more elements could be added. However, the author felt that this latter option would be more laborious and that the same final topology would be obtained in most cases.

Obviously, with so many possible placements being attempted, the efficiency of the algorithm to detect the success or failure of each addition is paramount. It was observed that, when a new element was inserted into an existing model, the moduli of the Gauss Newton corrections to be applied to the existing elements were usually much smaller than the modulus of the correction to be applied to the new element. This fact was capatilized upon by the scheme devised for element addition summarised in Figure 5.10.

Thus, when attempting to add a new element, first the Gauss Newton corrections are calculated. If the new element does not give rise to the maximum modulus correction, then the Gauss Newton algorithm proceeds normally. However, if the maximum modulus correction does apply to the new element, then this correction, up to a maximum absolute value of ten in the logarithmic domain, is applied directly to the new element. The

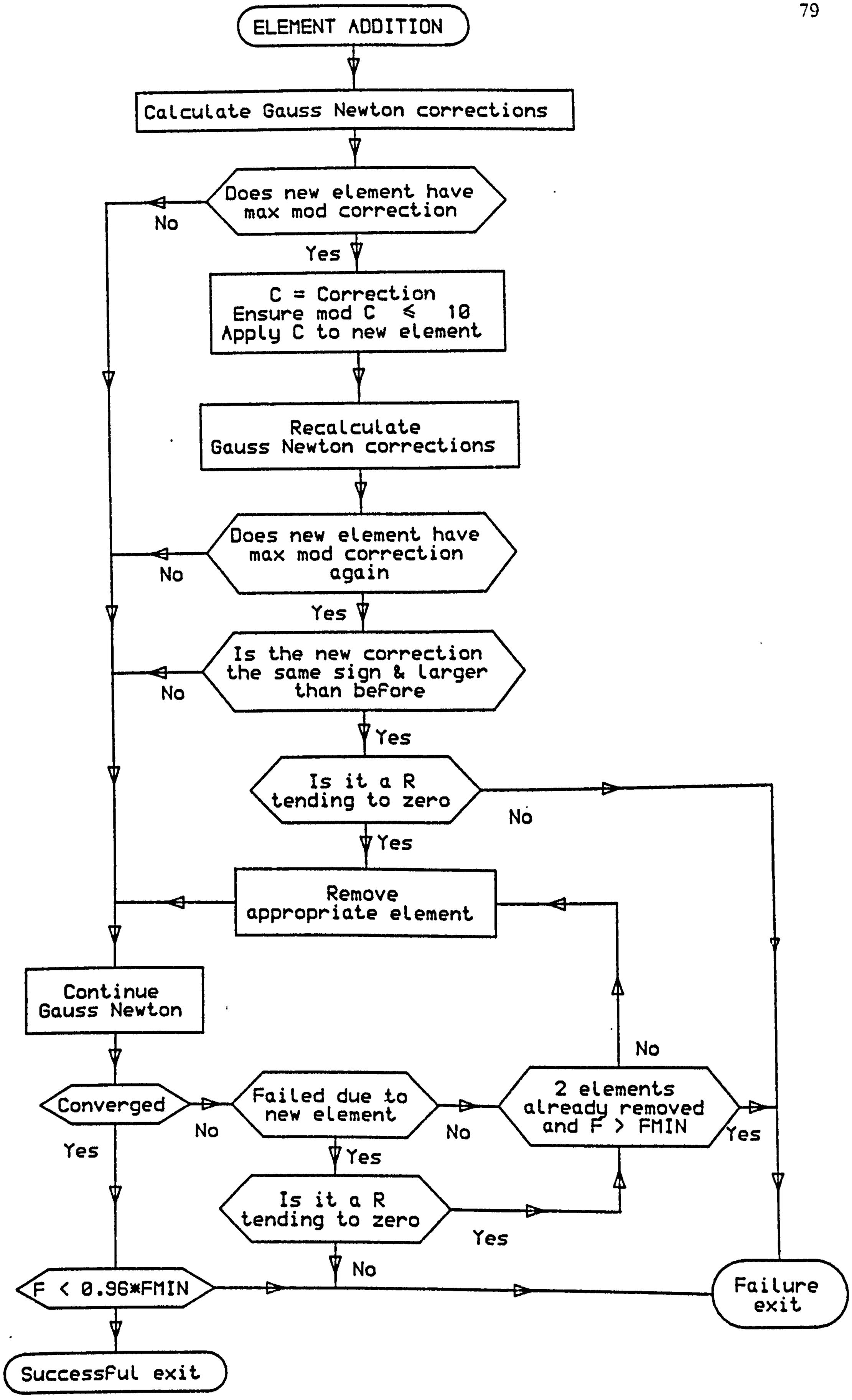

Figure 5.10 Scheme for Attempted Element Additions at Stage 2

Gauss Newton corrections are then re-calculated. If the new element is no longer the one generating the maximum modulus correction then the Gauss Newton algorithm is continued normally. Similarly, if the modulus correction to the new element is smaller than before, or if the correction is of the opposite sign, then again the Gauss Newton algorithm is allowed to proceed. If, however, the new correction is of the same sign and its absolute value is greater than before, then it is assumed that the new element is tending to a value of either zero or infinity. If the new element is a resistor and it is tending to zero, then the removal of the node that this suggests is permitted and the Gauss Newton algorithm is then applied to the reduced model. Otherwise, it is assumed that the new element is unsuitable for addition into the model. By applying the Gauss Newton correction to the new element in this way, the author is attempting both to detect failure of element addition more quickly, and to aid more rapid convergence of the Gauss Newton algorithm by ensuring that the starting value of the new element is reasonable.

It has been found that the Gauss Newton algorithm is very reliable even when the starting values of new elements are quite inaccurate. Thus, with this additional aid to rapid convergence, the values at which new elements of capacitance and resistance are added, were chosen quite arbitrarily. It was felt that the new elements should be of such values that they would not have too great an effect on the existing model. Therefore, the initial value chosen for new elements of capacitance was 1pF and of resistance was 1 KΩ . Alternative choices could have been based on the actual values of each type of element already present in the model at the time of the addition, but it was felt that this would not offer any improvement.

Those cases where the Gauss Newton algorithm is allowed to proceed now continue in a similar manner to Stage 1 except that in certain cases

the element addition is deemed to have failed before convergence of the Gauss Newton algorithm onto a local minimum has been obtained. These cases are:

(i) if failure of the Gauss Newton algorithm is due to the new element and it is not a resistor tending to short circuit a pair of nodes

(ii) if further element removals are indicated when two or more elements have already been removed and the current value of the objective function F is still greater than the value for the currently accepted model, F_{min}.

If the Gauss Newton algorithm converges at a new local minimum, the new model is only accepted if the value of the objective function is 4% lower than F_{min}, the value for the currently accepted model. This is to ensure that the model contains only those elements that make a significant contribution to the model accuracy and to avoid adding an excessive number of elements to the model.

Thus, Stage 2 ends when no further successful additions are possible. If the model is still not accurate enough then the next step is to attempt to add elements in such a way that a new node is generated.

5.6.3. Stage 3 - Node Addition

Savage[8] in his work on network synthesis discussed a number of methods by which nodes could be introduced into an existing network. Among these methods are to:

(i) split an existing element to form a new node to which attempted element additions should be made

(ii) duplicate an existing T-network

(iii) perform a delta-wye transformation

(iv) substitute a T-network in place of a negative virtual element.

Savage found that the most effective technique was the last of these, where if a potential element addition indicated that the element should take a negative value then a T-network, based on that element type and its corresponding proposed negative value, should be inserted in its place. However, the author felt that each of these methods which, apart from (iii), caused the generation of at least two extra elements, ignored the most likely method for the improvement of a model.

If we assume that the current model is basically correct then, rather than disturb the internal structure of the model, new nodes should be developed at the external nodes. This way, the addition of a new node can be achieved by the addition of only one new element as in the examples in Figure 5.5. If internal nodes are to be added then a method which again involves the addition of only one new element, is to insert a new element, of a different type, in series with one of the existing elements.

Thus, the author's method of node addition, which is shown in Figure 5.11, is based on the addition of only one element. Since we assume that the number of nodes in a model should be kept to a minimum, this involves the evaluation of each possible placement in order to select the best new node and element. The restrictions on the placements of new elements can be seen in Figure 5.11 and include the following.

1. Expansion at an external node is only permitted if there is not an inductor already at that external node. Then the addition of elements of inductance, resistance or capacitance is permitted.

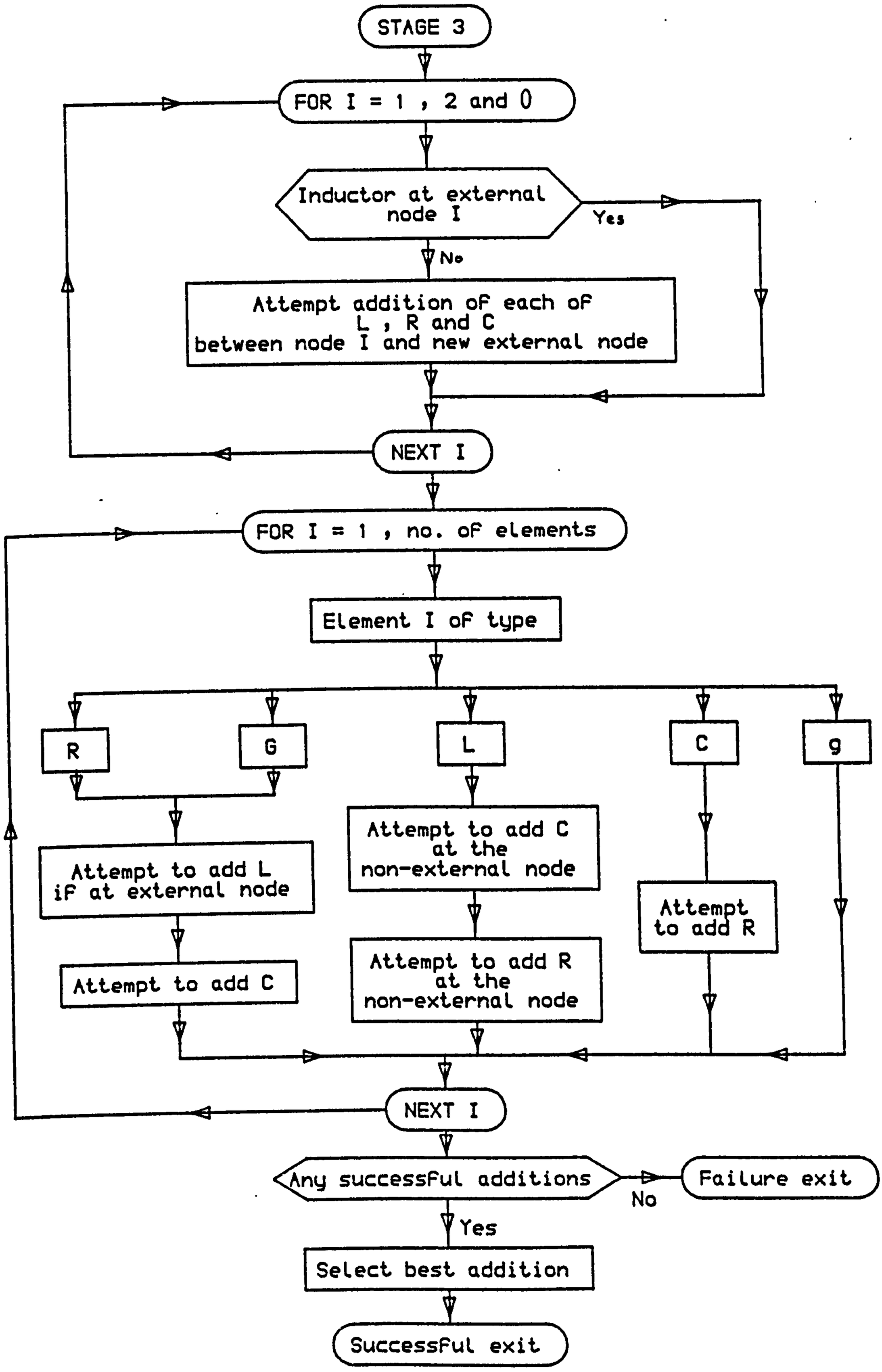

Figure 5.11 Scheme for Stage 3

2. An element of resistance or conductance may have an inductor added in series with it only if by so doing the inductor will be connected to an external node which does not already have an inductor connected.

3. Elements of resistance or conductance may have a capacitor added in series.

4. Elements of inductance may have an element of resistance or capacitance added in series at the non-external node.

5. An element of capacitance may have a resistor added in series.

6. A voltage controlled current source may not have any element added in series.

Further clarification of the way in which some of these elements are added is given below.

1. The addition of a particular element is not attempted if there is already an element of that type in series in that branch of the model.

2. The new elements are only added on one side of any particular element, usually on the side having the highest node number.

3. When an element is connected at a node at which a controlling voltage of a current generator is taken, then the controlling voltage is taken across the new element also.

Thus, although most topologies are possible with repeated entries to Stages 2 and 3, some could take an inordinate time to develop.

The method used to determine whether a node addition is successful is shown in Figure 5.12. As with the element addition at Stage 2, it is

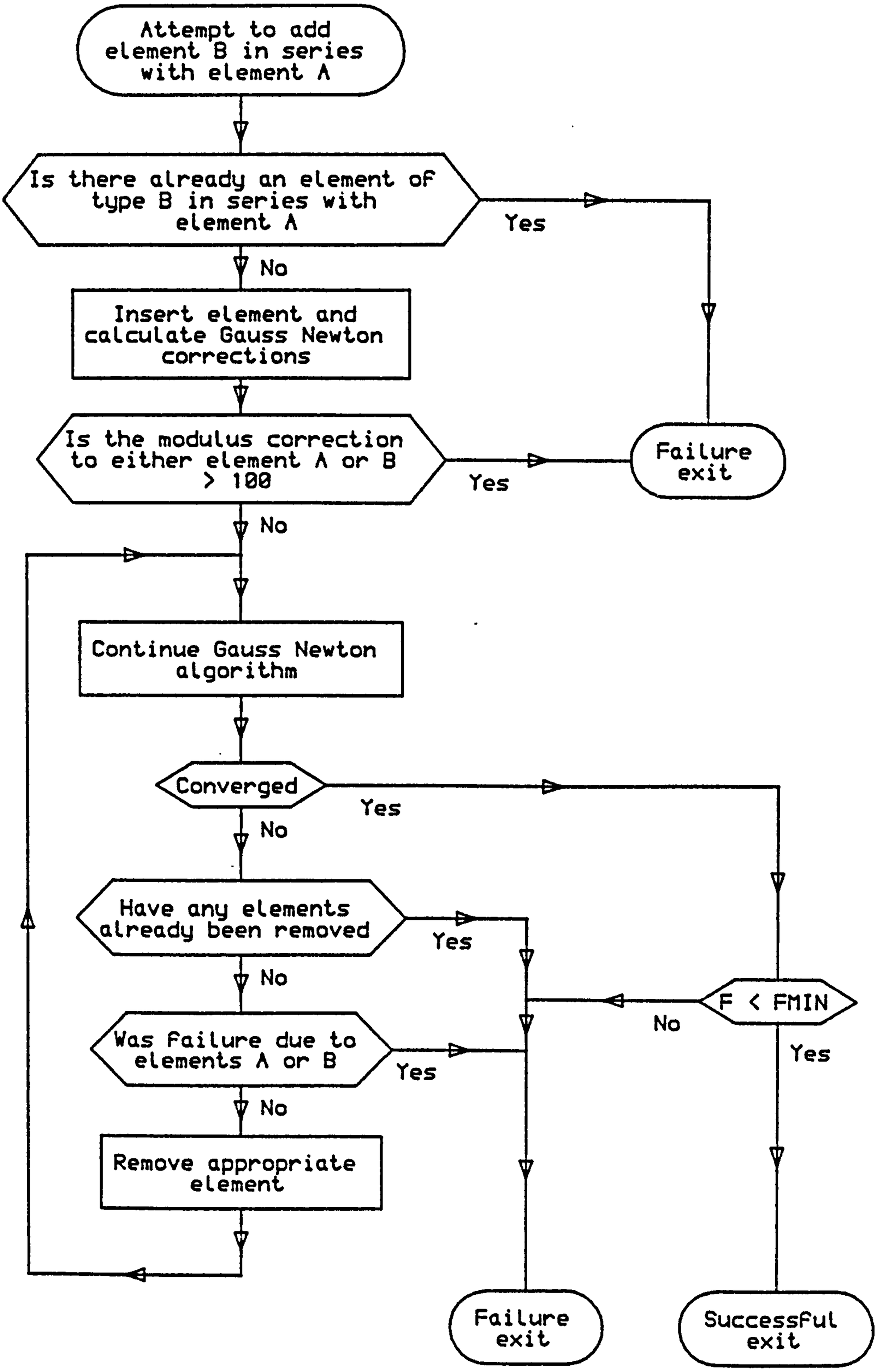

Figure 5.12 Scheme for Attempted Node Addition at Stage 3

based on the Gauss Newton algorithm. The initial values for new elements of resistance and capacitance were set at 100 Ω and 0.1 pF respectively, one order of magnitude smaller than at Stage 2. The initial value for elements of inductance was set at 10 nH .

It was found more difficult to reduce the computational effort at this stage and the only early prediction of failure is if the absolute correction (in the logarithmic domain) to either of the elements connected to the new node, calculated by Gauss Newton, exceeds 1000. Otherwise, the Gauss Newton algorithm is entered normally. If the algorithm fails to converge then, provided the failure to converge was not due to either of the elements connected to the new node, the appropriate element is removed and the Gauss Newton algorithm restarted. If it fails to converge again then the addition is deemed to have failed. If the Gauss Newton algorithm finds a new local minimum that is lower than F_{min}, the best minimum obtained before entry to Stage 3, then the addition is said to be successful.

Each successful node addition is saved for future reference by the user and the best of these is then used as the new model. Although the user may decide at which stage the model should be accepted, the author's recommendation is that it should be after completion of Stage 2, in order that the maximum benefit be gained from any particular number of nodes. It might be suggested that to save time, rather than re-entering Stage 2, further element additions should be attempted only in the vicinity of the new node. However, the author has found that the addition of a new node can affect the whole model and that, therefore, it is better if all permitted element additions are attempted using Stage 2 again.

5.7 Checking the Final Modelling Algorithm

As a final check on the modelling algorithm described in the previous section, after the models described in Chapters 6 and 7 had been developed, the first modelling exercise, to model a lateral p-n-p transistor, was repeated but this time using the final version of the modelling algorithm instead of the trial and error method used to produce the models in Figures 5.3 to 5.6. In addition, the s parameters of the models were calculated by the analysis routine using pivotal condensation written by the author, in place of di Mambro's routine.

From the initial model shown in Figure 5.2, the algorithm proceeded to remove elements G_{1-3} and C_{3-0} and then stopped with an indication that g_{0-3} should also be removed. On removing this element manually and re-starting the algorithm, it then went on to obtain the model shown in Figure 5.3. Continuing from there into Stage 2, the algorithm added the elements C_{1-0}, C_{2-0} and R_{1-0}. This model was thus the same as the last model in Figure 5.4 even though the element addition was in a different order to that given in Figure 5.4. Owing to the differences in the analysis routines, the element values and the overall error function value were slightly different and the new value of the overall error function, F , was 50.97 compared with 56.50. The algorithm then entered Stage 3 and the new element and node added was L_{4-0}. Thus the algorithm had produced the same model as the first model shown in Figure 5.5. The values of the elements were, here, quite different from those given in Figure 5.5 due to the errors in the analysis routine and the value of F , which had not been recalculated in the earlier trials, was found to be 13.50.

From this point, the model developed differently from the model in Figure 5.5 in which case the next step was to add an inductor at node 1, thus immediately generating an additional node. Although at the time it was thought that this made a significant improvement, it can now be seen

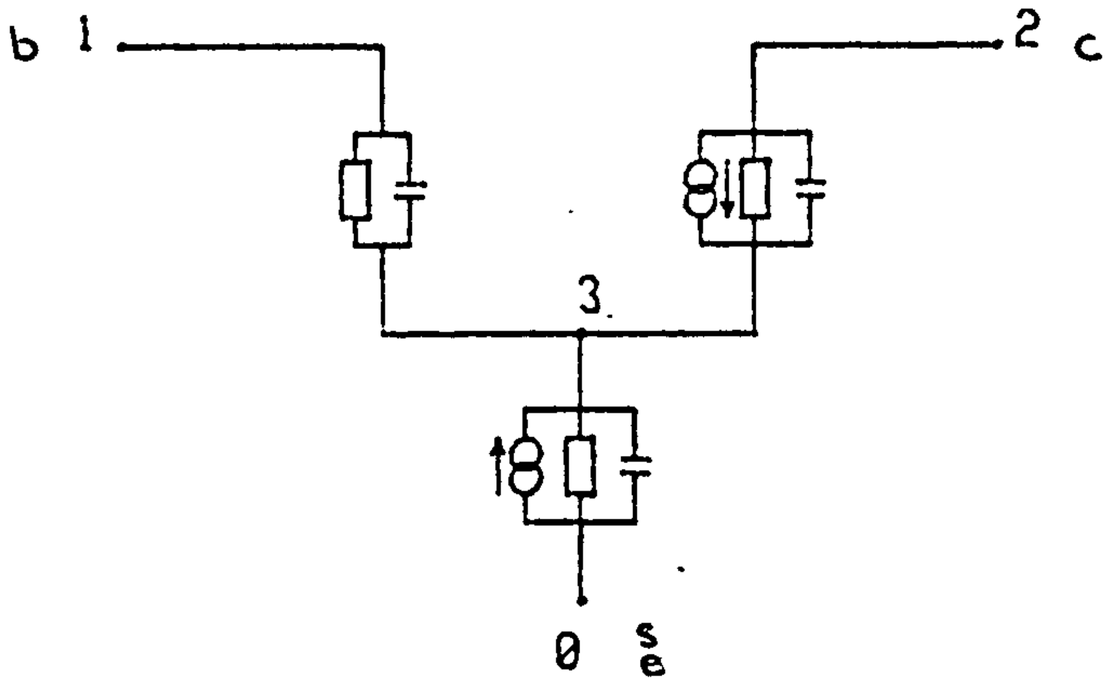

F = 3.84E+02

No. of nodes = 4
No. of elements = 8

g (2-3) = 3.53E-03 S
(T = 0)
(V across nodes $\frac{i}{j}$)
g (0-3) = 2.07E-05 S
(T = 0)
(V across nodes $\frac{i}{j}$)
G (1-3) = 6.12E-10 S
C (1-3) = 8.68E-02 nF
G (2-3) = 5.22E-05 S
C (2-3) = 5.06E-04 nF
G (0-3) = 6.77E-03 S
C (0-3) = 3.71E-06 nF

Delete G(1-3) ; C(2-0) ; g(0-3)
Add C(1-0) ; C(2-0) ; R(1-0)
Add new node with L(4-0)

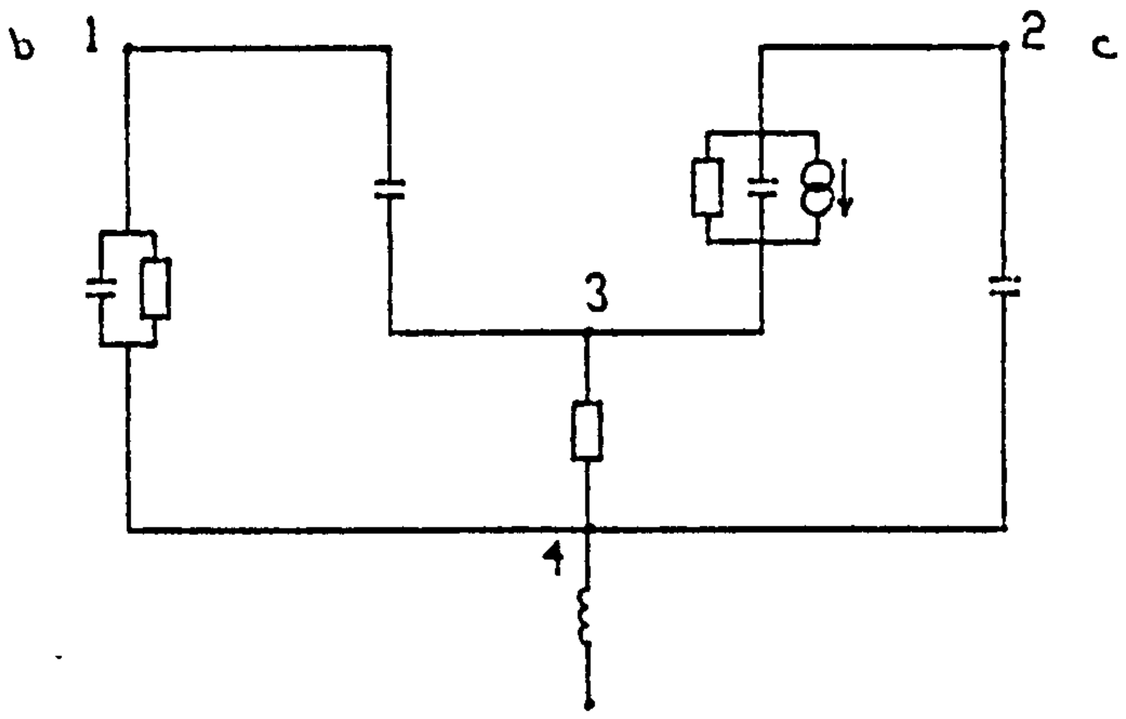

F = 1.35E+01

No. of nodes = 5
No. of elements = 9

C (1-3) = 1.26E-01 nF
G (2-3) = 1.64E-05 S
C (2-3) = 3.67E-04 nF
g (2-3) = 9.23E-03 S
(T = 0)
(V across nodes $\frac{i}{j}$)
G (4-3) = 3.27E-03 S
C (1-4) = 2.97E-02 nF
C (2-4) = 1.30E-04 nF
R (1-4) = 7.76E+03 ohm
L (0-4) = 4.28E+02 nH

Add C(1-2) ; Delete C(2-3)
Add C(2-0)
Add new node with C(0-3)

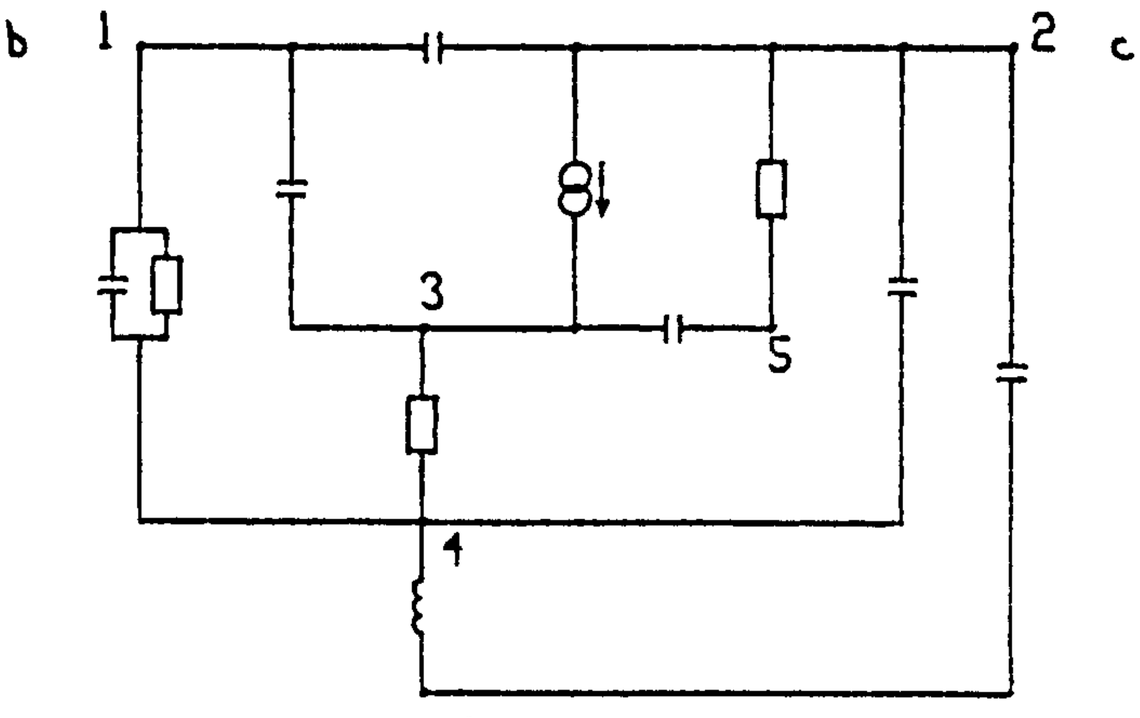

F = 7.36E+00

No. of nodes = 6
No. of elements = 11

C (1-3) = 1.15E-01 nF
G (2-5) = 8.28E-06 S
g (2-3) = 8.14E-03 S
(T = 0)
(V across nodes $\frac{i}{j}$)
G (4-3) = 3.42E-03 S
C (1-4) = 2.86E-02 nF
C (2-4) = 1.67E-04 nF
R (1-4) = 8.28E+03 ohm
L (0-4) = 4.15E+02 nH
C (1-2) = 3.94E-04 nF
C (2-0) = 2.01E-03 nF
C (5-3) = 3.00E-03 nF

Add C(2-3) ; Delete C(1-2)
Add R(4-5)

Node 1 - Base
Node 2 - Collector
Node 0 - Substrate and Emitter

Figure 5.13 Modelling the Lateral P-N-P Transistor

that the change in the value of F was actually from 13.50 to 12.27.

In the final modelling algorithm, after one successful node addition, Stage 2 is re-entered. In this section the algorithm added two new elements C_{1-2} and C_{2-0}, deleting C_{2-3} while adding C_{1-2}, to obtain a value of F = 12.26. On re-entry to Stage 3, the addition of an inductor at the input node only gave a very small reduction in the value of F and the new node selected by the algorithm was formed by the addition of an element of capacitance in series with G_{2-3}, and gave a value of F = 7.36. This sequence is shown in Figure 5.13 together with the additions made in the final entry to Stage 2. These additions were to add C_{2-3} while deleting C_{1-2}, followed by the addition of R_{4-5}. It is interesting that elements C_{1-2} and C_{2-3} appear to be mutually exclusive. However, the addition of C_{2-3} at this late stage after its earlier deletion serves to confirm the point made in Section 5.6.2 that attempted element additions should be repeated at each stage of a model's development.

b

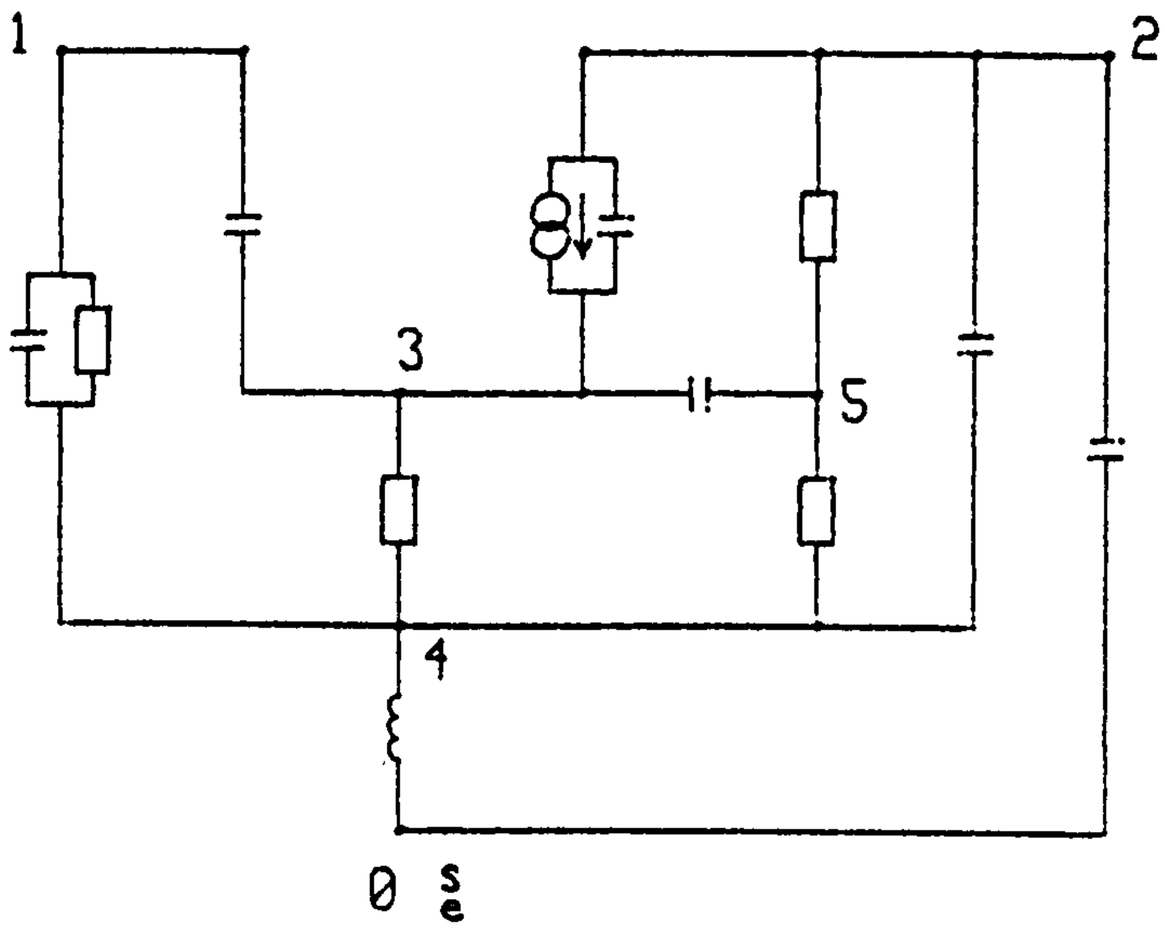

c

F = 5.77E+00

No. of nodes = 6
No. of elements = 12

C (1-3) = 1.19E-01 nF
G (2-5) = 4.63E-05 S
g (2-3) = 8.47E-03 S
(T = 0)
(V across nodes 1/3)
G (4-3) = 2.98E-03 S
C (1-4) = 2.89E-02 nF
C (2-4) = 1.18E-04 nF
R (1-4) = 8.10E+03 ohm
L (0-4) = 4.10E+02 nH
C (2-0) = 2.16E-03 nF
C (5-3) = 7.57E-01 nF
C (2-3) = 3.53E-04 nF
R (4-5) = 2.44E+03 ohm

Node 1 - Base
Node 2 - Collector
Node 0 - Substrate and Emitter

Figure 5.14 Final Model of the Lateral P-N-P Transistor

This final model, shown in Figure 5.14, had a value of F = 5.77, giving r.m.s. errors of 0.04 dB and 0.4° and consisted of 6 nodes and 12 elements which included only one voltage controlled current generator. The values of the s parameters and the errors are given in Table 5.3.

	Frequency MHz	Modulus (dB)			Phase (degrees)		
		Measured	Model	Error	Measured	Model	Error
S_{11}	0.5	-0.10	-0.11	0.01	-1.40	-1.14	-0.26
	2.0	-0.20	-0.16	-0.04	-5.40	-4.52	-0.88
	5.0	-0.40	-0.43	0.03	-11.20	-10.89	-0.31
	10.0	-1.20	-1.20	0.00	-19.40	-19.75	0.35
S_{12}	0.5	*	-76.89	0.00	*	99.54	0.00
	2.0	-64.70	-64.77	0.07	88.70	89.10	-0.40
	5.0	-57.20	-57.12	-0.08	84.00	82.76	1.24
	10.0	-52.00	-52.01	0.01	76.30	76.85	-0.55
S_{21}	0.5	-12.50	-12.44	-0.06	178.10	178.28	-0.18
	2.0	-12.50	-12.50	-0.00	169.90	169.81	0.09
	5.0	-12.80	-12.88	0.08	155.00	154.72	0.28
	10.0	-14.00	-13.97	-0.03	132.90	133.11	-0.21
S_{22}	0.5	0.00	-0.01	0.01	-0.20	-0.02	-0.18
	2.0	0.00	-0.01	0.01	-0.30	-0.19	-0.11
	5.0	0.00	-0.01	0.01	-0.50	-0.49	-0.01
	10.0	0.00	-0.01	0.01	-0.90	-0.97	0.07
* A measurement of s_{12} at 0.5 MHz was not available							

Table 5.3 s Parameters of Lateral P-N-P Transistor and Final Model

Although the value of F is smaller for this model than for the final intuitive model in Figure 5.6, these values being 5.77 and 6.13 respectively, the maximum absolute errors for this model are 0.08 dB and 1.24° compared with 0.13 dB and 1.03°. Thus the errors are again comparable with the errors in the measurements.

In the author's opinion both of these models are equally valid and she would suggest that the original model proposed by PRL contained two voltage controlled current generators in an attempt to model the substrate interaction of a lateral p-n-p transistor in the manner suggested by Callahan[75]. However, Callahan's model was for the lateral p-n-p transistor operating in

the saturated region and therefore, probably not applicable to the set of data provided by PRL. This could explain why the second current generator in the final intuitive model is reversed. By adding a supplementary current generator to a model needing only one, a model of much greater complexity, and potential effectiveness, is produced. The author would suggest that although the model in Figure 5.14 has one element more than that in Figure 5.6, it is actually the more simple of the two models.

The time taken to produce this final model was approximately 50 minutes of c.p.u. time on the Leicester University CDC Cyber 73. However, the point should be made that the author's intention was to produce an effective method for the development of models and that the computing time was not considered to be of prime importance. In Chapter 8, some suggestions are made for means of reducing the computing time, but with the present trend of faster computers constantly being developed, in the author's opinion the main priority should be the development of an algorithm that produces results regardless of the time taken. There is little point in developing a fast algorithm if it neglects to produce a good model.

CHAPTER 6

MODELLING A VERTICAL N-P-N TRANSISTOR

The second set of data provided by PRL was for a vertical n-p-n transistor. Like the lateral p-n-p transistor this is a component of an integrated circuit and the term 'vertical' refers to the way in which the transistor is produced in the integrated circuit. The data provided is reproduced in Appendix 1, together with an example of the data's original form.

It can be seen that the data consists of S parameter measurements at 12 frequencies between 0.1 GHz and 1.0 GHz for each of the common emitter, common base and common collector configurations. The original modulus measurements were simply the magnitude and were converted to decibels on input to the computer program. Similarly, the measurements of the phase angles in degrees were discontinuous in an erratic manner, for example, the original phase readings for S_{11} in the common base configuration (included in Appendix 1) between the frequencies of 0.6 GHz and 0.9 GHz are 355.3°, -11.7°, -17.6° and 336.1° on consecutive readings. Therefore, although the data was read in to the computer program exactly as it was given, the phase angles were immediately converted to values between -180° and +180°. As the calculated phase angles of the models were produced in the same range, this made the calculation of the errors easier although the algorithm still had to check for cases where, for example, the measured phase angle was -178° and the calculated phase angle was +176°. In this case the correct absolute error is 6° and not 354°, thus the maximum absolute error possible in a phase angle is 180°. In the graphs that are shown later, the phase angles are made continuous over the frequency range, therefore the absolute values of the phase angles exceed 180° in some cases.

PRL also provided a general model which they had developed. This

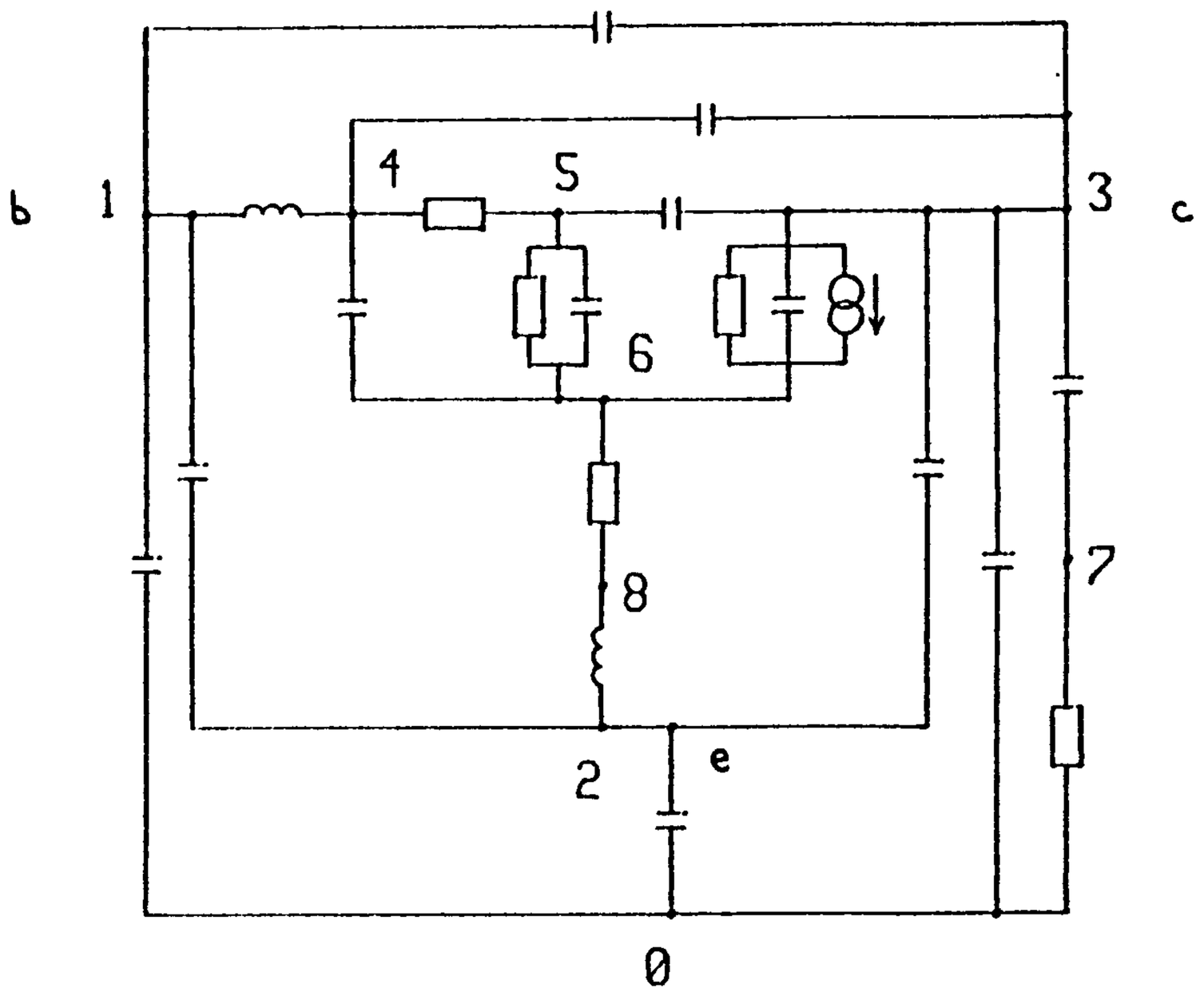

No. of nodes = 9
No. of elements = 20

R (4-5) = 1.13E+02 ohm
R (5-6) = 2.51E+03 ohm
R (3-6) = 9.43E+04 ohm
R (6-8) = 4.99E+00 ohm
R (7-0) = 6.03E+00 ohm
L (1-4) = 4.70E+00 nH
L (8-2) = 4.10E+00 nH
C (4-6) = 1.74E-03 nF
C (5-6) = 1.09E-02 nF
C (5-3) = 8.00E-05 nF
C (3-6) = -8.00E-05 nF
C (3-7) = 1.34E-03 nF
C (4-3) = 1.60E-04 nF
C (1-3) = 5.00E-05 nF
C (1-0) = 1.23E-03 nF
C (3-0) = 5.50E-04 nF
g (3-6) = 3.00E-02 S
(T = -1.00E-02 ns)
(V across nodes $^{5}_{6}$)
C (2-0) = 1.02E-03 nF
C (1-2) = 5.00E-05 nF
C (2-3) = 5.00E-05 nF

Node 1 - Base
Node 2 - Emitter
Node 3 - Collector
Node 0 - Ground

Figure 6.1 General Model of Vertical N-P-N Transistor Produced by Philips Research Laboratories

model is shown in Figure 6.1. In this diagram, node 1 is the base, node 2 is the emitter, node 3 is the collector and node 0 is ground. Thus, to obtain any particular configuration, the appropriate node has to be connected to node 0. This model was primarily a low frequency model and its s parameters give good agreement with the measurements at frequencies in the range 0.1 GHz to 0.3 GHz. However, at higher frequencies the errors become very large as can be seen in the graphs shown later. In each of these graphs, the black graph refers to this original model and is used for comparison purposes.

One interesting point about this model is that, although PRL stated a strong preference for the presence of physically realistic elements only in models produced for them, this model contains a negative-valued capacitor C_{3_6}.

This modelling problem was approached by attempting to model each configuration separately and to produce a single general model. The aim in each case was to improve the frequency range of the model without too great an increase in the numbers of nodes and elements in the model. Each of the parameters at every frequency was weighted equally, with a 1 dB error in the modulus having the same weighting as a 10° error in the phase.

The first individual models attempted were for the common emitter and common collector configurations. In each case the initial model was taken as the PRL general model with the appropriate terminal connected to ground. Of these two models, the common collector model produced a good result very quickly and with relatively few changes in the topology of the model. In the common emitter case, one node and several elements were deleted in Stage 1. The author therefore decided to try using the final common collector model, connected appropriately, as another initial model for the common emitter case. This model developed more rapidly to give another satisfactory result, which was included in the author's paper[73] describing the modelling algorithm. Following this,

the common base case was also attempted using the final common collector model as the basis for the initial model.

In attempting to develop a single general model for all three configurations, the major problem was one of size. In spite of this, two models were produced. The first of these used the PRL model as the initial model and this attempt was terminated when the model had reached such a level of complexity that firstly, it was considered that a more complex model would be inappropriate, and secondly, problems of computing time were being caused by the amount of calculation required. The second general model that was produced used as the initial model, a combination of those elements of the first individual models that were common to two or more of those models. The model developed from this contained one node more than the first model, but had fewer elements, and its overall error function value and maximum individual errors were smaller.

Full details of the development of these models together with graphs showing the accuracy of the results are given in the following sections of this chapter. In the graphs, in order to aid comparison of the errors, the vertical scales for each graph of modulus and of phase cover the same absolute ranges and the ranges of the modulus and phase are in the same ratio as the weighting factors applied to these.

Each of the models developed still bears some resemblance to the PRL model. The major feature of each of the new models is that there are more interconnections between the internal nodes. This would probably be expected since the PRL model was based on the primary theoretical aspects of the device being modelled. The new models improve on this approximation by including elements that model less significant characteristics of the device.

6.1. Common Collector Configuration

The initial model for the common collector configuration derived from the PRL general model in Figure 6.1 is the first model shown in Figure 6.2. Since the author's algorithm constrained the element values to take positive values only, the negative-valued capacitor, C_{4_7}, was given a value of 0.1 pF instead of -0.8 pF. This change in value actually reduced the overall error function, F, from 5.84E + 04 to 5.54E + 04. The r.m.s. errors given by the value of F = 5.54E + 04 were 2.4 dB and 24°. The maximum absolute errors were 3.6 dB and 85°, these occurring at the highest frequency.

After Stage 1, the model had been reduced from 7 nodes and 15 elements to 7 nodes and 12 elements. The new value of F was 1.12E + 03, already a significant reduction. This is the second model shown in Figure 6.2.

In Stage 2, there were several additions and deletions of elements and the details of these are given in Figure 6.2. The model obtained in Stage 2 was sufficiently accurate that Stage 3 was not entered. The final model thus obtained, the last model shown in Figure 6.2, consisted of 7 nodes and 15 elements and the value of F had been reduced in Stage 2 by a further factor of ten to 1.61E + 02. The r.m.s. errors of this final model were 0.13 dB and 1.3° and the maximum absolute errors were 0.32 dB and 1.74°. This model is extremely accurate and it could be that many people would find the simpler model obtained at the end of Stage 1 quite acceptable.

The graphs in Figures 6.3a and 6.3b show the s parameters of the final model in blue. As has already been mentioned, the scales of the Y axes of all the graphs in this chapter have been standardised to aid comparison of the errors. Thus the modulus scales cover a total range of 30 dB and the phase scales cover a total range of 300°. The black points

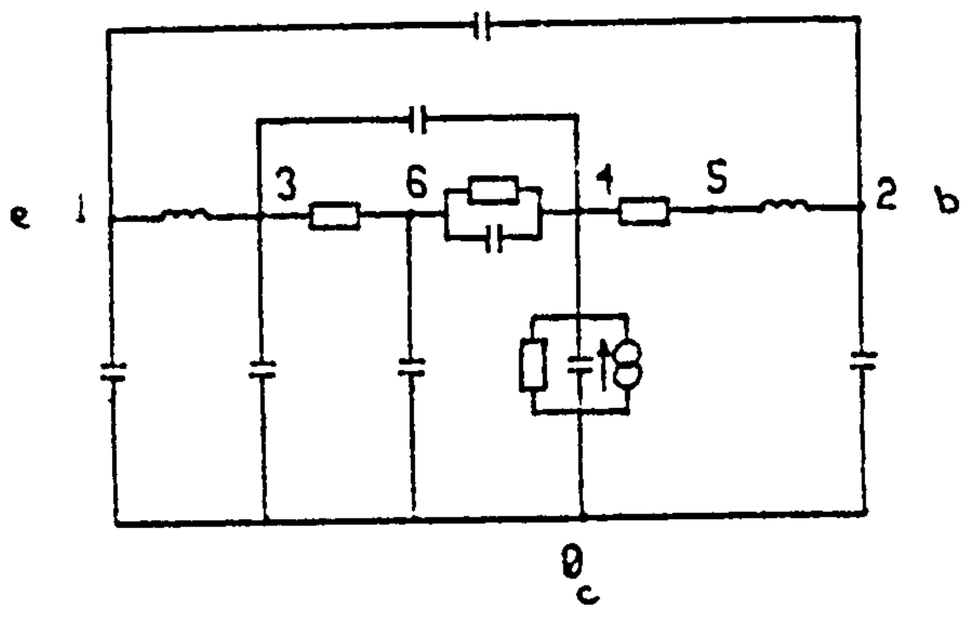

F = 5.54E+04

No. of nodes = 7
No. of elements = 15

R (3-6) = 1.12E+02 ohm
R (4-6) = 2.50E+03 ohm
R (4-0) = 9.43E+04 ohm
R (4-5) = 4.99E+00 ohm
L (1-3) = 4.70E+00 nH
L (5-2) = 4.10E+00 nH
C (1-0) = 5.00E-05 nF
C (3-0) = 1.60E-04 nF
C (3-4) = 1.74E-03 nF
C (4-6) = 1.09E-02 nF
C (6-0) = 8.00E-05 nF
C (4-0) = 1.00E-05 nF
C (2-0) = 5.00E-05 nF
C (1-2) = 5.00E-05 nF
g (0-4) = 3.00E-02 S
(T =-9.00E-03 ns, $^{6}_{4}$)
(V across nodes)

Delete R(4-6) , R(4-0)
Replace C(1-0) by R(1-0)
Delete C(2-0)

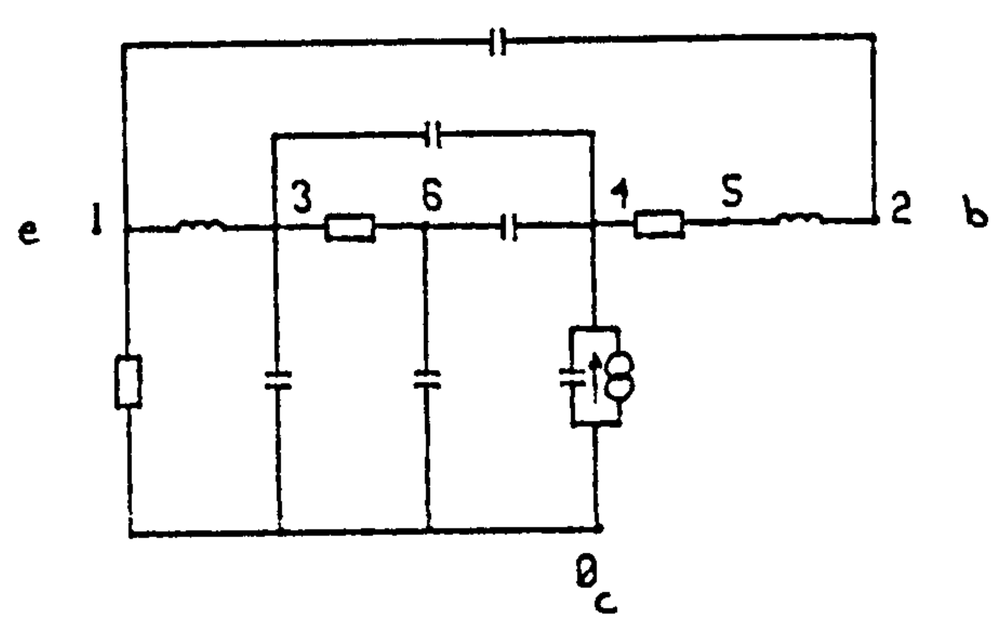

F = 1.12E+03

No. of nodes = 7
No. of elements = 12

R (3-6) = 8.92E+01 ohm
R (4-5) = 2.17E+01 ohm
L (1-3) = 6.52E+00 nH
L (5-2) = 3.09E+00 nH
R (1-0) = 3.20E+03 ohm
C (3-0) = 9.49E-04 nF
C (3-4) = 1.65E-03 nF
C (4-6) = 2.00E-02 nF
C (6-0) = 4.02E-04 nF
C (4-0) = 1.66E-03 nF
C (1-2) = 6.24E-04 nF
g (0-4) = 5.56E-02 S
(T = 3.55E-02 ns, $^{6}_{4}$)
(V across nodes)

Add C(1-4)
Replace C(1-2) by R(1-2)
Add C(1-6)
Add C(2-3) , Delete R(1-2)
Add C(2-0)
Add R(1-6) , Delete C(1-6) , C(2-3)

Add R(3-0) , Delete R(1-0)
Add C(5-6)
Add C(5-0) , Delete C(4-0)

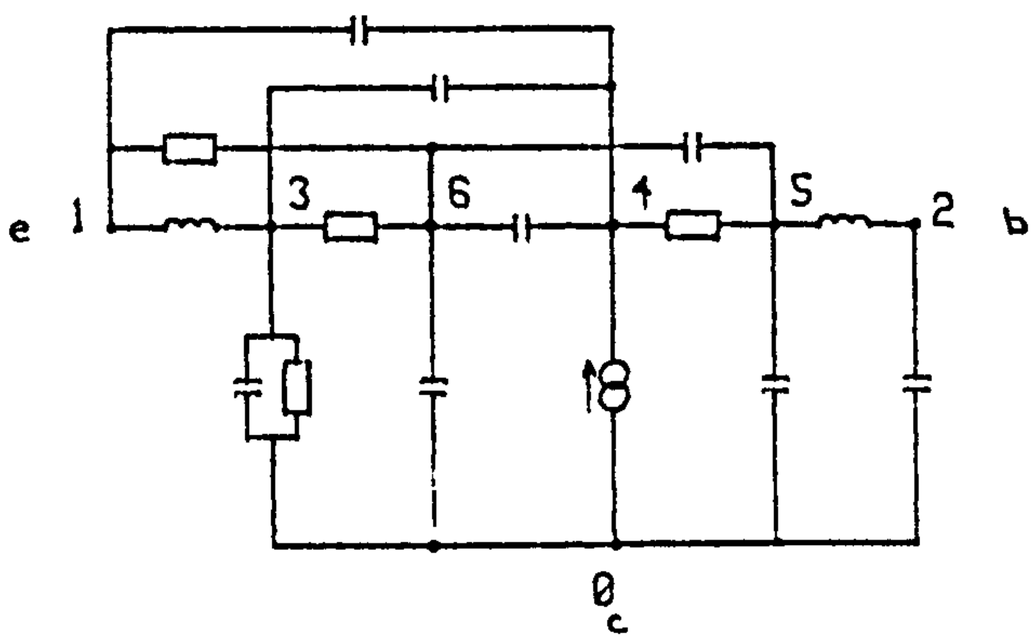

F = 1.61E+02

No. of nodes = 7
No. of elements = 15

R (3-6) = 2.01E+02 ohm
R (4-5) = 2.22E+01 ohm
L (1-3) = 1.08E+01 nH
L (5-2) = 7.70E+00 nH
C (3-0) = 1.41E-03 nF
C (3-4) = 2.12E-04 nF
C (4-6) = 1.94E-02 nF
C (6-0) = 1.86E-04 nF
g (0-4) = 5.71E-02 S
(T = 7.00E-02 ns, $^{6}_{4}$)
(V across nodes)
C (1-4) = 2.56E-03 nF
C (2-0) = 8.25E-04 nF
R (1-6) = 1.41E+02 ohm
R (3-0) = 1.48E+04 ohm
C (5-6) = 8.95E-04 nF
C (5-0) = 1.83E-04 nF

Node 1 - Emitter
Node 2 - Base
Node 0 - Collector

Figure 6.2 Modelling the Common Collector Configuration

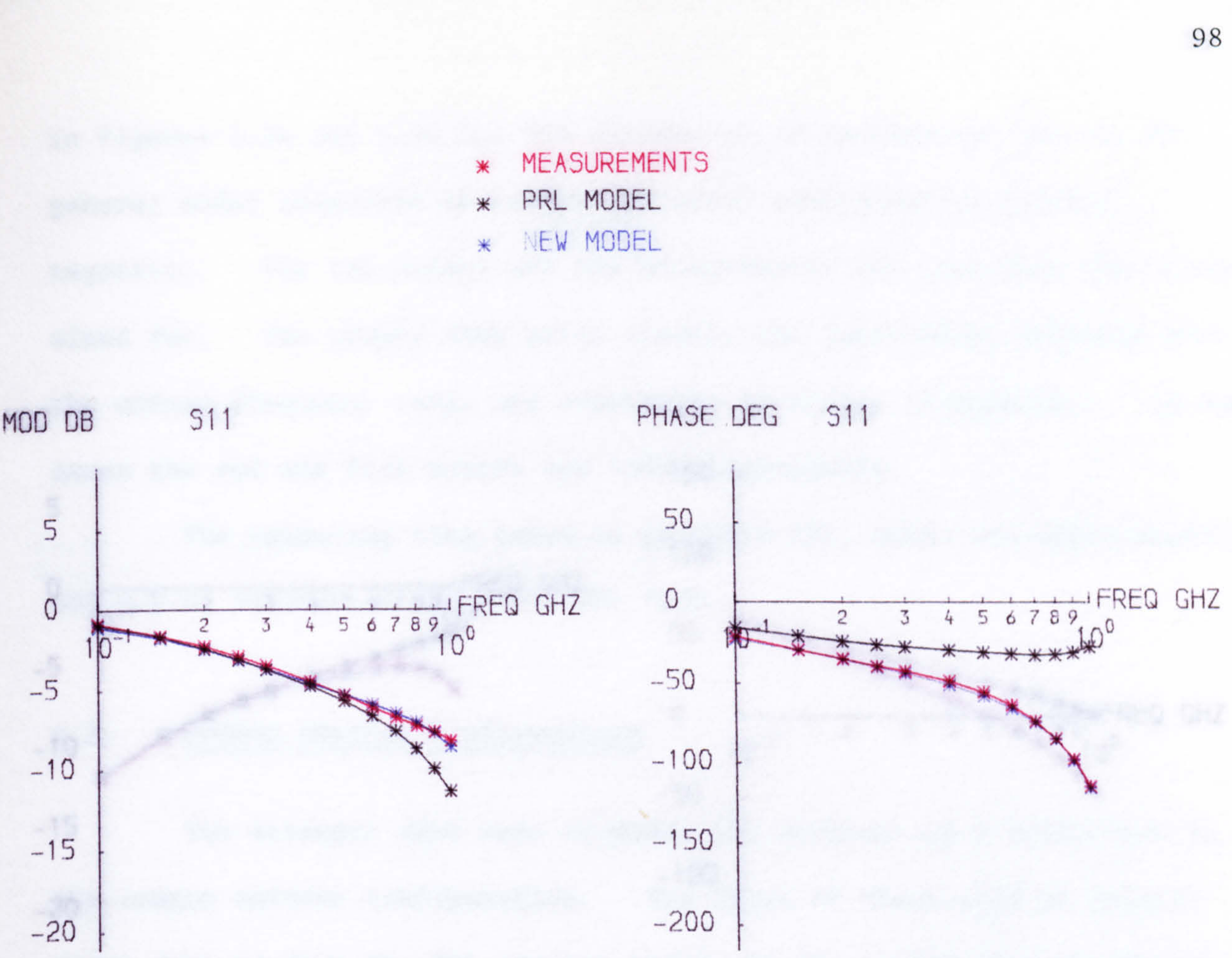

Figure 6.3a S_{11} and S_{21} in Common Collector Configuration

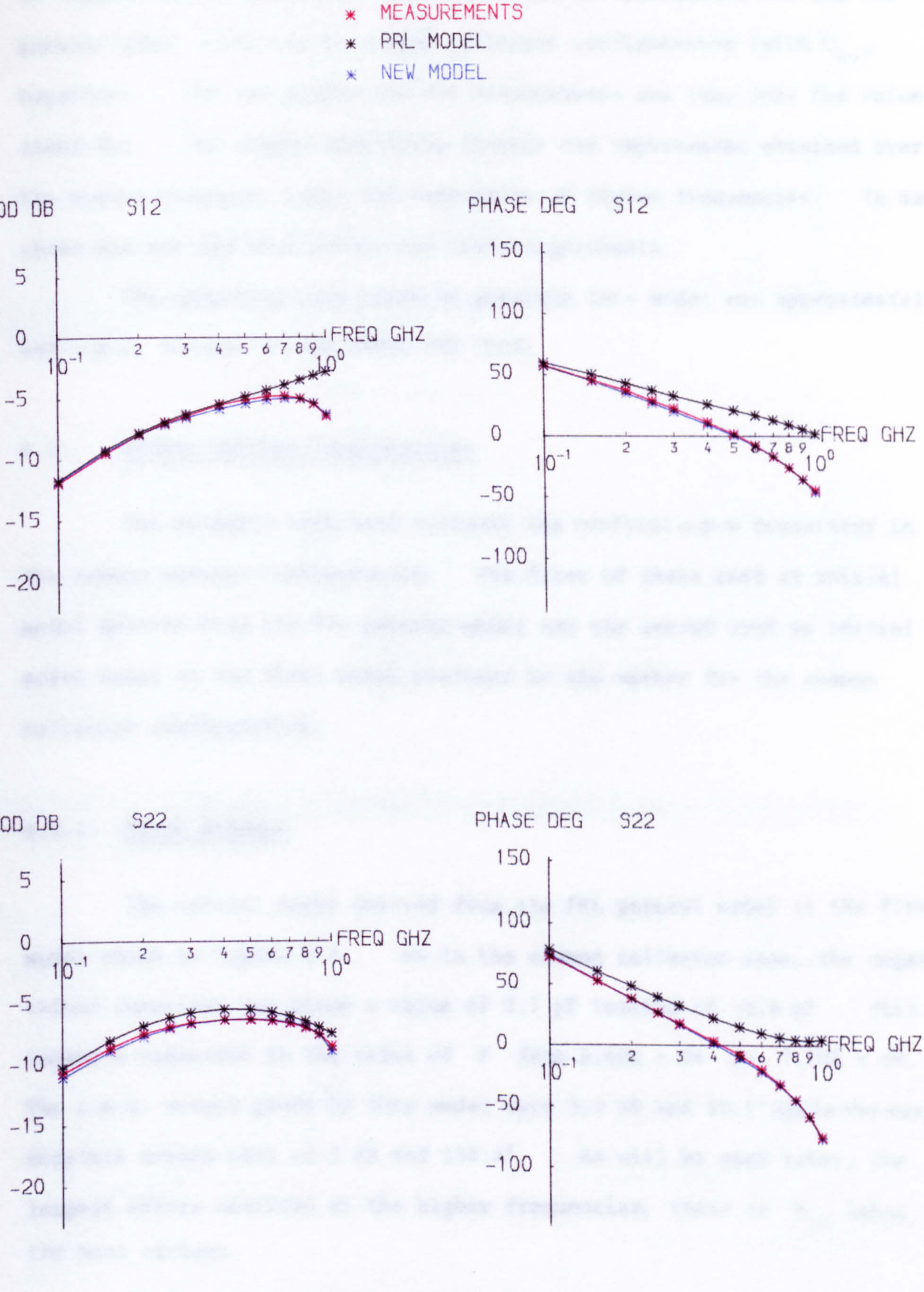

Figure 6.3b S_{12} and S_{22} in Common Collector Configuration

in Figures 6.3a and 6.3b are the calculated s parameters for the PRL general model connected in common collector configuration (with C_{4-7} negative). The red points are the measurements and thus show the values aimed for. The graphs show quite clearly the improvement obtained over the entire frequency range and especially at higher frequencies. In many cases the red and blue points are indistinguishable.

The computing time taken to generate this model was approximately 600 c.p.u. seconds on the UMRCC CDC 7600.

6.2. Common Emitter Configuration

Two attempts were made to model the vertical n-p-n transistor in the common emitter configuration. The first of these used an initial model derived from the PRL general model and the second used an initial model based on the final model produced by the author for the common collector configuration.

6.2.1. First Attempt

The initial model derived from the PRL general model is the first model shown in Figure 6.4. As in the common collector case, the negative-valued capacitor was given a value of 0.1 pF instead of -0.8 pF. This caused a reduction in the value of F from 8.60E + 04 to 7.72E + 04. The r.m.s. errors given by this model were 3.0 dB and 30.1° while the maximum absolute errors were 10.3 dB and 134.4°. As will be seen later, the largest errors occurred at the higher frequencies, those on s_{12} being the most obvious.

After Stage 1, the model had been reduced to 6 nodes and 10 elements giving a value of F = 1.45E + 04. The model giving this first local minimum is the second model in Figure 6.4. The maximum errors in

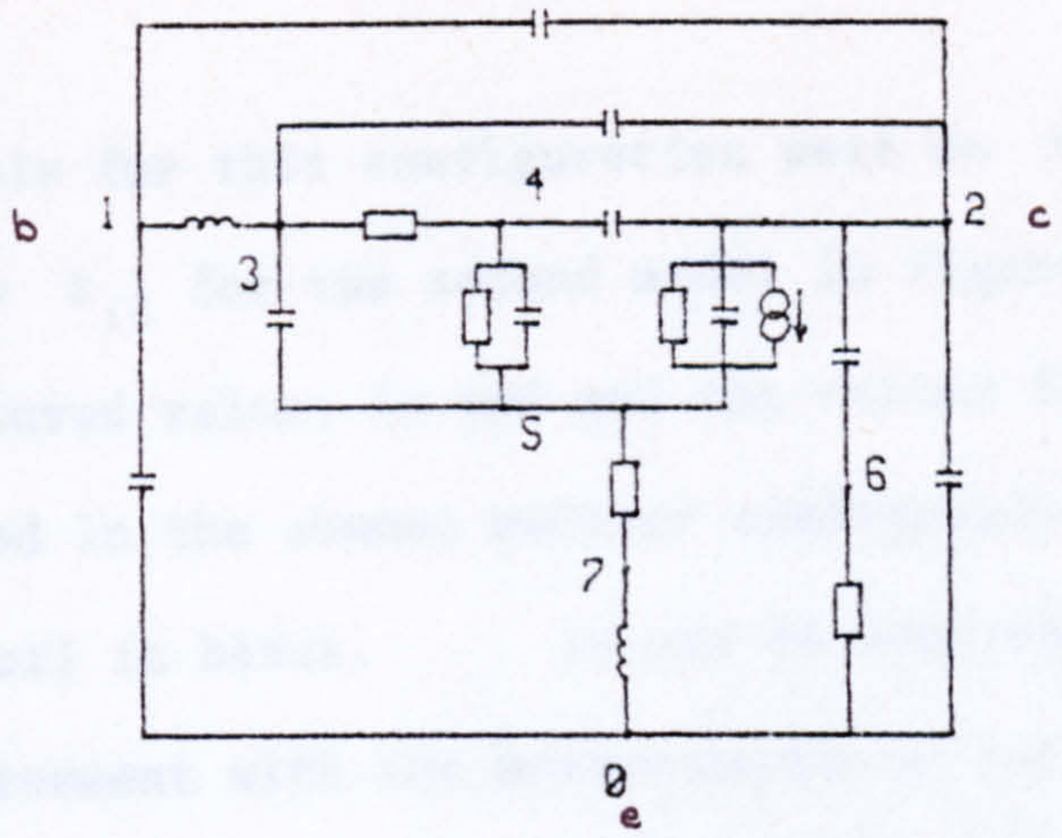

F = 7.72E+01

No. of nodes = 8
No. of elements = 17

R (3-4) = 1.13E+02 ohm
R (4-5) = 2.50E+03 ohm
R (2-5) = 9.43E+04 ohm
R (5-7) = 4.99E+00 ohm
R (6-0) = 6.03E+00 ohm
L (1-3) = 4.70E+00 nH
L (7-0) = 4.10E+00 nH
C (3-5) = 1.74E-03 nF
C (4-5) = 1.09E-02 nF
C (4-2) = 8.00E-05 nF
C (2-5) = 1.00E-05 nF
C (2-6) = 1.34E-03 nF
C (3-2) = 1.60E-04 nF
C (1-2) = 5.00E-05 nF
C (1-0) = 1.23E-03 nF
C (2-0) = 5.50E-04 nF
g (2-5) = 3.00E-02 S
(T =-1.00E-02 ns)
(V across nodes $^{4}_{5}$)

Delete L(1-3) (deleting node) , Combine C(1-2) with C(3-2)
Delete R(2-5) , R(5-7) , C(2-5) , C(1-0) , C(2-0)

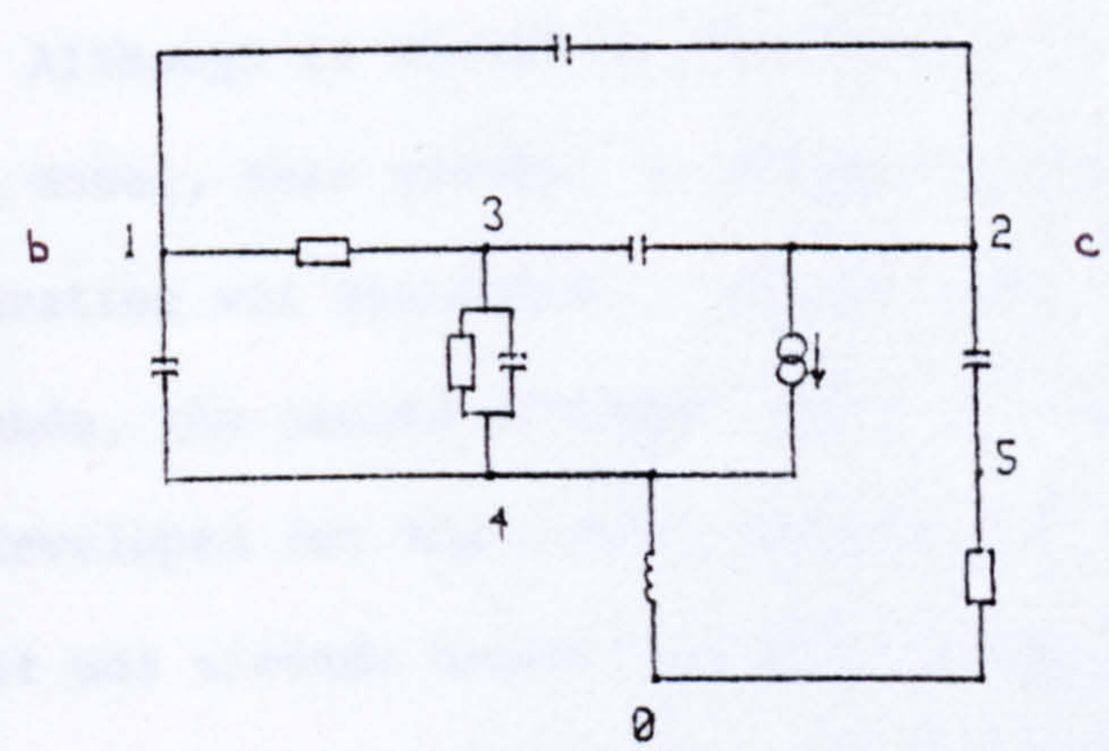

F = 1.45E+01

No. of nodes = 6
No. of elements = 10

R (1-3) = 9.60E+01 ohm
R (3-4) = 3.46E+02 ohm
R (5-0) = 2.83E+01 ohm
L (4-0) = 7.14E+00 nH
C (1-4) = 2.03E-03 nF
C (3-4) = 1.10E-02 nF
C (3-2) = 4.31E-04 nF
C (2-5) = 1.90E-03 nF
C (1-2) = 1.09E-04 nF
g (2-4) = 2.61E-02 S
(T =-1.26E-01 ns)
(V across nodes $^{3}_{1}$)

Node 1 - Base
Node 2 - Collector
Node 0 - Emitter

Figure 6.4 Modelling the Common Emitter Configuration (First Attempt)

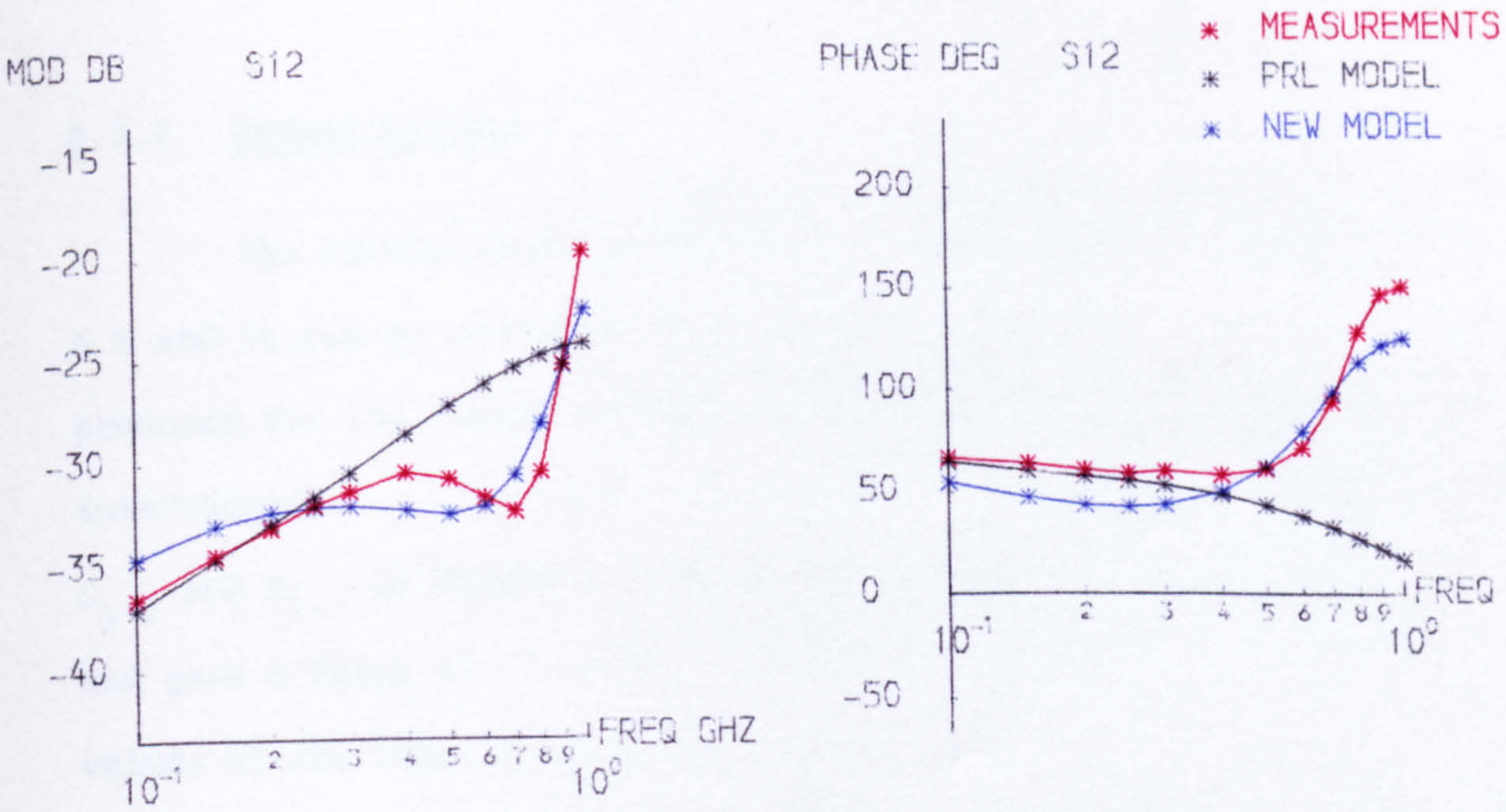

Figure 6.5 Graphs of S_{12} for Model in Figure 6.4

the models for this configuration were on s_{12} and the graphs in Figure 6.5 show s_{12} for the second model in Figure 6.4 in blue, together with the measured values in red and the values for the PRL general model connected in the common emitter configuration (with the negative-valued capacitor) in black. It can be seen that while the PRL model gives good agreement with the measurements at low frequencies the model is very poor at high frequencies, but the reduced model gives similar errors over the entire frequency range.

Although it should be feasible to build up a model from this reduced model, this attempt to produce a model for the common emitter configuration was abandoned. At the same time as this first attempt was being made, the second attempt, using an initial model based on the final model developed for the common collector case, was also being made. Thus, it was already known that the second attempt had produced, after Stage 1, a model with more nodes and elements which gave a considerably lower value of F . It was therefore decided that the second attempt showed more promise and should be continued in preference to the first attempt.

6.2.2. Second Attempt

The initial model used in the second attempt is shown in Figure 6.6 and it can be seen that this model is identical to the final model produced for the common collector configuration but with nodes 2 and 0 interchanged. This model, in particular, lacked the substrate elements, C_{3-7} and R_{7-0} in Figure 6.1, that were present in the PRL general model, and gave a value of F = 4.95E + 05 with correspondingly high absolute values of the individual errors.

However, in Stage 1 only one element was deleted together with one capacitor being replaced by a resistor, resulting in the second model

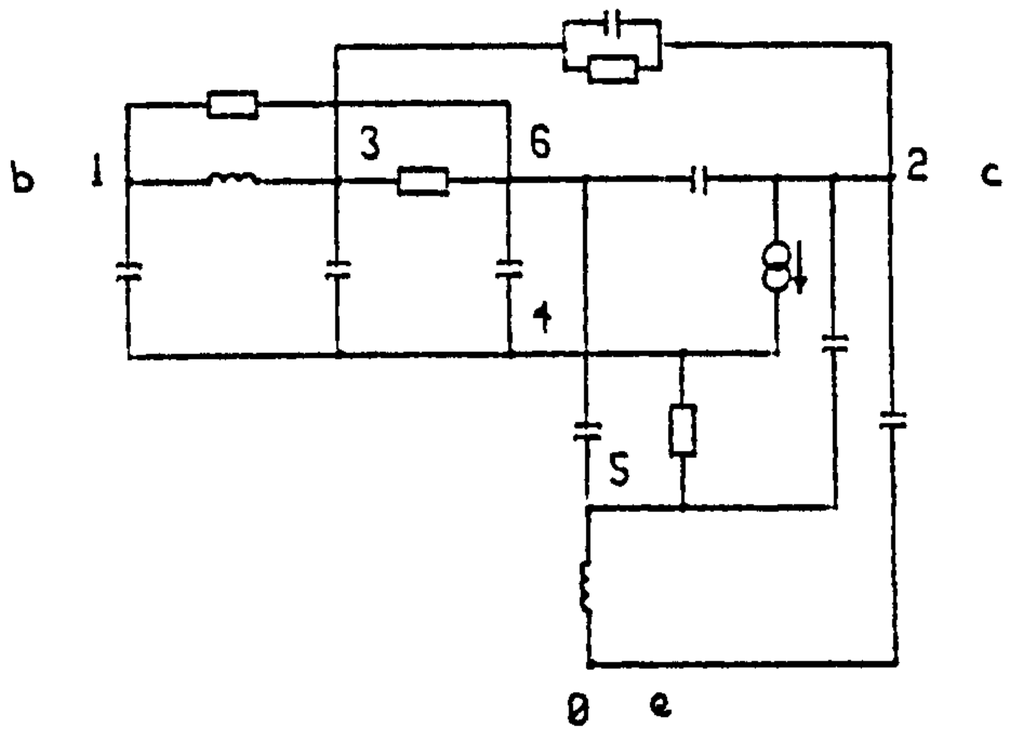

F = 4.95E+05

No. of nodes = 7
No. of elements = 15

R (3-6) = 2.01E+02 ohm
R (4-5) = 2.22E+01 ohm
L (1-3) = 1.08E+01 nH
L (5-0) = 7.70E+00 nH
C (3-2) = 1.41E-03 nF
C (3-4) = 2.12E-04 nF
C (4-6) = 1.94E-02 nF
C (6-2) = 1.86E-04 nF
g (2-4) = 5.71E-03 S
(T = 7.00E-02 ns)
(V across nodes $\frac{6}{4}$)
C (1-4) = 2.56E-03 nF
C (2-0) = 8.25E-04 nF
R (1-6) = 1.41E+02 ohm
R (3-2) = 1.48E+04 ohm
C (5-6) = 8.95E-04 nF
C (5-2) = 1.83E-04 nF

Delete C(3-4)
Replace C(5-6) by R(5-6)

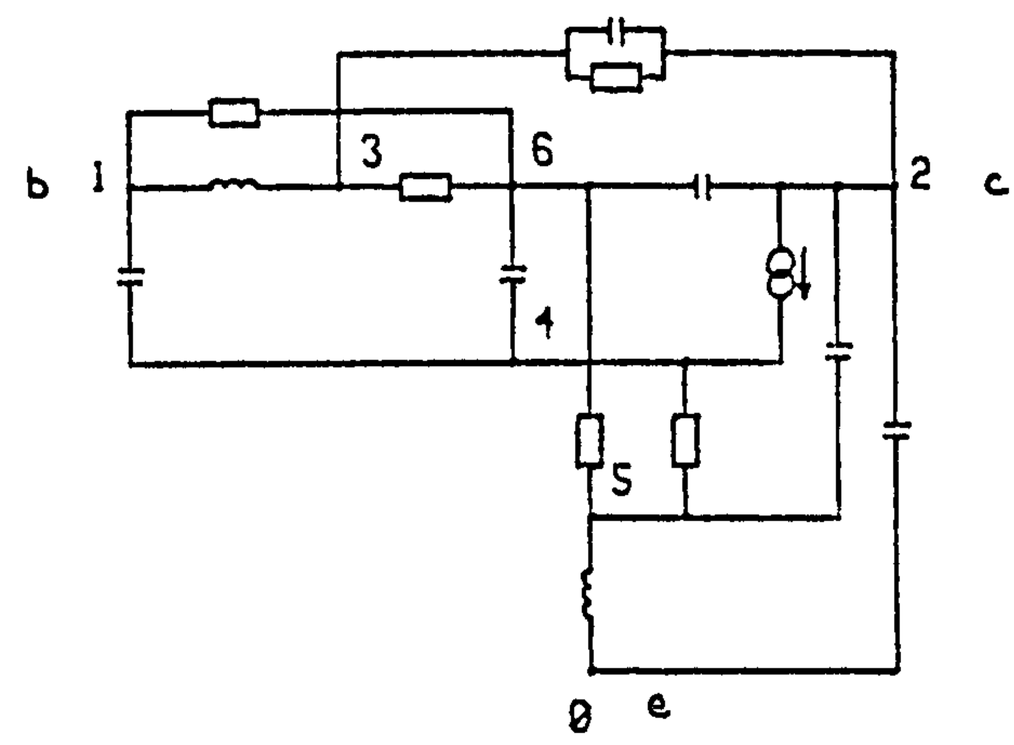

F = 1.77E+03

No. of nodes = 7
No. of elements = 14

R (3-6) = 9.19E+02 ohm
R (4-5) = 2.22E+01 ohm
L (1-3) = 1.17E+02 nH
L (5-0) = 3.33E+00 nH
C (3-2) = 2.42E-04 nF
C (4-6) = 1.73E-02 nF
C (6-2) = 3.68E-05 nF
g (2-4) = 4.31E-02 S
(T =-5.76E-02 ns)
(V across nodes $\frac{6}{4}$)
C (1-4) = 3.34E-03 nF
C (0-2) = 8.90E-04 nF
R (1-6) = 8.05E+01 ohm
R (3-2) = 3.63E+04 ohm
R (5-6) = 1.94E+03 ohm
C (5-2) = 1.19E-03 nF

Add R(1-4) ; Delete R(5-6)
Add R(1-5) ; Delete R(1-4)
Add R(1-0) ; Delete R(1-5)
Add R(2-4) ; Delete C(6-2)
Add R(2-0)
Add new node with L(2-7)

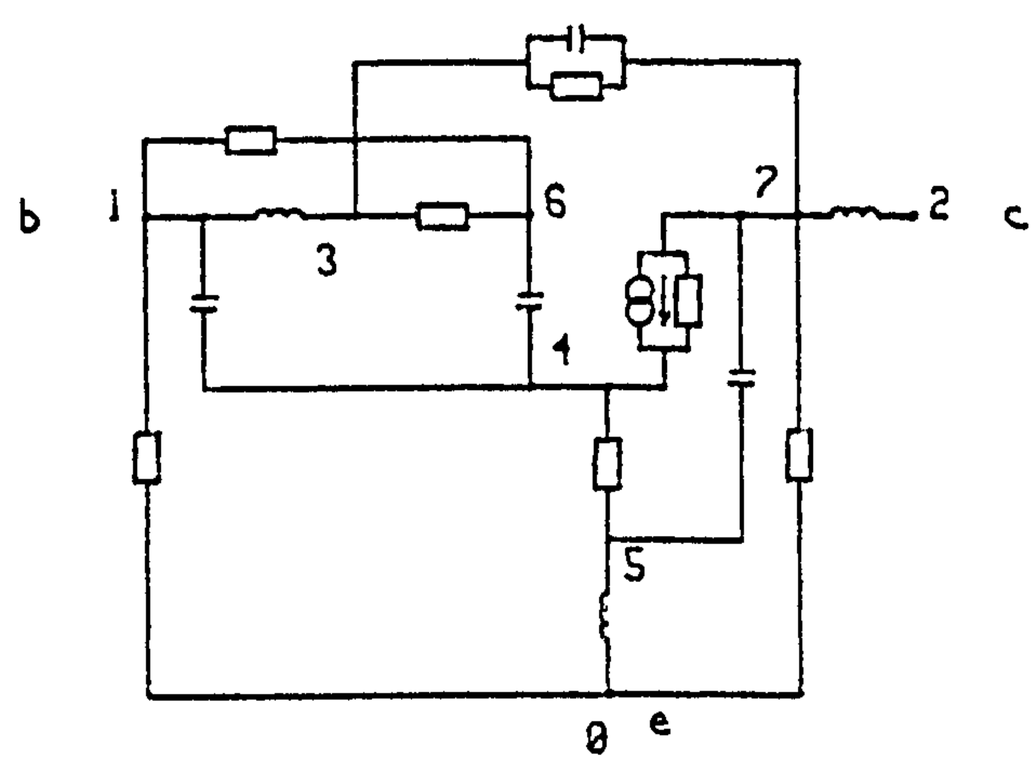

F = 9.84E+02

No. of nodes = 8
No. of elements = 15

R (3-6) = 1.21E+03 ohm
R (4-5) = 3.32E+01 ohm
L (1-3) = 1.65E+02 nH
L (5-0) = 2.37E+00 nH
C (3-7) = 1.97E-04 nF
C (4-6) = 2.94E-02 nF
g (7-4) = 7.72E-02 S
(T =-3.62E-02 ns)
(V across nodes $\frac{6}{4}$)
C (1-4) = 4.29E-03 nF
R (1-6) = 8.10E+01 ohm
R (3-7) = 1.66E+05 ohm
C (5-7) = 1.69E-03 nF
R (1-0) = 8.95E+02 ohm
R (7-4) = 2.90E+03 ohm
R (7-0) = 1.18E+04 ohm
L (2-7) = 3.48E+00 nH

Add R(3-5)

Node 1 - Base
Node 2 - Collector
Node 0 - Emitter

Figure 6.6 Modelling the Common Emitter Configuration (Second Attempt)

shown in Figure 6.6 which had a value of F = 1.77E + 03.

In Stage 2 a number of additions and deletions were made resulting in a model consisting of 7 nodes and 15 elements giving a value of F = 1.45E + 03.

On entry to Stage 3 a new node was added by inserting an inductor at node 2, the collector terminal. This was an interesting development since PRL had stated that they had wanted an inductor at the collector terminal of their model but had been unable to insert one successfully. This new addition gave the last model shown in Figure 6.6 which had a value of F = 9.84E + 02.

Re-entry to Stage 2 resulted in one further element addition giving the final model shown in Figure 6.7. This final model consisted of 8 nodes and 16 elements and gave a value of F = 8.81E + 02. The r.m.s. errors were 0.30 dB and 3.0° and the maximum absolute errors were 1.56 dB and 4.1°.

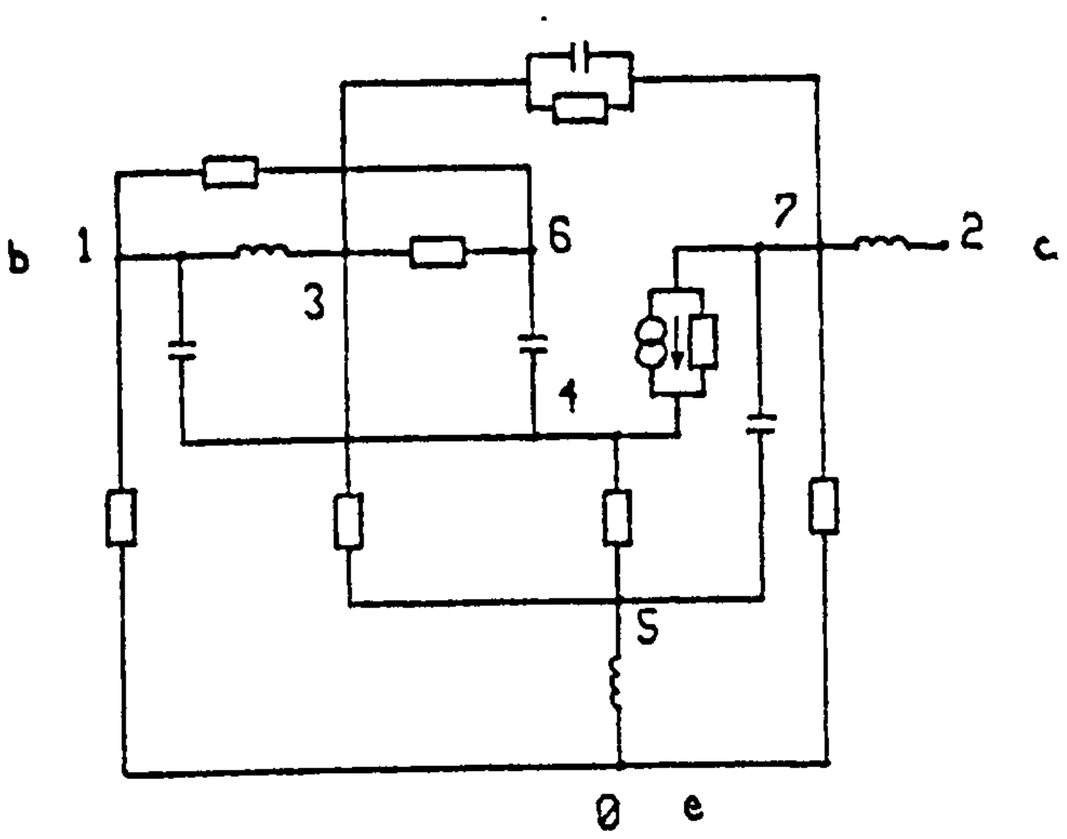

F = 8.81E+02

No. of nodes = 8
No. of elements = 16

R (3-6) = 1.63E+03 ohm
R (4-5) = 3.27E+01 ohm
L (1-3) = 1.39E+02 nH
L (5-0) = 2.38E+00 nH
C (3-7) = 2.09E-04 nF
C (4-6) = 3.11E-02 nF
g (7-4) = 8.20E-02 S
(T = -3.06E-02 ns)
(V across nodes 5,4)
C (1-4) = 4.41E-03 nF
R (1-6) = 8.18E+01 ohm
R (3-7) = 7.15E+05 ohm
C (5-7) = 1.65E-03 nF
R (1-0) = 1.41E+03 ohm
R (7-4) = 3.23E+03 ohm
R (7-0) = 5.98E+03 ohm
L (2-7) = 3.59E+00 nH
R (3-5) = 3.32E+03 ohm

Node 1 - Base
Node 2 - Collector
Node 0 - Emitter

Figure 6.7 Final Model for Common Emitter Configuration

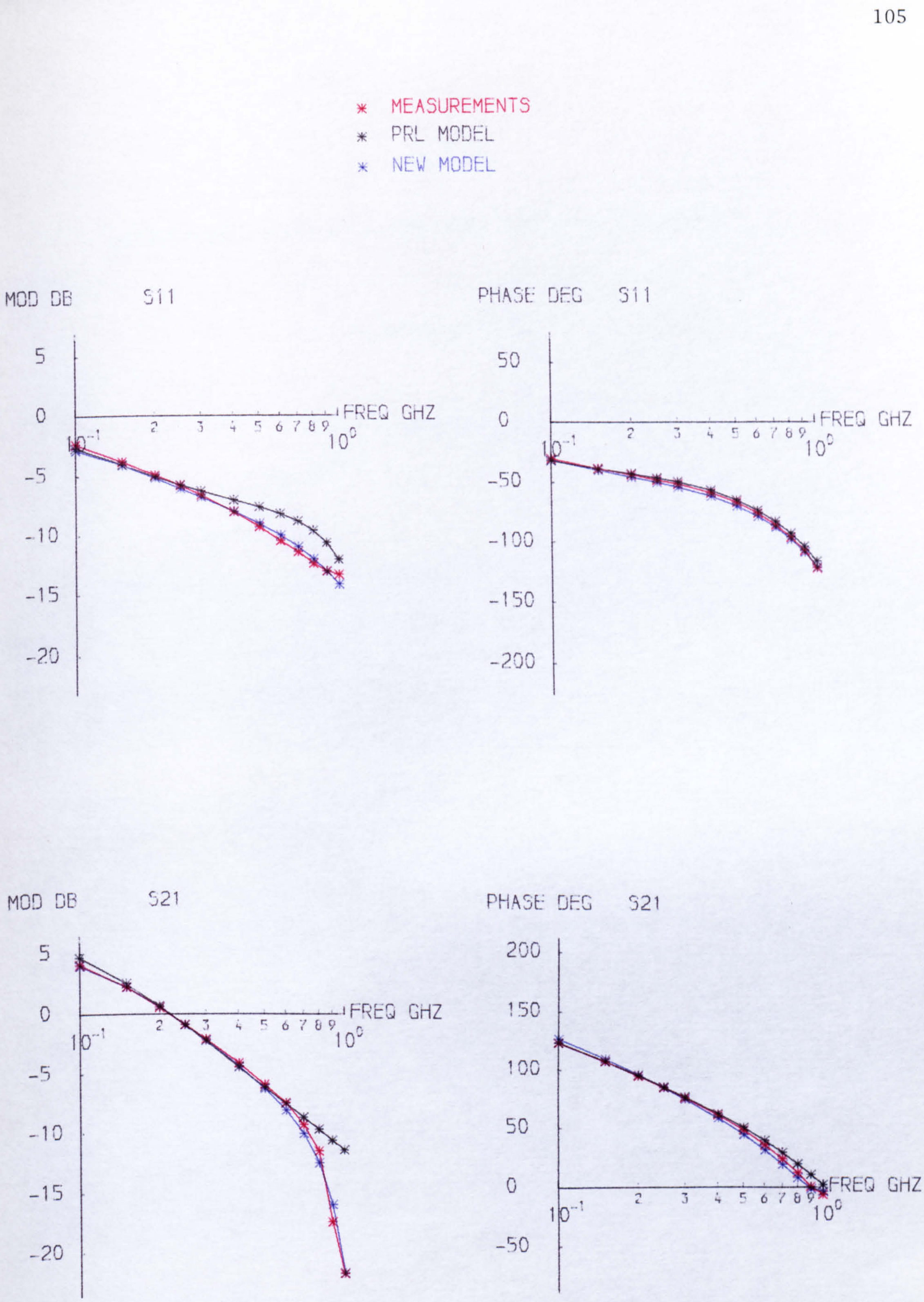

Figure 6.8a S_{11} and S_{21} of Final Model for Common Emitter Configuration

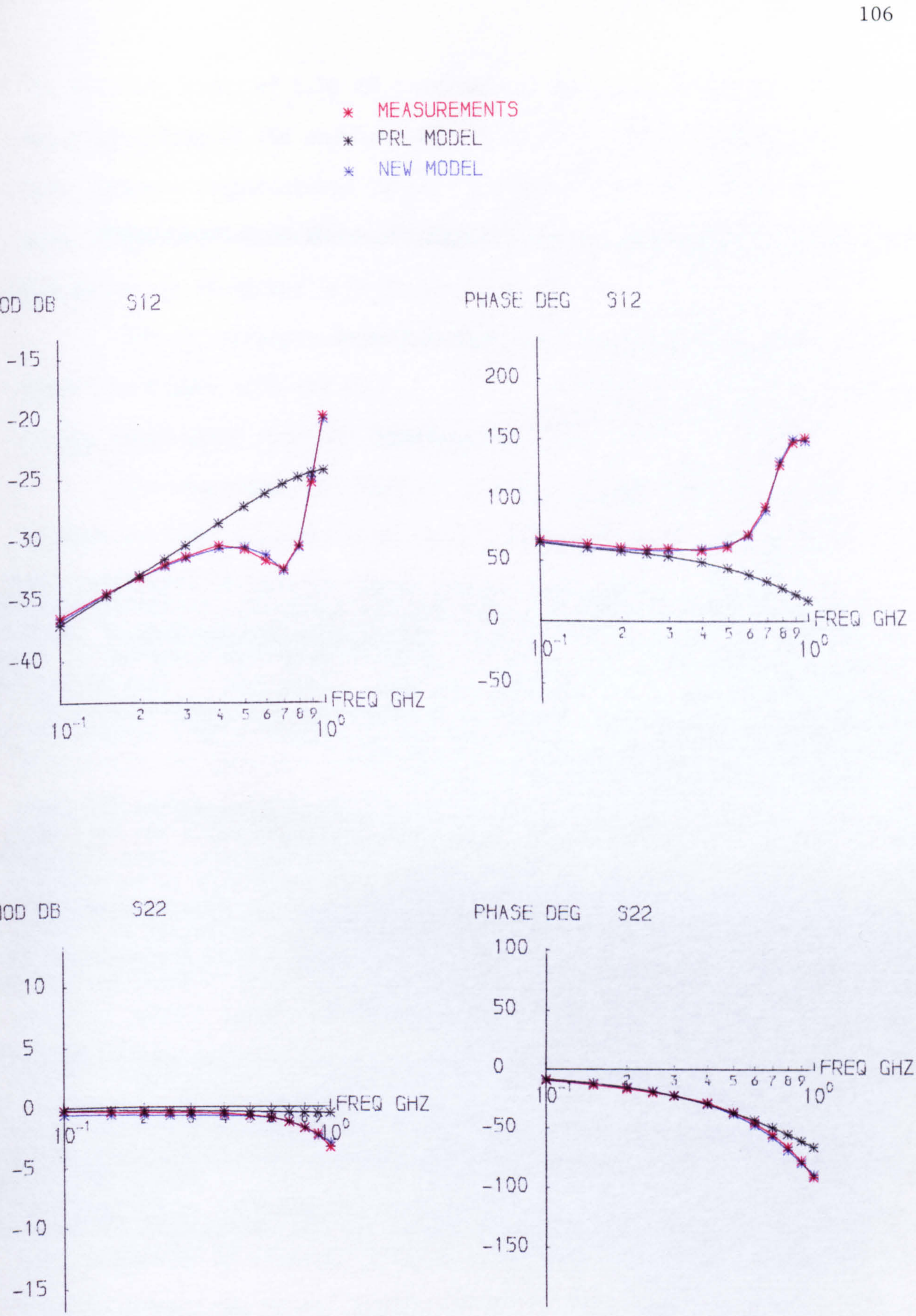

Figure 6.8b $\underline{S}_{12}$ and $\underline{S}_{22}$ of Final Model for Common Emitter Configuration

The absolute error of 1.56 dB occurred on s_{21} at a frequency of 0.9 GHz where the value of the modulus was -17.52 dB. Thus, although this error appears comparatively large, it might not be considered to be of great significance. The next highest absolute errors in the moduli were 0.9 dB in -11.54 dB and 0.73 dB in -13.23 dB.

The s parameters of this final model are shown in blue in the graphs in Figure 6.8a and 6.8b. It can be seen that they are a considerable improvement over the values given by the PRL general model.

The computing time taken to generate the final model in the second attempt was approximately 1900 c.p.u. seconds on the UMRCC CDC 7600.

6.3. Common Base Configuration

The model for the common base configuration based on the PRL general model with the negative-valued capacitor gave a value of F = 1.67E + 05. Changing the value of this capacitor from -0.8 pF to 0.1 pF, changed the value of F to 2.12E + 05. Using this model consisting of 8 nodes and 17 elements as an initial model, Stage 1 failed to find a local minimum. The attempt was terminated after indications that either the voltage controlled current generator should be removed or the nodes across which the controlling voltage was taken should be made short-circuit.

In view of the results described in Section 6.2, an initial model based on the author's final model for the common collector configuration was then used. This is the first model shown in Figure 6.9 and consisted of 7 nodes and 15 elements giving a value of F = 8.65E + 05. As with the initial model used in the second attempt for the common emitter configuration, this initial model lacked the substrate elements that were present in the PRL general model.

In Stage 1, three elements were removed, resulting in the second model shown in Figure 6.9, which gave a value of F = 3.09E + 03.

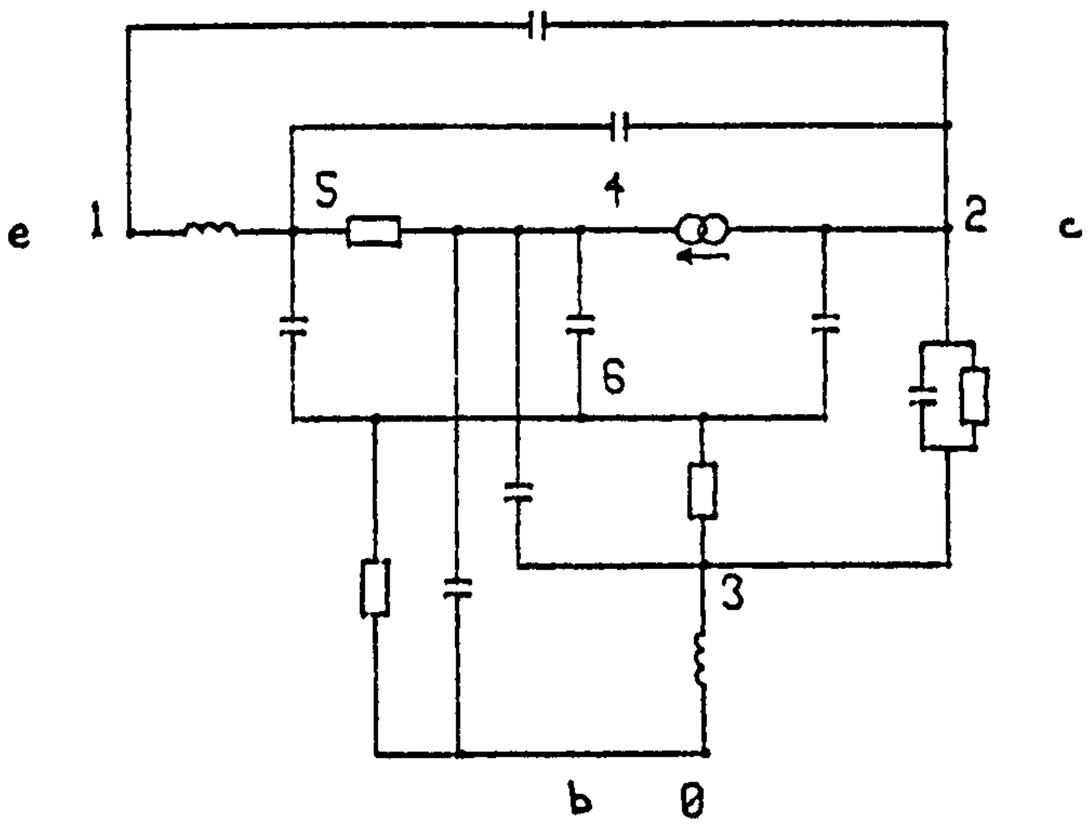

F = 8.65E+05

No. of nodes = 7
No. of elements = 15

R (3-6) = 2.01E+02 ohm
R (4-5) = 2.22E+01 ohm
L (0-3) = 1.08E+01 nH
L (5-1) = 7.70E+00 nH
C (3-2) = 1.41E-03 nF
C (3-4) = 2.12E-04 nF
C (4-6) = 1.94E-02 nF
C (6-2) = 1.86E-04 nF
g (2-4) = 5.71E-02 S
(T = 7.00E-02 ns)
(V across nodes 5,4)
C (0-4) = 2.56E-03 nF
C (1-2) = 8.25E-04 nF
R (0-6) = 1.41E+02 ohm
R (3-2) = 1.48E+04 ohm
C (5-6) = 8.95E-04 nF
C (5-2) = 1.83E-04 nF

Delete R(3-6) , C(4-6) , C(5-2)
Replace C(1-2) by R(1-2)

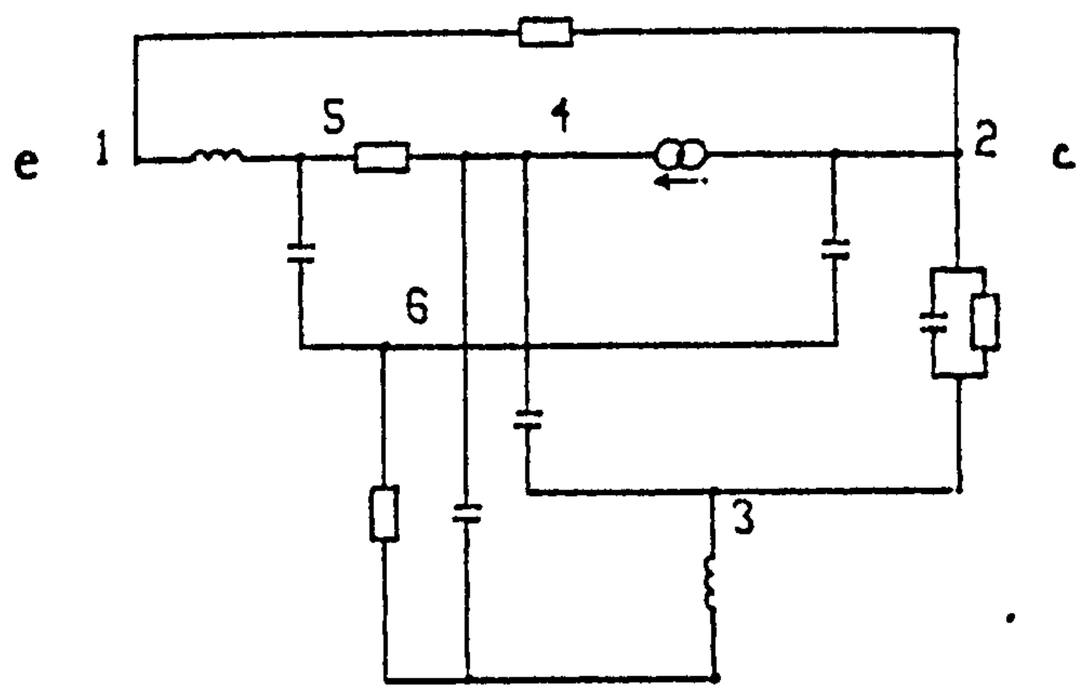

F = 3.09E+03

No. of nodes = 7
No. of elements = 12

R (4-5) = 4.98E+00 ohm
L (0-3) = 8.50E+00 nH
L (5-1) = 4.24E+00 nH
C (3-2) = 1.55E-03 nF
C (3-4) = 4.48E-04 nF
C (6-2) = 1.02E-04 nF
g (2-4) = 2.90E-02 S
(T =-1.39E-01 ns)
(V across nodes 5,4)
C (0-4) = 8.77E-04 nF
R (1-2) = 4.20E+04 ohm
R (0-6) = 7.64E+01 ohm
R (3-2) = 1.35E+03 ohm
C (5-6) = 1.36E-02 nF

Add C(1-3) , C(1-0)
Add C(2-0) , Delete R(1-2) , R(4-5) (deleting node)

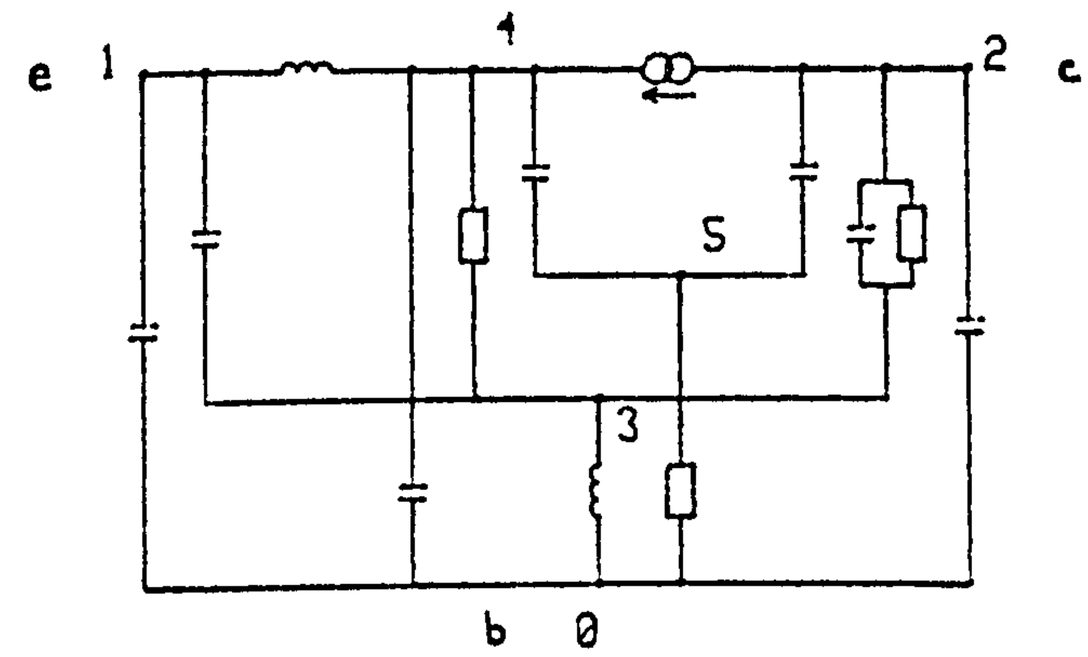

F = 1.88E+03

No. of nodes = 6
No. of elements = 13

L (0-3) = 1.78E+01 nH
L (4-1) = 1.31E+01 nH
C (3-2) = 7.35E-04 nF
R (3-4) = 1.40E+03 ohm
C (5-2) = 8.91E-05 nF
g (2-4) = 2.51E-02 S
(T =-9.27E-03 ns)
(V across nodes 5,4)
C (0-4) = 1.77E-03 nF
R (0-5) = 9.35E+01 ohm
R (3-2) = 1.81E+03 ohm
C (4-5) = 8.64E-03 nF
C (1-3) = 4.32E-04 nF
C (1-0) = 1..8E-03 nF
C (2-0) = 1.26E-03 nF

Add C(1-2) , C(5-0)
Add R(1-4) , Delete C(0-4) , C(1-2) , R(3-4)
Add C(1-2) , C(4-0)
Add new node with R(6-2)

Node 1 - Emitter
Node 2 - Collector
Node 0 - Base

Figure 6.9 Modelling the Common Base Configuration

In Stage 2, during the addition and deletion of elements, one node was also deleted. The model produced after deletion of this node is the third model in Figure 6.9. This model gave a value of F = 1.88E + 03. Continuing in Stage 2, further elements were added and deleted, C_{1-2} being added, then removed and then added again, until a model having 6 nodes and 15 elements giving a value of F = 6.92E + 02 was produced.

Although sufficient accuracy had already been obtained, an entry into Stage 3 resulted in the addition of a new node which created the substrate elements in a similar form to those in the PRL general model. The value of F was also reduced to 3.63E + 02. This final model, which is shown in Figure 6.10 gave r.m.s. errors of 0.2 dB and 1.9°. The maximum absolute errors were 0.7 dB and 3.4°.

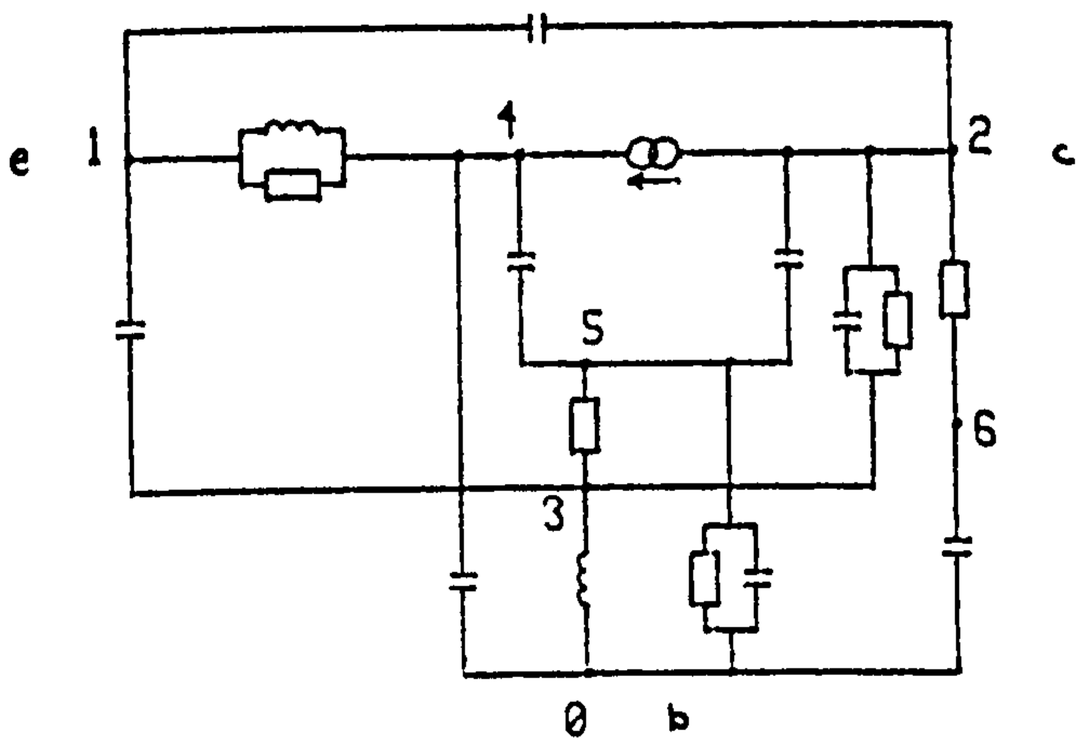

F = 3.63E+02

No. of nodes = 7
No. of elements = 16

L (0-3) = 1.88E+01 nH
L (4-1) = 3.03E+01 nH
C (3-2) = 6.77E-04 nF
C (5-2) = 1.99E-04 nF
g (2-4) = 2.62E-02 S
(T =-1.88E-01 ns)
(V across nodes 5,4)
R (0-5) = 3.40E+01 ohm
R (3-2) = 1.47E+04 ohm
C (4-5) = 1.04E-02 nF
C (1-3) = 3.91E-04 nF
C (6-0) = 1.42E-03 nF
C (5-0) = 1.11E-02 nF
R (1-4) = 8.75E+01 ohm
R (3-5) = 8.98E+02 ohm
C (1-2) = 5.97E-05 nF
C (4-0) = 1.75E-03 nF
R (6-2) = 4.98E+01 ohm

Node 1 - Emitter
Node 2 - Collector
Node 0 - Base

Figure 6.10 Final Model for Common Base Configuration

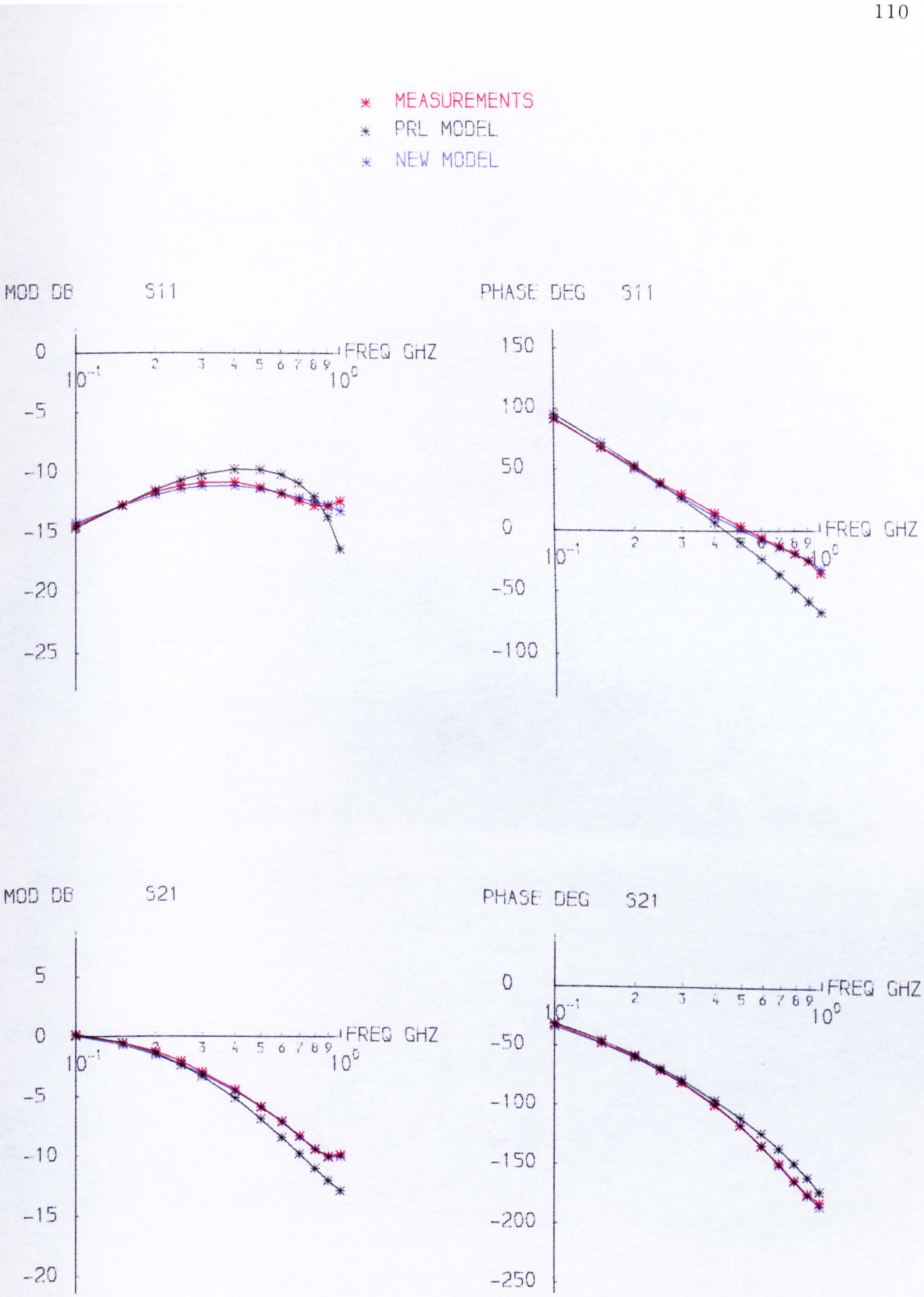

Figure 6.11a S_{11} and S_{21} in Common Base Configuration

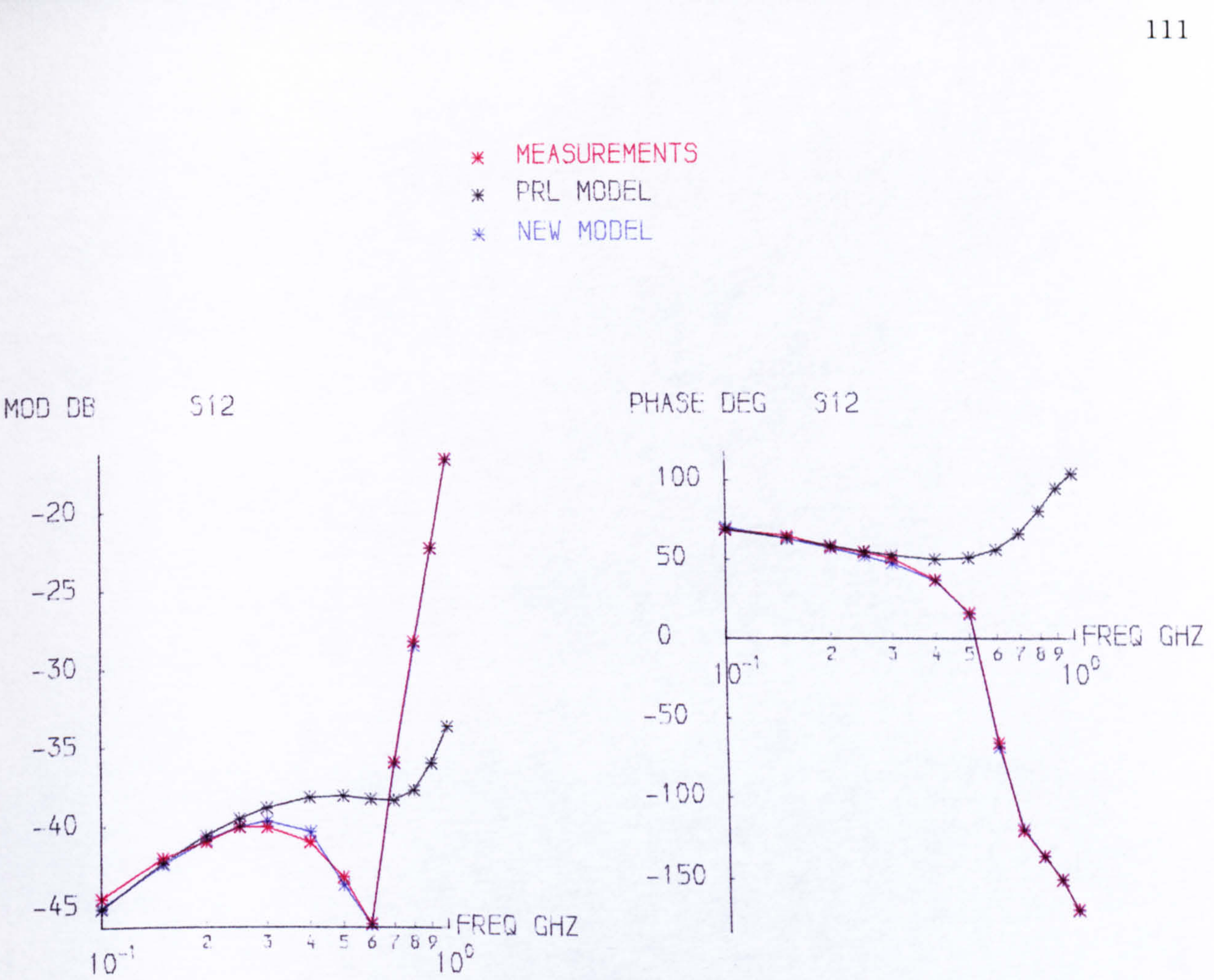

Figure 6.11b S_{12} and S_{22} in Common Base Configuration

As can be seen from the graphs in Figures 6.11a and 6.11b, this final model gives excellent agreement with the measured s parameters and is a considerable improvement over the PRL general model.

The computing time taken to generate this model was approximately 1120 c.p.u. seconds on the UMRCC CDC 7600.

6.4. General Model

The total computing time taken to generate the three individual models for the different configurations of the vertical n-p-n transistor was approximately 3620 c.p.u. seconds. If all the available data was to be used in an attempt to produce a general model, then it was only to be expected that the analysis of the errors at any particular stage would take at least three times as long as for the individual models. Furthermore, as the number of nodes and elements in a general model would be expected to be greater than for the individual models, this could contribute to a considerable increase in the required computing time. The amount of computation in the analysis of a model increases by the order of the square of the number of nodes for each additional node.

The simplest way to reduce the computing time would be to fit the measured s parameter data at fewer frequencies. However, the author decided to proceed using all the available data.

The initial model used in the first attempt to develop an improved general model was the PRL general model. In the second attempt, the author produced an initial model based on the final models generated for each of the common collector, common emitter and common base configurations.

6.4.1. First Attempt

The PRL general model shown in Figure 6.1 gave an overall error function value of F = 3.11E + 05. The r.m.s. errors were 3.3 dB and

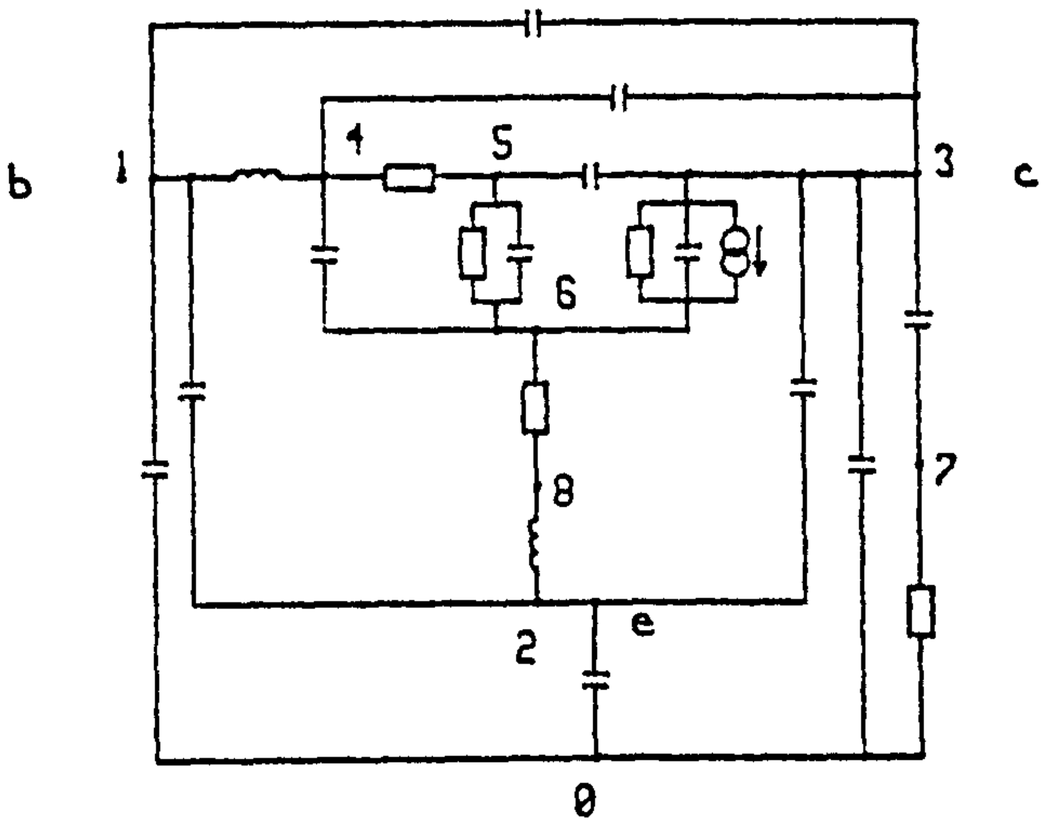

F = 3.11E+05

No. of nodes = 9
No. of elements = 20

R (4-5) = 1.13E+02 ohm
R (5-6) = 2.51E+03 ohm
R (3-6) = 9.43E+04 ohm
R (6-8) = 4.99E+00 ohm
R (7-0) = 6.03E+00 ohm
L (1-4) = 4.70E+00 nH
L (8-2) = 4.10E+00 nH
C (4-6) = 1.74E-03 nF
C (5-6) = 1.09E-02 nF
C (5-3) = 8.00E-05 nF
C (3-6) = 1.00E-05 nF
C (3-7) = 1.34E-03 nF
C (4-3) = 1.60E-04 nF
C (1-3) = 5.00E-05 nF
C (1-0) = 1.23E-03 nF
C (3-0) = 5.50E-04 nF
g (3-6) = 3.00E-02 S
(T =-1.00E-02 ns)
(V across nodes 5 6)
C (2-0) = 1.02E-03 nF
C (1-2) = 5.00E-05 nF
C (2-3) = 5.00E-05 nF

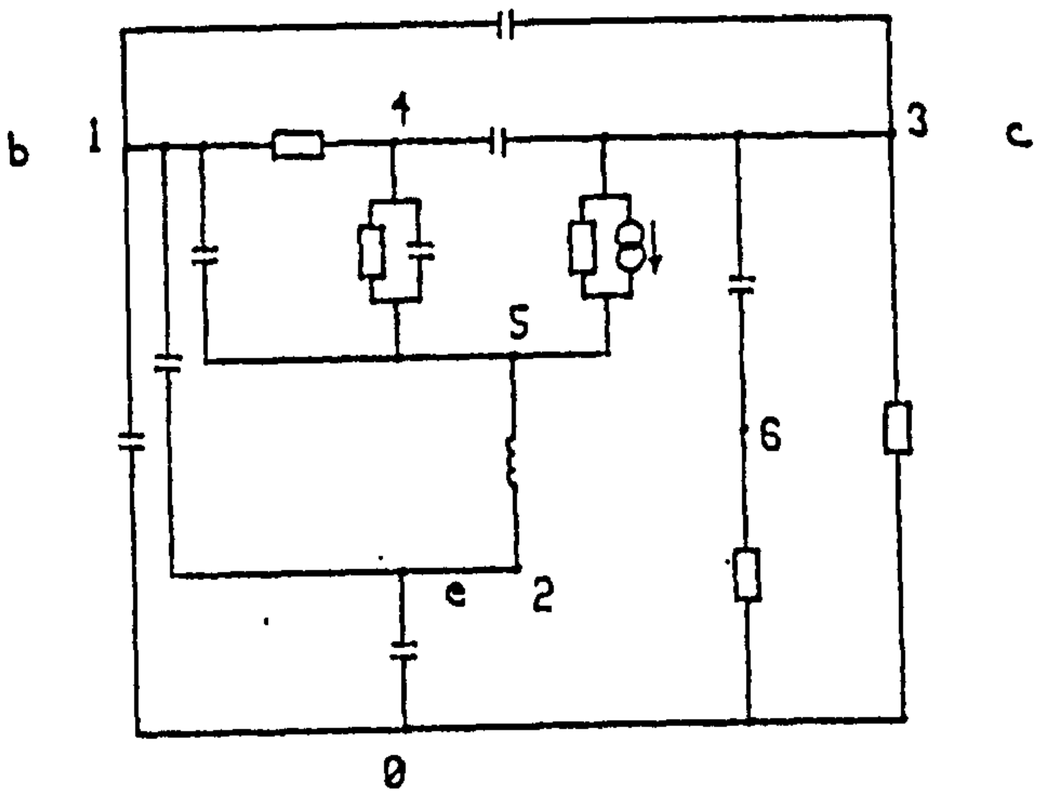

F = 1.67E+05

No. of nodes = 7
No. of elements = 15

R (1-4) = 1.07E+02 ohm
G (4-5) = 1.38E-03 S
R (6-0) = 1.85E+01 ohm
L (5-2) = 1.48E+01 nH
C (1-5) = 2.44E-03 nF
C (4-5) = 7.88E-03 nF
C (4-3) = 7.45E-05 nF
R (3-5) = 1.47E+05 ohm
C (3-6) = 2.43E-03 nF
C (1-3) = 1.62E-04 nF
C (1-0) = 1.83E-03 nF
R (3-0) = 3.63E+03 ohm
g (3-5) = 2.87E-02 S
(T = 1.75E-02 ns)
(V across nodes 5 6)
C (2-0) = 1.67E-03 nF
C (1-2) = 5.84E-04 nF

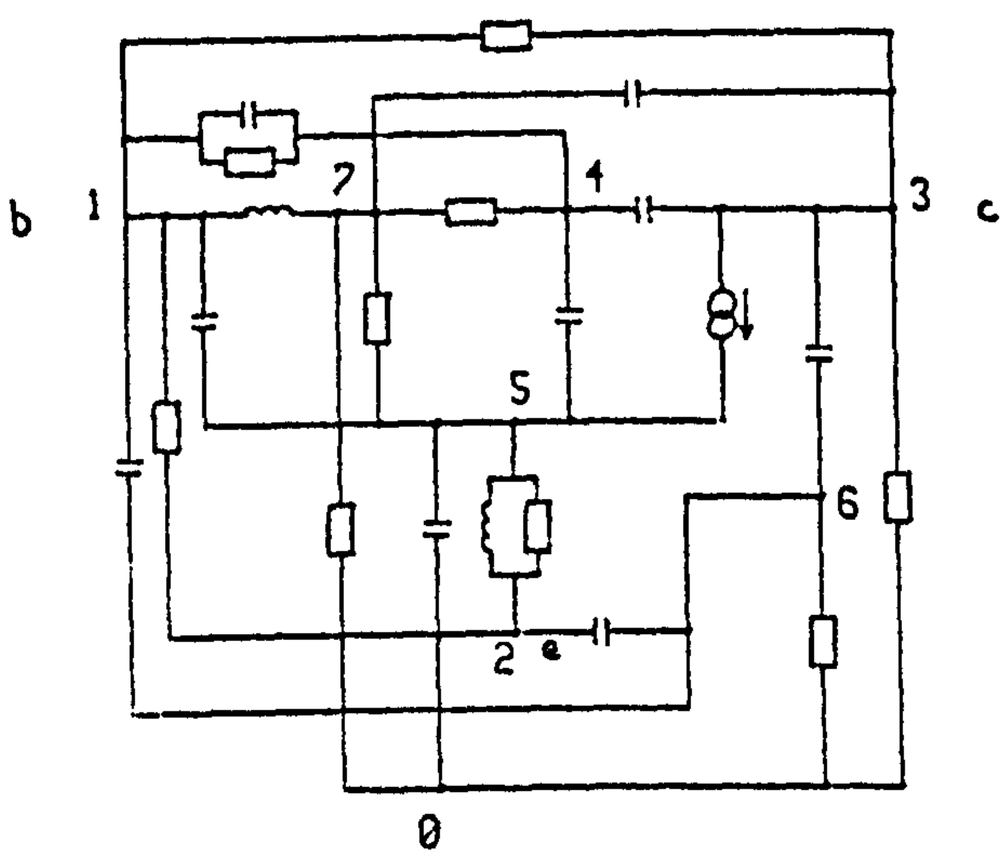

F = 6.07E+04

No. of nodes = 8
No. of elements = 21

R (7-4) = 9.35E+03 ohm
R (6-0) = 1.01E+01 ohm
L (5-2) = 2.32E+01 nH
C (1-5) = 2.35E-03 nF
C (4-5) = 3.37E-03 nF
C (4-3) = 5.18E-05 nF
C (3-6) = 2.25E-03 nF
R (3-0) = 8.47E+03 ohm
g (3-5) = 2.59E-02 S
(T =-4.53E-02 ns)
(V across nodes 5 6)
C (1-6) = 2.39E-03 nF
C (2-6) = 1.48E-03 nF
R (1-2) = 2.91E+02 ohm
R (1-3) = 1.81E+05 ohm
R (2-5) = 6.00E+02 ohm
C (1-4) = 7.57E-04 nF
L (7-1) = 4.17E+02 nH
C (3-7) = 1.86E-04 nF
R (5-7) = 1.71E+07 ohm
C (5-0) = 2.82E-06 nF
R (7-0) = 2.90E+03 ohm
R (1-4) = 1.97E+02 ohm

Node 1 - Base
Node 2 - Emitter
Node 3 - Collector
Node 0 - Ground

Figure 6.12 General Model - First Attempt

32.8°. As can be seen from the graphs shown earlier, the model gave a good fit at low frequencies but there were gross errors at higher frequencies.

On using this model as the initial model for the general case, Stage 1 caused the reduction of the model from 9 nodes and 20 elements to 7 nodes and 15 elements. These are the first two models shown in Figure 6.12. The two node deletions were attained by (i) the deletion of the base terminal inductor and (ii) the deletion of the resistor in series with the emitter terminal inductor. The value of F after Stage 1 was 1.67E + 05. The individual errors now became more evenly distributed although they were still smallest for the common collector configuration.

After one entry each to Stages 2 and 3, during the latter of which the base terminal inductor was re-inserted, and one further entry to Stage 2, the final model shown in Figure 6.12 had been produced. This model consisted of 8 nodes and 21 elements and gave a value of F = 6.07E + 04. The r.m.s. errors of this model were 1.45 dB and 14.5°, but the maximum absolute errors were 1.5 dB and 38° in the common collector configuration, 6.3 dB and 53° in the common emitter configuration and 8.0 dB and 59° in the common base configuration. Thus, although a large improvement had been achieved, the errors were still rather large.

This model had taken approximately 6000 c.p.u. seconds on the UMRCC CDC 7600 to develop. Because of the size of the model each further element addition was now taking an excessive amount of time. It was therefore decided to make another attempt to produce a general model using a different initial model.

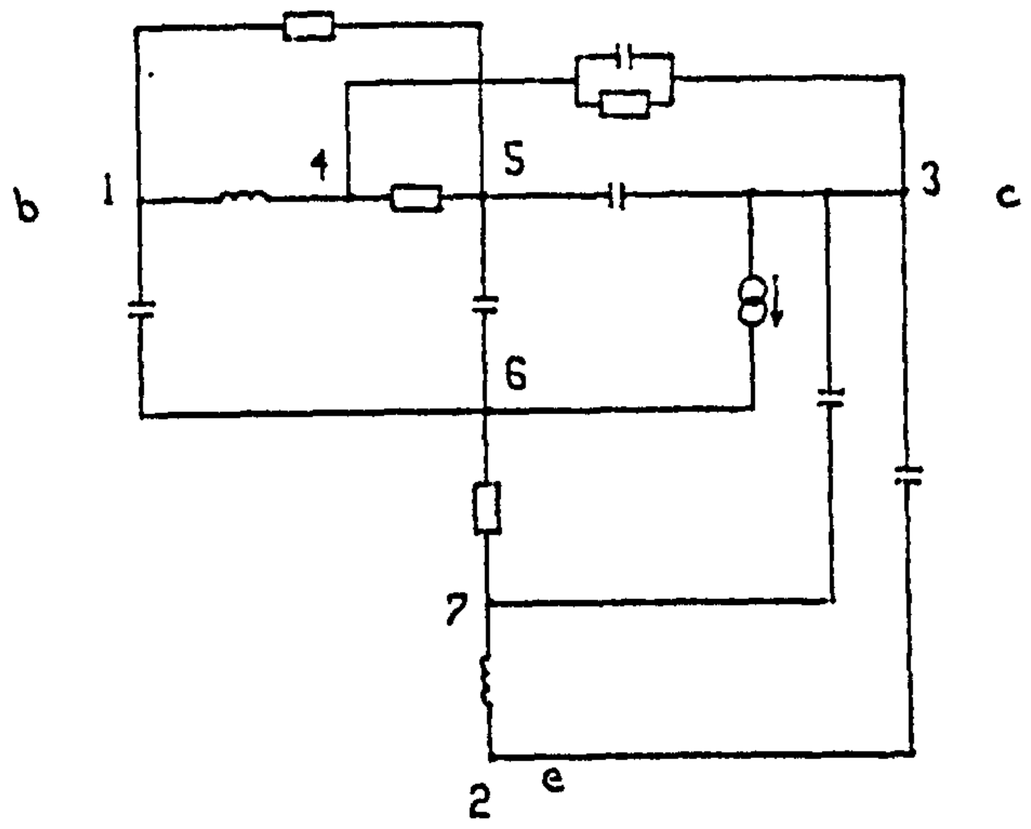

F = 9.78E+05

No. of nodes = 8
No. of elements = 13

L (1-4) = 3.00E+01 nH
R (4-5) = 2.00E+02 ohm
R (1-5) = 8.00E+01 ohm
C (4-3) = 7.00E-04 nF
R (4-3) = 1.00E+04 ohm
C (5-6) = 2.00E-02 nF
g (3-6) = 5.00E-02 S
(T = 1.00E-02 ns,)
(V across nodes 5, 6)
L (7-2) = 5.00E+00 nH
C (1-6) = 3.00E-03 nF
C (5-3) = 2.00E-04 nF
R (6-7) = 3.00E+01 ohm
C (3-7) = 5.00E-04 nF
C (3-2) = 1.00E-05 nF

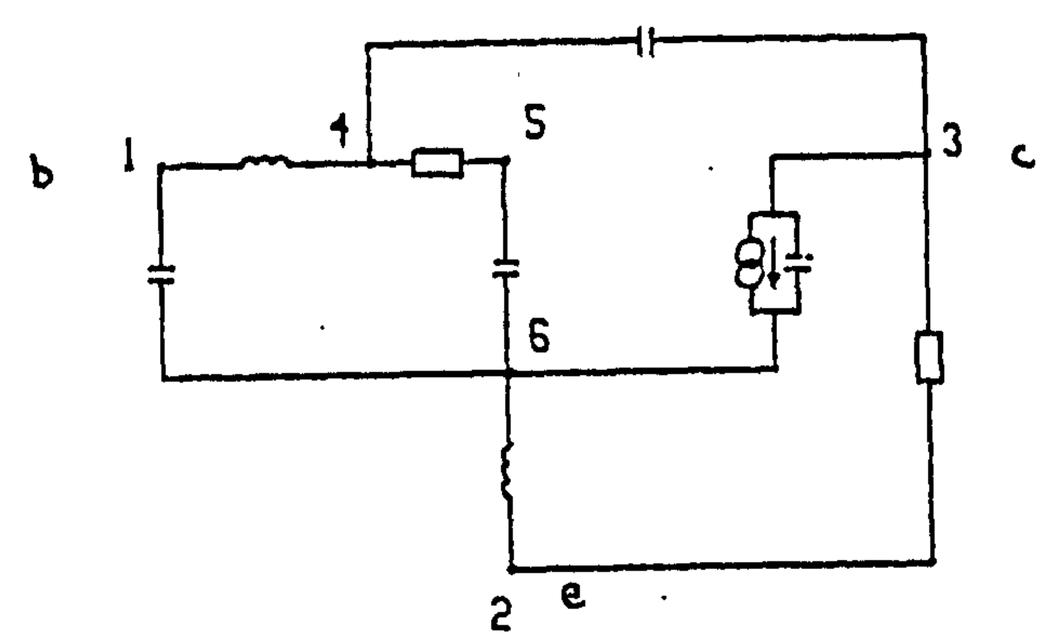

F = 3.05E+05

No. of nodes = 7
No. of elements = 9

L (1-4) = 5.67E+00 nH
R (4-5) = 9.01E+01 ohm
C (4-3) = 2.57E-04 nF
C (5-6) = 1.15E-02 nF
g (3-6) = 2.37E-02 S
(T = -5.80E-02 ns,)
(V across nodes 5, 6)
L (6-2) = 5.86E+00 nH
C (1-6) = 2.25E-03 nF
C (3-6) = 4.37E-06 nF
R (3-2) = 5.75E+03 ohm

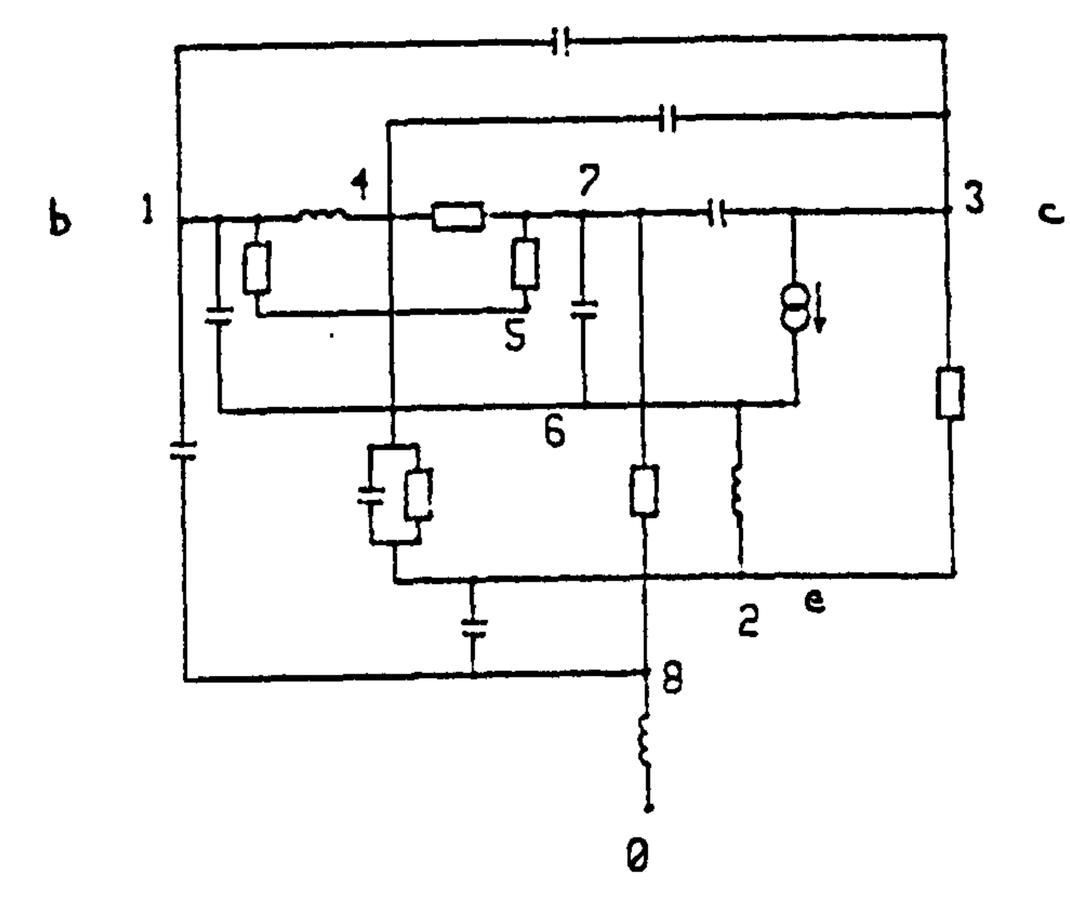

F = 4.78E+04

No. of nodes = 9
No. of elements = 18

L (1-4) = 1.79E+01 nH
C (4-3) = 6.64E-05 nF
g (3-6) = 2.02E-02 S
(T = -1.60E-01 ns,)
(V across nodes 3, 6)
L (6-2) = 3.29E+01 nH
C (1-6) = 3.87E-03 nF
C (1-8) = 1.08E-03 nF
C (2-4) = 1.01E-03 nF
C (2-8) = 1.12E-03 nF
R (1-5) = 6.51E+03 ohm
R (2-4) = 2.72E+02 ohm
C (7-3) = 2.03E-03 nF
R (5-7) = 4.49E+04 ohm
R (7-8) = 3.30E+01 ohm
R (4-7) = 1.33E+03 ohm
C (6-7) = 8.20E-04 nF
R (2-3) = 2.33E+04 ohm
L (8-8) = 2.17E+00 nH
C (1-3) = 1.72E-04 nF

Node 1 - Base
Node 2 - Emitter
Node 3 - Collector
Node 0 - Ground

Figure 6.13 General Model - Second Attempt

6.4.2. Second Attempt

For the second attempt, the first model shown in Figure 6.13 was used as the initial model. This model was derived by combining those elements of the three individual models developed by the author that appeared in any two models. This model consisted of 8 nodes and 13 elements and gave a value of F = 9.78E + 05. After Stage 1 the model was reduced to 7 nodes and 9 elements giving a value of F = 3.05E + 05. This simple model, which is the second model in Figure 6.13, gave r.m.s. errors of 3.3 dB and 32.5° and maximum errors of 11.0 dB and 152°.

After two entries to each of Stages 2 and 3, the final model shown in Figure 6.13 had been obtained. There are two points about this model that provoke comment. The first point is that node 5, at which the controlling voltage of the current generator is taken, can be seen to be merely splitting an element of resistance between nodes 1 and 7. However, this situation was developed by a complicated series of additions and deletions and until a late stage other elements had been connected to node 5. The second point to be made concerns the inductor L_{0-8}. This element was added in the second entry to Stage 3 to generate a new node. In common base configuration, there is thus one inductor at each of the emitter, collector and base terminals, but in common emitter and common collector configurations, a rather complicated structure is formed in the region of the ground node. However, the addition of this element and node caused a significant reduction in the objective function from 7.23E + 04 immediately prior to their inclusion to 4.78E + 04.

This model therefore gives a better overall result than that obtained in the first attempt. The r.m.s. errors of this model are 1.3 dB and 12.9° and the maximum absolute errors are 4.8 dB and 28.1° in the common collector configuration, 2.3 dB and 26.2° in the common emitter configuration and 6.2 dB and 36.5° in the common base configuration. It

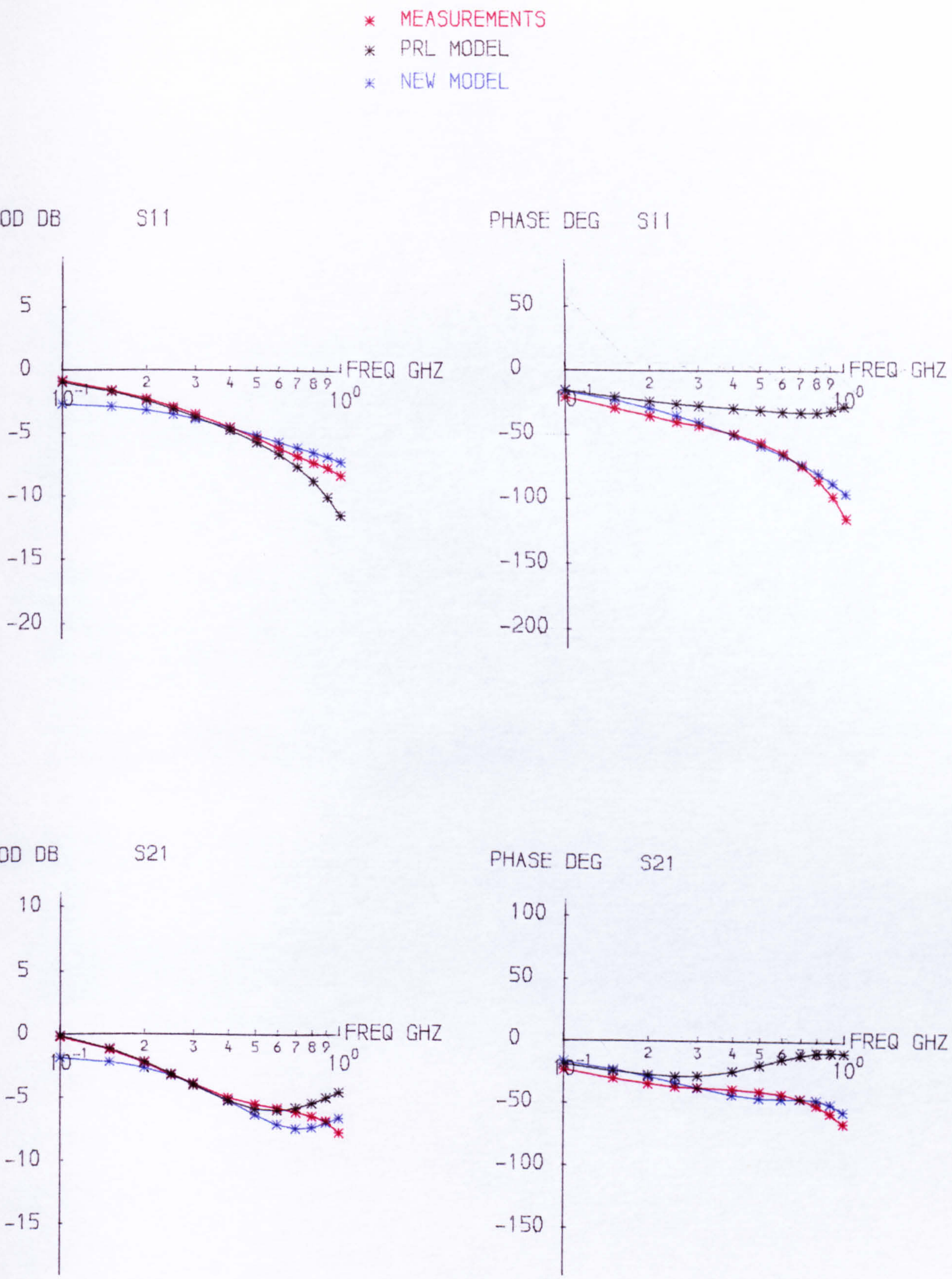

Figure 6.14a S_{11} and S_{21} for General Model in Common Collector Configuration

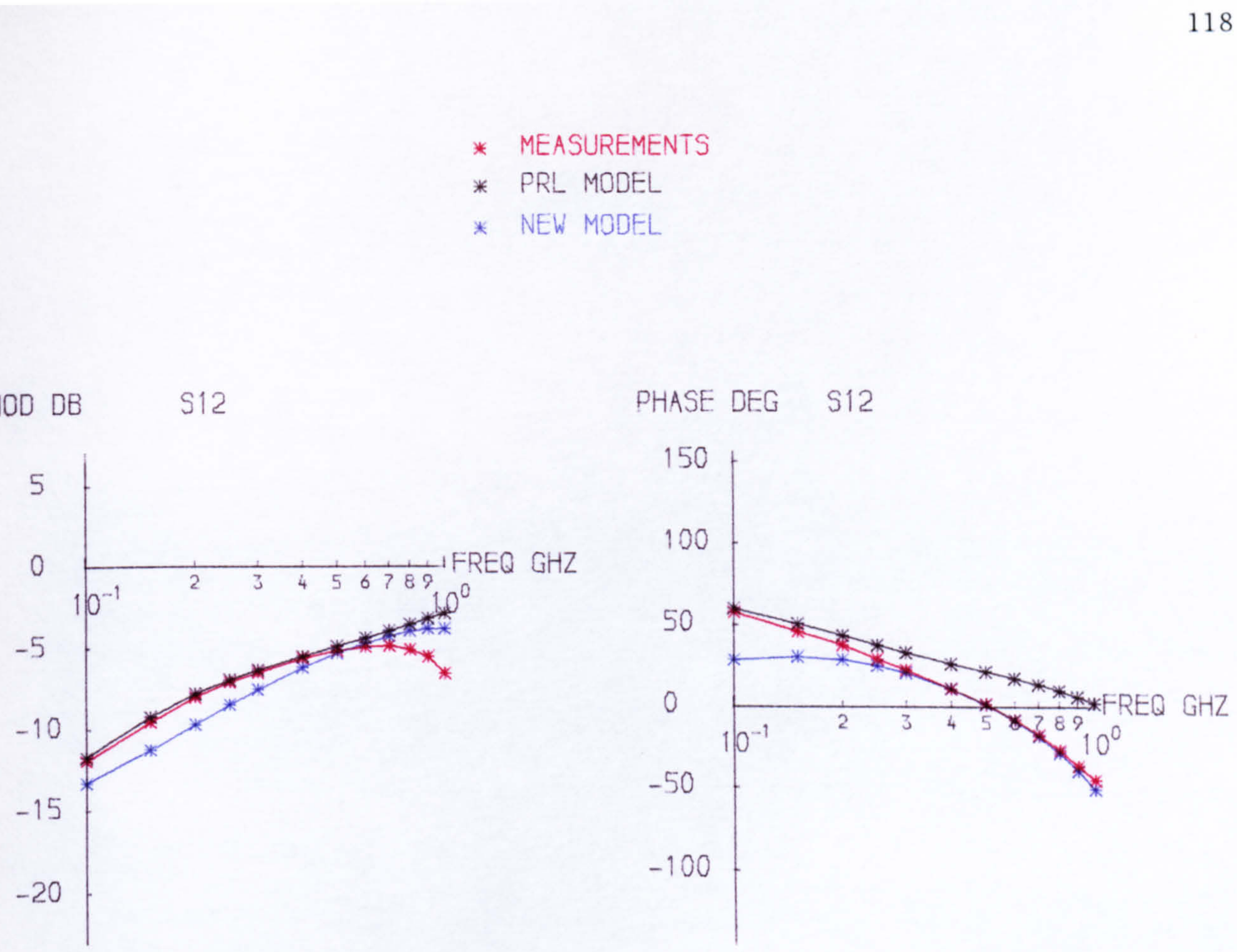

Figure 6.14b S_{12} and S_{22} for General Model in Common Collector Configuration

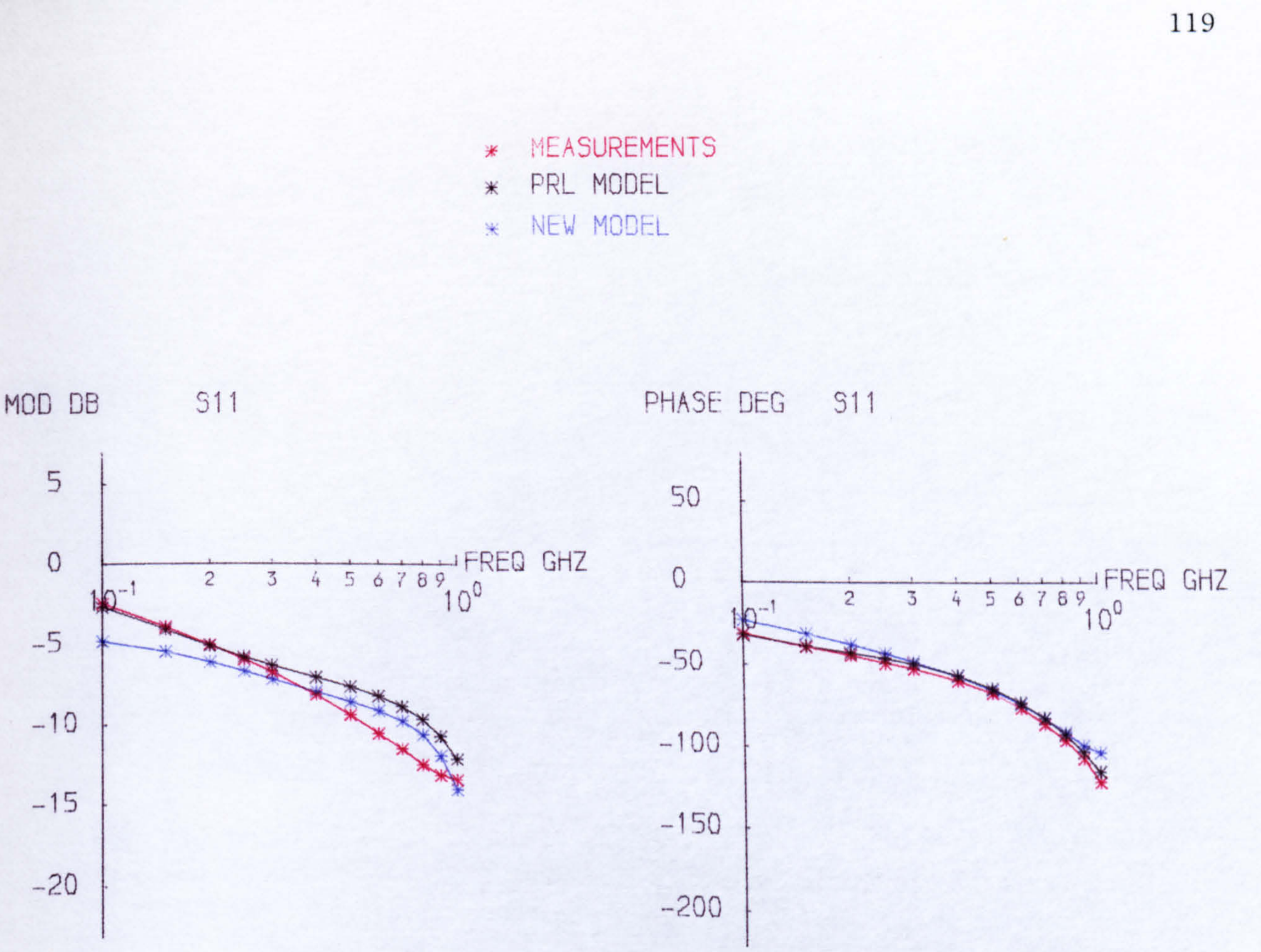

Figure 6.15a $\underline{S_{11}}$ and $\underline{S_{21}}$ for General Model in Common Emitter Configuration

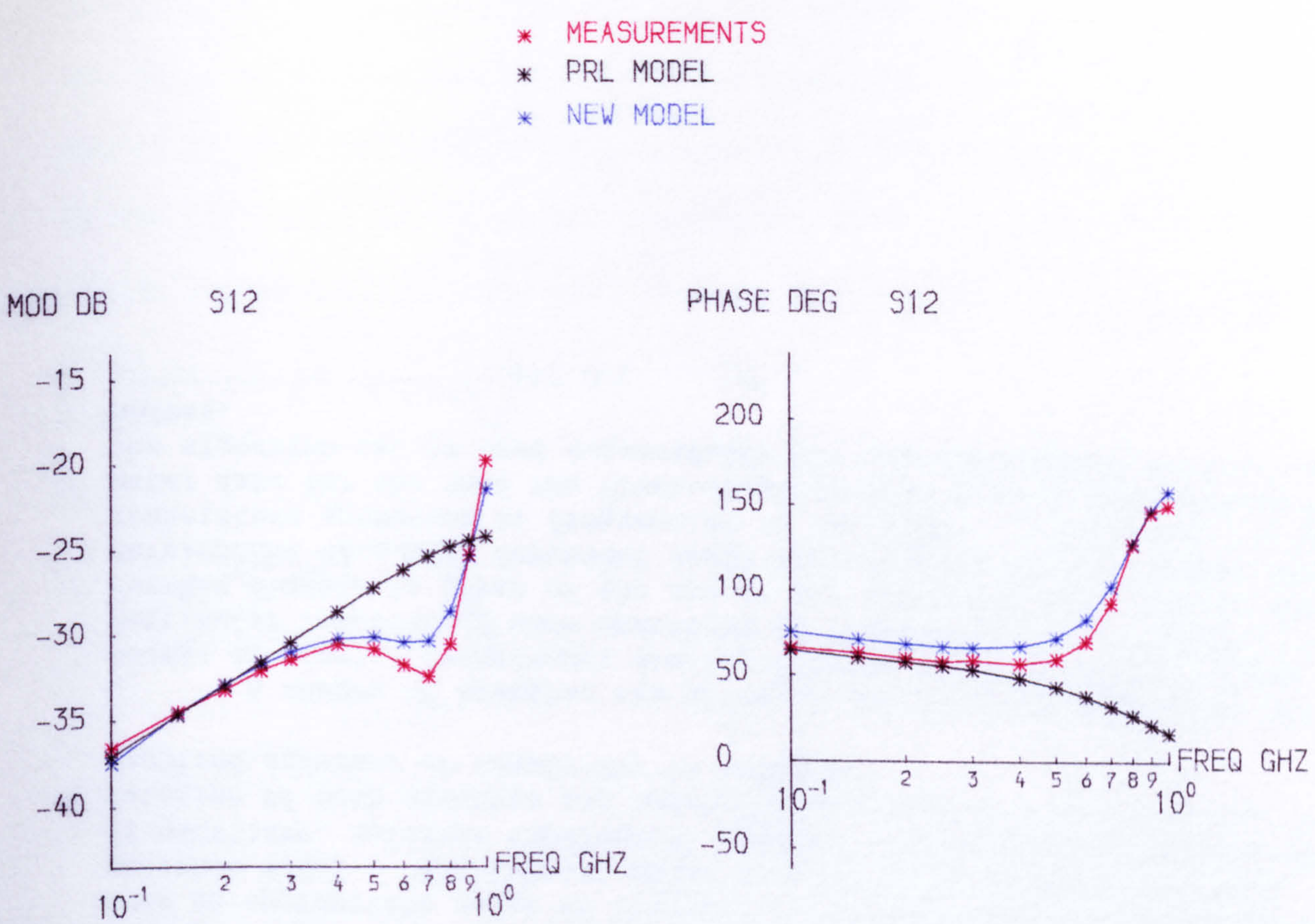

Figure 6.15b S_{12} and S_{22} for General Model in Common Emitter Configuration

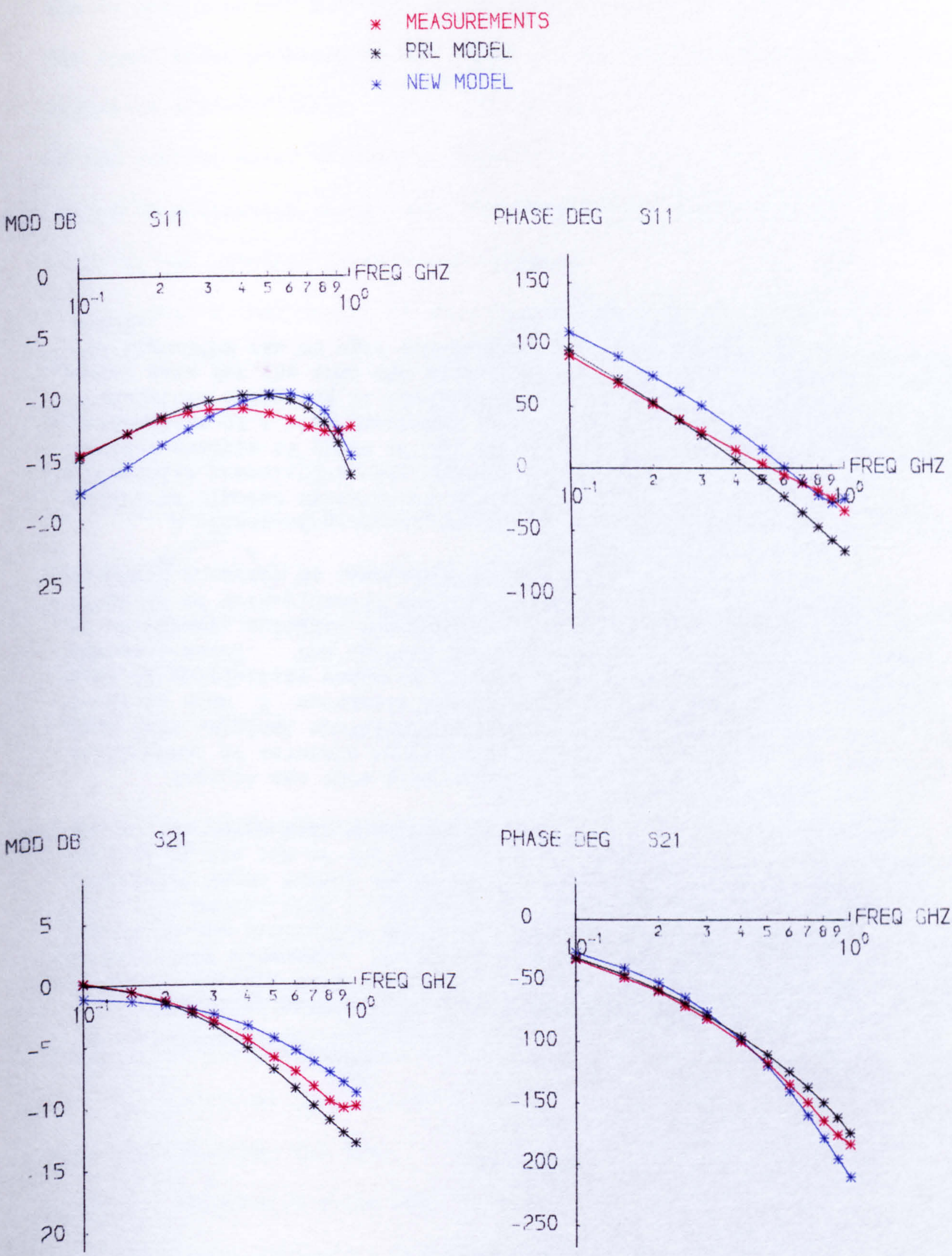

Figure 6.16a S_{11} and S_{21} for General Model in Common Base Configuration

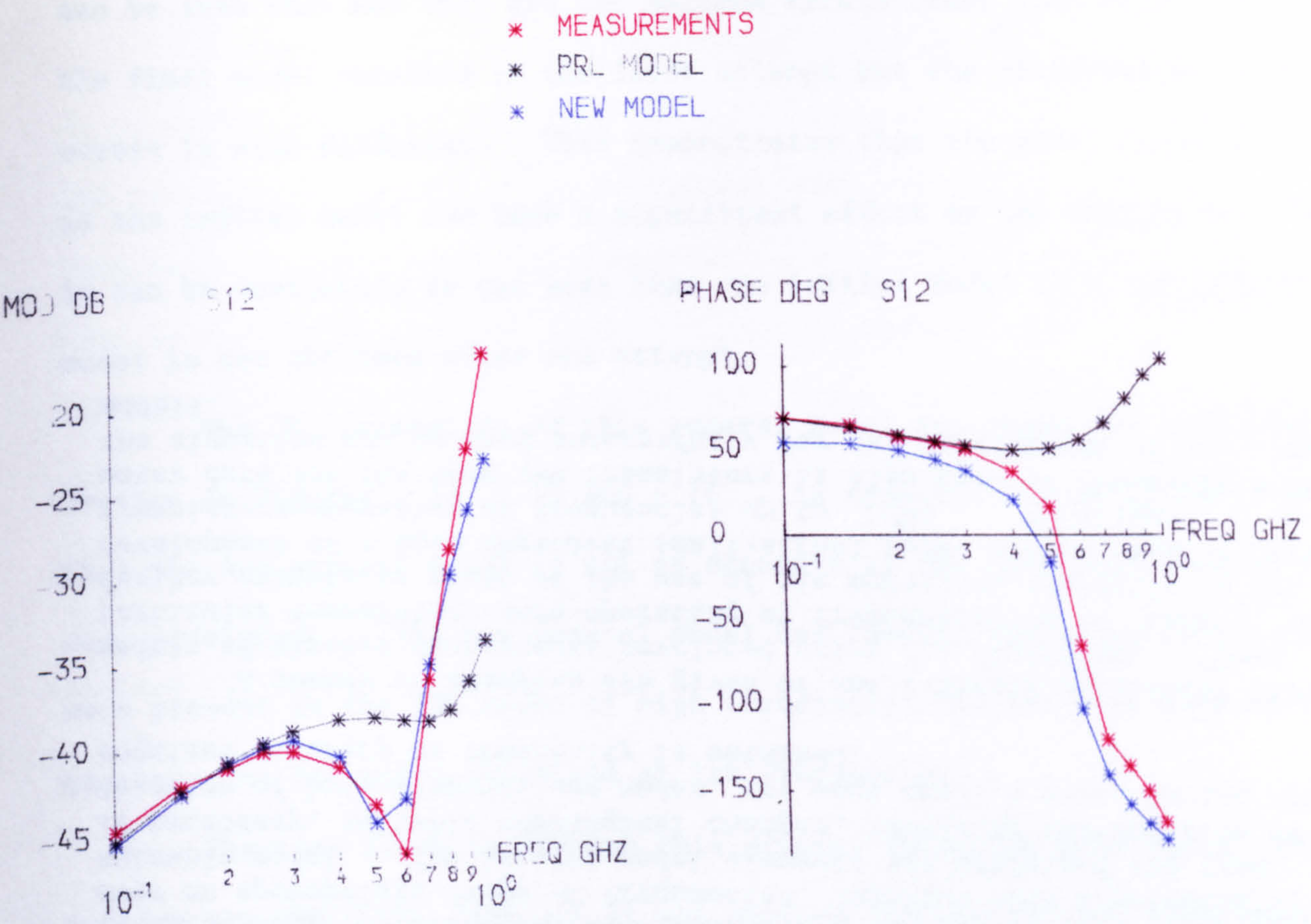

Figure 6.16b S_{12} and S_{22} for General Model in Common Base Configuration

can be seen that not only are the maximum errors lower than those for the final model obtained in the first attempt but the distribution of the errors is also different. This demonstrates that the model chosen for use as the initial model can have a significant effect on the results and that it can be worthwhile to use more than one initial model if a satisfactory model is not obtained after one attempt.

The s parameters of this general model are shown for each configuration in Figures 6.14, 6.15 and 6.16. As expected, these graphs show that the new general model is not as accurate as the individual models that were developed. The new general model has removed the gross errors that were present in the PRL model at high frequencies but has lost some of the accuracy the PRL model exhibited at low frequencies.

The time taken to develop this general model was 8300 c.p.u. seconds on the UMRCC CDC 7600 and it was decided that no further improvements should be attempted.

6.4.3. Suggested Alternative Approaches

With the benefit of hindsight, the author now feels that the approach used to produce the two general models was too ambitious.

Knowing that both the size of the problem and the computing time required would be large, the first priority should have been to ensure that the algorithm operated as efficiently as possible even if this meant that some accuracy was lost. Therefore, in the analysis routine single precision arithmetic could have been used and, as shown in Section 3.1.5, this would have achieved a 50% reduction in the computing time required for the analysis of the models. Furthermore, as mentioned in Section 5.2.2, the calculation of the approximation to the Jacobian matrix could have employed forward differences rather than central differences, and although this, too, involves a loss of accuracy, it would have halved the

number of function evaluations required in that calculation.

Further savings could also have been made by using less of the s parameter data that was provided. For example, instead of using the measured s parameters at every frequency given, they could have been taken at every alternate frequency given. This certainly might have been a better approach using the initial model used in the second attempt. However, in the first attempt, since the PRL model gave good results at low frequencies, it might have been better to have attempted to improve the model in stages by initially matching the s parameters at low frequencies and gradually increasing the number of frequencies and the maximum frequency at which the s parameters were matched.

CHAPTER 7

A BIAS DEPENDENT MODEL FOR TWO SIMILAR BIPOLAR TRANSISTORS

The third set of data provided by PRL[15] consisted of the sets of s parameter measurements, given in the appendix, for two similar bipolar transistors in common emitter configuration. These transistors had the reference numbers 1E2M and 3E2M and were isolated n-p-n transistors made in silicon with implanted arsenic emitters and diffused boron bases. The 1E2M had one emitter stripe and the 3E2M had three emitter stripes.

The data provided consisted of the s parameter measurements for the two devices at 16 frequencies in the range 0.1 GHz to 2 GHz with collector-emitter voltages, V_{ce}, of 0.5 V and 3 V and with emitter currents, I_e, in the ranges 0.5 mA to 10 mA for the 1E2M and 0.5 mA to 27 mA for the 3E2M. The graphs in Figure 7.1 showing f_T and the modulus

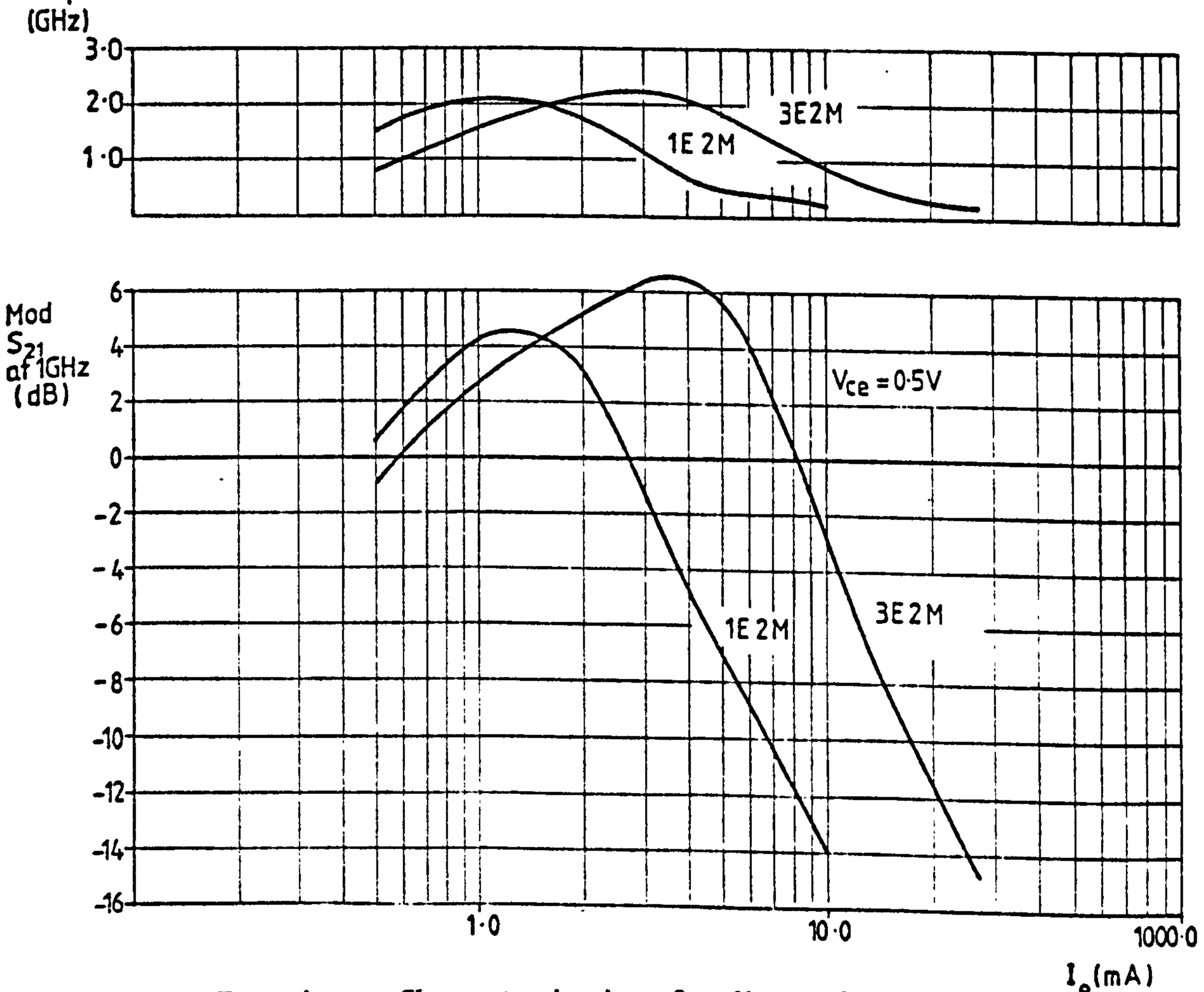

Figure 7.1 Transistor Characteristics for V_{ce} = 0.5 V

of s_{21} at 1 GHz plotted against emitter current for a collector-emitter voltage of 0.5 V, lead to the assumption that the small-signal operating ranges of the transistors up to 1 GHz were 0.5 mA to 2 mA for the 1E2M and 0.6 mA to 8 mA for the 3E2M.

A bias dependent model for these devices had been developed by Slatter[16,17]. This model was designed to represent the small signal behaviour of the transistors up to a frequency of 1 GHz for emitter currents such that f_T was still less than its peak value. The model was based on the physical structure of the device and contained a number of bias dependent elements. Some of the values of the model elements were chosen using the construction of the devices as a guide, while others were chosen using optimisation techniques. The relationships for the bias dependent elements were based on theoretical considerations.

The results published by Slatter[17] for this model show that in general a good fit to the measured s parameters had been obtained for frequencies up to 1 GHz with the bias variation well simulated for emitter currents of up to 2 mA for the 1E2M and up to 4 mA for the 3E2M. Slatter[16] states that the model for the 3E2M fits the measured s parameters more accurately than that for the 1E2M and that s_{11} for the 1E2M shows larger errors than expected. He also states that the higher frequency limits for the models might be 1 GHz for the 1E2M and 1.6 GHz for the 3E2M.

The author decided that an interesting experiment would be to apply the modelling algorithm described earlier, to this problem. By producing optimised models for each of the bias conditions, an alternative method of studying the bias dependence of the model elements could be achieved. Some of the results of this experiment were published by the author[76] in 1981.

7.1. Optimisation of the Model

The author started by producing a model for the 1E2M using the modelling algorithm described earlier and using the same weightings on the individual errors in the modulus and phase as were used when modelling the vertical n-p-n transistor described in the previous chapter. The initial model used is shown in Figure 7.2. This model, which consisted of 8 nodes and 12 elements, and the initial element values shown, were based on the PRL bias dependent model. A new model was produced for the 1E2M over the frequency range 0.1 GHz to 2 GHz for V_{ce} = 0.5 V and I_e = 4 mA. This model consisted of 6 nodes and 14 elements and gave an overall crror function, F , of 5.15E + 02. However, this model was at the limit of the linear region of operation of the 1E2M and when it was used as the initial model for the same transistor with V_{ce} = 3 V and I_e = 0.5 mA, further changes were made resulting in the less complicated model shown in Figure 7.3. This model consisted of 6 nodes and 9 elements and gave a value of F = 4.35E + 02 for the 1E2M with V_{ce} = 3 V and I_e = 0.5 mA. The r.m.s. errors of this model were 0.2 dB and 1.8°, and the maximum absolute individual errors were 0.7 dB and 3.8°. The graphs in Figure 7.4 show the s parameters of this model compared with the measured s parameters. The scales of the graphs cover the same absolute ranges as those in the previous chapter. This very accurate model was developed in approximately 2200 c.p.u. seconds on the UMRCC CDC 7600. This time includes the two stages in the development of the model, from the initial model in Figure 7.2, through the first model developed for V_{ce} = 0.5 V , to this final model for V_{ce} = 3 V .

Now, using this latest model as the initial model for the 1E2M with V_{ce} = 0.5 V and I_e = 0.5 mA, it was found that excellent results were obtained without any further topology changes. Furthermore, it was found that this model, with the element values optimised, also gave good

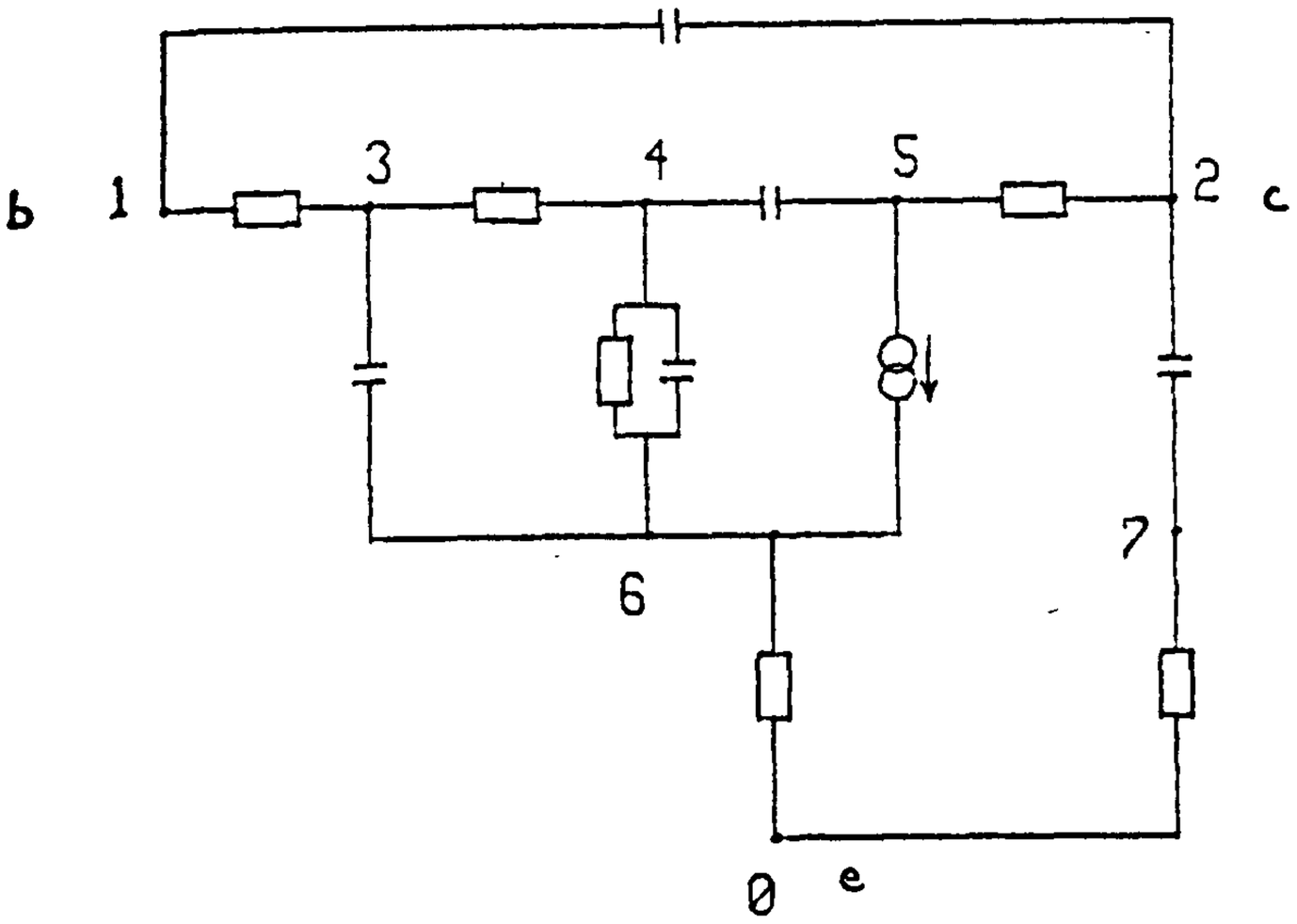

No. of nodes = 8
No. of elements = 12

R (1-3) = 1.00E+01 ohm
R (3-4) = 2.00E+01 ohm
C (4-5) = 3.00E-05 nF
R (5-2) = 1.00E+01 ohm
C (3-6) = 1.00E-03 nF
R (4-6) = 5.00E+01 ohm
C (4-6) = 1.00E-04 nF
g (5-6) = 1.00E-02 S
(T =-2.50E-03 ns)
(V across nodes $\frac{4}{6}$)
R (6-0) = 1.00E+00 ohm
C (2-7) = 1.00E-03 nF
R (7-0) = 2.00E+02 ohm
C (1-2) = 1.00E-05 nF

Node 1 - Base
Node 2 - Collector
Node 0 - Emitter

Figure 7.2 Initial Model Based on PRL Bias Dependent Model

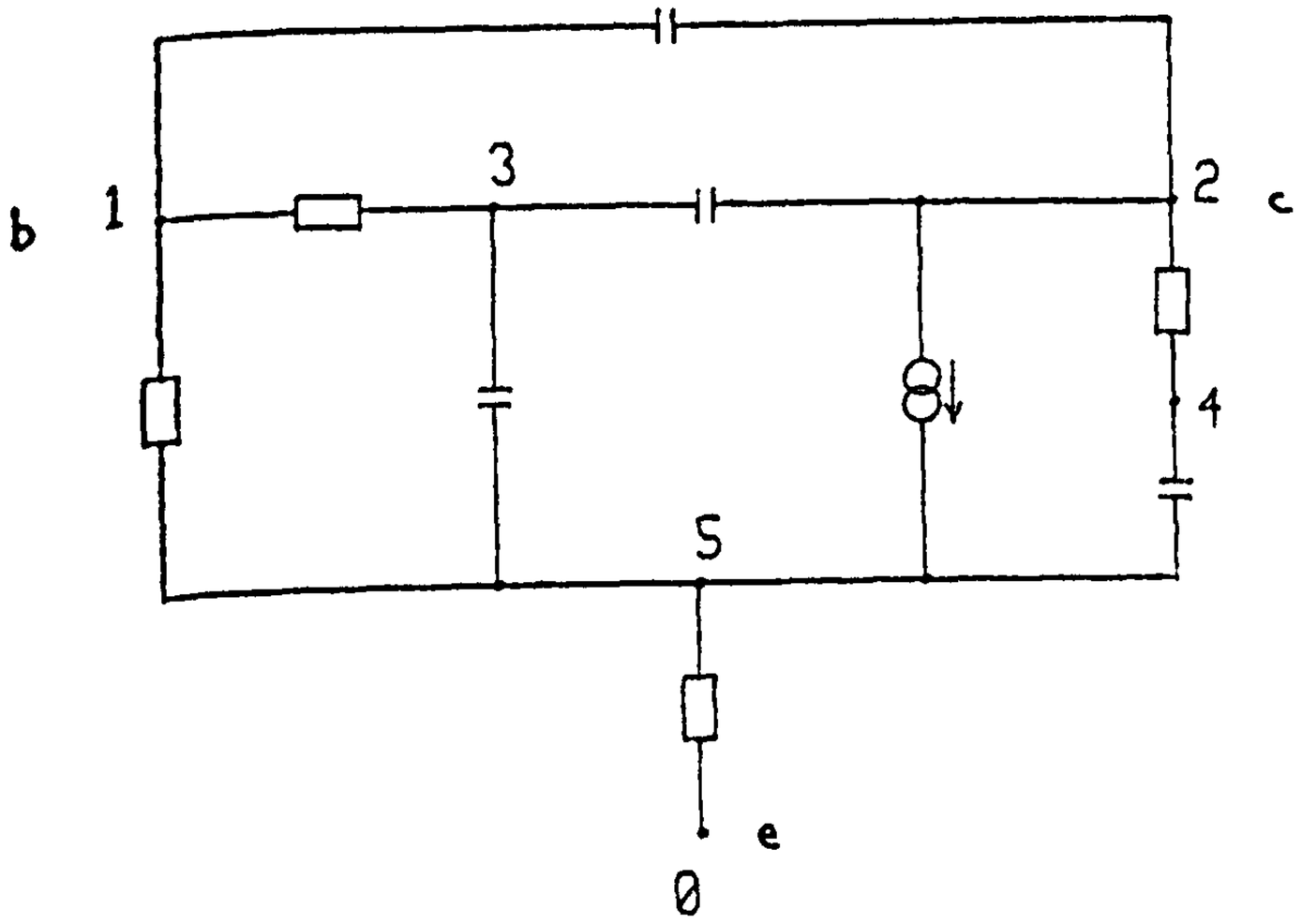

F = 4.35E+02

No. of nodes = 6
No. of elements = 9

C (1-2) = 1.33E-04 nF
g (2-5) = 2.59E-02 S
(T =-2.66E-02 ns)
(V across nodes $\frac{3}{5}$)
C (4-5) = 8.16E-04 nF
C (3-5) = 1.57E-03 nF
R (3-1) = 4.04E+01 ohm
R (4-2) = 1.91E+02 ohm
R (1-5) = 1.58E+03 ohm
R (0-5) = 1.97E+01 ohm
C (2-3) = 9.07E-05 nF

Node 1 - Base
Node 2 - Collector
Node 0 - Emitter

Figure 7.3 Final Model for 1E2M for V_{ce} = 3 V and I_e = 0.5 mA

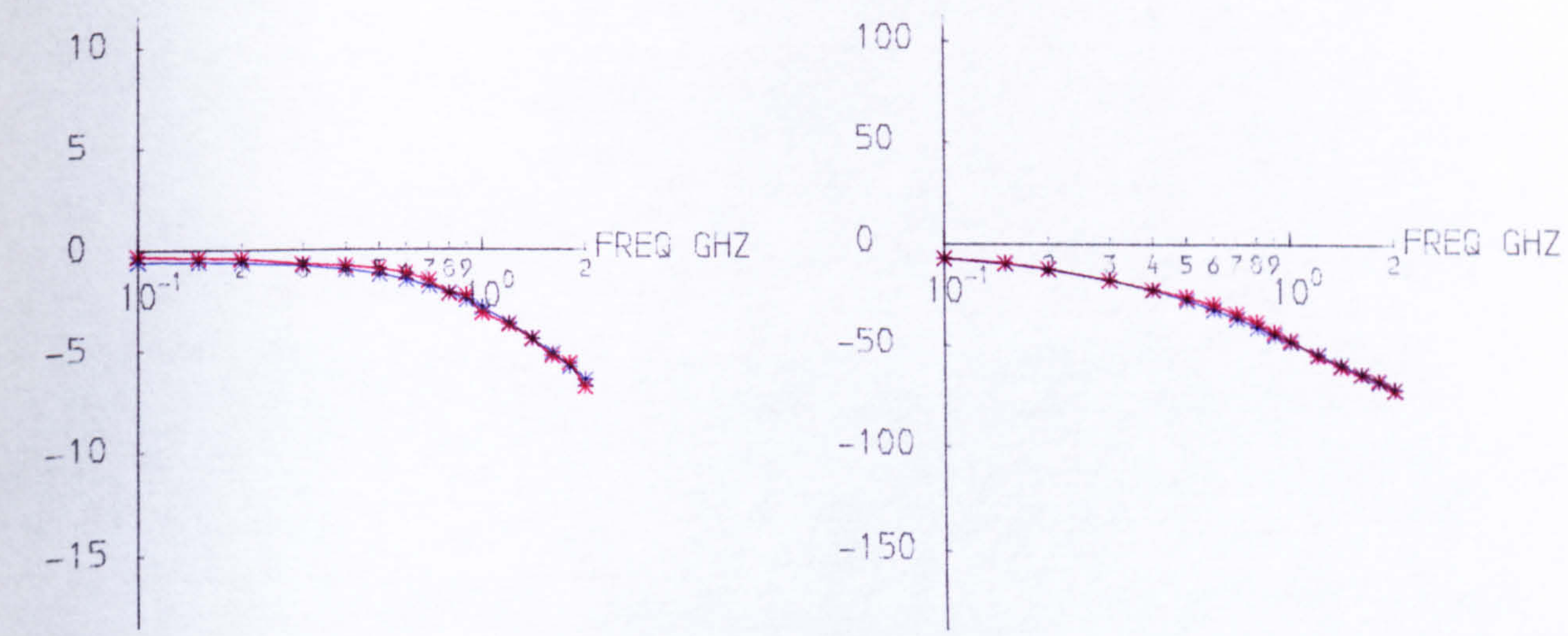

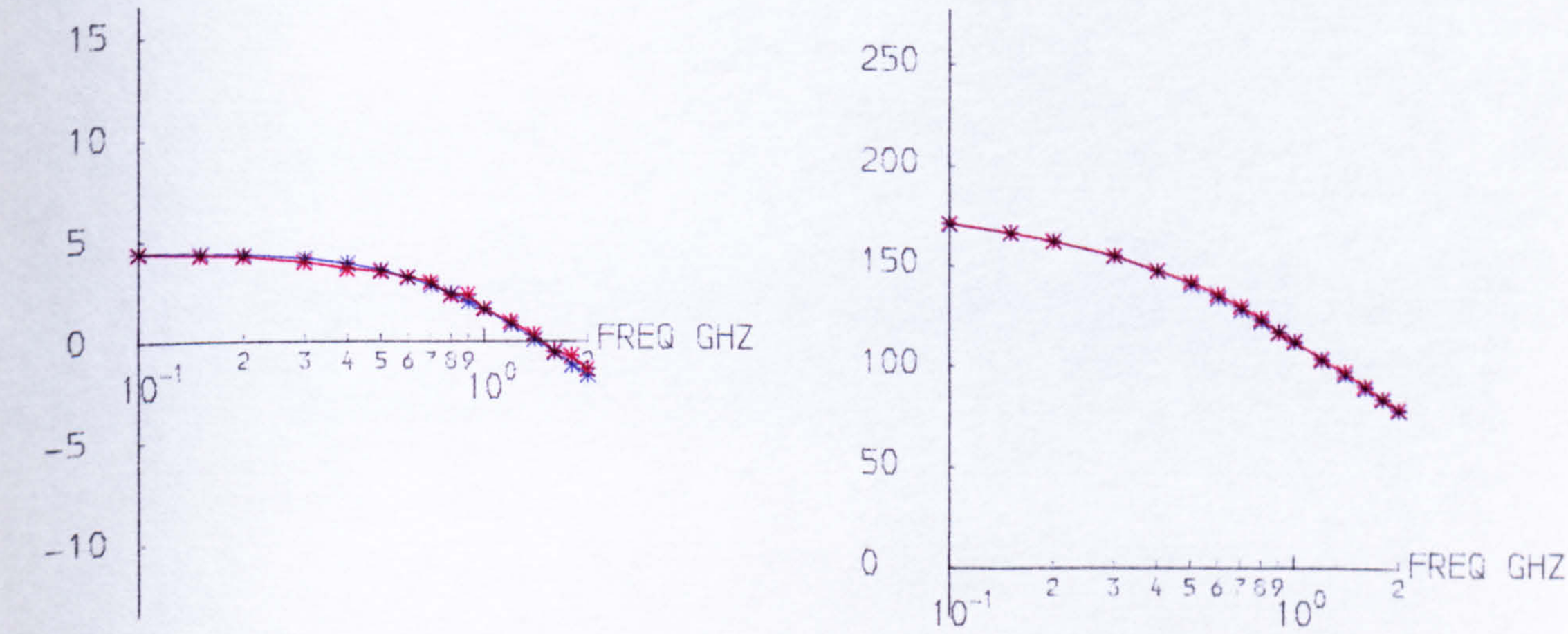

Figure 7.4a S_{11} and S_{21} of Optimised Model for V_{ce} = 3 V and I_e = 0.5 mA

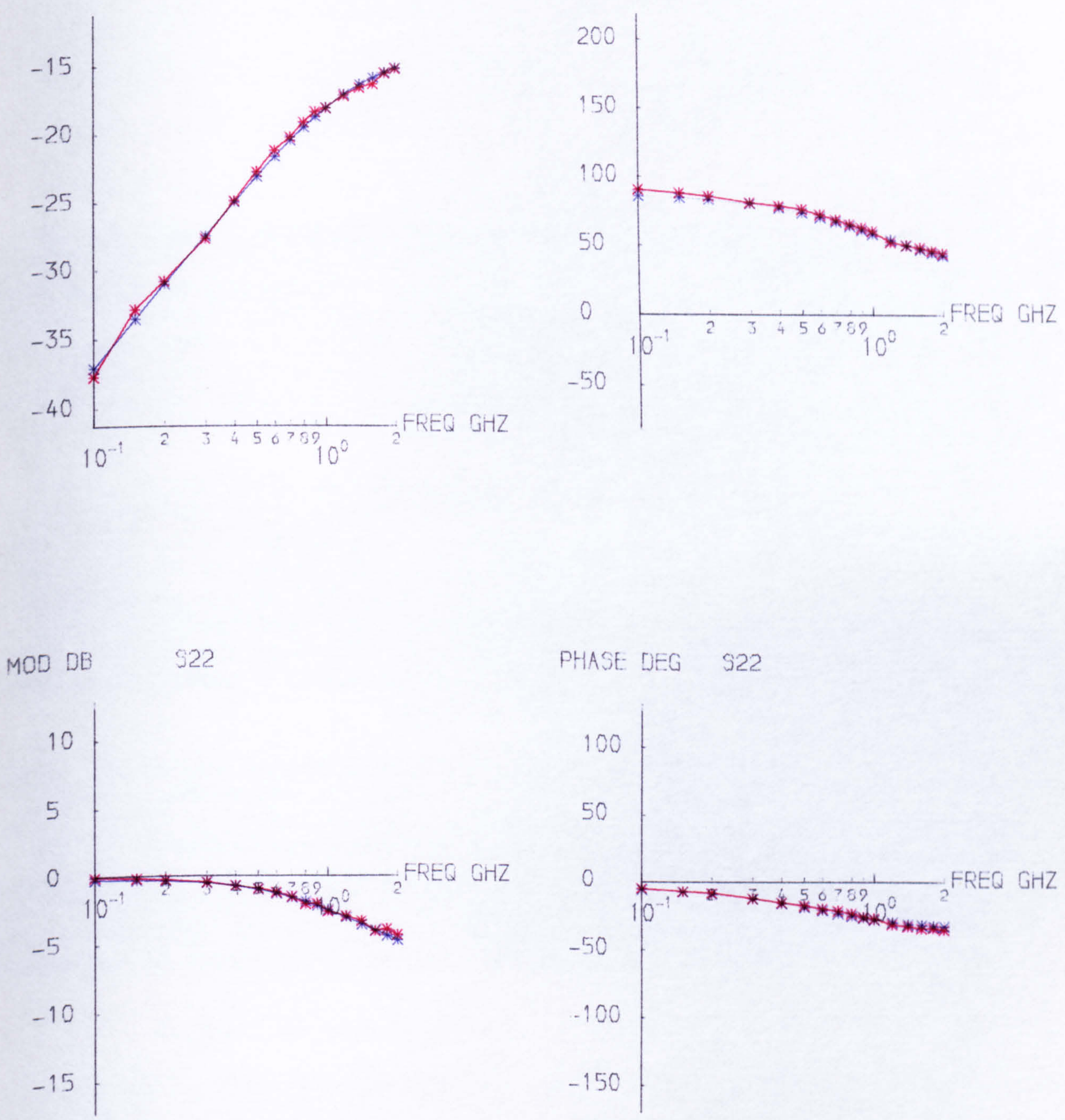

Figure 7.4b S_{12} and S_{22} of Optimised Model for V_{ce} = 3 V and I_e = 0.5 mA

results for the 3E2M with I_e = 0.5 mA and with both of the values of V_{ce}.

Following this, each of the four new models was used as the initial model for the same transistor and the same value of V_{ce} with the next higher value of I_e. Excellent results were again obtained without further changes in the topology and in every case the optimisation of the model element values took less than 200 c.p.u. seconds on the Leicester University CDC Cyber 73. Therefore the process was repeated for still higher values of I_e, until the results indicated that a topology change was necessary to achieve similar accuracy. The values of the objective function for each of the models having the same topology as that shown in Figure 7.3 are given in Table 7.1.

I_e mA	Objective Function, F			
	1E2M		3E2M	
	V_{ce} = 0.5 V	V_{ce} = 3 V	V_{ce} = 0.5 V	V_{ce} = 3 V
0.5	3.33E + 02	4.35E + 02	4.12E + 02	5.82E + 02
1.0	6.62E + 02	8.94E + 02	4.04E + 02	6.96E + 02
2.0	6.80E + 02	1.22E + 03	3.75E + 02	3.99E + 02
4.0	3.80E + 03	1.65E + 03	3.94E + 02	6.27E + 02
8.0	-	-	1.46E + 03	1.11E + 03

Table 7.1. Values of the Objective Function for Optimised Models of the 1E2M and 3E2M Transistors

It was felt that satisfactory accuracy had been obtained at values of I_e up to 4 mA for the 1E2M and up to 8 mA for the 3E2M. Although the value of F = 3.80E + 03 for the 1E2M with V_{ce} = 0.5 V and I_e = 4.0 mA, giving r.m.s. errors of 0.5 dB and 5.4°, was relatively high, it was still considered acceptable since the maximum absolute errors of 1.7 dB and 15.2° occurred at 2 GHz, the highest frequency, where the moduli of the s parameters ranged from -8.9 dB to -15.28 dB. The effective ranges of I_e of

this model for the two types of transistor agree with the suggested small-signal operating ranges of the devices given earlier. Thus a single accurate model for the small-signal operation of the two similar bipolar transistors covering the frequency range 0.1 GHz to 2.0 GHz had been developed.

Although the modelling process had gone through a number of different stages, this new model was quite similar to the PRL bias dependent model. Looking at the elements in the final model in Figure 7.3 those which have obvious equivalents in the PRL model in Figure 7.2 are C_{1-2}, C_{3-2} and g_{2-5}. Those having a slightly weaker resemblance to elements in the PRL model are R_{2-4}, C_{4-5} and R_{5-6}. The remaining elements: R_{1-3}, R_{1-5} and C_{3-5}, seem to form a Π arrangement where in the PRL model there was a T arrangement. The well-known T-Π or star-delta transformation is described by Weinberg[77] and the author suggests that there is the possibility that the Π arrangement in the final model is a transformation of the T arrangement in the PRL model, with some of the extra elements that would be present by this transformation rendered unnecessary by the optimisation process. Thus, by the T-Π transformation, R_{1-3} in the new model would be equal to $R_{1-3} + R_{3-4}$ in the PRL model and should also have a series inductor. The Π arm between nodes 1 and 5 should consist of a resistor, equal to R_{1-3} in the PRL model, in series with a capacitor, and the Π arm between nodes 3 and 5 should consist of a resistor and a capacitor in series. Thus it could be conjectured that in the new model R_{1-3} is equivalent to $R_{1-3} + R_{3-4}$ in the PRL model, R_{1-5} is equivalent to R_{1-3} in the PRL model and C_{3-5} in the new model is due to C_{4-6} plus some additional capacitance from the T-Π transformation.

Having developed the new model, the next step was to examine the variation in the values of the elements in the model with the bias conditions. The results of this exercise are given in the next section.

At values of I_e greater than 4 mA for the 1E2M transistor and

8 mA for the 3E2M, topology changes were indicated. Details of some models developed for these cases are given in Section 7.4.

7.2. Examination of the Bias Dependent Elements

Taking each of the model elements in turn, graphs were drawn of the element values against the emitter current. These graphs are shown in Figures 7.5a and 7.5b. In each of these graphs the points are joined by straight lines. The red lines refer to the 1E2M transistor and the blue lines to the 3E2M. The solid-colour lines are for V_{ce} = 0.5 V and the dotted-colour lines are for V_{ce} = 3 V. The black dotted lines are the functions that were fitted to these points and will be described later.

These graphs were extremely encouraging as most of the elements showed a distinct pattern of variation with the emitter current and the collector-emitter voltage.

Although the model was different from the PRL bias dependent model, some of the elements in the two models could be compared. The bias relationships in the PRL model involved only $\sqrt{V}_{ce}$, V_{ce} and I_e, these being based on theoretical considerations. The author decided to use a curve fitting routine from the NAG library, E02ADF[78], to examine the fits obtained to each of the sets of points. First, only the relationships with I_e were studied, allowing functions of $\sqrt{I}_e$, I_e, I_e^2 and reciprocals thereof. Then the effect of V_{ce} was taken into consideration. The bias dependence of each element is discussed below with reference being made to the model shown in Figure 7.2 for the comparisons with the PRL bias dependent model.

C_{1-2} - This element had a direct equivalent in the PRL model which they suggested was not current dependent, with values of $0.33/\sqrt{V}_{ce}$ pF for the 1E2M and $0.62/\sqrt{V}_{ce}$ pF for the 3E2M. In the author's model the

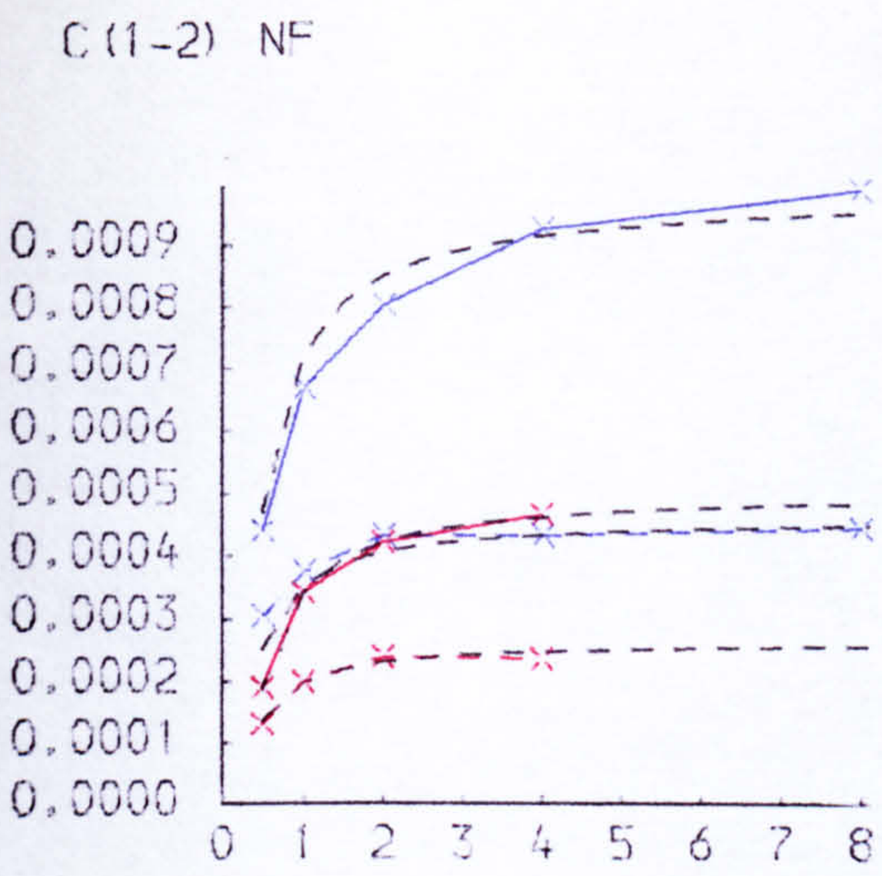

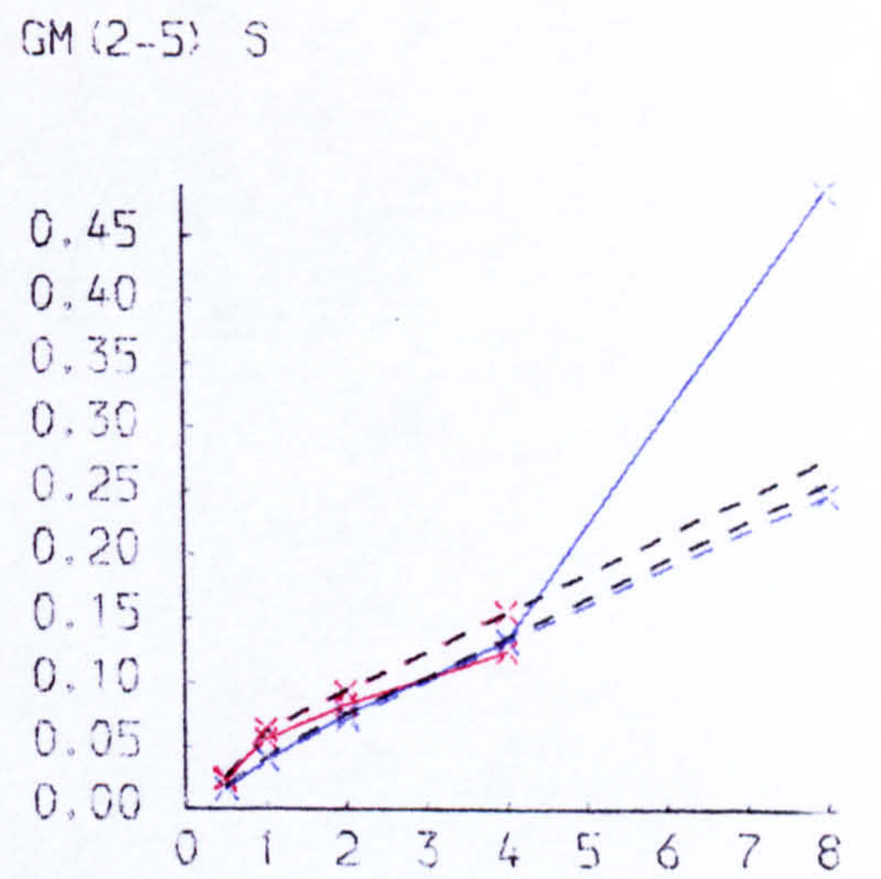

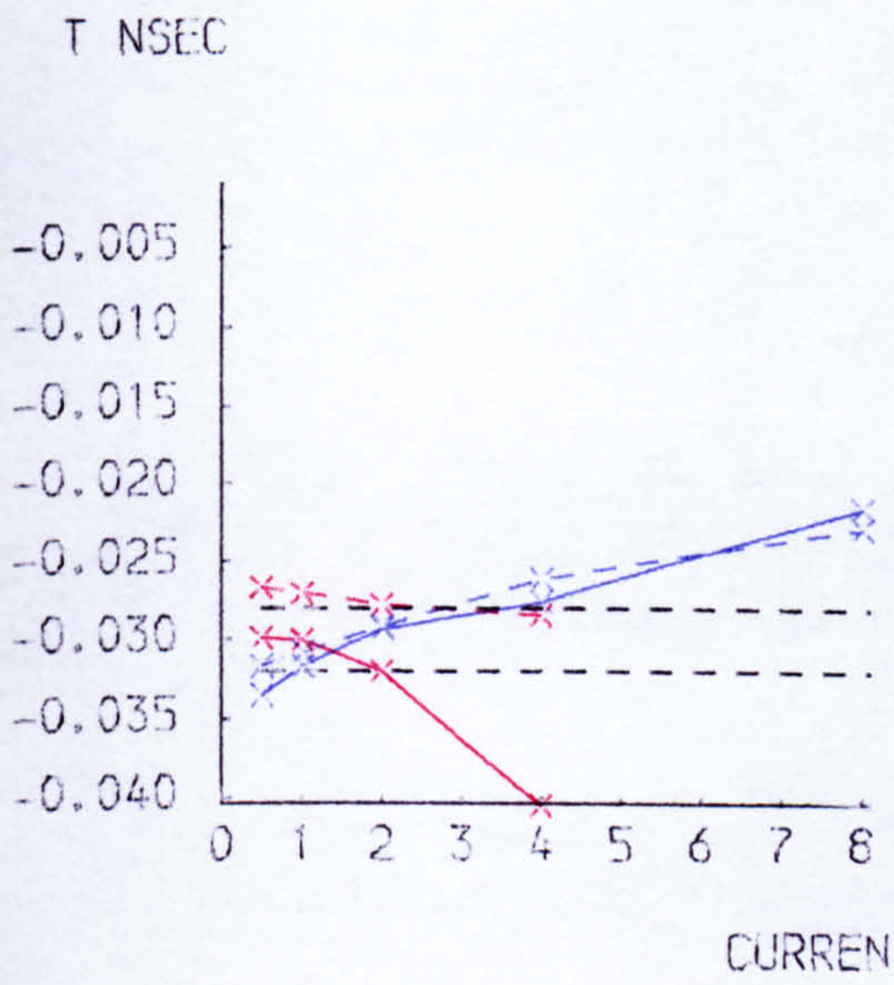

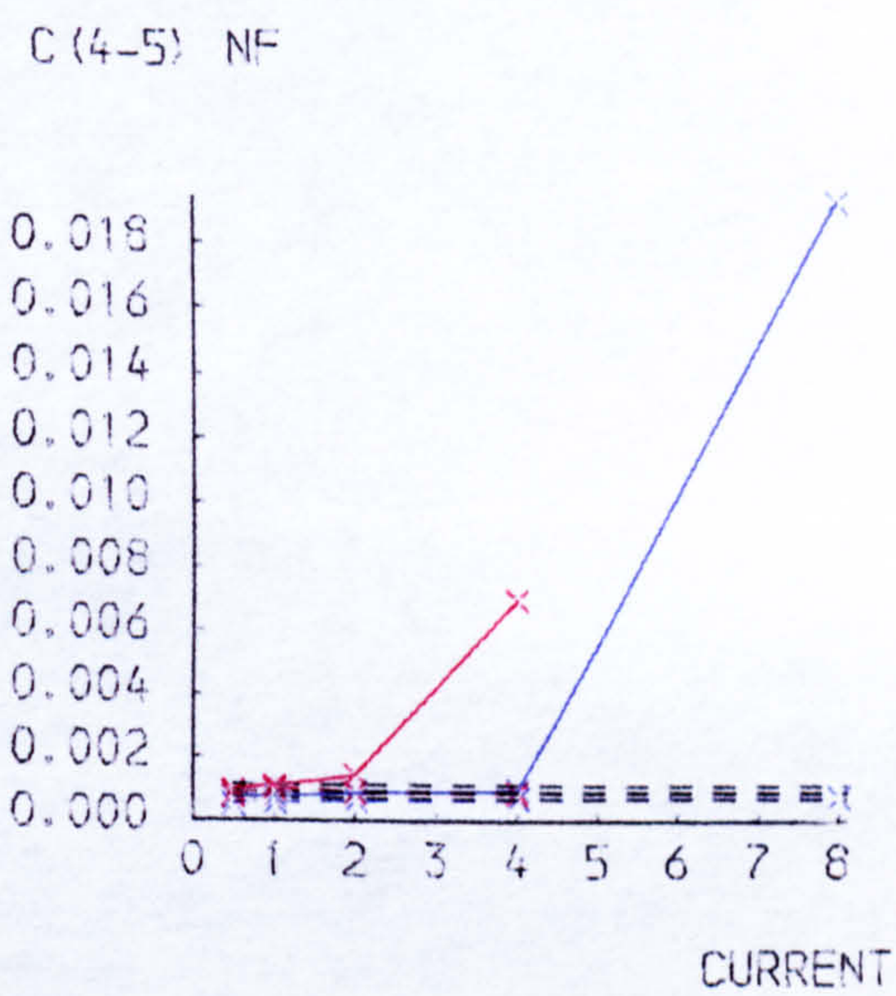

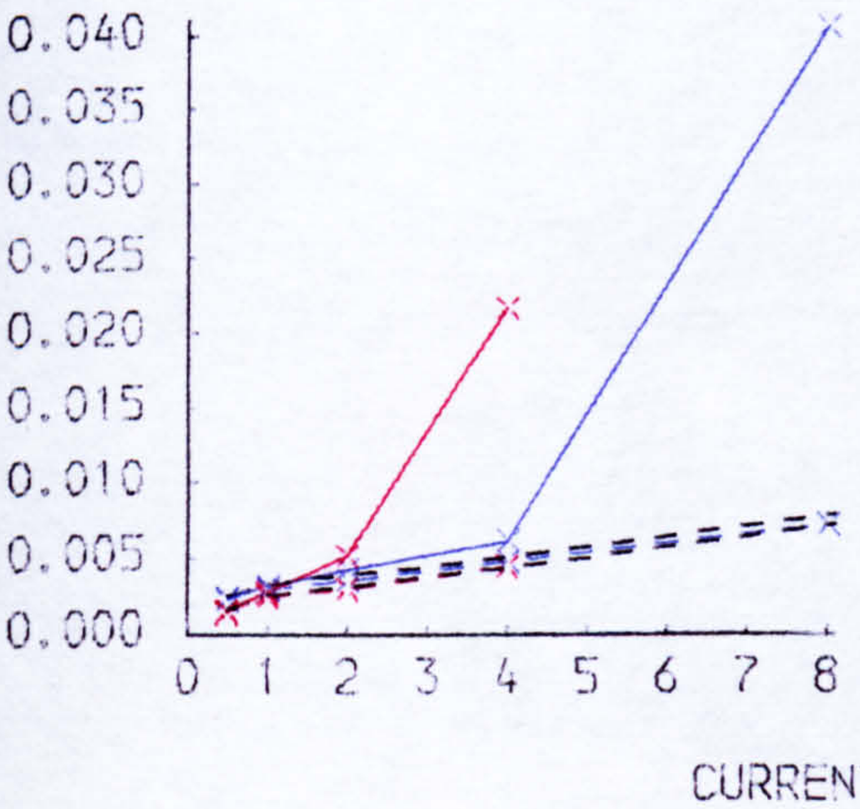

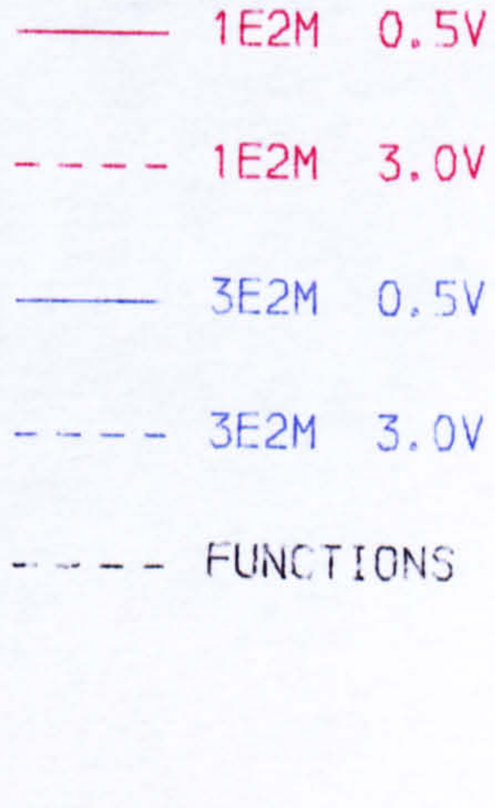

Figure 7.5a Variation of Model Element Values with Emitter Current

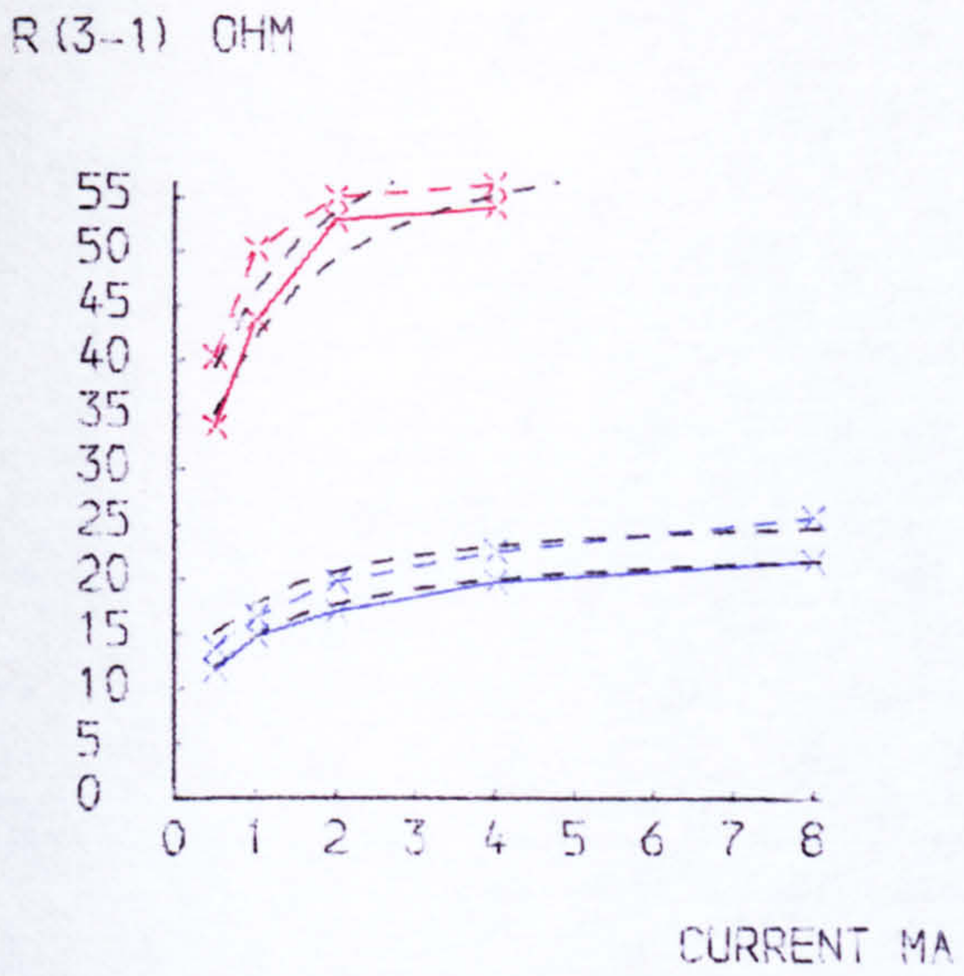

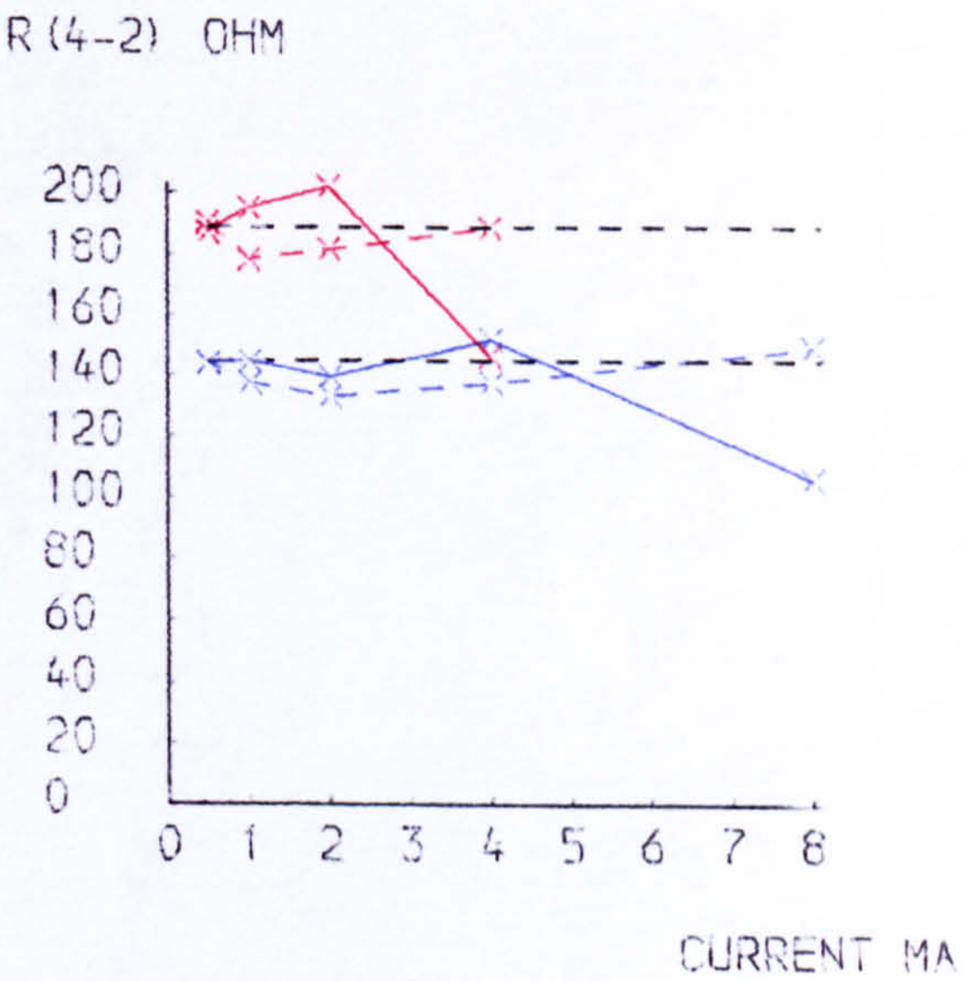

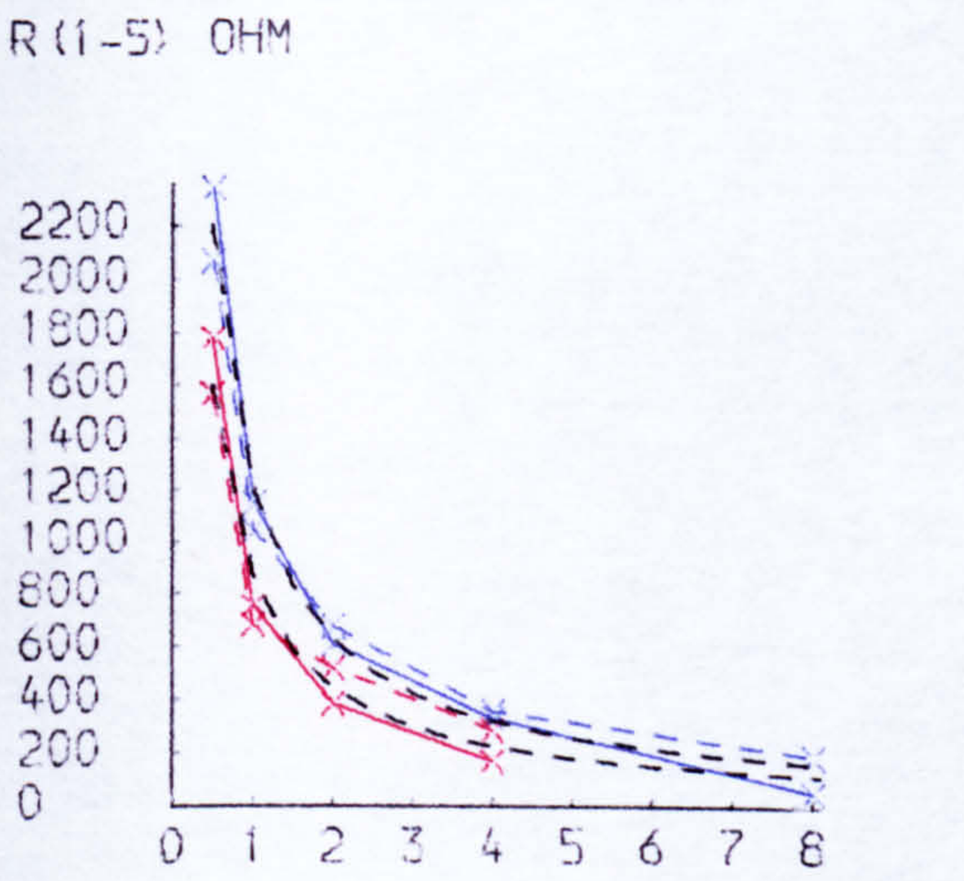

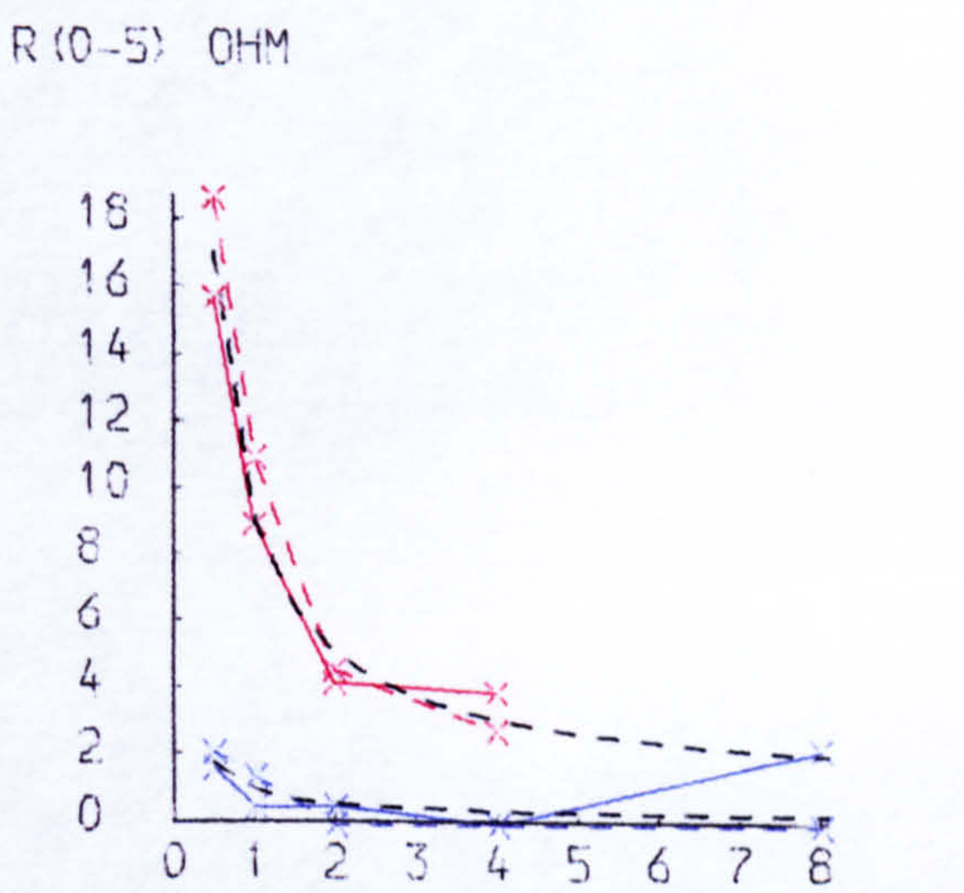

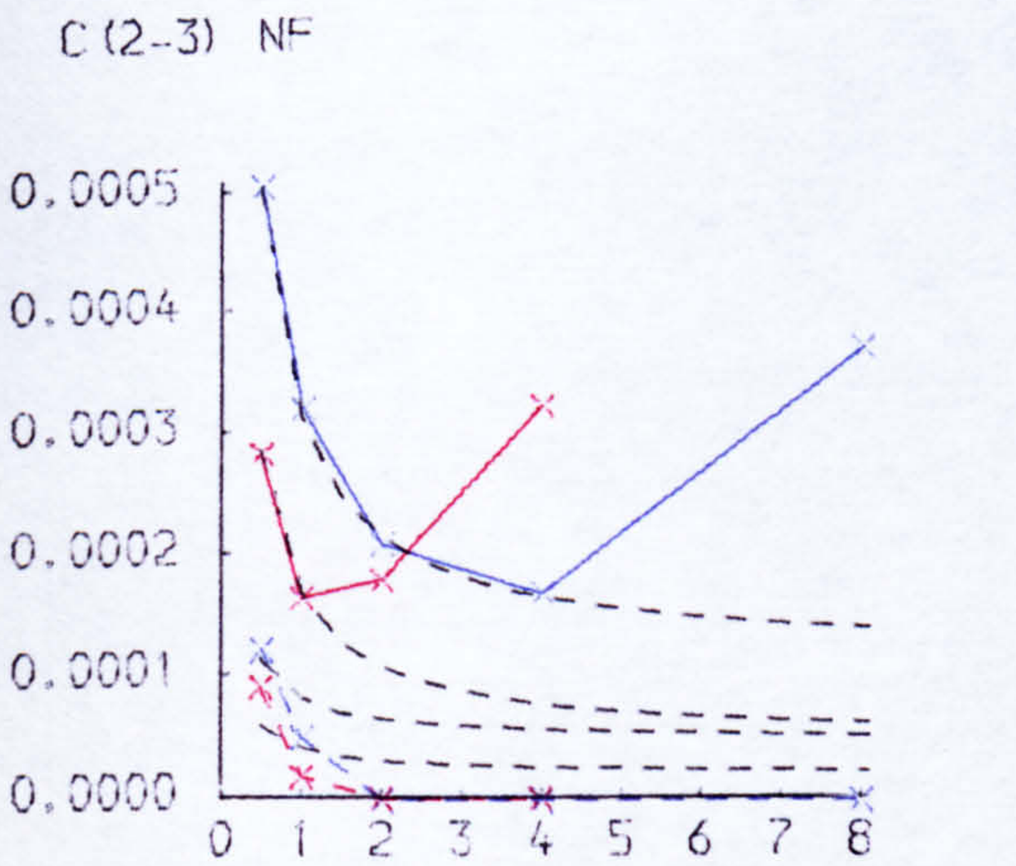

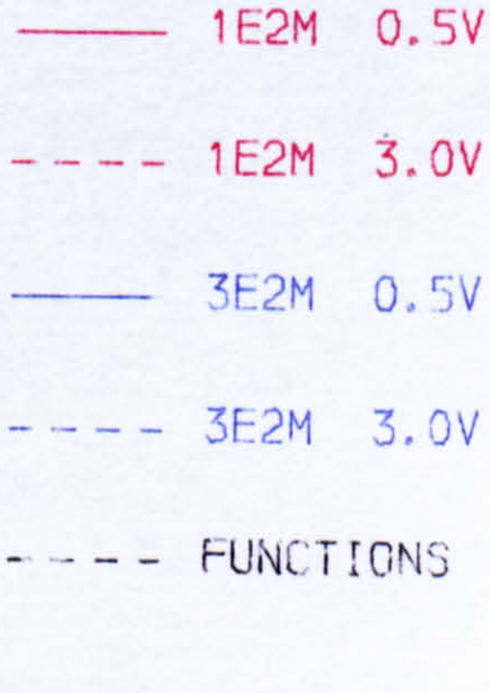

Figure 7.5b Variation of Model Element Values with Emitter Current

value of C_{1-2} appeared to reach a limit where the maximum values obtained in the ranges of I_e under consideration were

0.47 pF for 1E2M at 0.5 V giving $0.33/\sqrt{V_{ce}}$ pF ,

0.24 pF for 1E2M at 3 V giving $0.42/\sqrt{V_{ce}}$ pF ,

0.99 pF for 3E2M at 0.5 V giving $0.70/\sqrt{V_{ce}}$ pF

and 0.45 pF for 3E2M at 0.5 V giving $0.78/\sqrt{V_{ce}}$ pF .

However, the value of C_{1-2} was definitely varying with the value of I_e at lower values of I_e . The model was also sufficiently sensitive to the value of C_{1-2} that a 5% change in the optimum value of C_{1-2} made a significant change in the value of the objective function, F . Thus the functions chosen for C_{1-2} were functions of both I_e and V_{ce} as shown in Table 7.2. The black dotted lines on the graphs of C_{1-2} in Figure 7.5a show the function evaluated at the appropriate values of V_{ce} and I_e.

g_{2-5} - PRL suggested that the value of the current generator should be proportional to I_e . A further relationship stated by PRL was that $g_{2-5} = \frac{1}{r_e}$ where $h_{fe}r_e$ was element R_{4-6} in Figure 7.2 and $h_{fe} = 50$. It is possible that R_{4-6} in Figure 7.2 could be equivalent to element R_{1-5} in Figure 7.3. If this were so then g_{2-5} could be equal to $50/R_{1-5}$. Checking the optimised values of g_{2-5} and R_{1-5} led to the conclusion that although this type of relationship was possible, the value of 50 was not quite right. The average values were 44.4 for 1E2M and 46.3 for 3E2M. However, taking these average values with the optimised values of R_{1-5}, the values calculated for g_{2-5} were not sufficiently accurate. Thus the relationship chosen for g_{2-5} was a piecewise linear function dependent only on I_e. The sudden change in the value of this element for the 3E2M at $I_e = 8$ mA with $V_{ce} = 0.5$ V was taken as a sign that the device was becoming non-linear. This effect can be seen in several of the model elements and in each case it occurs at the highest value of I_e for which an acceptable

value of F had been obtained with V_{ce} = 0.5 V. No attempt was made to model this effect and the fits of the piecewise linear functions chosen can be seen as the black dotted lines on the graphs of g_{2-5} in Figure 7.5a.

τ - The time constant applied to the current generator in the PRL model was given the independent values of -25 ps for the 1E2M and -26 ps for the 3E2M. It can be seen that the optimised values of τ in the author's model vary with the emitter current and that the values of τ for the 1E2M also vary with the collector-emitter voltage. However, as there was no apparent pattern in the variations in the values of τ and bearing in mind the PRL values for τ, it was decided that constant values should be chosen based on the optimum values at low emitter currents since these were the values when the devices were most certainly in the linear region of operation. The values chosen were therefore -28 ps for the 1E2M, the emphasis being on the values for the higher voltage, and -32 ps for the 3E2M.

C_{4-5} - The function given for the equivalent element in the PRL model was A/F where A took a constant value of 1.12 $pF.V^{\frac{1}{2}}$ for the 1E2M and 1.16 $pF.V^{\frac{1}{2}}$ for the 3E2M and F was a function of the collector-substrate voltage $V_{c\text{-}sub}$ such that $F = \sqrt{V_{c\text{-}sub} + 0.75}$. This element was one where the optimised values changed drastically at high values of emitter current while at lower values the element values were almost constant. Therefore, it was decided that, ignoring the high current effects, an inverse square root function of V_{ce} as given in Table 7.2 was appropriate.

C_{3-5} - The optimised values of this element, as with C_{4-5}, underwent large changes at higher values of emitter current and again, these effects were not modelled. C_{3-5} could be considered equivalent to element C_{4-6} in the PRL model in Figure 7.2 perhaps with some additional capacitance due to the T-Π transformation discussed earlier. C_{4-6} in the PRL model

was dependent on the value of the current generator. Investigating the possibilities of this type of relationship showed that similar smooth curves were obtained for both transistors on plotting the optimised values of C_{3-5}/g_{2-5} against emitter current. The function dependent on the value of g_{2-5}, given in Table 7.2, was found to give a best fit for this element.

R_{3-1} - This element could be taken as equivalent to R_{1-3} and R_{3-4} in the PRL model in Figure 7.2. These resistors together with C_{3-6} in Figure 7.2 were used by PRL to model some of the high frequency effects of the transistors and the combined constant values of these two resistors in the PRL model were 66 Ω for the 1E2M and 23 Ω for the 3E2M. In the author's model, R_{3-1} appeared to depend on both I_e and V_{ce} as can be seen from the graphs in Figure 7.5b. The maximum values this element attained for the 1E2M were 54 Ω with V_{ce} = 0.5 V and 56 Ω with V_{ce} = 3 V and for the 3E2M were 22 Ω with V_{ce} = 0.5 V and 26 Ω with V_{ce} = 3 V. These values were quite similar to the constant values used in the PRL model. However the sensitivity of the model to the value of R_{3-1} meant that the effect of changing current was significant. Therefore, it was decided that both the current and voltage effects should be included. The effect of increasing voltage appeared to be to increase the value of R_{3-1} by a constant amount over the entire range of I_e plotted in Figure 7.5b. The function developed for this element is given in Table 7.2.

R_{4-2} - The equivalent element in the PRL model was given constant values of 209 Ω for the 1E2M and 185 Ω for the 3E2M. It was felt that constant values were the most appropriate and the values chosen by the author were 189 Ω for the 1E2M and 145 Ω for the 3E2M. It can be seen from the graphs in Figure 7.5b that these values were based on the optimised values of this element at I_e = 0.5 mA.

R_{1-5} - This element has already been mentioned during the discussion of g_{2-5}. No relationship between these two elements was discovered. It was also decided that there was no dependence on V_{ce} exhibited by R_{1-5}. Functions of I_e were therefore fitted to the average element values for the two values of V_{ce} for each transistor. The functions giving the best fit are given in Table 7.2 and are plotted in Figure 7.5b.

R_{0-5} - This element could be equivalent to R_{0-8} in the PRL model in Figure 7.2. PRL gave R_{0-8} constant values of 1.1 Ω for the 1E2M and 0.8 Ω for the 3E2M. These values did not agree with the values of R_{0-5} in the author's model. This element appeared to depend on I_e particularly for the 1E2M for which the value of R_{0-5} at I_e = 0.5 mA was as high as 18 Ω , reducing to 4 Ω at I_e = 2 mA. Functions of I_e were therefore developed for this element.

C_{2-3} - In the PRL model, the equivalent element, C_{4-5}, was defined as a function of the voltage between nodes 5 and 8 in Figure 7.2. This voltage was calculated as $(V_{ce} - I_e.R_{2-5})$. In the author's model there is no element equivalent to PRL's R_{2-5}. However, the optimised values of C_{2-3} seemed to depend on both I_e and V_{ce}. Fitting functions to the element values proved difficult because the element values at V_{ce} = 3 V became zero. The final compromise was to fit a function of I_e to the element values for V_{ce} = 0.5 V first and then to modify this function as necessary for the higher value of V_{ce}. The final complicated function given in Table 7.2 is not entirely satisfactory and the fits obtained using the function are shown in Figure 7.5b. It can be seen that the values with V_{ce} = 0.5 V are considerably more accurate than those with V_{ce} = 3 V . Fortunately, the model was not highly sensitive to these low values of C_{2-3}.

Element	Bias Dependent Value of Element (I_e in mA, V_{ce} in V)	Constants for 1E2M	Constants for 3E2M
C_{1-2} . nF	$\left[1 + \frac{\left(A + \frac{B}{I_e}\right)}{\sqrt{V_{ce}}}\right].10^{-4}$	A = 2.84 B = - 1.12	A = 6.22 B = - 1.81
g_{2-5} S	$(A + B.I_e).10^{-2}$	A = - 1.12, B = 7.21 } $I_e \leq 1$ mA A = 3.4, B = 3.0 } $I_e > 1$ mA	A = - 0.47, B = 4.64 } $I_e \leq 1$ mA A = 1.5, B = 3.0 } $I_e > 1$ mA
τ ns	A	A = - 0.028	A = - 0.032
C_{4-5} nF	$\left(A + \frac{1}{1 + \sqrt{V_{ce}}}\right).10^{-3}$	A = 0.54	A = 0.34
C_{3-5} nF	$\left(A + \frac{B}{I_e}\right).g_{2-5}$	A = 0.024 B = 0.018	A = 0.024 B = 0.055
R_{3-1} Ω	$A - \frac{B}{1 + I_e} + C.V_{ce}$	A = 62.9 B = 43.1 C = 1.7	A = 22.9 B = 17.2 C = 1.2
R_{4-2} Ω	A	A = 189	A = 145
R_{1-5} Ω	$\frac{1}{A + B.I_e}.10^5$	A = 8.385 B = 108.32	A = 7.371 B = 76.19
R_{6-5} Ω	$A + \frac{B}{C}$	A = 1.0 B = 8.0	A = 0.1 B = 0.8
C_{2-3} nF	$\left(\frac{A}{\sqrt{V_{ce}}} + \frac{B}{I_e.V_{ce}}\right)10^{-5}$	A = 3.27 B = 5.95	A = 8.2 B = 9.7

Table 7.2. Bias Dependent Relationships for the Model in Figure 6.3

7.3. Resultant Bias Dependent Model

The effect of the different bias conditions on the values of the model elements was discussed in Section 7.2 and functions were developed for each of the elements. This exercise could be seen as a feasibility study for the determination of the effects of different bias conditions using optimised models of transistors. Although the effects of different emitter currents on the model element values could generally be seen, the number of values of collector-emitter voltage, V_{ce}, for which data was provided was too small to give confidence in the proposed functions of V_{ce}. However, a bias dependent model had been developed.

It was known that some of the functions would not give the optimised values of certain elements for $V_{ce} = 0.5\,V$ when I_e was greater than $2\,mA$ for the 1E2M and greater than $4\,mA$ for the 3E2M. As a check on the effectiveness of the new bias dependent model, graphs were drawn of the calculated and measured values of the modulus of s_{21} at $1\,GHz$ against emitter current. These graphs are shown in Figure 7.6. As expected they show that the model is accurate for values of modulus s_{21} up to its peak value. This appears to be slightly better than the PRL model which, in the paper by Slatter[17], is shown to lose accuracy for the 3E2M before the peak value of modulus s_{21} is reached. Graphs of the s parameters calculated using the author's bias dependent model, together with the measured s parameters, against frequency are shown in Figures 7.7 and 7.8 for the 1E2M and 3E2M respectively, at the arbitrary bias values of $V_{ce} = 3\,V$ and $I_e = 2\,mA$. Looking at these graphs the author has some doubts about the accuracy of the measurements of s_{12} for the 1E2M. However, the graphs show good agreement between the measured and calculated values of all the s parameters and would appear to offer an improvement on those shown by Slatter[17], especially as the agreement continues up to a frequency of $2\,GHz$ while Slatter's model was only valid

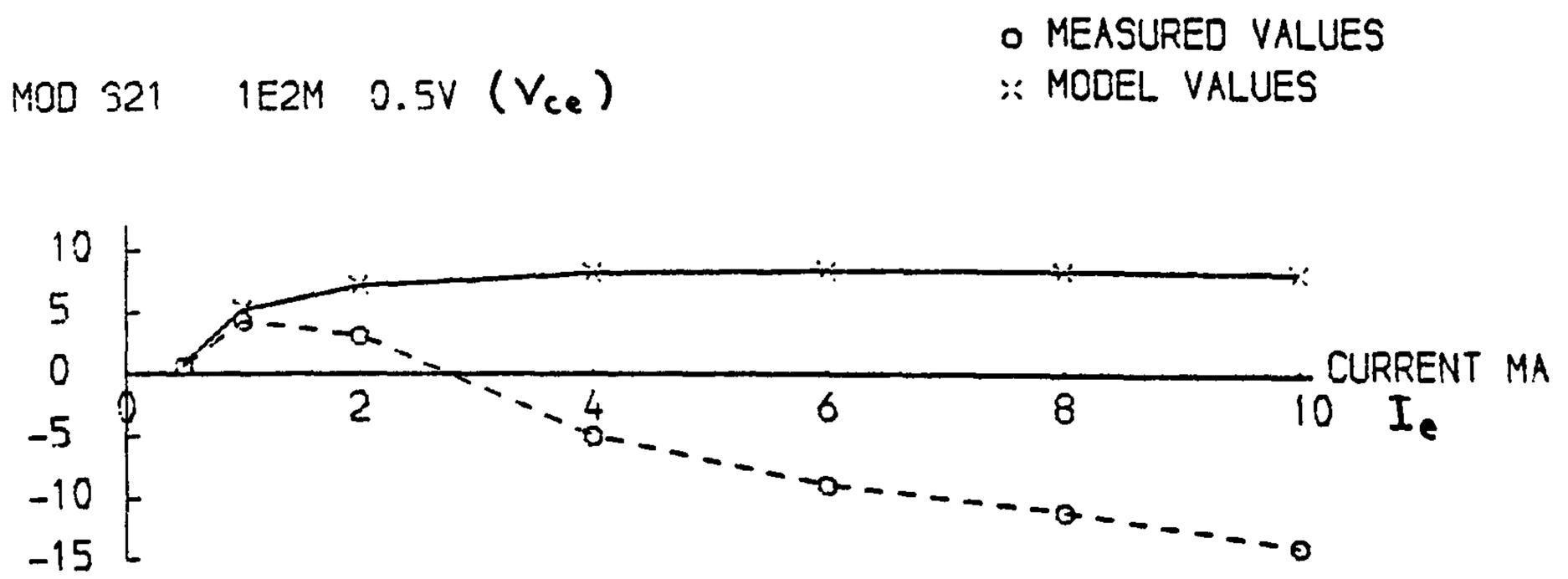

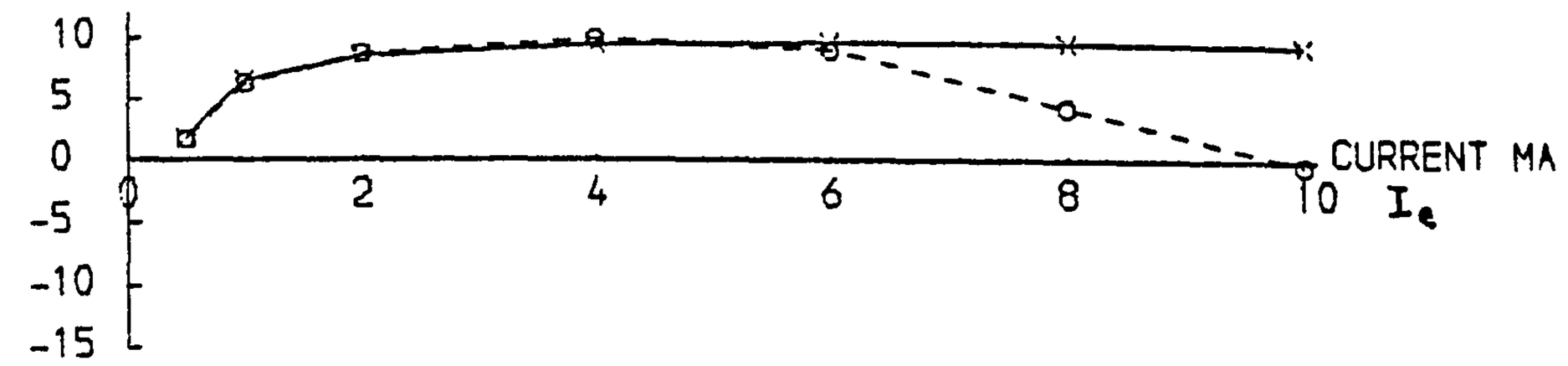

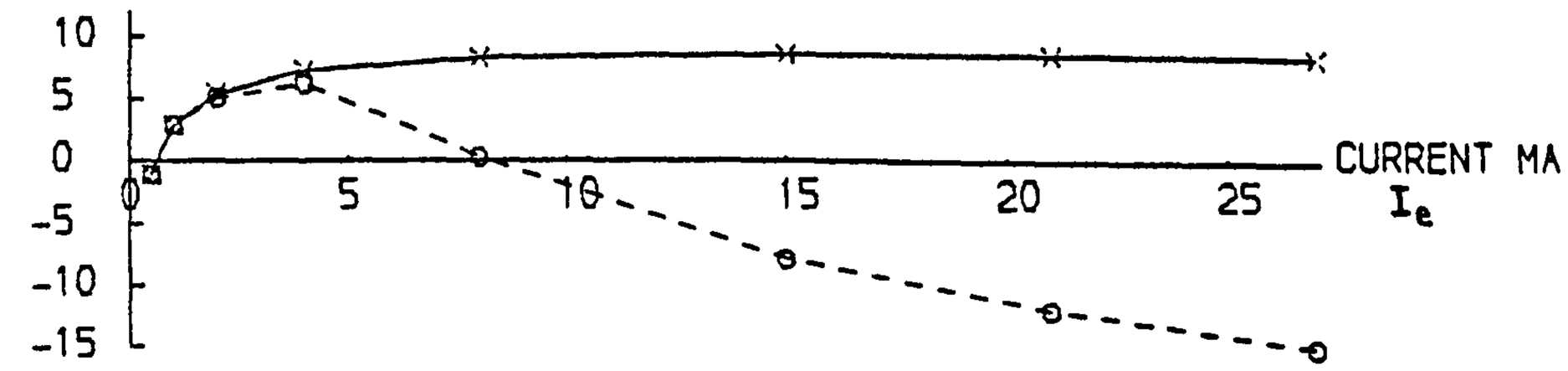

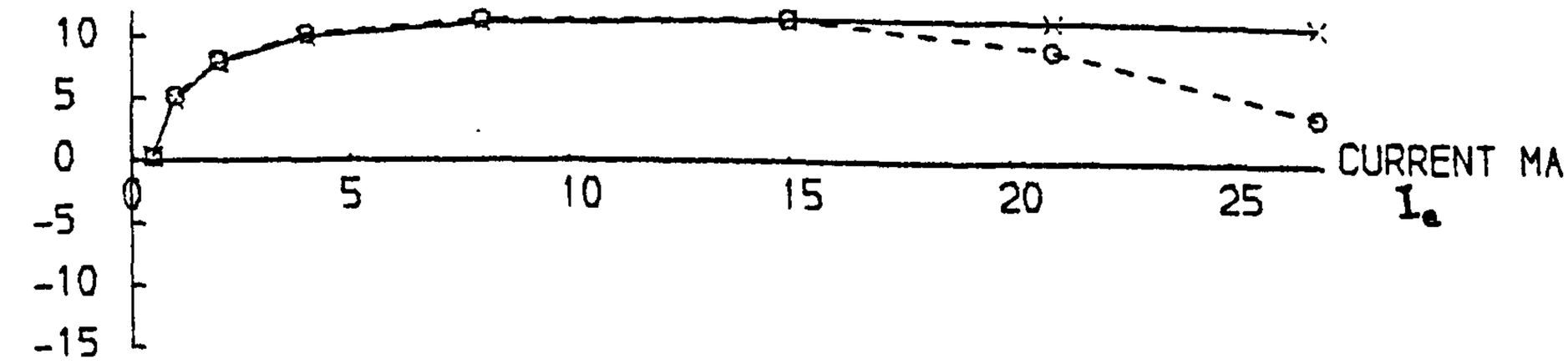

Figure 7.6 Modulus S_{21} at 1 GHz for the Bias Dependent Model

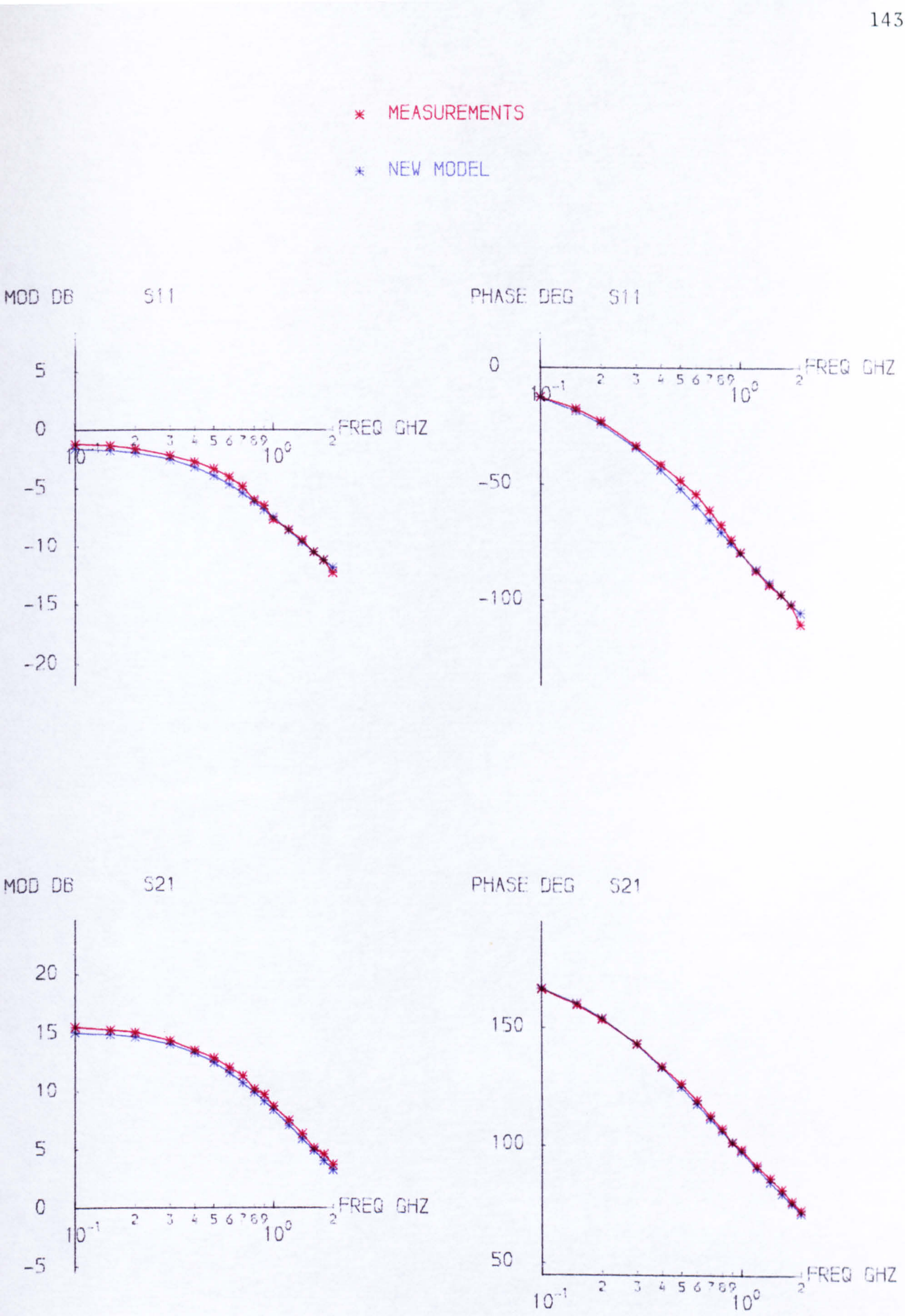

Figure 7.7a S_{11} and S_{21} for 1E2M for V_{ce} = 3 V and I_e = 2 mA

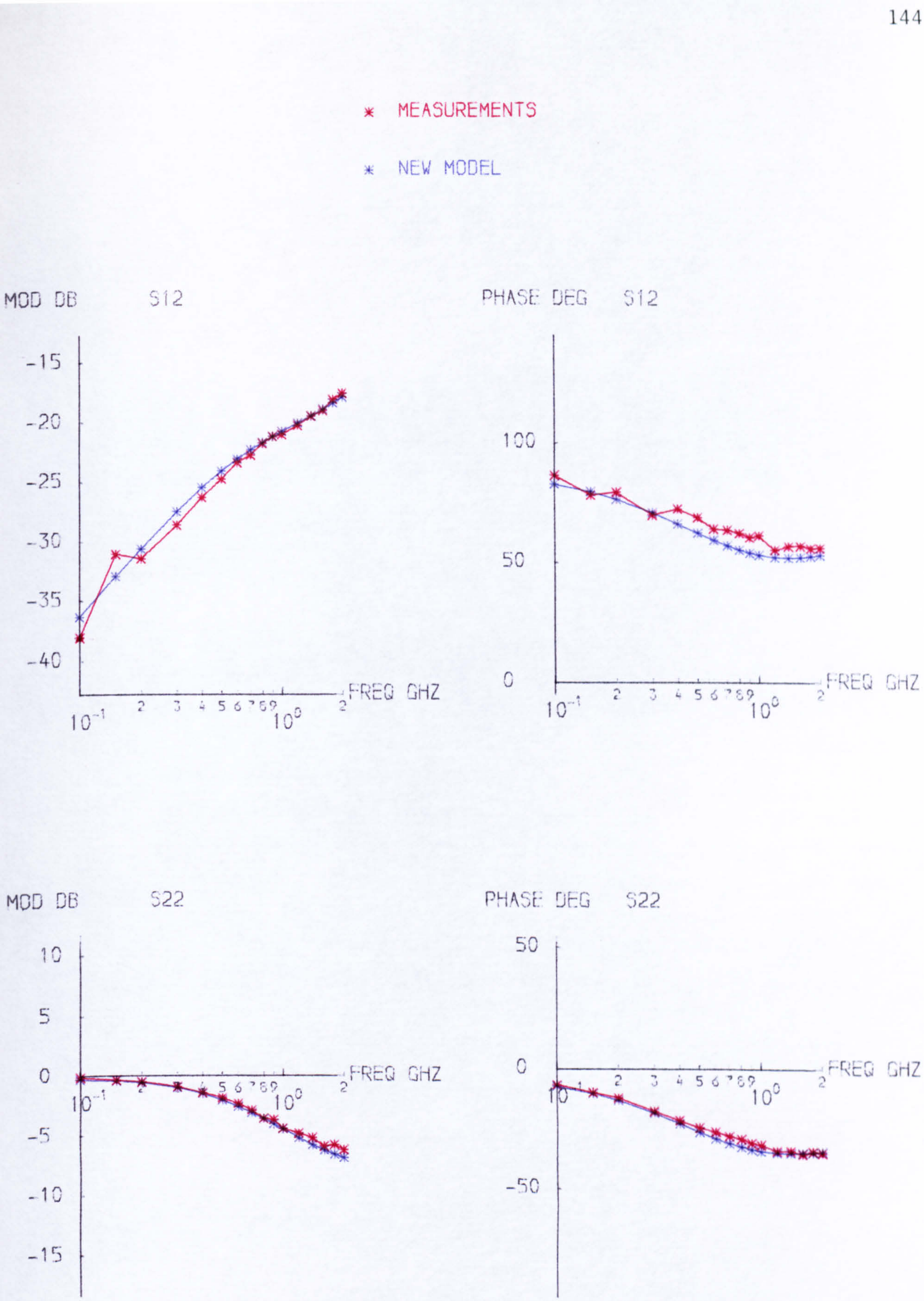

Figure 7.7b S_{12} and S_{22} for 1E2M for V_{ce} = 3 V and I_e = 2 mA

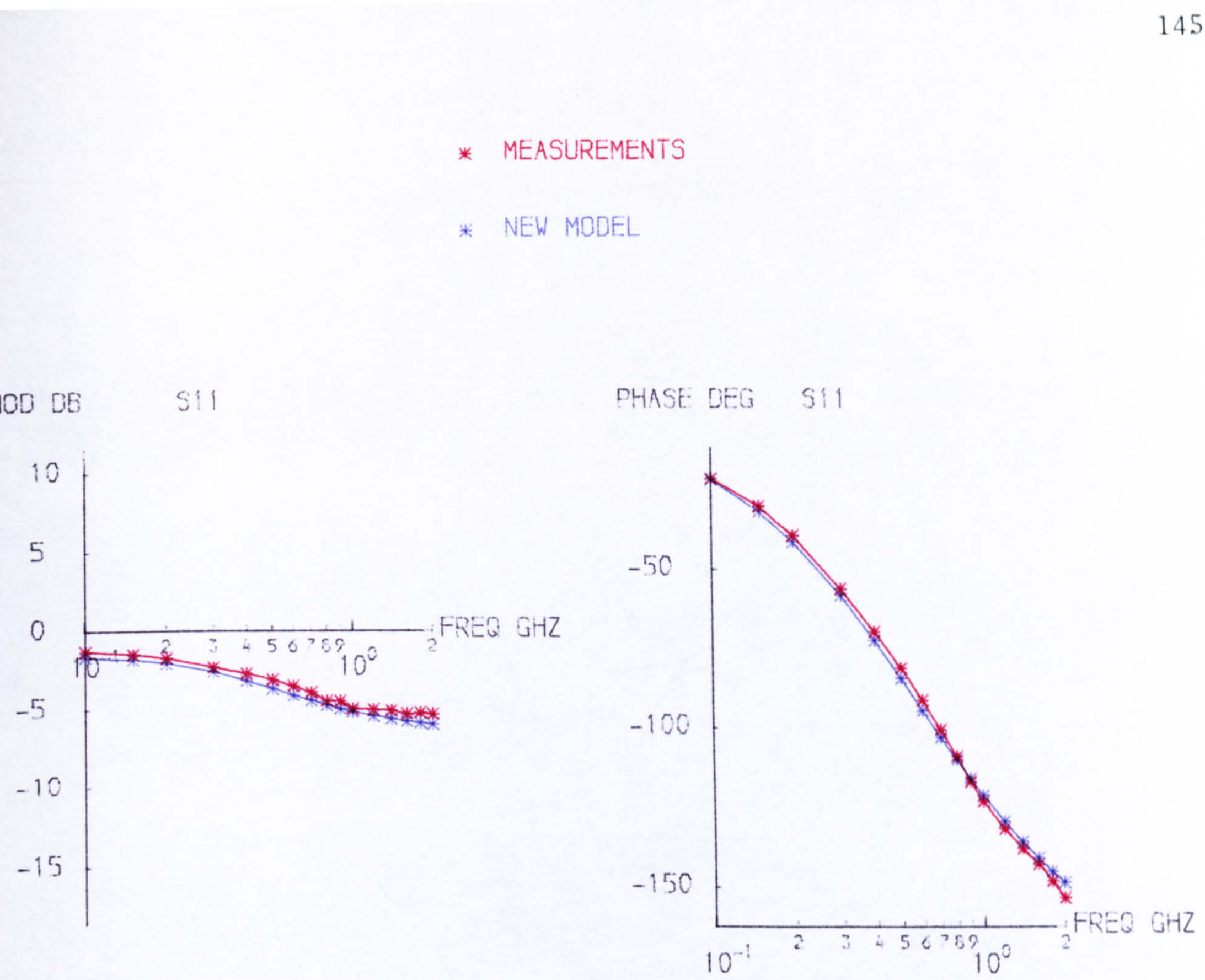

Figure 7.8a S_{11} and S_{21} for 3E2M for V_{ce} = 3 V and I_e = 2 mA

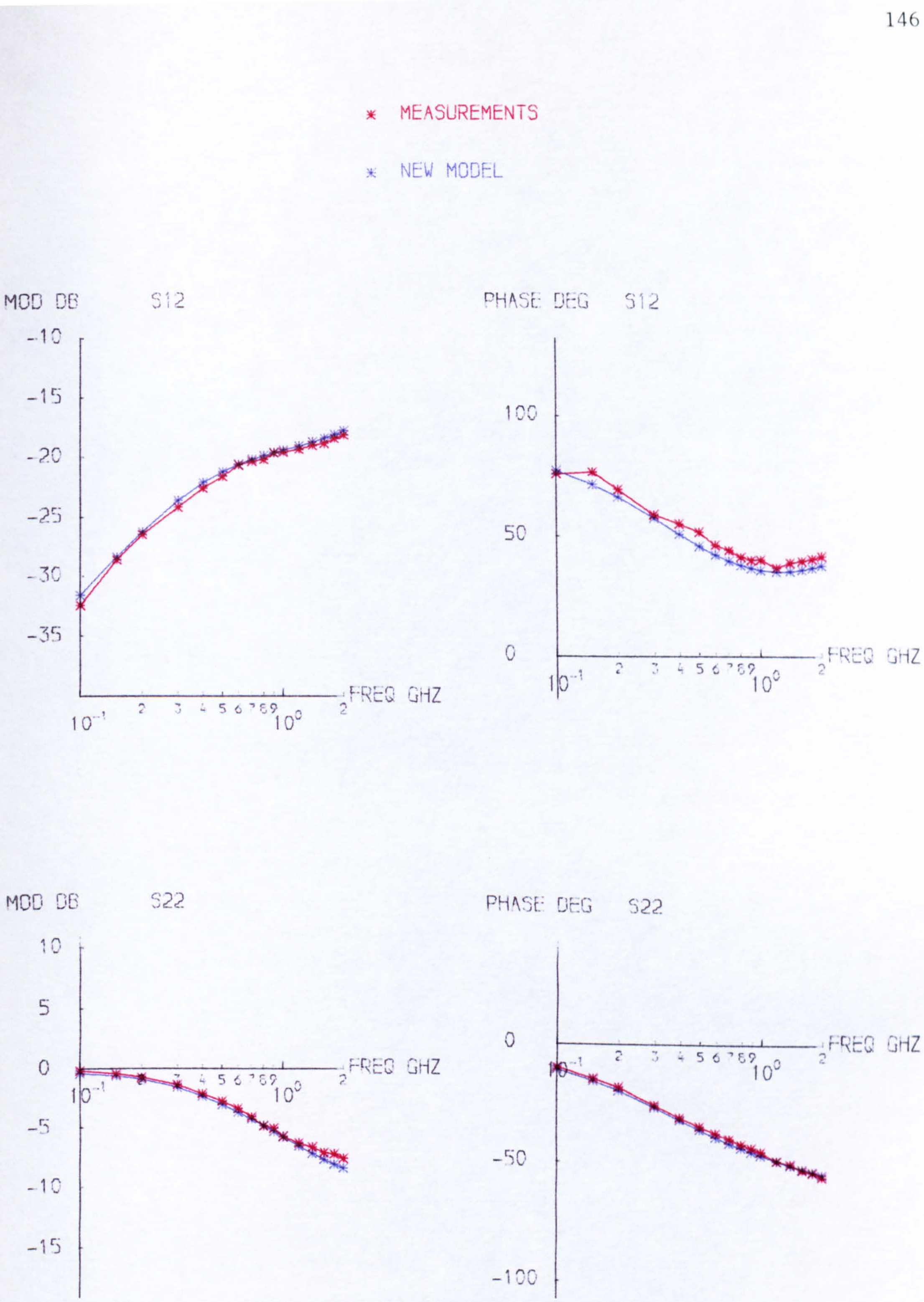

Figure 7.8b S_{12} and S_{22} for 3E2M for V_{ce} = 3 V and I_e = 2 mA

up to 1 GHz.

The conclusions drawn from this were that accurate bias dependent models could be developed using the author's modelling algorithm and that it was possible to develop quite simple functions describing the dependence of the model elements on the bias conditions. Although some theoretical indications of likely relationships could be useful, they were not absolutely necessary. Examination of the variation of the model element values at different bias conditions could indicate the possible forms the function could take. Then the use of a curve fitting technique with a number of different functions of the bias variables could assist in the final choice of the most suitable function.

7.4. Models for High Emitter Currents

After the bias dependent model for the linear region of operation had been successfully developed, attempts were made to develop models for the transistors at the highest values of emitter current for which data was provided.

For each transistor, using the s parameter data at the highest values of I_e given and with both values of V_{ce} given, the initial model used was the appropriate optimised model for I_e = 4 mA or I_e = 8 mA from the earlier work. Applying the modelling algorithm to these four cases produced four different models. However, re-optimising each of these four models for each of the four cases, one of the models proved to be the most effective with V_{ce} = 0.5 V and I_e = 10 mA and 28 mA for the 1E2M and 3E2M respectively, while another model was the most effective for both transistors with V_{ce} = 3 V and their respective highest values of I_e. These models are shown in Figure 7.9. The value of the objective function in each case was less than 4.3E + 03 and the maximum absolute individual errors were 1.5 dB and 12°. The models were again effective

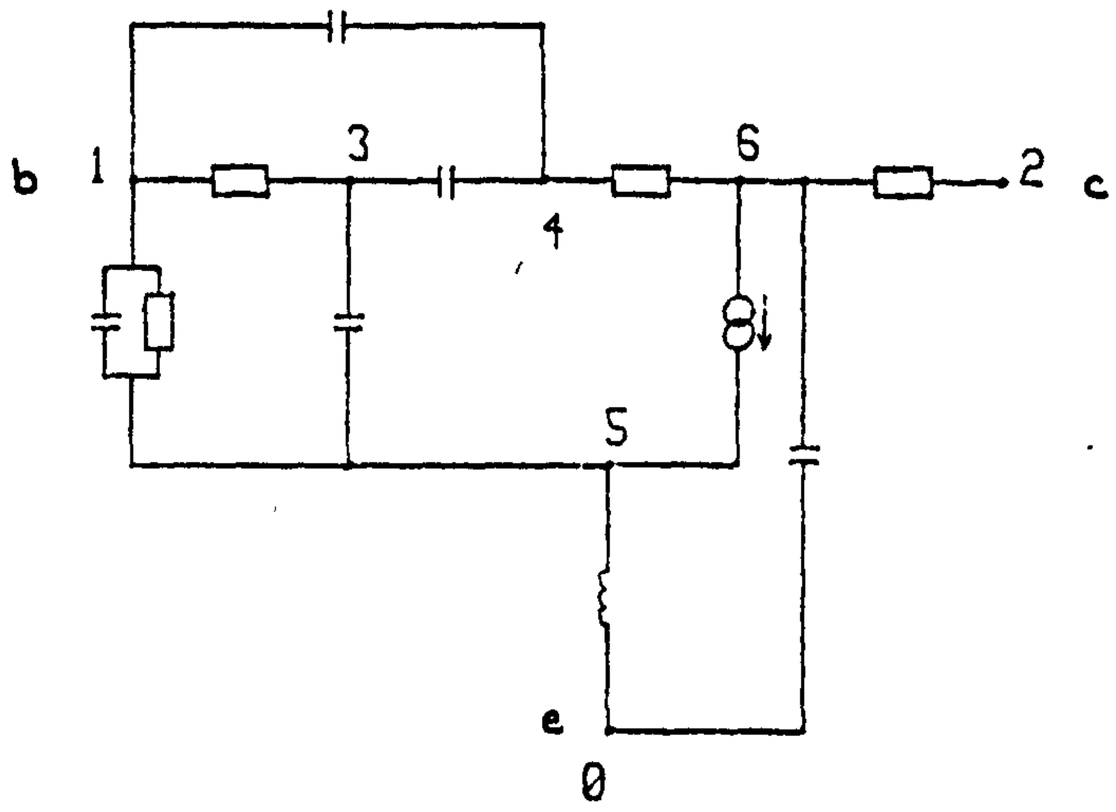

No. of nodes = 7
No. of elements = 11

Node 1 - Base
Node 2 - Collector
Node 0 - Emitter

1E2M 0.5V 10mA

F = 1.26E+03

g (6-5) = 1.80E-01 S
(T =-1.07E-01 ns)
(V across nodes $\frac{3}{5}$)
C (3-5) = 6.40E-02 nF
R (3-1) = 3.61E+01 ohm
R (4-6) = 1.92E+01 ohm
L (0-5) = 1.13E+00 nH
C (1-4) = 1.18E-03 nF
C (3-4) = 4.80E-03 nF
C (1-5) = 6.86E-04 nF
C (6-0) = 1.30E-03 nF
R (1-5) = 1.33E+02 ohm
R (2-6) = 1.73E+01 ohm

3E2M 0.5V 27mA

F = 1.55E+03

g (6-5) = 4.97E-01 S
(T =-3.09E-02 ns)
(V across nodes $\frac{3}{5}$)
C (3-5) = 1.20E-01 nF
R (3-1) = 1.36E+01 ohm
R (4-6) = 2.36E+00 ohm
L (0-5) = 5.10E-01 nH
C (1-4) = 3.06E-03 nF
C (3-4) = 9.04E-03 nF
C (1-5) = 4.03E-03 nF
C (6-0) = 1.90E-03 nF
R (1-5) = 4.62E+01 ohm
R (2-6) = 1.15E+01 ohm

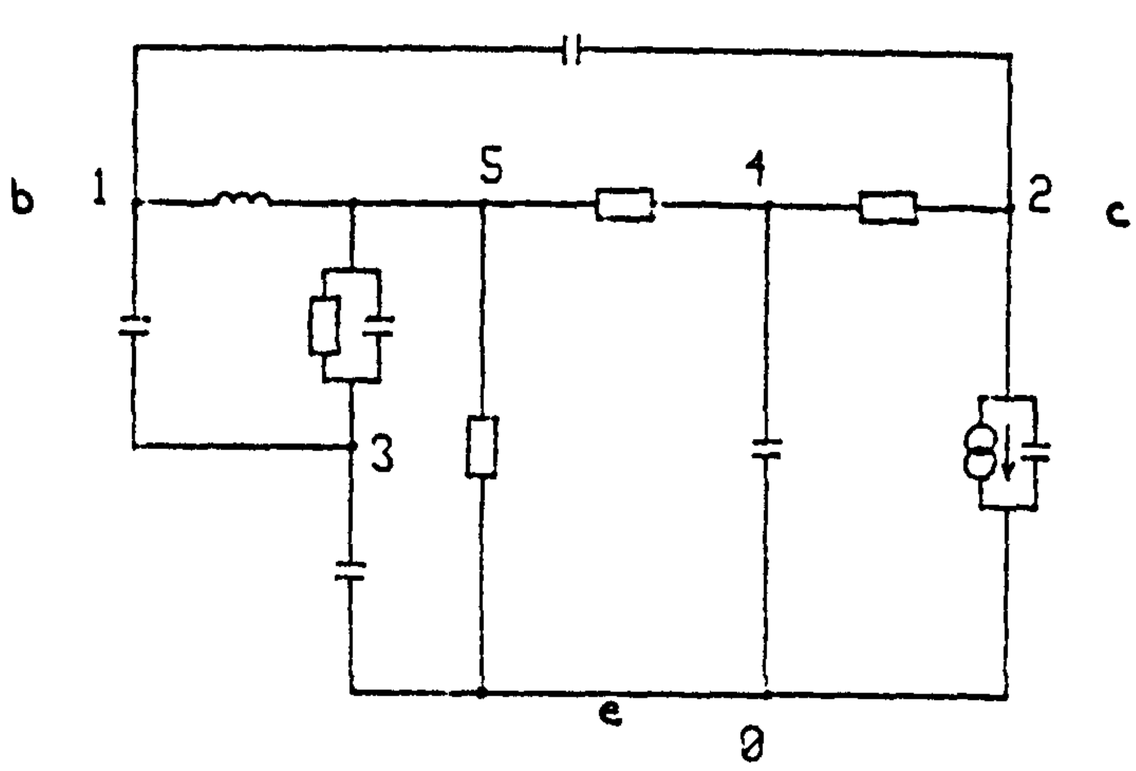

No. of nodes = 6
No. of elements = 12

Node 1 - Base
Node 2 - Collector
Node 0 - Emitter

1E2M 3.0V 10mA

F = 1.25E+03

g (2-0) = 1.50E-01 S
(T =-4.35E-02 ns)
(V across nodes $\frac{3}{0}$)
C (4-0) = 1.80E-03 nF
C (3-0) = 1.84E-02 nF
R (3-5) = 5.83E+01 ohm
R (4-2) = 2.91E+02 ohm
R (5-0) = 1.58E+02 ohm
C (5-3) = 9.42E-04 nF
R (5-4) = 1.88E+01 ohm
C (2-0) = 1.38E-04 nF
L (1-5) = 1.93E+00 nH
C (1-2) = 2.72E-04 nF
C (1-3) = 4.02E-04 nF

3E2M 3.0V 27mA

F = 1.42E+03

g (2-0) = 4.54E-01 S
(T =-3.21E-02 ns)
(V across nodes $\frac{3}{0}$)
C (4-0) = 3.16E-03 nF
C (3-0) = 3.97E-02 nF
R (3-5) = 2.28E+01 ohm
R (4-2) = 2.10E+02 ohm
R (5-0) = 6.57E+01 ohm
C (5-3) = 2.55E-03 nF
R (5-4) = 1.47E+01 ohm
C (2-0) = 1.53E-04 nF
L (1-5) = 9.92E-01 nH
C (1-2) = 5.15E-04 nF
C (1-3) = 9.72E-04 nF

Figure 7.9 Models for High Emitter Currents

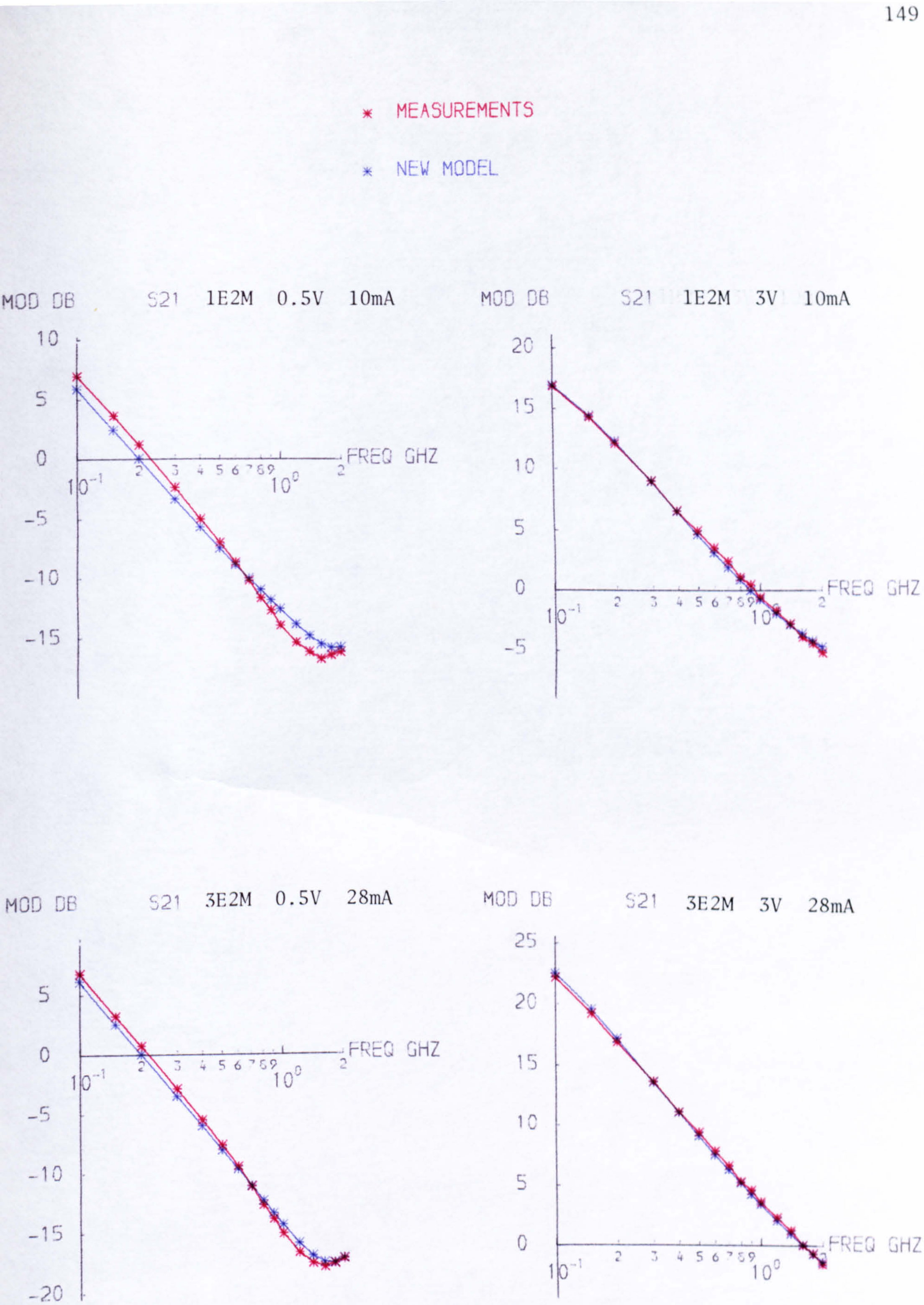

Figure 7.10 Modulus S_{21} Against Frequency for the High Current Models

up to 2 GHz and graphs of modulus s_{21} against frequency for each case are shown in Figure 7.10.

The author found this result interesting as it seems to confirm the similarity of the two transistors. The effect of the extra emitter stripes in the 3E2M would appear to enable the transistor to operate in a similar manner to the 1E2M at higher emitter currents for the same values of collector-emitter voltages. The fact that there were different models at the two values of collector-emitter voltage demonstrates that there are major effects on changing V_{ce} in this region of operation of the transistors.

CHAPTER 8

CONCLUSIONS AND SUGGESTIONS FOR FURTHER WORK

In Chapter 2, the standard models for bipolar transistors were described together with methods by which the values of the elements in a model of any particular device could be determined. Where the model chosen gives adequate accuracy there are no problems. However, the author felt that there was insufficient guidance on the choice of alternative models and on the determination of their element values.

Chapters 3 and 4 provided some background information relevant to the author's modelling algorithm which was developed for those cases where a suitable model of a particular device was not readily available. Chapter 3 described transistor parameter measurements and gave details of how models could be analysed in order to compare their performance with a device for which parameter measurements were available. Chapter 4 then described a number of methods of numerical optimisation.

The development of the author's modelling algorithm was described in Chapter 5. The algorithm started as one to optimise the element values of particular models in order to reduce the errors between the s parameter measurements of a transistor and the s parameters of the model. From this, techniques were developed whereby, if necessary, the topology of the model could also be optimised. The development of a model for a lateral p-n-p transistor was used to illustrate the development of the algorithm. Then, after a complete description of the modelling algorithm, details were given of the development of a model for the lateral p-n-p transistor using the final version of the modelling algorithm.

As a further demonstration of the efficacy of the modelling algorithm, in Chapter 6 details were given of the models produced for a vertical n-p-n transistor in each of common base, common emitter and

common collector configurations. The models produced were highly accurate, but attempts to produce a single general model for all three configurations was not so successful. This was mainly because of the size of the problem and the computing time required.

The final example of use of the modelling algorithm was in Chapter 7, which described the development of a bias dependent model of two similar bipolar transistors. The modelling algorithm was first used to develop a suitable model and then to optimise the element values of the model for different bias conditions of the transistors. Using these optimised element values as a guide, suitable expressions for the model elements as functions of the bias conditions were suggested by the author.

The modelling algorithm was developed with the main aim of producing accurate models of particular transistors. The emphasis, therefore, was on the achievement of results rather than on producing a small, fast computer program. The author's view is that computers are ever becoming faster and larger; therefore, although computer programs should be written efficiently, they should not take short-cuts that could cause the failure to find a solution to a particular problem. However, the development of the general model for the vertical n-p-n transistor demonstrated that, with the facilities available to the author, some sacrifices of accuracy might be necessary in order to achieve satisfactory models for some large problems. However, these sacrifices might not have a detrimental effect on the efficacy of the modelling algorithm and tests could be conducted to check the effect of a number of ways in which the modelling algorithm could be made faster. These include

(i) the use of single precision arithmetic in the analysis of the models,

(ii) the use of forward differences in the calculation of the approximation to the Jacobian matrix.

The use of a smaller increment in the calculation of the approximation to the Jacobian matrix could improve the accuracy of this calculation. This could offset the loss of accuracy due to (ii) above, and would not cause any increase in the required computing time.

In Stage 2 of the modelling algorithm, the author decided that each successful addition should remain in the model. One effect of this was that sometimes elements were added and then removed again during the addition of a different element. Cases have been seen where a particular element is added and removed several times. There are two alternative techniques that the author considers would be worth evaluating.

The first of these would be to test each possible addition and to select only the best of these. Then a suitable technique for further additions in Stage 2 could be, either, to attempt to add the remaining successful elements, one at a time, in order of effectiveness, or, to re-evaluate all the possible additions, taking only the best again. The former suggestion for further additions might seem to be the most efficient method, but changing a model by the addition of only one element could cause such differences that elements which could be successfully added prior to the change, could no longer be inserted.

A second, alternative technique for Stage 2 could be to evaluate each possible element addition and then to insert all the successful additions together at their optimum values. The model could then be re-optimised in a similar manner to Stage 1 so that any elements that were not necessary could be removed. In this way a number of element additions might be achieved in one operation.

For large problems such as the general model of the vertical n-p-n transistor, even these suggestions might not reduce the required computing

time sufficiently. Therefore, in view of the large amount of data available for that particular problem, as suggested in Chapter 6, it might be feasible to use only part of the available data.

In the development of the bias dependent model described in Chapter 7, the modelling algorithm was used to calculate the optimum element values at each of the different bias conditions. Instead of choosing the constant values in the rather arbitrary manner used by the author it might be possible to use an optimisation technique both to choose which elements should take constant values and to ascertain their optimum values. This would, like the general model of the vertical n-p-n transistor, create a very large scale optimisation problem and it might be necessary to use only a selection of the available S parameter data.

After the constant element values have been ascertained, more accurate functions for the bias dependent elements might be obtained if the models are then re-optimised with the constant element values fixed.

The development of bias dependent models valid beyond the linear region of operation could be possible using the author's modelling algorithm. The author's approach to this problem would be to develop new models for progressively higher values of I_e and V_{ce}. Hopefully the topology of the models would only change slowly and these changes could, perhaps, be incorporated into the models by the use of mathematical functions which would allow, for example, the gradual reduction of a resistor to zero, after which it would remain as a short-circuit. Alternatively, elements or groups of elements could be made part of the model under certain bias conditions by the use of diodes in much the same way as in the Ebers Moll models described in Chapter 2.

It is the author's opinion that the aims of the research stated in the Introduction have been achieved. A modelling algorithm has been

developed which will optimise model element values and topologies in order to produce accurate models of bipolar transistors using the s parameter measurements of the devices. The effectiveness of this algorithm has been demonstrated by the modelling of several different transistors. Although suggested model topologies were provided for these cases, the author feels that an initial model based on the modified hybrid pi model described in Section 2.2.2 would be suitable for the modelling of most bipolar transistors. The author has also shown that the modelling algorithm can be used in the development of bias dependent models. A model for the linear region of operation of two similar bipolar transistors using simple functions for the bias dependent elements was developed by the author.

It was hoped that this research might indicate how the standard models of bipolar transistors could be improved especially at high frequencies. Although a number of different accurate models have been described here, the author is of the opinion that a much larger selection of devices must be modelled before any conclusions can be drawn concerning the general applicability of the non-standard elements. However, by the development of the new modelling algorithm, the author has provided a means by which this can now be achieved.

APPENDIX 1

S PARAMETER DATA PROVIDED BY PHILIPS RESEARCH LABORATORIES

S - Parameter Data - Lateral pnp in Common Emitter at 0.1mA

freq MHz	Sinput		Sreverse		Sforward		Soutput	
	dB	degrees	dB	degrees	dB	degrees	dB	degrees
0.5	- 0.1	- 1.4	N.M.	N.M.	- 12.5	178.1	0.0	- 0.2
2.0	- 0.2	- 5.4	- 64.7	88.7	- 12.5	169.9	0.0	- 0.3
5.0	- 0.4	- 11.2	- 57.2	84.0	- 12.8	155.0	0.0	- 0.5
10.0	- 1.2	- 19.4	- 52.0	76.3	- 14.0	132.9	0.0	- 0.9

N.M. = Not measurable

Author's Note

Z_0 = 50 ohms

Frequency in MHz

U=	1.5		I=		.778			
FREQ	S11		S12		S21		S22	
100.000	.191	91.9	.006	69.4	1.004	-31.5	1.002	-8.9
150.000	.232	69.4	.008	65.5	.948	-46.5	.985	-13.5
200.000	.264	53.0	.009	58.3	.867	-58.3	.979	-17.4
250.000	.280	40.2	.010	55.0	.798	289.8	.975	-21.0
300.000	.289	30.7	.010	51.2	.715	279.4	.971	336.1
400.000	.291	375.4	.009	37.5	.601	-99.7	.954	329.3
500.000	.278	364.4	.007	16.8	.507	-117.0	.929	321.1
600.000	.261	355.3	.005	-65.2	.443	-134.2	.892	311.7
700.000	.244	-11.7	.016	-120.5	.386	211.0	.849	-58.3
800.000	.234	-17.6	.039	224.2	.337	196.2	.792	-68.9
900.000	.233	336.1	.077	209.7	.316	184.7	.734	280.2
1000.000	.245	325.9	.148	-168.7	.321	-182.8	.687	267.7

Original Form of Data for Vertical N-P-N Transistor in Common Base Configuration

S PARAMETERS OF VERTICAL NPN TRANSISTOR IN COMMON COLLECTOR CONFIGURATION

FREQUENCY	S11		S12		S21		S22	
GHZ	MOD DB	PHASE DEG	MOD DB	PHASE DEG	MOD DB	PHASE DEG	MOD DB	PHASE DEG
.10	-.73	-20.30	-11.87	58.30	-.11	-22.40	-10.63	73.50
.15	-1.51	-28.70	-9.45	46.40	-1.14	-29.40	-8.66	53.20
.20	-2.17	-34.30	-7.89	38.30	-2.18	-34.00	-7.44	38.80
.25	-2.81	-39.00	-6.96	29.70	-3.15	-36.40	-6.44	26.90
.30	-3.36	-42.00	-6.38	23.30	-3.84	-37.20	-6.61	13.50
.40	-4.41	-48.30	-5.48	12.00	-4.93	-38.40	-6.38	4.00
.50	-5.26	-55.10	-5.04	2.80	-5.43	-40.10	-6.38	-7.30
.60	-6.04	-63.20	-4.74	-7.00	-5.76	-42.20	-6.47	-19.50
.70	-6.65	-73.20	-4.73	-16.30	-6.11	-45.30	-6.67	-31.60
.80	-7.19	-84.30	-4.97	-25.50	-6.43	-51.10	-7.05	-44.00
.90	-7.58	-96.70	-5.42	-35.20	-6.82	-57.50	-7.60	-58.00
1.00	-8.13	-114.10	-6.43	-43.90	-7.77	-65.90	-8.59	-74.40

S PARAMETERS OF VERTICAL NPN TRANSISTOR IN COMMON EMITTER CONFIGURATION

FREQUENCY	S11		S12		S21		S22	
GHZ	MOD DB	PHASE DEG	MOD DB	PHASE DEG	MOD DB	PHASE DEG	MOD DB	PHASE DEG
.10	-2.28	-29.80	-36.48	67.20	4.19	124.40	-.17	-9.00
.15	-3.75	-36.00	-34.42	64.40	2.35	107.80	-.33	-13.10
.20	-4.85	-43.00	-33.15	61.30	.65	95.30	-.38	-16.40
.25	-5.75	-47.70	-32.04	59.50	-.79	85.80	-.42	-19.50
.30	-6.54	-50.90	-31.37	60.50	-2.05	77.00	-.41	-22.00
.40	-7.90	-56.20	-30.46	58.60	-4.10	62.40	-.51	-28.10
.50	-9.10	-65.80	-30.75	61.40	-5.88	49.50	-.67	-35.90
.60	-10.37	-74.70	-31.70	71.70	-7.43	36.80	-.88	-44.40
.70	-11.34	-84.50	-32.40	94.40	-9.27	25.20	-1.22	-54.90
.80	-12.32	-94.60	-30.46	128.50	-11.54	12.90	-1.72	-65.70
.90	-12.96	-105.80	-25.19	146.90	-17.52	1.00	-2.24	-77.00
1.00	-13.23	-120.20	-19.66	150.80	-21.83	-5.60	-3.29	-90.70

S PARAMETERS OF VERTICAL NPN TRANSISTOR IN COMMON BASE CONFIGURATION

FREQUENCY	S11		S12		S21		S22	
GHZ	MOD DB	PHASE DEG	MOD DB	PHASE DEG	MOD DB	PHASE DEG	MOD DB	PHASE DEG
.10	-14.38	91.90	-44.44	69.40	.29	-31.50	.02	-8.90
.15	-12.69	69.40	-41.94	65.50	-.46	-46.50	-.13	-15.50
.20	-11.57	53.00	-40.92	58.30	-1.24	-58.30	-.18	-17.80
.25	-11.06	40.20	-40.00	55.00	-2.03	-70.20	-.22	-21.00
.30	-10.78	30.70	-40.00	51.20	-2.91	-80.60	-.26	-25.40
.40	-10.72	15.40	-40.92	37.50	-4.42	-99.70	-.41	-33.70
.50	-11.12	4.40	-43.10	16.80	-5.90	-117.00	-.64	-38.90
.60	-11.67	-4.70	-46.02	-65.20	-7.07	-134.20	-.94	-48.30
.70	-12.25	-11.70	-35.92	-120.50	-6.27	-149.00	-1.42	-58.30
.80	-12.62	-17.60	-28.18	-135.00	-9.45	-163.80	-2.03	-68.90
.90	-12.85	-23.90	-22.27	-150.30	-10.01	-175.30	-2.59	-79.80
1.00	-12.22	-34.10	-16.59	-168.70	-9.87	177.20	-3.92	-92.30

20TH NOVEMBER 1975

SEAN LEAD P/N ISOLATED PAIRS
V=VCE I=IE S PARAMETERS IN DB,DEG

(SEAN 1 EMITTER; EMITTER WIDTH 2 MICRONS)

VOLTS= .5 CURRENT MA= .5

FREQ	S11		S12		S21		S22	
100.000	-.27	-8.5	-30.94	86.7	4.42	168.6	-.01	-6.6
150.000	-.39	-11.5	-26.56	85.9	4.23	162.3	-.01	-15.6
200.000	-.49	-15.1	-24.63	79.9	4.14	157.7	-.42	-12.9
300.000	-.64	-22.6	-21.50	73.5	3.64	148.7	-.76	-18.4
400.000	-1.06	-28.3	-19.27	67.9	3.21	139.7	-1.26	-23.1
500.000	-1.31	327.0	-17.59	64.2	2.93	132.6	-1.66	330.5
600.000	-1.67	322.1	-16.37	-300.0	2.53	-234.9	-2.06	330.7
700.000	-2.20	316.7	-15.57	55.0	2.17	-241.0	-2.54	328.0
800.000	-2.96	311.4	-15.02	51.7	1.46	-248.0	-3.07	325.6
900.000	-3.22	306.2	-14.65	48.6	1.02	104.3	-3.80	322.3
1000.000	-4.17	301.7	-14.05	46.5	.61	99.7	-4.02	-38.5
1200.000	-4.90	-66.4	-13.37	39.9	-.11	90.2	-4.59	-43.2
1400.000	-5.60	287.7	-12.95	37.7	-.76	82.8	-5.02	315.1
1600.000	-6.49	282.9	-12.85	-324.3	-1.56	-284.4	-5.74	312.8
1800.000	-7.01	279.3	-12.25	33.8	-1.82	66.7	-5.83	312.1
1999.999	-8.13	273.4	-12.09	31.7	-2.40	63.5	-6.34	-49.4

20TH NOVEMBER 1975

SEAN LEAD P/N ISOLATED PAIRS
V=VCE I=IE S PARAMETERS IN DB,DEG

(SEAN 1 EMITTER; EMITTER WIDTH 2 MICRONS)

VOLTS= .5 CURRENT MA= 1

FREQ	S11		S12		S21		S22	
100.000	-.71	-12.8	-30.80	84.5	10.89	165.0	-.09	-9.3
150.000	-.91	-17.8	-25.46	77.8	10.58	158.1	-.24	-14.2
200.000	-1.15	-23.4	-24.48	76.5	10.35	151.8	-.58	-17.1
300.000	-1.78	-34.2	-21.87	64.2	9.56	141.0	-1.28	-24.7
400.000	-2.32	317.8	-19.83	61.6	8.79	131.2	-1.98	-29.7
500.000	-2.98	310.6	-18.57	57.5	8.07	123.5	-2.58	326.6
600.000	-3.54	304.6	-17.54	-307.1	7.38	-242.0	-3.25	323.3
700.000	-4.35	297.7	-16.90	50.2	6.66	-250.6	-3.97	321.6
800.000	-5.38	291.5	-16.55	46.0	5.58	103.2	-4.78	319.2
900.000	-5.90	285.2	-15.98	44.2	5.20	96.8	-4.98	317.6
1000.000	-7.00	279.7	-15.83	44.4	4.32	92.3	-5.75	-40.3
1200.000	-7.76	-88.7	-15.16	39.9	3.05	85.0	-6.37	-47.4
1400.000	-8.54	264.8	-14.79	46.2	2.30	78.8	-6.81	311.7
1600.000	-9.48	260.2	-14.63	-360.5	1.21	-287.2	-7.48	309.6
1800.000	-10.12	255.2	-13.68	38.8	.71	67.1	-7.81	309.3
1999.999	-11.16	247.4	-13.56	37.9	-.05	62.6	-8.11	-52.0

S parameters of 1E2M and 3E2M transistors as a function of frequency and bias.

Table 1 Sht. 1 of 16

20TH NOVEMBER 1975

BEAM LEAD P/N ISOLATED PAIRS
V=VCE I=IC & PARAMETERS IN DB,DEG

(SEMI EMITTER; EMITTER WIDTH 2 MICRONS)

VOLTS= .5 CURRENT MA= 2

FREQ	S11		S12		S21		S22	
100.000	-1.94	-65.3	-29.59	73.4	14.35	152.7	-.54	-14.1
150.000	-2.60	-84.1	-26.36	65.4	13.59	142.5	-1.11	-20.2
200.000	-3.26	-46.4	-24.71	61.6	12.85	134.0	-1.71	-23.9
300.000	-4.76	-56.3	-22.63	53.5	11.17	120.9	-2.68	-26.5
400.000	-6.06	294.5	-21.46	51.6	9.54	110.7	-3.92	-33.5
500.000	-7.22	287.3	-20.56	51.0	8.27	103.2	-4.67	324.7
600.000	-8.36	281.6	-19.79	-311.1	7.03	-262.9	-5.27	323.8
700.000	-9.32	275.3	-19.23	48.9	6.01	-268.3	-5.93	323.0
800.000	-10.57	269.2	-18.80	48.1	4.69	87.2	-6.63	321.5
900.000	-11.68	262.8	-18.12	48.4	4.11	82.1	-6.75	320.5
1000.000	-12.67	256.9	-17.85	49.2	3.10	79.3	-7.36	-40.4
1200.000	-13.48	250.2	-16.99	46.4	1.85	73.0	-7.64	-44.1
1400.000	-12.66	245.7	-16.18	47.6	.75	68.2	-7.88	315.0
1600.000	-13.61	242.5	-15.71	-312.7	-.41	-296.4	-8.40	312.3
1800.000	-14.66	237.2	-14.80	47.0	-.93	59.1	-8.33	311.0
1999.999	-14.48	228.2	-14.27	45.4	-1.71	55.4	-8.73	-56.3

20TH NOVEMBER 1975

BEAM LEAD P/N ISOLATED PAIRS
V=VCE I=IE S PARAMETERS IN DB,DEG

(SEMI EMITTER; EMITTER WIDTH 2 MICRONS)

VOLTS= .5 CURRENT MA= 4

FREQ	S11		S12		S21		S22	
100.000	-6.84	-62.4	-27.95	46.4	12.99	120.5	-3.49	-20.9
150.000	-9.24	-75.3	-27.24	47.3	10.30	108.2	-4.40	-22.5
200.000	-11.10	-83.9	-26.53	41.0	8.06	100.0	-5.14	-22.0
300.000	-13.57	264.2	-24.93	40.6	4.76	91.0	-5.80	-24.3
400.000	-14.66	258.1	-24.17	46.9	2.33	83.6	-6.29	-25.4
500.000	-15.89	252.8	-23.16	51.7	.56	78.4	-6.62	332.9
600.000	-16.59	247.1	-21.91	-307.1	-.93	-285.7	-6.91	331.4
700.000	-16.96	241.2	-21.11	53.7	-2.16	-289.8	-7.03	329.8
800.000	-17.47	235.9	-20.44	53.7	-3.43	67.0	-7.75	327.4
900.000	-17.16	229.0	-19.39	54.7	-4.05	63.2	-7.66	324.9
1000.000	-17.09	223.3	-19.05	56.2	-5.06	61.6	-8.20	-37.3
1200.000	-16.37	222.6	-17.93	58.0	-6.19	56.1	-8.37	-43.2
1400.000	-15.81	222.0	-16.95	52.8	-7.10	53.0	-8.33	313.7
1600.000	-16.65	221.5	-16.46	-308.3	-8.08	-309.9	-8.87	309.7
1800.000	-15.74	216.8	-15.47	50.7	-8.35	47.3	-8.77	307.5
1999.999	-15.28	209.2	-14.93	49.5	-8.87	45.5	-9.11	-55.6

20TH NOVEMBER 1975

BEAM LEAD P/N ISOLATED PAIRS
V=VCE I=IE S PARAMETERS IN DB,DEG

(SEMI EMITTER; EMITTER WIDTH 2 MICRONS)

VOLTS= .5 CURRENT MA= 6

FREQ	S11		S12		S21		S22	
100.000	-10.62	-94.7	-28.24	33.6	10.66	105.8	-5.40	-21.9
150.000	-12.65	-110.6	-27.53	35.5	7.54	94.9	-6.08	-21.9
200.000	-13.53	238.4	-26.98	39.9	5.13	87.6	-6.68	-22.3
300.000	-14.48	226.1	-25.96	39.6	1.70	77.7	-7.14	-25.4
400.000	-14.97	219.5	-24.65	46.7	-.90	70.0	-7.65	-28.6
500.000	-15.24	215.6	-23.56	50.8	-2.77	63.6	-7.96	328.5
600.000	-15.31	210.2	-22.26	-307.8	-4.36	-301.5	-8.19	325.8
700.000	-15.14	207.1	-21.58	52.8	-5.72	53.4	-8.58	323.1
800.000	-15.36	203.3	-20.87	52.2	-7.11	49.6	-9.14	320.0
900.000	-14.61	199.6	-19.91	52.6	-7.91	45.7	-9.11	316.3
1000.000	-14.55	198.7	-19.52	53.5	-8.97	44.5	-9.67	-46.6
1200.000	-14.06	199.3	-18.57	50.1	-10.38	39.6	-9.74	-54.1
1400.000	-13.75	200.7	-17.66	52.1	-11.41	39.0	-9.89	302.2
1600.000	-14.05	200.3	-17.16	-308.8	-12.42	-321.1	-10.39	297.3
1800.000	-13.56	197.2	-16.80	51.0	-12.68	39.0	-10.25	294.6
1999.999	-13.06	193.0	-15.82	50.0	-13.09	40.7	-10.67	-69.3

20TH NOVEMBER 1975

BEAM LEAD P/N ISOLATED PAIRS
V=VCE I=IE S PARAMETERS IN DB,DEG

(SEMI EMITTER; EMITTER WIDTH 2 MICRONS)

VOLTS= .5 CURRENT MA= 8

FREQ	S11		S12		S21		S22	
100.000	-11.51	-117.3	-28.74	32.6	9.38	99.8	-6.59	-23.0
150.000	-12.54	227.2	-27.61	42.3	6.13	89.4	-7.41	-24.5
200.000	-12.88	218.1	-26.90	40.3	3.67	81.6	-7.83	-24.9
300.000	-13.19	208.9	-25.31	42.9	.17	70.7	-8.27	-29.6
400.000	-13.41	204.1	-24.43	45.5	-2.46	61.9	-8.80	-34.1
500.000	-13.44	201.1	-23.31	48.0	-4.38	54.7	-9.12	321.6
600.000	-13.43	197.4	-22.16	-310.6	-6.06	-311.4	-9.41	317.8
700.000	-13.20	195.7	-21.37	49.4	-7.51	42.8	-9.65	314.3
800.000	-13.41	193.1	-20.85	49.0	-8.96	38.8	-10.45	310.2
900.000	-12.72	190.8	-20.01	49.5	-9.91	35.2	-10.45	305.5
1000.000	-12.75	189.8	-19.68	51.1	-11.13	34.4	-11.05	-58.4
1200.000	-12.43	191.3	-18.88	47.9	-12.65	30.8	-11.06	-66.7
1400.000	-12.21	193.6	-18.03	49.7	-13.80	32.5	-11.13	289.0
1600.000	-12.51	193.8	-17.56	-310.7	-14.81	-324.8	-11.56	283.6
1800.000	-12.04	190.6	-16.69	49.1	-14.87	38.6	-11.51	280.8
1999.999	-11.61	187.4	-16.23	48.7	-14.93	41.1	-11.80	-83.9

30TH NOVEMBER 1975

BEAM LEAD P-N ISOLATED PAIRS
V=VCE I=IE S PARAMETERS IN DB,DEG

1E2N11 EMITTER: EMITTER WIDTH 2 MICRONS)

VOLTS= .5 CURRENT MA= 10

FREQ	S11		S12		S21		S22	
100.000	-10.79	-144.2	-27.36	33.4	7.10	92.7	-9.52	-33.6
150.000	-11.01	205.5	-25.91	30.9	3.76	82.0	-10.50	-35.3
200.000	-11.01	200.2	-25.32	36.2	1.30	73.4	-10.86	-38.1
300.000	-11.01	194.6	-23.86	37.9	-2.26	61.2	-11.29	-45.8
400.000	-11.16	192.7	-22.73	41.0	-4.90	50.8	-11.78	306.1
500.000	-11.12	190.8	-21.66	41.6	-6.87	42.2	-12.07	298.4
600.000	-11.06	189.3	-20.67	-319.1	-8.57	-324.0	-12.27	292.1
700.000	-10.93	188.3	-20.31	41.4	-10.13	29.9	-12.53	285.9
800.000	-11.15	186.6	-19.88	40.3	-11.62	26.7	-13.01	279.2
900.000	-10.61	185.1	-19.26	41.2	-12.64	24.1	-12.80	272.4
1000.000	-10.67	184.9	-19.21	42.3	-13.91	24.7	-13.19	-92.8
1200.000	-10.34	186.4	-18.50	39.3	-15.30	24.3	-12.68	-101.3
1400.000	-10.26	187.8	-17.67	41.3	-16.09	23.8	-12.64	254.5
1600.000	-10.52	187.8	-17.57	-317.5	-16.67	-325.6	-12.79	249.8
1800.000	-10.02	186.1	-16.79	42.7	-16.35	38.2	-12.49	246.2
1999.999	-9.74	184.8	-16.44	42.8	-16.13	41.2	-12.53	-117.7

TEXT CUT OFF IN ORIGINAL

20TH NOVEMBER 1975

BEAM LEAD P-N ISOLATED PAIRS
VCBO= 15 IE= 5 PARAMETERS IN DB,DEG

(SEGMENT EMITTER; EMITTER WIDTH 2 MICRONS)

VOLTS= .5 CURRENT MA= .5

FREQ	S11		S12		S21		S22	
100.000	-.32	-16.0	-25.12	78.8	4.56	164.0	-.65	-10.8
150.000	-.48	-22.9	-21.14	74.1	4.26	156.5	-.81	-15.5
200.000	-.65	-29.6	-19.39	69.8	4.14	148.6	-.98	-19.0
300.000	-1.14	-43.4	-16.53	59.1	3.44	136.5	-1.18	-27.4
400.000	-1.47	305.6	-14.74	51.0	2.69	124.7	-1.61	-33.4
500.000	-1.77	296.0	-13.62	45.0	2.17	115.2	-2.00	321.7
600.000	-2.15	287.3	-12.85	-300.4	1.55	-254.0	-2.00	317.8
700.000	-2.58	278.3	-12.27	34.7	.95	-262.5	-3.50	314.2
800.000	-3.07	270.1	-11.96	30.4	.17	90.0	-4.04	316.5
900.000	-3.33	262.6	-11.63	26.9	-.32	82.5	-4.30	307.6
1000.000	-3.84	255.5	-11.56	23.8	-1.04	77.3	-4.81	-55.6
1200.000	-4.14	246.6	-11.52	18.3	-1.96	67.6	-5.35	-61.4
1400.000	-4.15	238.7	-11.55	15.6	-2.66	59.4	-5.53	294.9
1600.000	-4.27	232.6	-11.58	12.7	-3.24	-300.3	-5.76	290.3
1800.000	-4.38	227.0	-11.64	10.5	-3.99	45.0	-5.96	287.5
1999.999	-4.63	220.6	-11.83	8.9	-4.65	39.6	-6.20	-76.4

20TH NOVEMBER 1975

BEAM LEAD P-N ISOLATED PAIRS
VCBO= 15 IE= 5 PARAMETERS IN DB,DEG

(SEGMENT EMITTER; EMITTER WIDTH 2 MICRONS)

VOLTS= .5 CURRENT MA= 1

FREQ	S11		S12		S21		S22	
100.000	-.77	-22.4	-25.65	76.5	11.62	161.9	-.80	-14.3
150.000	-1.03	-31.9	-21.83	68.6	10.78	152.5	-.55	-21.1
200.000	-1.32	-41.4	-19.76	63.1	10.43	144.4	-1.00	-26.4
300.000	-1.98	-58.6	-17.04	56.6	9.34	131.7	-1.92	-36.6
400.000	-2.45	287.9	-15.79	45.2	8.17	120.3	-2.91	315.7
500.000	-2.87	276.4	-14.97	40.1	7.30	111.6	-3.74	310.3
600.000	-3.29	266.7	-14.24	-305.4	6.32	-256.5	-4.44	306.2
700.000	-3.71	257.4	-14.06	31.1	5.45	-263.6	-5.27	302.5
800.000	-4.12	249.3	-13.84	27.6	4.44	90.0	-5.96	298.6
900.000	-4.26	242.0	-13.67	25.4	3.72	83.8	-6.35	295.6
1000.000	-4.61	236.0	-13.61	23.4	2.66	79.9	-6.98	-67.1
1200.000	-4.72	228.8	-13.56	18.9	1.65	72.6	-7.43	-73.3
1400.000	-4.73	221.8	-13.58	19.4	.65	65.1	-7.79	284.9
1600.000	-4.83	216.5	-13.53	18.6	-.26	-301.3	-7.83	279.6
1800.000	-4.83	212.1	-13.56	17.9	-1.08	50.8	-8.04	276.7
1999.999	-4.95	206.8	-13.53	17.7	-1.87	48.0	-8.24	-66.6

20TH NOVEMBER 1975

BEAM LEAD P/N ISOLATED PAIRS
V=VCE I=IE S PARAMETERS IN DB,DEG

BEAMIS EMITTER; EMITTER WIDTH 2 MICRONS)

VOLTS= .5 CURRENT MA= 2

FREQ	S11		S12		S21		S22	
100.000	-1.52	-31.7	-55.39	72.3	15.90	156.4	-.44	-20.0
150.000	-1.65	-4.8	-21.91	68.0	15.89	146.5	-1.01	-39.4
200.000	-2.24	-57.6	-20.47	57.1	14.67	137.4	-1.74	-35.8
300.000	-2.99	282.1	-18.51	46.4	13.09	124.3	-3.07	-47.9
400.000	-3.46	267.1	-17.42	39.4	11.52	113.4	-4.43	303.6
500.000	-3.79	255.0	-16.87	36.1	10.32	105.2	-5.49	297.7
600.000	-4.12	245.2	-16.30	32.8	9.07	-261.7	-6.39	293.4
700.000	-4.40	236.5	-16.16	29.9	8.00	-267.9	-7.18	289.3
800.000	-4.67	229.2	-16.05	28.6	6.82	87.5	-8.05	285.4
900.000	-4.69	222.4	-15.90	27.4	5.98	82.3	-8.50	282.0
1000.000	-4.90	216.4	-15.75	27.1	5.10	79.0	-9.11	-61.6
1200.000	-4.92	211.7	-15.74	25.4	3.77	72.5	-9.52	-66.5
1400.000	-4.85	207.7	-15.42	27.0	2.67	66.6	-9.77	270.7
1600.000	-4.92	203.4	-15.25	27.2	1.65	-299.1	-9.78	266.7
1800.000	-4.87	200.1	-15.03	28.1	.73	56.0	-9.94	263.9
1999.999	-4.88	195.9	-14.87	28.1	-.09	51.8	-10.09	-99.6

20TH NOVEMBER 1975

BEAM LEAD P/N ISOLATED PAIRS
V=VCE I=IE S PARAMETERS IN DB,DEG

BEAMIS EMITTER; EMITTER WIDTH 2 MICRONS)

VOLTS= .5 CURRENT MA= 4

FREQ	S11		S12		S21		S22	
100.000	-2.99	-51.5	-25.91	64.6	19.69	146.7	-1.06	-30.0
150.000	-3.30	-9.3	-22.48	58.1	18.81	135.0	-2.15	-41.8
200.000	-3.68	-65.1	-21.84	49.2	17.75	125.9	-3.03	-46.8
300.000	-4.18	252.6	-20.44	39.3	15.55	113.6	-5.17	-63.1
400.000	-4.44	238.7	-19.96	35.9	13.54	103.9	-6.80	307.1
500.000	-4.51	228.8	-19.46	34.6	12.03	96.8	-8.00	301.3
600.000	-4.58	220.7	-19.03	33.2	10.59	-266.6	-8.95	296.5
700.000	-4.66	214.4	-18.91	33.7	9.37	-273.6	-9.86	292.1
800.000	-4.81	209.1	-18.70	33.3	8.11	82.6	-10.50	287.1
900.000	-4.69	204.7	-18.39	34.1	7.20	78.7	-10.82	283.8
1000.000	-4.81	201.5	-18.17	34.9	6.21	76.3	-11.37	-99.4
1200.000	-4.83	196.7	-17.99	37.0	4.64	71.1	-11.50	-105.6
1400.000	-4.68	194.7	-17.63	38.3	3.78	65.7	-11.64	253.8
1600.000	-4.70	191.8	-16.67	-320.5	2.66	-299.1	-11.47	250.1
1800.000	-4.64	189.3	-16.80	40.1	1.73	56.5	-11.50	247.3
1999.999	-4.61	186.4	-15.63	40.4	.85	52.9	-11.52	-115.9

20TH NOVEMBER 1975
BEAM LEAD P/N ISOLATED PAIRS
V=VCE I=IE S PARAMETERS IN DB,DEG

SERIES EMITTER: EMITTER WIDTH 2 MICRONS)
VOLTS= .5 CURRENT MA= 8

FREQ	S11		S12		S21		S22	
100.000	-5.43	-114.9	-28.68	37.1	16.84	116.5	-6.46	-55.1
150.000	-5.49	127.2	-25.54	39.4	16.13	107.5	-8.87	-64.6
200.000	-5.51	116.5	-25.26	38.8	13.84	100.3	-10.47	-78.8
300.000	-5.55	105.1	-24.69	38.7	10.56	92.5	-12.30	885.3
400.000	-5.64	99.5	-23.96	36.1	8.01	87.0	-13.06	873.7
500.000	-5.55	96.9	-23.38	40.5	6.19	82.5	-13.85	875.6
600.000	-5.52	93.4	-22.63	-316.8	4.63	-281.3	-14.09	870.6
700.000	-5.41	91.4	-21.96	45.1	3.39	-285.1	-14.17	867.3
800.000	-5.48	89.5	-21.32	46.3	2.14	76.5	-14.19	866.1
900.000	-5.25	87.7	-20.66	48.1	1.23	69.3	-13.69	856.9
1000.000	-5.33	86.5	-20.12	49.3	.30	67.4	-13.77	-104.3
1200.000	-5.19	85.7	-19.13	46.2	-1.03	62.7	-13.13	855.4
1400.000	-5.11	85.2	-18.16	51.3	-2.10	58.6	-12.37	848.1
1600.000	-5.08	84.2	-17.37	-308.5	-3.07	-305.4	-11.76	845.6
1800.000	-4.91	82.9	-16.74	51.5	-3.87	50.9	-11.34	841.8
1999.999	-4.78	81.3	-16.15	51.1	-4.63	46.2	-10.99	-121.4

20TH NOVEMBER 1975
BEAM LEAD P/N ISOLATED PAIRS
V=VCE I=IE S PARAMETERS IN DB,DEG

SERIES EMITTER: EMITTER WIDTH 2 MICRONS)
VOLTS= .5 CURRENT MA= 14

FREQ	S11		S12		S21		S22	
100.000	-4.92	202.1	-28.35	36.1	12.11	98.3	-14.32	-86.9
150.000	-4.79	195.3	-27.41	39.9	8.76	90.8	-15.59	-97.8
200.000	-4.75	191.6	-27.58	39.6	6.38	85.4	-16.45	-108.9
300.000	-4.74	188.2	-26.86	38.5	2.87	78.3	-16.37	851.1
400.000	-4.78	186.2	-25.58	36.9	.28	72.6	-15.68	845.8
500.000	-4.71	185.0	-24.58	34.5	-1.60	66.6	-14.91	842.8
600.000	-4.68	184.2	-23.48	-311.3	-3.24	-297.3	-14.16	839.1
700.000	-4.60	183.2	-22.83	49.3	-4.62	57.5	-13.66	838.1
800.000	-4.68	182.5	-22.18	50.3	-5.91	54.7	-13.10	833.1
900.000	-4.43	181.4	-21.49	51.3	-6.88	51.3	-12.88	836.5
1000.000	-4.52	181.0	-20.83	52.5	-7.82	49.5	-12.53	-131.6
1200.000	-4.33	180.7	-19.81	51.3	-9.67	45.1	-10.95	824.0
1400.000	-4.33	180.4	-18.93	55.1	-10.28	43.7	-10.34	824.9
1600.000	-4.30	179.8	-18.12	-304.9	-11.18	-317.7	-9.77	821.8
1800.000	-4.18	178.6	-17.44	54.8	-11.81	41.9	-9.39	819.7
1999.999	-4.05	537.7	-16.78	54.8	-12.26	42.7	-8.99	-142.9

20TH NOVEMBER 1975
BEAM LEAD P/N ISOLATED PAIRS
V=VCE I=IE 3 PARAMETERS IN DB,DEG

3 SEGMENT EMITTER; EMITTER WIDTH 2 MICRONS)

VOLTS= .5 CURRENT MA= 21

FREQ	S11		S12		S21		S22	
100.000	-4.11	176.4	-29.66	24.6	9.00	91.7	-14.74	-121.3
150.000	-4.07	168.6	-27.83	26.6	5.66	84.0	-14.07	129.6
200.000	-4.01	166.4	-27.69	25.0	3.20	77.6	-14.57	124.3
300.000	-3.99	164.4	-26.64	28.1	-.34	66.6	-13.79	119.1
400.000	-4.04	163.1	-25.66	21.9	-3.01	60.6	-12.83	121.4
500.000	-3.97	162.3	-24.66	26.6	-4.96	53.7	-11.88	120.5
600.000	-3.96	161.5	-23.57	-311.7	-6.74	-312.1	-11.16	119.1
700.000	-3.89	161.0	-22.99	29.0	-8.20	46.5	-10.67	117.4
800.000	-4.01	160.3	-22.45	30.2	-9.72	39.5	-10.20	115.3
900.000	-3.75	179.4	-21.66	31.7	-10.84	34.4	-9.52	113.1
1000.000	-3.90	538.9	-21.25	32.6	-11.91	25.5	-9.30	-146.1
1200.000	-3.77	179.0	-20.27	32.2	-13.57	33.4	-8.55	109.0
1400.000	-3.73	178.6	-19.36	35.3	-14.66	36.1	-8.16	108.6
1600.000	-3.71	178.0	-18.51	-304.6	-15.45	-320.0	-7.77	106.5
1800.000	-3.55	176.9	-17.95	35.6	-15.74	42.6	-7.40	105.1
1999.999	-3.49	535.9	-17.23	36.1	-15.71	46.7	-7.22	-156.6

20TH NOVEMBER 1975
BEAM LEAD P/N ISOLATED PAIRS
V=VCE I=IE 3 PARAMETERS IN DB,DEG

3 SEGMENT EMITTER; EMITTER WIDTH 2 MICRONS)

VOLTS= .5 CURRENT MA= 27

FREQ	S11		S12		S21		S22	
100.000	-3.55	187.9	-29.31	25.4	6.78	87.8	-12.46	-143.5
150.000	-3.51	185.4	-28.26	25.4	3.32	79.4	-12.19	111.6
200.000	-3.47	183.9	-27.88	26.0	.84	72.4	-11.64	110.5
300.000	-3.52	182.4	-26.87	23.4	-2.76	61.8	-10.85	108.3
400.000	-3.55	181.5	-25.26	42.3	-5.41	52.5	-10.17	106.7
500.000	-3.54	181.2	-24.51	45.6	-7.46	44.5	-9.58	105.8
600.000	-3.46	180.3	-23.29	-314.6	-9.25	-321.5	-8.79	104.2
700.000	-3.45	179.9	-22.61	47.5	-10.98	33.0	-8.38	104.3
800.000	-3.57	179.2	-22.25	48.0	-12.48	30.3	-8.04	103.5
900.000	-3.34	178.4	-21.65	46.7	-13.63	27.0	-7.48	102.7
1000.000	-3.45	538.1	-21.19	50.0	-14.64	29.0	-7.38	-157.4
1200.000	-3.32	178.0	-20.41	51.2	-16.39	30.5	-6.79	100.3
1400.000	-3.31	177.6	-19.51	54.0	-17.29	31.0	-6.52	134.5
1600.000	-3.31	177.1	-18.69	-305.0	-17.61	-317.2	-6.31	136.1
1800.000	-3.21	176.1	-18.02	55.3	-17.29	47.3	-6.03	137.0
1999.999	-3.13	535.1	-17.40	55.6	-16.90	51.2	-5.94	-164.6

20TH NOVEMBER 1975

BEAM LEAD P/N ISOLATED PAIRS
V=VCE I=IE S PARAMETERS IN DB,DEG

1E2M(1 EMITTER; EMITTER WIDTH 2 MICRONS)

VOLTS= 3 CURRENT MA= .5

FREQ	S11		S12		S21		S22	
100.000	-.22	-6.4	-37.62	91.3	4.45	171.8	.05	-4.0
150.000	-.32	-8.4	-32.81	88.8	4.31	167.4	-.06	-6.5
200.000	-.36	-11.2	-30.76	86.4	4.27	163.3	-.15	-7.5
300.000	-.62	-16.8	-27.62	81.8	3.98	156.4	-.35	-11.6
400.000	-.72	-21.2	-24.63	79.7	3.67	149.0	-.60	-14.7
500.000	-.86	335.2	-22.70	77.3	3.52	143.2	-.82	343.1
600.000	-1.06	331.5	-21.12	-286.6	3.24	-223.1	-1.08	340.8
700.000	-1.42	327.8	-20.18	-290.2	3.00	-229.1	-1.42	339.0
800.000	-2.08	322.7	-19.08	66.6	2.35	-235.3	-1.96	337.2
900.000	-2.17	318.0	-18.31	63.9	2.39	118.4	-1.91	334.9
1000.000	-3.08	314.0	-18.02	61.6	1.70	114.1	-2.52	-26.6
1200.000	-3.65	-53.5	-17.12	53.8	1.03	105.3	-2.85	-30.6
1400.000	-4.34	301.4	-16.50	51.3	.33	98.6	-3.24	-32.0
1600.000	-5.20	297.8	-16.25	-310.5	-.46	-268.5	-3.96	336.2
1800.000	-5.57	294.1	-15.46	47.5	-.68	85.2	-3.83	326.4
1999.999	-6.73	289.4	-15.13	45.6	-1.31	79.8	-4.25	-34.8

20TH NOVEMBER 1975

BEAM LEAD P/N ISOLATED PAIRS
V=VCE I=IE S PARAMETERS IN DB,DEG

1E2M(1 EMITTER; EMITTER WIDTH 2 MICRONS)

VOLTS= 3 CURRENT MA= 1

FREQ	S11		S12		S21		S22	
100.000	-.59	-8.8	-39.06	81.3	11.03	169.5	.03	-5.0
150.000	-.71	-12.4	-32.45	83.0	10.85	164.4	-.06	-7.8
200.000	-.81	-16.0	-30.60	85.7	10.74	159.5	-.23	-9.5
300.000	-1.21	-24.0	-27.62	77.8	10.27	151.0	-.46	-14.2
400.000	-1.48	-30.1	-25.33	75.9	9.71	142.8	-.84	-17.4
500.000	-1.81	324.7	-23.39	73.6	9.35	136.2	-1.19	339.3
600.000	-2.25	319.5	-22.05	-291.8	8.83	-230.7	-1.54	337.0
700.000	-2.82	313.9	-21.26	65.1	8.35	-237.2	-2.06	335.1
800.000	-3.75	308.6	-20.29	63.7	7.43	-243.2	-2.66	333.3
900.000	-4.69	303.0	-19.64	60.2	7.21	110.4	-2.69	331.2
1000.000	-5.17	298.6	-19.37	60.1	6.31	107.0	-3.39	-29.9
1200.000	-5.95	-69.3	-18.68	58.0	5.36	98.9	-3.81	-33.4
1400.000	-6.84	285.1	-18.08	53.0	4.44	92.6	-4.33	-33.9
1600.000	-7.85	280.7	-17.81	-307.7	3.33	-273.5	-4.99	324.6
1800.000	-8.42	277.3	-16.85	51.3	2.89	81.1	-4.88	325.4
1999.999	-9.76	271.4	-16.53	50.4	2.05	76.6	-5.29	-35.5

20TH NOVEMBER 1975

BEAM LEAD P/N ISOLATED PAIRS
V=VCE I=IE S PARAMETERS IN DB,DEG

(2EMI1 EMITTER; EMITTER WIDTH 2 MICRONS)

VOLTS= 3 CURRENT MA= 2

FREQ	S11		S12		S21		S22	
100.000	-1.14	-12.1	-37.96	66.6	15.64	166.7	-.01	-6.3
150.000	-1.27	-17.6	-30.99	78.5	15.37	160.3	-.23	-9.5
200.000	-1.54	-22.2	-31.38	79.7	15.15	154.2	-.36	-11.7
300.000	-2.15	-32.9	-28.56	70.3	14.43	143.9	-.78	-17.3
400.000	-2.67	319.0	-26.22	72.8	13.59	134.5	-1.28	-21.1
500.000	-3.25	312.2	-24.78	69.2	12.92	127.0	-1.74	336.0
600.000	-3.95	306.4	-23.30	-295.4	12.12	-240.1	-2.21	334.2
700.000	-4.76	299.5	-22.67	64.1	11.39	-246.6	-2.78	332.5
800.000	-5.91	293.4	-21.72	62.8	10.27	-252.1	-3.50	331.2
900.000	-6.41	287.2	-21.12	61.0	9.79	101.8	-3.58	329.6
1000.000	-7.60	281.8	-20.96	61.8	8.77	98.9	-4.32	-31.2
1200.000	-8.45	-86.2	-20.17	55.8	7.59	91.9	-4.72	-33.8
1400.000	-9.35	267.2	-19.42	57.3	6.44	86.7	-5.14	-33.8
1600.000	-10.37	263.6	-18.95	-302.5	5.21	-278.3	-5.63	325.6
1800.000	-11.08	259.2	-18.02	56.5	4.66	76.6	-5.70	326.0
1999.999	-12.19	250.9	-17.49	56.6	3.78	72.8	-6.10	-34.6

20TH NOVEMBER 1975

BEAM LEAD P/N ISOLATED PAIRS
V=VCE I=IE S PARAMETERS IN DB,DEG

(2EMI1 EMITTER; EMITTER WIDTH 2 MICRONS)

VOLTS= 3 CURRENT MA= 4

FREQ	S11		S12		S21		S22	
100.000	-2.18	-18.1	-39.73	90.9	19.73	161.7	-.11	-8.0
150.000	-2.46	-25.3	-33.68	76.2	19.33	153.4	-.39	-11.9
200.000	-2.89	-33.3	-32.38	77.5	18.84	145.6	-.67	-14.5
300.000	-3.92	-47.2	-30.24	73.1	17.66	133.3	-1.27	-26.3
400.000	-4.84	302.7	-27.63	69.9	16.32	122.7	-1.98	-23.5
500.000	-5.74	294.7	-26.28	68.3	15.36	115.1	-2.54	334.3
600.000	-6.78	287.6	-25.06	-293.3	14.08	-251.4	-3.11	333.2
700.000	-7.67	280.3	-24.63	65.6	13.09	-257.4	-3.66	332.5
800.000	-8.96	272.9	-23.51	66.3	11.78	98.1	-4.39	331.7
900.000	-9.46	265.8	-22.79	65.6	11.13	92.8	-4.43	330.7
1000.000	-10.55	259.5	-22.33	66.7	9.99	90.5	-5.13	-29.6
1200.000	-11.12	251.4	-21.49	61.7	8.67	84.6	-5.44	-31.9
1400.000	-11.80	245.2	-20.54	64.0	7.38	80.2	-5.76	-31.5
1600.000	-12.70	241.1	-19.90	-295.9	6.04	-284.0	-6.39	327.3
1800.000	-13.16	235.1	-18.79	63.6	5.36	71.7	-6.31	328.3
1999.999	-13.71	225.3	-18.08	63.1	4.45	68.7	-6.52	-32.2

20TH NOVEMBER 1975

BEAM LEAD P/N ISOLATED PAIRS
V=VCE I=IE S PARAMETERS IN DB,DEG

1E8M(1 EMITTER; EMITTER WIDTH 2 MICRONS)

VOLTS= 3 CURRENT MA= 6

FREQ	S11		S12		S21		S22	
100.000	-3.55	-27.6	-38.89	66.0	21.35	153.3	-.28	-9.2
150.000	-4.24	-37.7	-34.01	78.4	20.63	142.9	-.62	-13.4
200.000	-4.69	-46.8	-33.20	71.8	19.79	134.2	-1.08	-15.6
300.000	-6.44	-62.6	-30.76	61.9	18.00	121.4	-1.77	-19.9
400.000	-7.64	286.8	-29.08	68.8	16.21	111.5	-2.48	-21.9
500.000	-8.71	278.4	-27.59	71.6	14.64	104.5	-3.01	337.0
600.000	-9.81	271.4	-26.37	-290.8	13.48	-266.7	-3.43	336.4
700.000	-10.58	263.6	-25.57	-288.9	12.37	-265.8	-3.87	335.9
800.000	-11.78	255.8	-24.47	71.5	10.96	90.7	-4.49	335.4
900.000	-12.61	248.1	-23.40	70.9	10.26	85.9	-4.45	334.4
1000.000	-12.82	241.4	-23.05	72.7	9.09	84.2	-5.06	-25.9
1200.000	-12.93	234.7	-22.15	66.9	7.71	79.1	-5.22	-28.5
1400.000	-13.30	229.9	-20.89	68.5	6.39	75.2	-5.49	-28.8
1600.000	-13.90	226.3	-20.19	-292.0	5.02	-288.3	-6.06	329.9
1800.000	-14.13	220.8	-19.01	67.7	4.40	67.5	-5.83	330.5
1999.999	-14.09	211.0	-18.28	66.7	3.45	64.6	-6.10	-30.4

20TH NOVEMBER 1975

BEAM LEAD P/N ISOLATED PAIRS
V=VCE I=IE S PARAMETERS IN DB,DEG

1E2M(1 EMITTER; EMITTER WIDTH 2 MICRONS)

VOLTS= 3 CURRENT MA= 8

FREQ	S11		S12		S21		S22	
100.000	-5.59	-42.4	-38.93	65.3	20.27	140.2	-.70	-8.8
150.000	-7.14	-54.7	-36.22	64.1	18.66	127.6	-1.14	-11.4
200.000	-8.49	-65.1	-34.37	71.4	16.93	118.4	-1.47	-12.0
300.000	-10.77	281.1	-32.11	64.0	14.14	107.9	-1.88	-14.5
400.000	-12.17	273.4	-30.75	73.9	11.74	100.8	-2.27	-16.0
500.000	-13.19	267.2	-29.68	77.8	10.08	96.1	-2.55	342.7
600.000	-14.26	261.4	-26.66	-283.1	8.56	-267.1	-2.78	341.7
700.000	-14.68	254.9	-26.00	-282.8	7.40	-270.6	-3.08	340.7
800.000	-15.51	247.4	-24.82	77.6	6.06	87.2	-3.57	339.6
900.000	-15.44	240.8	-23.69	76.3	5.37	83.3	-3.46	338.1
1000.000	-15.76	233.3	-22.94	77.1	4.30	82.1	-3.99	-23.0
1200.000	-15.15	229.5	-21.58	70.2	3.02	77.9	-4.13	-26.7
1400.000	-15.01	226.3	-20.89	71.4	1.83	74.8	-4.37	-27.9
1600.000	-15.27	223.8	-20.07	-289.6	.62	-268.4	-4.96	330.3
1800.000	-15.08	218.0	-18.97	69.1	.10	68.1	-4.69	330.2
1999.999	-14.78	209.1	-18.25	67.8	-.70	65.4	-5.02	-31.3

20TH NOVEMBER 1975

TEAM LEAD P/N ISOLATED PPIPS
U=UCE I=IE S PARAMETERS IN DB,DEG

TEEN(1 EMITTER; EMITTER WIDTH 2 MICRONS)

VOLTS= 3 CURRENT MA= 10

FREQ	S11		S12		S21		S22	
100.000	-9.42	-67.1	-40.37	57.4	16.97	124.2	-1.11	-7.5
150.000	-11.40	-81.1	-38.64	63.3	14.43	113.1	-1.39	-8.8
200.000	-12.92	-92.1	-37.11	67.3	12.23	106.4	-1.66	-9.1
300.000	-14.63	253.5	-34.08	64.8	9.10	99.0	-1.92	-11.8
400.000	-15.42	246.9	-31.79	78.9	6.64	94.1	-2.17	-13.6
500.000	-15.84	239.9	-29.62	82.2	4.99	90.5	-2.38	344.9
600.000	-16.20	233.8	-27.89	-281.8	3.59	-272.4	-2.56	343.6
700.000	-16.66	228.2	-26.79	-279.6	2.47	-275.7	-2.82	342.6
800.000	-16.28	221.8	-25.41	79.9	1.20	82.3	-3.07	341.2
900.000	-15.60	215.5	-24.18	79.6	.58	78.4	-3.13	339.5
1000.000	-15.56	211.3	-23.53	79.3	-.48	77.2	-3.64	-21.6
1200.000	-14.71	210.7	-22.61	72.8	-1.63	72.2	-3.75	-25.8
1400.000	-14.40	209.1	-21.35	73.8	-2.70	68.6	-3.98	-27.3
1600.000	-14.64	207.2	-20.59	-287.6	-3.82	-295.1	-4.53	330.6
1800.000	-14.14	202.6	-19.37	72.1	-4.32	60.9	-4.27	330.4
1999.999	-13.70	195.3	-18.57	70.6	-5.06	57.9	-4.54	-31.1

20TH NOVEMBER 1975

BEAM LEAD P/N ISOLATED PAIRS
V=VCE I=IE S PARAMETERS IN DB,DEG

SEEMIG EMITTER; EMITTER WIDTH 2 MICRONS)

VOLTS= 3 CURRENT MA= .5

FREQ	S11		S12		S21		S22	
100.000	-.27	-16.5	-36.45	64.4	4.61	166.6	.02	-5.6
150.000	-.35	-17.4	-27.83	66.6	4.40	162.8	-.12	-8.6
200.000	-.46	-22.6	-25.52	78.8	4.35	157.3	-.20	-10.5
300.000	-.79	-34.2	-22.96	67.1	3.90	148.2	-.47	-15.6
400.000	-.95	317.1	-20.58	64.6	3.41	138.3	-.60	-19.7
500.000	-1.15	309.8	-19.12	59.2	3.11	130.8	-1.10	337.0
600.000	-1.40	301.1	-17.84	-306.2	2.64	-237.2	-1.38	334.3
700.000	-1.78	292.9	-17.24	49.4	2.20	-244.8	-1.83	331.8
800.000	-2.36	284.6	-16.86	45.2	1.32	-251.6	-2.40	329.1
900.000	-2.46	277.8	-16.19	41.8	1.12	101.0	-2.39	326.8
1000.000	-3.13	270.3	-16.00	38.9	.35	96.6	-2.92	-35.2
1200.000	-3.36	-100.3	-15.64	32.3	-.53	87.3	-3.33	-40.4
1400.000	-3.57	251.2	-15.54	29.9	-1.30	79.6	-3.58	317.3
1600.000	-3.92	244.4	-15.56	-331.8	-2.17	-287.8	-4.04	313.9
1800.000	-4.01	237.9	-15.43	26.6	-2.77	65.5	-4.07	312.9
1999.999	-4.34	230.9	-15.43	24.7	-3.49	60.0	-4.38	-50.1

20TH NOVEMBER 1975

BEAM LEAD P/N ISOLATED PAIRS
V=VCE I=IE S PARAMETERS IN DB,DEG

SEEMIG EMITTER; EMITTER WIDTH 2 MICRONS)

VOLTS= 3 CURRENT MA= 1

FREQ	S11		S12		S21		S22	
100.000	-.64	-16.1	-32.96	77.9	11.38	166.5	.00	-7.3
150.000	-.81	-22.6	-27.45	81.0	11.11	160.1	-.19	-11.2
200.000	-.93	-29.8	-25.42	74.7	10.96	153.9	-.29	-13.5
300.000	-1.40	-43.9	-23.26	66.9	10.32	143.6	-.79	-19.9
400.000	-1.69	305.2	-21.42	59.4	9.50	133.9	-1.28	-24.8
500.000	-2.01	295.3	-20.10	55.8	8.99	126.0	-1.75	331.6
600.000	-2.35	286.3	-18.98	-310.1	8.23	-241.7	-2.10	328.6
700.000	-2.80	277.8	-18.63	46.2	7.59	-248.9	-2.61	326.1
800.000	-3.43	268.5	-18.35	42.6	6.45	-254.8	-3.46	323.4
900.000	-3.53	260.5	-17.66	39.5	6.06	98.3	-3.59	321.5
1000.000	-4.13	253.6	-17.72	38.4	5.19	92.6	-4.17	-40.4
1200.000	-4.30	243.7	-17.42	33.1	4.06	86.6	-4.68	-45.1
1400.000	-4.42	236.1	-17.33	33.5	3.07	80.1	-4.99	313.3
1600.000	-4.74	230.1	-17.20	-326.7	1.98	-286.2	-5.50	310.3
1800.000	-4.75	224.2	-16.99	32.8	1.23	67.9	-5.55	309.3
1999.999	-4.94	218.1	-16.96	33.1	.38	63.3	-5.90	-53.0

20TH NOVEMBER 1975

BEAM LEAD P/N ISOLATED PAIRS
V=VCE I=IE S PARAMETERS IN DB,DEG

3E2N(3 EMITTER; EMITTER WIDTH 2 MICRONS)

VOLTS= 3 CURRENT MA= 2

FREQ	S11		S12		S21		S22	
100.000	-1.23	-21.2	-32.39	76.0	16.28	163.7	-.11	-9.6
150.000	-1.41	-29.9	-28.53	76.6	15.91	156.2	-.36	-14.3
200.000	-1.66	-39.0	-26.40	69.6	15.62	146.9	-.66	-17.6
300.000	-2.25	-56.6	-24.14	59.2	14.69	127.6	-1.27	-22.4
400.000	-2.66	290.5	-22.56	55.5	13.56	126.9	-2.03	-30.6
500.000	-3.05	279.2	-21.56	52.2	12.75	119.0	-2.69	325.7
600.000	-3.46	269.1	-20.61	-313.2	11.76	-240.3	-3.30	322.9
700.000	-3.86	259.8	-20.29	44.7	10.88	-255.9	-4.01	320.6
800.000	-4.42	251.4	-20.14	41.9	9.63	99.9	-4.78	318.1
900.000	-4.41	243.5	-19.61	40.7	9.05	93.9	-4.97	316.6
1000.000	-4.92	237.1	-19.53	40.8	8.03	91.1	-5.66	-45.0
1200.000	-4.96	228.6	-19.29	37.4	6.78	84.3	-6.20	-49.0
1400.000	-5.01	222.4	-18.96	39.6	5.67	78.6	-6.53	309.7
1600.000	-5.24	217.5	-18.78	-319.7	4.51	-206.7	-7.00	307.1
1800.000	-5.16	212.3	-18.35	41.1	3.69	67.9	-7.12	306.1
1999.999	-5.25	207.0	-18.06	42.3	2.79	63.8	-7.47	-55.9

20TH NOVEMBER 1975

BEAM LEAD P/N ISOLATED PAIRS
V=VCE I=IE S PARAMETERS IN DB,DEG

3E2N(3 EMITTER; EMITTER WIDTH 2 MICRONS)

VOLTS= 3 CURRENT MA= 4

FREQ	S11		S12		S21		S22	
100.000	-2.37	-29.9	-33.64	74.1	20.89	158.9	-.28	-13.4
150.000	-2.65	-42.5	-29.20	74.0	20.36	149.7	-.73	-19.7
200.000	-2.93	-54.7	-28.26	65.2	19.79	141.3	-1.19	-23.9
300.000	-3.54	284.3	-25.76	54.0	18.39	128.7	-2.25	-32.3
400.000	-3.99	269.3	-24.44	51.8	16.85	118.0	-3.29	326.6
500.000	-4.31	257.1	-23.68	50.3	15.70	110.2	-4.14	319.2
600.000	-4.62	247.3	-22.78	-312.2	14.41	-256.1	-4.88	317.0
700.000	-4.87	238.2	-22.56	46.4	13.34	-262.0	-5.73	315.2
800.000	-5.27	231.0	-22.41	45.0	11.96	93.9	-6.58	313.1
900.000	-5.12	224.3	-21.79	45.9	11.25	88.8	-6.81	311.5
1000.000	-5.44	219.2	-21.72	48.0	10.19	86.7	-7.56	-49.7
1200.000	-5.34	212.5	-21.09	45.9	8.83	81.0	-8.16	-53.3
1400.000	-5.31	208.3	-20.55	49.5	7.61	76.8	-8.43	306.8
1600.000	-5.51	204.5	-20.02	-308.8	6.37	-268.4	-8.86	303.6
1800.000	-5.32	200.7	-19.32	52.3	5.50	67.1	-9.60	303.1
1999.999	-5.30	196.5	-18.73	53.2	4.56	63.8	-9.34	-59.3

20TH NOVEMBER 1975

SEAM LEAD P/N ISOLATED PAIRS
U=VCE I=IE S PARAMETERS IN DB;DEG

SEGM(3 EMITTER; EMITTER WIDTH 2 MICRONS)

VOLTS= 3 CURRENT MA= 8

FREQ	S11		S12		S21		S22	
100.000	-4.42	-47.0	-34.71	71.7	25.02	151.6	-.68	-19.0
150.000	-4.70	-65.1	-29.54	65.8	24.11	146.4	-1.50	-27.6
200.000	-4.83	-81.1	-30.10	61.7	23.07	130.8	-2.39	-31.2
300.000	-5.11	255.6	-28.00	49.4	21.03	117.9	-3.76	-39.0
400.000	-5.27	241.6	-27.15	51.0	19.02	102.2	-5.06	317.6
500.000	-5.27	231.4	-26.65	53.3	17.54	101.3	-6.06	314.5
600.000	-5.33	223.4	-25.55	-307.2	16.05	-263.9	-6.87	313.4
700.000	-5.37	216.5	-25.10	54.8	14.85	-268.6	-7.67	312.3
800.000	-5.64	211.3	-24.70	55.0	13.37	92.1	-8.56	310.6
900.000	-5.30	206.1	-23.75	56.1	12.58	83.9	-8.80	309.9
1000.000	-5.51	202.9	-23.51	58.8	11.46	82.3	-9.51	-51.6
1100.000	-5.33	198.8	-22.70	57.5	10.05	77.5	-9.99	-55.2
1200.000	-5.30	196.2	-21.60	61.1	8.81	73.4	-10.38	304.6
1300.000	-5.45	193.9	-20.78	-297.5	7.50	-290.5	-10.63	302.2
1400.000	-5.20	191.1	-19.90	62.8	6.62	65.6	-10.70	301.3
1500.000	-5.13	188.1	-19.10	63.3	5.64	62.6	-11.67	-60.9

20TH NOVEMBER 1975

SEAM LEAD P/N ISOLATED PAIRS
U=VCE I=IE S PARAMETERS IN DB;DEG

SEGM(3 EMITTER; EMITTER WIDTH 2 MICRONS)

VOLTS= 3 CURRENT MA= 14

FREQ	S11		S12		S21		S22	
100.000	-6.55	-71.3	-36.50	65.0	27.17	143.7	-1.27	-23.4
150.000	-6.27	-93.1	-31.45	66.6	25.80	131.0	-2.42	-30.7
200.000	-6.01	251.1	-30.27	57.4	24.34	121.5	-3.45	-34.2
300.000	-5.78	231.5	-31.06	50.5	21.80	109.5	-5.08	-40.2
400.000	-5.68	220.5	-29.48	54.8	19.50	101.2	-6.40	317.8
500.000	-5.48	213.2	-28.38	61.7	17.84	95.1	-7.27	316.6
600.000	-5.46	207.9	-27.12	-299.4	16.25	-269.2	-8.00	316.1
700.000	-5.36	203.4	-26.62	62.6	14.98	-273.3	-8.72	315.4
800.000	-5.54	199.4	-26.03	63.2	13.48	84.1	-9.53	314.0
900.000	-5.15	195.6	-24.91	65.7	12.67	80.2	-9.73	313.9
1000.000	-5.32	193.6	-24.24	68.2	11.55	78.9	-10.32	-48.2
1100.000	-5.13	191.1	-23.23	65.9	10.10	74.5	-10.70	-51.7
1200.000	-5.16	189.7	-22.12	69.4	8.82	70.7	-10.84	307.8
1300.000	-5.24	188.1	-21.18	-290.2	7.48	-292.9	-11.10	305.4
1400.000	-4.93	186.8	-20.27	69.1	6.59	63.4	-11.69	304.6
1500.000	-4.83	183.6	-19.38	69.2	5.60	60.6	-11.40	-58.2

20TH NOVEMBER 1975
SEAM LEAD P/N ISOLATED PAIRS
V=VCE I=IE S PARAMETERS IN DB,DEG

SEGMENT EMITTER; EMITTER WIDTH 2 MICRONS)

VOLTS= 3 CURRENT MA= 21

FREQ	S11		S12		S21		S22	
100.000	-7.25	-104.7	-37.38	58.0	26.42	131.8	-2.19	-33.5
150.000	-6.59	-123.8	-32.53	60.4	24.44	119.2	-3.03	-37.9
200.000	-6.15	224.7	-30.69	55.2	22.56	110.9	-3.35	-38.4
300.000	-5.67	211.3	-28.42	54.6	19.64	101.4	-5.53	-30.2
400.000	-5.74	204.8	-31.09	61.9	17.15	94.7	-6.69	-31.1
500.000	-5.60	200.5	-29.46	69.2	15.40	89.9	-6.79	328.0
600.000	-5.47	197.0	-28.06	-292.3	13.79	-273.5	-7.28	327.1
700.000	-5.38	194.4	-27.16	-289.3	12.48	-277.3	-7.64	326.0
800.000	-5.56	191.9	-26.71	69.4	11.01	80.8	-8.21	324.5
900.000	-5.13	189.5	-25.25	72.8	10.20	77.1	-8.21	322.6
1000.000	-5.27	188.2	-24.74	72.1	9.08	76.1	-8.70	-28.9
1200.000	-5.05	186.7	-23.58	69.9	7.64	71.9	-8.91	-43.6
1400.000	-5.00	186.1	-22.22	73.4	6.38	68.3	-8.95	314.6
1600.000	-5.13	185.0	-21.33	-287.1	5.08	-295.2	-9.21	311.1
1800.000	-4.78	183.4	-20.27	72.7	4.24	60.9	-9.13	309.4
1999.999	-4.71	181.6	-19.50	72.2	3.25	58.1	-9.41	-53.7

20TH NOVEMBER 1975
SEAM LEAD P/N ISOLATED PAIRS
V=VCE I=IE S PARAMETERS IN DB,DEG

SEGMENT EMITTER; EMITTER WIDTH 2 MICRONS)

VOLTS= 3 CURRENT MA= 27

FREQ	S11		S12		S21		S22	
100.000	-6.50	-138.5	-39.88	51.5	22.24	117.4	-3.38	-16.6
150.000	-5.93	216.5	-36.09	57.4	19.38	107.5	-4.09	-17.2
200.000	-5.79	203.2	-36.77	54.9	17.03	101.7	-4.47	-16.5
300.000	-5.55	196.4	-34.83	60.2	13.82	95.9	-4.87	-19.5
400.000	-5.57	193.3	-32.35	66.7	11.25	91.5	-5.21	-21.6
500.000	-5.44	191.0	-30.29	75.4	9.54	87.8	-5.47	336.5
600.000	-5.33	189.5	-28.68	-287.0	7.98	-274.4	-5.68	334.3
700.000	-5.22	188.3	-27.92	-284.6	6.77	-277.5	-5.99	332.4
800.000	-5.41	186.7	-26.91	74.3	5.41	81.1	-6.47	330.1
900.000	-4.96	185.8	-25.49	75.4	4.78	77.4	-6.36	327.5
1000.000	-5.10	184.4	-24.79	77.7	3.73	76.4	-6.87	-34.7
1200.000	-4.84	183.8	-23.89	73.1	2.44	72.1	-7.00	-40.6
1400.000	-4.75	183.6	-22.49	75.5	1.35	68.4	-7.09	316.4
1600.000	-4.90	182.7	-21.62	-284.9	.14	-295.3	-7.44	312.8
1800.000	-4.49	181.4	-20.47	75.0	-.57	60.6	-7.33	310.1
1999.999	-4.38	179.8	-19.83	75.0	-1.45	57.7	-7.59	-53.5

APPENDIX 2

RELEVANT PUBLICATIONS BY THE AUTHOR

International Conference on

Computer Aided Design and Manufacture of Electronic Components, Circuits and Systems

3-6 July 1979

Organised by the
Electronics Division of the
Institution of Electrical Engineers

in association with the
British Computer Society
Institute of Electrical and Electronics Engineers
(Circuits and Systems Society)
Institute of Electrical and Electronics Engineers
(Region 8)
Institute of Mathematics and its Applications
Institution of Electronic and Radio Engineers

with the support of the
Convention of National Societies of Electrical Engineers of Western Europe (EUREL)

Venue
University of Sussex

EXPERIENCE IN MODELLING INTEGRATED CIRCUIT TRANSISTORS

O.P.D. Cutteridge and Monica Dowson

University of Leicester, U.K.

INTRODUCTION

Industry is paying increasing attention to the linear modelling of integrated circuit transistors. The authors have been fortunate in receiving data from Philips Research Laboratories (1) on two such devices, firstly, a lateral pnp transistor, and secondly, a vertical npn transistor. The data provided in the first case is shown in Table 1 and consisted of measurements of the S-parameters of the lateral pnp transistor at four frequencies in the range 0.5 MHz to 10.0 MHz.

A brief account of the method used by the authors for modelling linear active devices is given in the following section. Figures 1, 2 and 3 show the models obtained for the lateral pnp transistor at three different stages in the modelling procedure, with the corresponding errors tabulated in Table 2.

MODELLING METHOD

Construction of Error Function

The modulus and phase of each S-parameter were matched at every real frequency for which measured values were given. Every modulus error was given the same weighting, as was every phase error, although these weightings were different. An overall error function was constructed by taking the sum of the squares of the individual weighted errors.

General Strategy

The method requires an initial model with element values to be provided. Although a topological model was suggested by the donors of the data, no element values were given. In order to obtain suitable starting values for the elements, the global search method described by Price (2) was used. With these starting values the main optimisation procedure, the modified Gauss Newton section of a computer program described by Cutteridge (3), was then utilised.

By running this optimisation algorithm in the domain of the logarithms of the independent variables (representing the element values) it is possible to determine from the values of the corrections generated at successive Gauss Newton iterations which, if any, elements should be removed. After eliminating all such elements the algorithm converges on to a local minimum of the overall error function. From such a point further improvement can only be obtained by the addition of new elements. By adding new elements one at a time it is possible to tell immediately whether or not they are effective in improving the model. Only such elements as are beneficial, with positive values, in reducing the overall error function are retained. After a point this results in later models having a greater number of nodes than did the original.

RESULTS OBTAINED

The S-parameter data shown in Table 1 refers to the lateral pnp transistor mentioned earlier. Table 2 contains the errors in the S-parameters of the models shown in Figures 1, 2 and 3.

The element values for the initial model shown in Figure 1 were those obtained using the global search method (2). The value of the overall error function at this stage was 384.2. After Gauss Newton optimisation of this model during which three elements were removed, the improved model shown in Figure 2, which gave an overall error function value of 114.9 , was obtained. Elements were then added until the final model shown in Figure 3, having an overall error function value of 6.1 , was produced. As can be seen from Table 2, the errors were reduced from maximum errors of 0.5 dB and 11 degrees in the initial model to 0.1 dB and 1 degree in the final model.

The order of element addition was found to be quite critical, especially that of the second generator g_2 . Although this element was present in the originally suggested model, the optimisation technique would not tolerate its insertion until the final stage. It might be noted that the direction of the current generator is reversed in the final model as compared with the initial model.

ACKNOWLEDGEMENT

The authors would like to express their gratitude to K.W.Moulding and P.J.Rankin of Philips Research Laboratories for providing them with the accurately measured S-parameter data for the two types of transistor.

REFERENCES

1. Moulding, K.W. and Rankin, P.J., 1977, Private communication.

2. Price, W.L., 1977, "A Controlled Random Search Procedure for Global Optimisation", Comn. J., 20, 367-370.

3. Cutteridge, O.P.D., 1974, "Powerful 2-part Program for Solution of Nonlinear Simultaneous Equations", Elect. Lett., 10, 182-184.

TABLE 1. Measured S-parameters of a lateral pnp transistor.

	S_{11}		S_{12}		S_{21}		S_{22}	
Frequency MHz	Modulus dB	Phase degrees	Modulus dB	Phase degrees	Modulus dB	Phase degrees	Modulus dB	Phase degrees
0.5	-0.10	-1.40	---*	---*	-12.50	178.10	0.00	-0.20
2.0	-0.20	-5.40	-64.70	88.70	-12.50	169.90	0.00	-0.30
5.0	-0.40	-11.20	-57.20	84.00	-12.80	155.00	0.00	-0.50
10.0	-1.20	-19.40	-52.00	76.30	-14.00	132.90	0.00	-0.90

* A measurement of S_{12} at 0.5 MHz was not available.

TABLE 2. Errors in the S-parameters of models of a lateral pnp transistor.

		S_{11}		S_{12}		S_{21}		S_{22}	
	Frequency MHz	Modulus dB	Phase degrees	Modulus dB	Phase degrees	Modulus dB	Phase degrees	Modulus dB	Phase degrees
Initial Model	0.5	-0.10	-0.37	0.00*	0.00*	0.27	0.17	0.03	-0.19
	2.0	-0.14	-1.33	0.55	-0.17	0.34	-1.89	0.03	-0.26
	5.0	-0.02	-1.60	0.20	-3.41	0.46	-5.12	0.03	-0.41
	10.0	0.05	-3.31	-0.36	-9.66	0.46	-11.02	0.03	-0.71
Improved Model	0.5	-0.09	-0.21	0.00*	0.00*	-0.30	0.52	0.03	-0.19
	2.0	-0.11	-0.71	0.08	2.19	-0.19	-0.49	0.03	-0.27
	5.0	0.10	-0.36	-0.05	1.97	0.07	-2.00	0.03	-0.42
	10.0	0.38	-2.21	-0.04	-1.48	0.43	-6.52	0.03	-0.74
Final Model	0.5	0.00	-0.21	0.00*	0.00*	-0.05	0.67	0.00	-0.14
	2.0	-0.04	-0.66	0.10	1.03	0.01	0.13	0.00	-0.07
	5.0	0.04	0.09	-0.13	0.04	0.07	0.06	0.00	0.07
	10.0	0.00	0.08	0.02	-0.19	-0.03	-0.05	0.00	0.24

* A measurement of S_{12} at 0.5 MHz was not available.

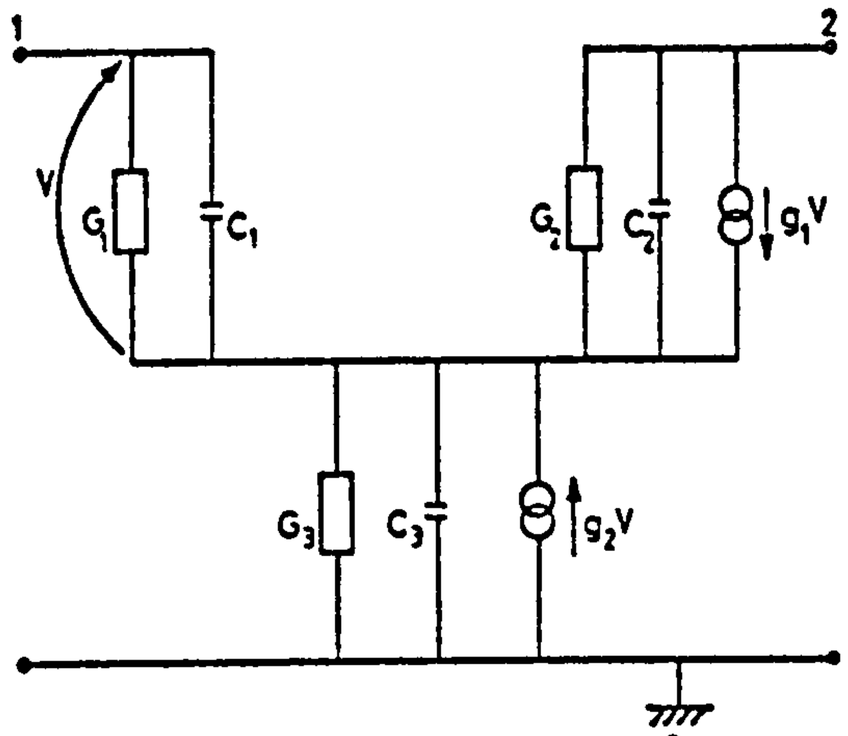

$G_1 = 6.12 \times 10^{-10}$S
$G_2 = 5.22 \times 10^{-5}$S
$G_3 = 6.77 \times 10^{-3}$S
$g_1 = 3.53 \times 10^{-3}$S
$g_2 = 2.07 \times 10^{-5}$S

$C_1 = 8.68 \times 10^{-5}$ µF
$C_2 = 5.06 \times 10^{-7}$ µF
$C_3 = 3.71 \times 10^{-9}$ µF

Figure 1 Initial model

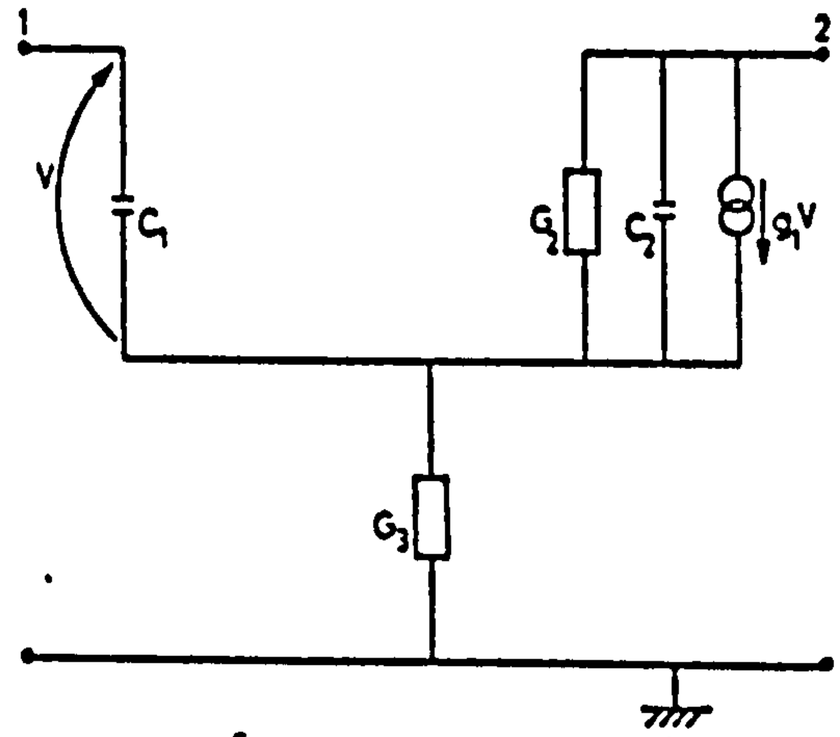

$G_2 = 4.67 \times 10^{-5}$S
$G_3 = 6.63 \times 10^{-3}$S
$g_1 = 3.94 \times 10^{-3}$S

$C_1 = 1.05 \times 10^{-4}$ µF
$C_2 = 3.90 \times 10^{-9}$ µF

Figure 2 Improved model

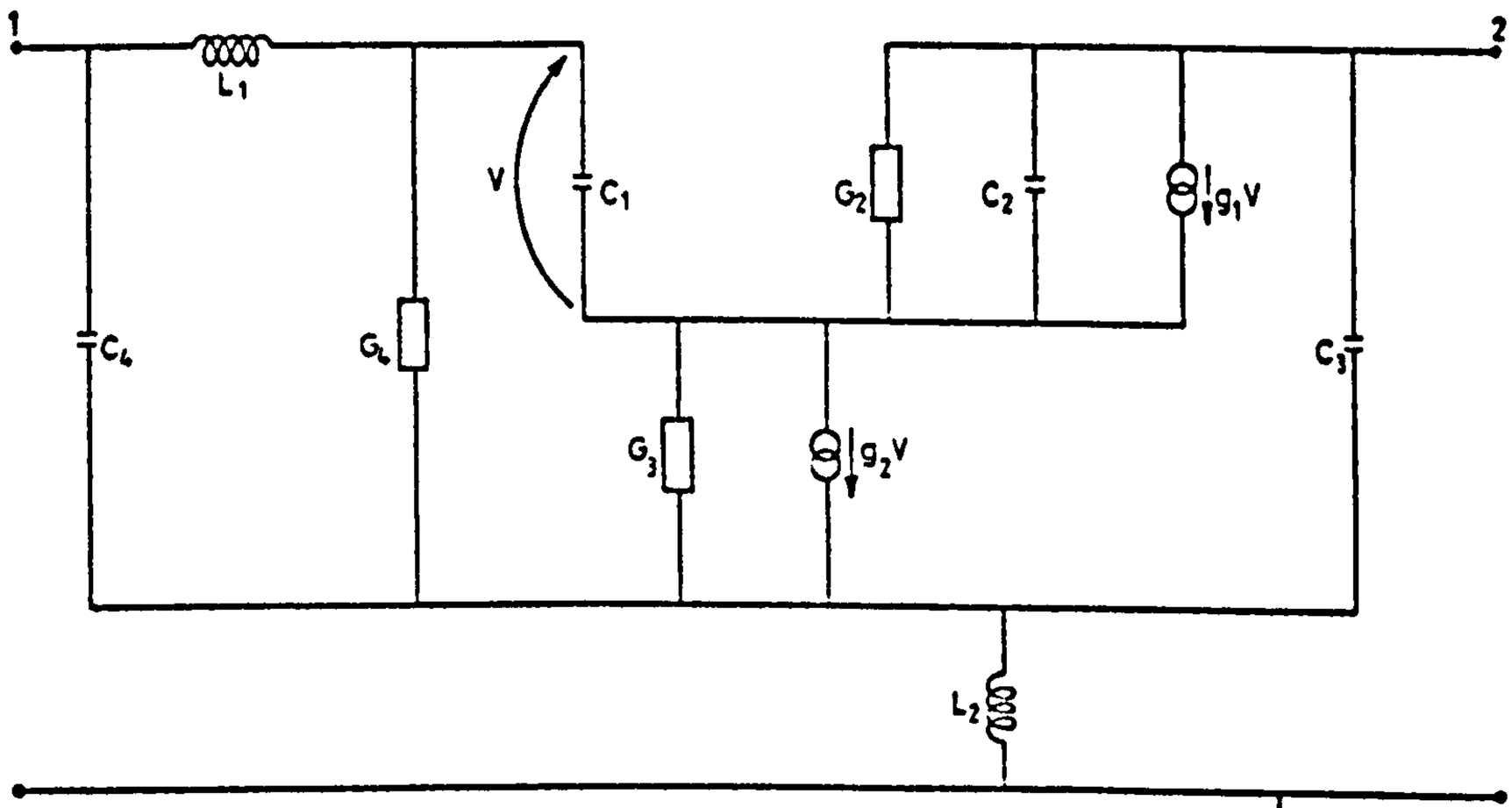

$G_2 = 4.43 \times 10^{-5}$S
$G_3 = 2.74 \times 10^{-3}$S
$G_4 = 1.15 \times 10^{-4}$S

$g_1 = 1.20 \times 10^{-4}$ S
$g_2 = 2.72 \times 10^{-3}$ S

$C_1 = 1.96 \times 10^{-6}$ µF
$C_2 = 6.19 \times 10^{-7}$ µF
$C_3 = 2.64 \times 10^{-6}$ µF
$C_4 = 3.73 \times 10^{-5}$ µF

$L_1 = 1.83$ µH
$L_2 = 0.16$ µH

Figure 3 Final model

Algorithms supplement

Note by the Editor
Algorithm No. 107 is published under our agreement with the Institute of Mathematics and its Applications, and is associated with the authors' article in the *JIMA*, Volume 24, Number 1, August 1979.

Algorithm 107
A WEIGHTED SIMPLEX PROCEDURE FOR THE SOLUTION OF SIMULTANEOUS NONLINEAR EQUATIONS
W. L. Price and M. Dowson

Authors' Notes
The weighted simplex (WS) procedure provides an alternative to the Newton-Raphson (NR) procedure for the solution of N simultaneous nonlinear equations in N real variables, rapid convergence being obtained from a sufficiently good initial approximation. In contrast to the NR the WS procedure does not involve the computation of derivatives. The principle of the WS method, together with the results of comparative performance tests, are published elsewhere (Price, 1979).

Given the set of equations $f_i(x_1, \ldots, x_N) = 0$, $i = 1, \ldots N$, the procedure operates on the data associated with a SIMPLEX of $N + 1$ points in N-space. Prior to each iteration the co-ordinates of these points, x_{ij} (where $i = 1, \ldots N; j = 1, \ldots N + 1$), and the corresponding function values, f_{ij}, are held in store. For each point j of the simplex a WEIGHT, w_j, is computed by solving (by Gauss elimination) the set of $N + 1$ linear equations $\Sigma w_j = 1; \Sigma w_j f_{ij} = 0$, $i = 1, \ldots N$. The co-ordinates $X_i = \Sigma_j w_j x_{ij}$ of the weighted centroid, X, of the simplex are then determined, and each of the N functions is evaluated at X. If, at X, the magnitude of every function is less than ACC, a user-supplied measure of the required accuracy, then the procedure terminates. Otherwise one of the simplex points is discarded, its place being taken by X, and the modified simplex which results forms the basis of the next iteration. The discard point is chosen to be L, that point of the simplex with the least positive (most negative) weight, unless L happens to be the X point of the previous iteration in which case the discard point is chosen randomly from the simplex but excluding the point M, that point with the most positive weight (Price, 1979 for full explanation). The procedure is initialised by generating a simplex of $N + 1$ points randomly positioned within a hypercube of linear dimension z (the zone size) the hypercube being centred on the initial approximation supplied by the user. The choice of z is not critical, but ideally the hypercube should be large enough to embrace the exact solution sought yet small enough to exclude other possible solutions to the given system of equations.

The procedure has been programmed in ANSI FORTRAN so as to be generally applicable and to require the minimum of user coding to run a specific problem. All arrays used by the program are declared in the main program so that the user has only to change the DIMENSION statement to adapt the program for use with any particular maximum value of N. The user must supply a subroutine FUNCT(X, F, N) which calculates the values of his set of functions F, corresponding to the variables X, where X and F are both of dimension N. He must also supply, as data, the value of N, the co-ordinates of the initial approximation, the zone size z, and the required accuracy ACC. The user must code a random number generator appropriate to his computer—RANF is a standard function on the Cyber 72 used by the authors.

As an example of the operation of the program a printout is supplied for a run relating to the specific two-variable problem in which the functions are

$$F_1 = 2x_1^3 x_2 - x_2^3$$
$$F_2 = 6x_1 - x_2^2 + x_2$$

The pair of equations $F_1 = 0$ and $F_2 = 0$ have three solutions, the approximate locations at (0,0), (1.5, 3.5) and (1.5, −2.5) having been obtained by a global search procedure. The WS procedure was used to obtain a refinement of the solution for which the initial approximation is $x_1 = 1.5$, $x_2 = 3.5$. A zone size $z = 1$ was chosen so as to exclude the neighbourhoods of the other two solution points. The precision was specified by ACC = 10^{-6}. The WS procedure achieves the exact solution at (2,4) in six iterations, the same number as is required by the NR procedure from the same starting point and with the same precision.

Reference
PRICE, W. L. (1979). A Weighted Simplex Procedure for the Solution of Simultaneous Nonlinear Equations, *JIMA*, Vol. 24 no. 1, pp. 1-8).

```
C
C     WEIGHTED SIMPLEX PROGRAM
C     WRITTEN BY W.L.PRICE
C     TRANSLATED INTO FORTRAN BY M.DOWSON
C
      DIMENSION V(3,4),U(3,4),X(2),F(2)
C
C     DIMENSIONS ARE SET AS FOLLOWS
C     V(N+1,2N),U(N+1,N+2),X(N),F(N)
C     WHERE N=NO. OF VARIABLES AND FUNCTIONS
C
C     SET I/O STREAMS
C
      IN=1
      IOUT=2
C
C     INPUT N AND STARTING VALUES OF VARIABLES X(N)
C
      READ(IN,1000)N
      READ(IN,1001)(X(I),I=1,N)
      NP1=N+1
      NP2=N+2
      N2=N*2
C
C     CALCULATE FUNCTION VALUES AND PRINT THEM
C
      CALL FUNCT(X,F,N)
      WRITE(IOUT,2000)
      WRITE(IOUT,2001)(I,X(I),I,F(I),I=1,N)
C
C     INPUT ZONE SIZE AND ACCURACY REQUIRED
C
      READ(IN,1001)Z,ACC
      WRITE(IOUT,2002)Z,ACC
C
C     CALL SIMPLEX ROUTINE
C
      CALL WSMPLX(X,F,N,V,U,NP1,NP2,N2,Z,ACC)
C
C     OUTPUT SOLUTION VALUES
C
      WRITE(IOUT,2003)
      WRITE(IOUT,2001)(I,X(I),I,F(I),I=1,N)
      STOP
C
 1000 FORMAT(I2)
 1001 FORMAT(8E10.3)
 2000 FORMAT(25H1WEIGHTED SIMPLEX PROGRAM///16H STARTING VALUES//
     1       5X,9HVARIABLES,19X,9HFUNCTIONS/)
 2001 FORMAT(3H X(,I2,4H) = ,1PE10.3,10X,2HF(,I2,4H) = ,1PE10.3)
 2002 FORMAT(//13H ZONE SIZE = ,1PE10.3/21H ACCURACY REQUIRED = ,
     1       1PE10.3)
 2003 FORMAT(//16H SOLUTION VALUES//5X,9HVARIABLES,19X,9HFUNCTIONS/)
      END
      SUBROUTINE WSMPLX(A,F,N,V,U,NP1,NP2,N2,Z,ACC)
C
C     WEIGHTED SIMPLEX SUBROUTINE
C     WRITTEN BY W.L.PRICE
C     TRANSLATED INTO FORTRAN BY M.DOWSON
C
C     A=ARRAY OF VARIABLES.  ON ENTRY = STARTING VALUES
C                            ON EXIT  = SOLUTION VALUES
C     F=ARRAY OF FUNCTION VALUES CORRESPONDING TO X
C     N=NUMBER OF FUNCTIONS AND VARIABLES
```

```
C     V AND U ARE ARRAYS USED BY NSMPLX
C     NP1=N+1
C     NP2=N+2
C     N2=N**2
C     Z=ZONE SIZE
C     ACC=REQUIRED ACCURACY
C
      DIMENSION V(NP1,N2),U(NP1,NP2),X(N),F(N)
      FNP1=FLOAT(NP1)
C
C     GENERATE INITIAL SIMPLEX
C
      CALL FUNCT(X,F,N)
      DO 10 K=1,N
      KN=K+N
      V(1,K)=X(K)
      V(1,KN)=F(K)
   10 CONTINUE
      DO 40 J=1,N
      JP1=J+1
      DO 20 K=1,N
      X(K)=V(1,K)+Z*(0.5-RANF(0.0))
C
C     RANF IS RANDOM NUMBER GENERATOR WITH DUMMY ARGUMENT
C     RETURNING UNIFORMLY DISTRIBUTED VALUES IN RANGE 0.0 TO 1.0
C
      V(JP1,K)=X(K)
   20 CONTINUE
      CALL FUNCT(X,F,N)
      DO 30 K=1,N
      KPN=K+N
      V(JP1,KPN)=F(K)
   30 CONTINUE
   40 CONTINUE
      ID=1
C
C     COMPUTE WEIGHTED CENTROID, X
C
   50 CALL WEIGHT(V,U,L,M,N,NP1,NP2,N2)
      DO 60 K=1,N
      X(K)=0.0
      DO 60 J=1,NP1
      X(K)=X(K)+U(J,NP2)*V(J,K)
   60 CONTINUE
C
C     EVALUATE AT X AND TEST FOR CONVERGENCE
C
      CALL FUNCT(X,F,N)
      DO 70 K=1,N
      IF (ABS(F(K)).GT.ACC) GO TO 80
   70 CONTINUE
C
C     EXIT IF CONVERGED
C
      RETURN
C
C     CHOOSE DISCARD POINT
C
   80 IF (L.NE.ID) GO TO 90
      L=1+INT(FNP1*RANF(0.0))
   90 ID=L
C
C     REPLACE DISCARD POINT BY X
C
      DO 100 K=1,N
      KPN=K+N
      V(ID,K)=X(K)
      V(ID,KPN)=F(K)
  100 CONTINUE
      GOTO 50
      END
      SUBROUTINE WEIGHT(V,U,L,M,N,NP1,NP2,N2)
C
C     COMPUTE WEIGHTS AND FIND MOST POSITIVE WEIGHT, M
C                          AND LEAST POSITIVE WEIGHT, L
C
      DIMENSION V(NP1,N2),U(NP1,NP2)
C
C     INITIALISE U ARRAY
C
      DO 10 K=1,NP2
      U(1,K)=1.0
   10 CONTINUE
      DO 20 K=2,NP1
      U(K,NP2)=0.0
   20 CONTINUE
      DO 30 J=1,N
      JP1=J+1
      JPN=J+N
      DO 30 K=1,NP1
      U(JP1,K)=V(K,JPN)
   30 CONTINUE
C
C     COMPUTE WEIGHTS
C
      DO 70 I=1,N
      IP1=I+1
      KKK=NP1+IP1
      DO 50 KK=IP1,NP1
      K=KKK-KK
      IF (ABS(U(K,I)).LE.ABS(U(K-1,I))) GO TO 50
      DO 40 J=I,NP2
      B=U(K,J)
      U(K,J)=U(K-1,J)
      U(K-1,J)=B
   40 CONTINUE
   50 CONTINUE
      DO 60 K=I,N
      KP1=K+1
      DO 60 J=I,NP1
      JP1=J+1
      U(KP1,JP1)=U(KP1,JP1)-U(I,JP1)*U(KP1,I)/U(I,I)
   60 CONTINUE
   70 CONTINUE
      U(NP1,NP2)=U(NP1,NP2)/U(NP1,NP1)
      L=NP1
      M=NP1
      DO 90 KK=1,N
      K=NP1-KK
      B=0.0
      KP1=K+1
      DO 80 J=KP1,NP1
      B=B+U(K,J)*U(J,NP2)
   80 CONTINUE
      U(K,NP2)=(U(K,NP2)-B)/U(K,K)
C
C     FIND M AND L
C
      IF (U(K,NP2).LT.U(L,NP2)) L=K
      IF (U(K,NP2).GT.U(M,NP2)) M=K
   90 CONTINUE
      RETURN
      END
      SUBROUTINE FUNCT(X,F,N)
      DIMENSION X(N),F(N)
      F(1)=2.0*X(1)**3*X(2)-X(2)**3
      F(2)=6.0*X(1)-X(2)**2+X(2)
      RETURN
      END
```


Algorithm 108

EFFICIENT SOLUTION OF TRIDIAGONAL LINEAR SYSTEMS

Ole Østerby
Computer Science Department
Aarhus University

Author's Note

The solution of a tridiagonal system of linear equations of the form

$$\begin{bmatrix} b_1 & c_2 & & & & \\ a_2 & b_2 & c_3 & & & \\ & \cdot & \cdot & \cdot & & \\ & & \cdot & \cdot & \cdot & \\ & & & a_n & b_n \end{bmatrix} \cdot \begin{bmatrix} x_1 \\ x_2 \\ \cdot \\ \cdot \\ x_n \end{bmatrix} = \begin{bmatrix} d_1 \\ d_2 \\ \cdot \\ \cdot \\ d_n \end{bmatrix} \qquad (1)$$

is carried out efficiently by means of Gaussian elimination. In the following we assume that pivoting is not necessary. The idea behind the algorithm is not new (Sprague, 1960; Leavenworth, 1960), but we have supplied the procedure for easy reference.

The operation count is: $2n - 1$ divisions, $3n - 3$ multiplications and $3n - 3$ additions. The only new feature in our procedure is a slightly more efficient use of simply subscripted variables. The number of such references is $10n - 5$ compared to $13n - 9$ in Leavenworth (1960) and Sprague (1960). The solution is returned in array D and array B is destroyed.

The reason for this very detailed operation count is that on most computers division is slower than multiplication, and floating point addition is not so much faster that it makes the time insignificant. Subscripted variables are counted not only because of the subscript handling but also because they imply memory references. In contrast, the simple variables can (and should, if possible) stay in fast registers, of which most modern computers have sufficiently many.

If several systems with the same coefficient matrix are to be solved subsequently, we can store the intermediate results from the LU-decomposition in array A for later use when the right hand sides become available. The operation count for subsequent systems

IEE

ELECTRONICS DIVISION

COLLOQUIUM ON

'MODEL PARAMETERS FOR CIRCUIT ANALYSIS'

ORGANISED BY

PROFESSIONAL GROUP E10
(CIRCUIT THEORY AND DESIGN)
AND PROFESSIONAL GROUP E3
(MICROELECTRONICS AND SEMICONDUCTOR DEVICES)
FRIDAY 27 MARCH 1981

DIGEST No: 1981/25

CONSIDERATIONS ON MODEL MODIFICATION

Monica Dowson

1. Introduction

A number of equivalent circuit models of electronic devices exist which can be optimised to match the measured characteristics of an actual device. Where the model does not give a sufficiently accurate agreement with the measured characteristics then modifications have to be made to the model. This paper discusses some aspects of model modification in order to match the S-parameter measurements of high frequency integrated circuit transistors.

2. Determination of original model

For any given device a model based on the physical aspects of the device is normally available where perhaps some of the elements are given fixed values but most of the element values are unknown. These element values must therefore be optimised to provide a fit to the required characteristics.

Given a set of S-parameter measurements of a device at a range of frequencies together with a suggested model, the optimisation method[1] favoured by the author involves setting up an error function given by the sum of the weighted absolute differences between the measured S-parameters and those calculated for the model. This error function can then be minimised using the Gauss Newton method. By running this optimisation algorithm in the domain of the logarithms of the variables (i.e. the element values), the element values are constrained to be positive. When convergence of the algorithm onto a minimum is obtained all the corrections to the element values are very close to zero and this is a positive indication that the model is a suitable one.

3. Modifications to the model

If the convergence of the Gauss Newton algorithm is not obtained this can be an indication that the model is not suitable. By looking at the values of the corrections to the individual elements it is possible to determine what action should be taken.

3.1. Removal of elements from the model

Since the algorithm is operating in the logarithmic domain it is possible to say that a large negative correction to an element could indicate that the element should be zero. If, after applying that correction to the element, the correction for that same element is still large and negative, this acts as confirmation. Thus, if for example, the element was a resistance then this should be short circuited. A

Monica Dowson is with the Department of Engineering, University of Leicester.

similar argument may be used for corrections that are large and positive. Fig.1 shows a suggested low frequency physical model for a vertical npn transistor operating at frequencies of 0.1 to 1.0 GHz . After application of the technique described here the model given in Fig.2 gave convergence in Guass Newton over the entire range of frequencies with an attendant improvement in the high frequency response of S_{12} in particular, as shown in Fig.3.

3.2. Addition of elements

Just as this technique can be used to remove unwanted elements, so it can be used to determine whether a particular element could be added to the model.

The placing of additional elements is the cause of some disagreement. One view is that all elements in a model must have a physical meaning within the construction of the device. To comply with this requirement, attempts should only be made to place elements in certain predetermined positions in the model. However, as shown by Cutteridge and Dowson[1], it should not be assumed that because the addition of a particular element has failed once, it will not be acceptable at a later stage.

Where a model is required that gives close agreement with the measured characteristics, the requirement of adding only physically based elements can be an unnecessary restriction particularly if the view is taken that any model is only an approximation to an infinite connection of elements. In order to be certain that each element added is the best one at that point in the model growth all possible placements must be attempted. This can be most time consuming and some restrictions are usually necessary. Thus, to add elements without creating a new node one can either attempt to add elements in parallel with elements already present in the model (an approach most physicists would not find too unorthodox) or attempt to add elements between each combination of nodes. To add a new node, the simplest way is to attempt to add one element in series with an existing element although, of course, this does not cover all possibilities.

4. Results

Fig.4 shows an example of a model grown from the reduced model in Fig.2. The frequency response of modulus S_{21} for this model is shown in Fig.5 and of modulus and phase S_{12} in Fig.6.[21] As can be seen this model now gives good agreement with the required characteristics.

References

1. Cutteridge, O.P.D. and Dowson M., "Experience in Modelling Integrated Circuit Transistors", I.E.E. Conference on Computer Aided Design and Manufacture of Electronic Components, Circuits and Systems, July 1979.

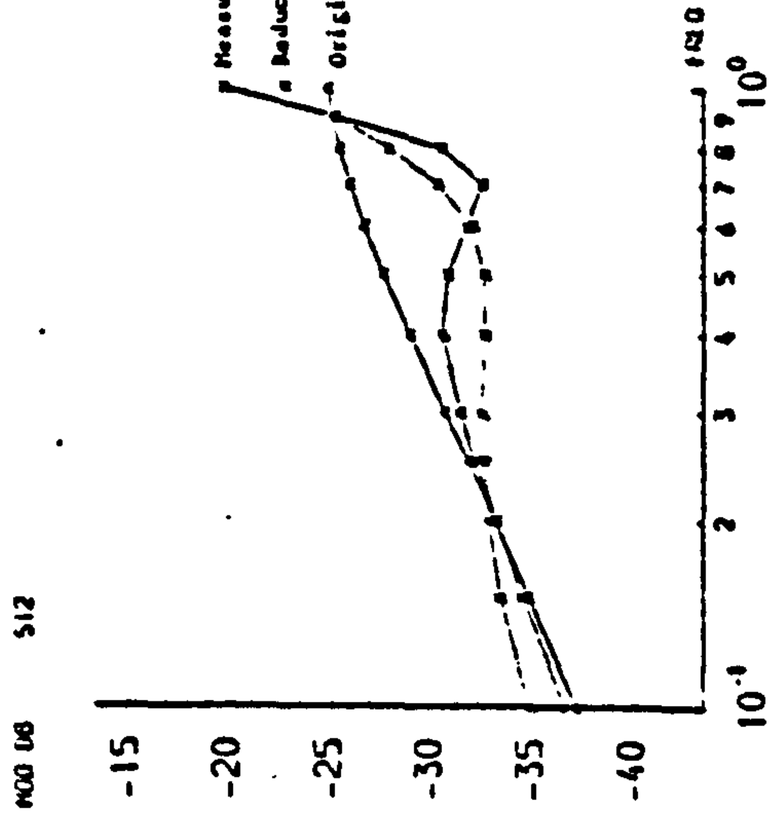

Measured and Calculated Values of S_{12}

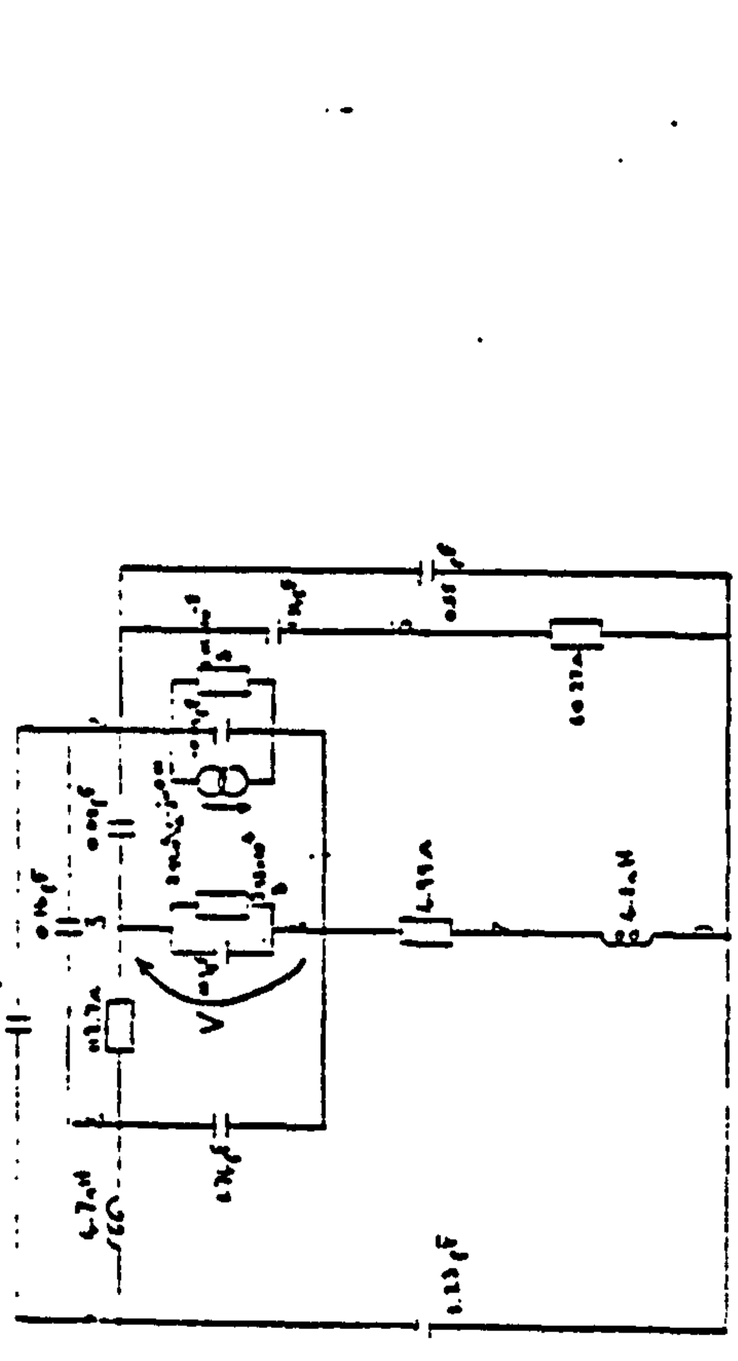

Original Model for Vertical NPN Translator

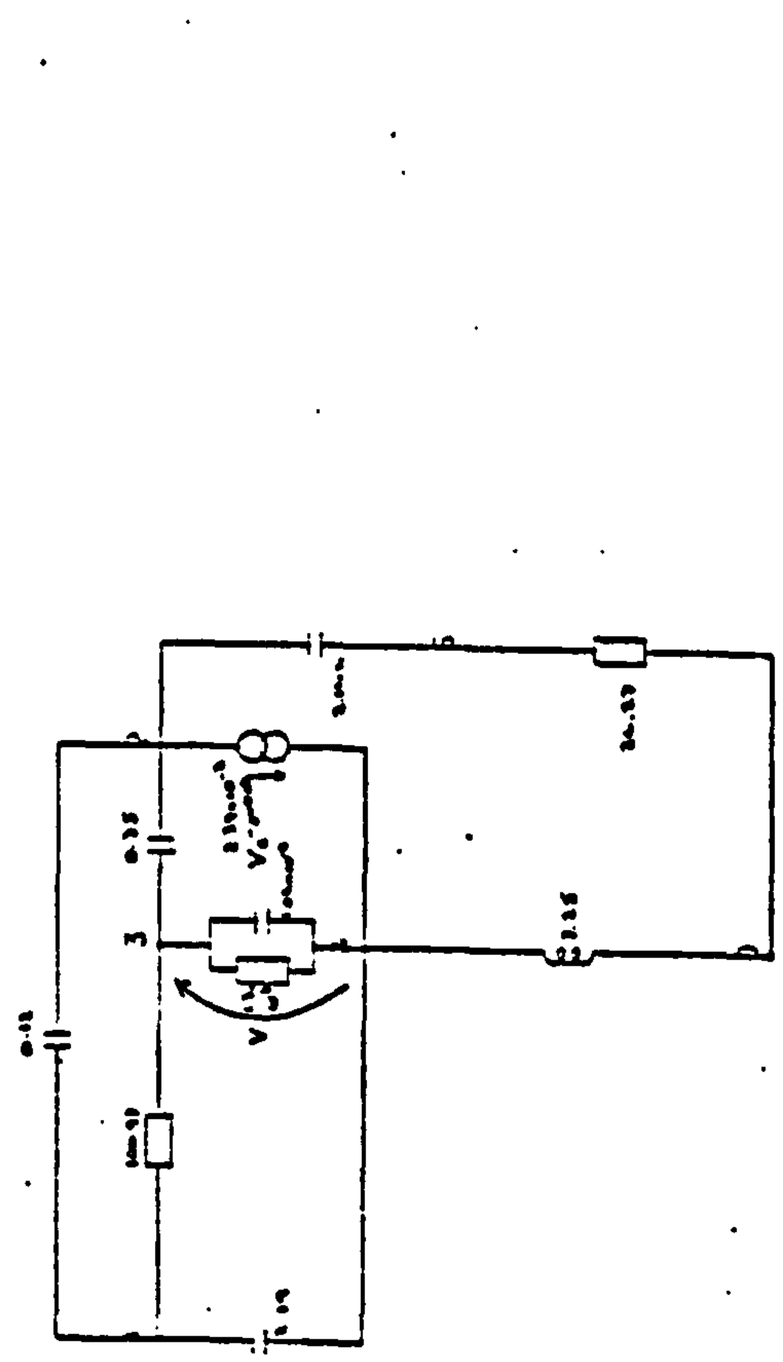

Reduced Model

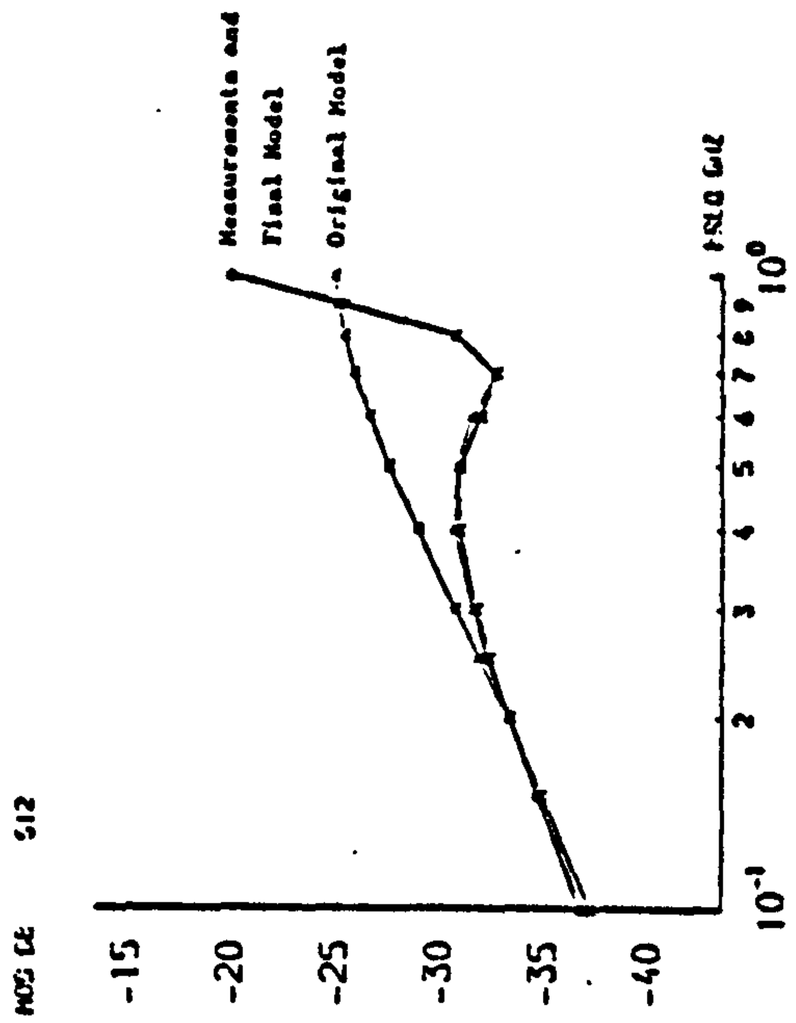

Fig 6 Measured and Calculated Values of S_{12}

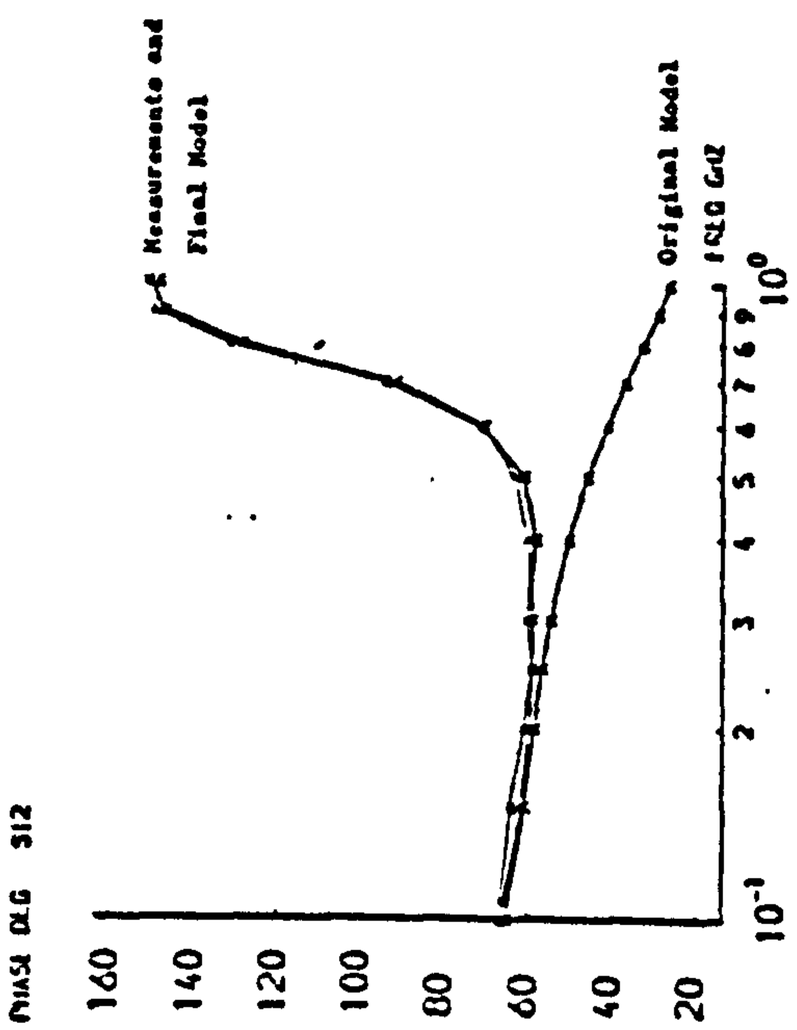

Fig 5 Final Model

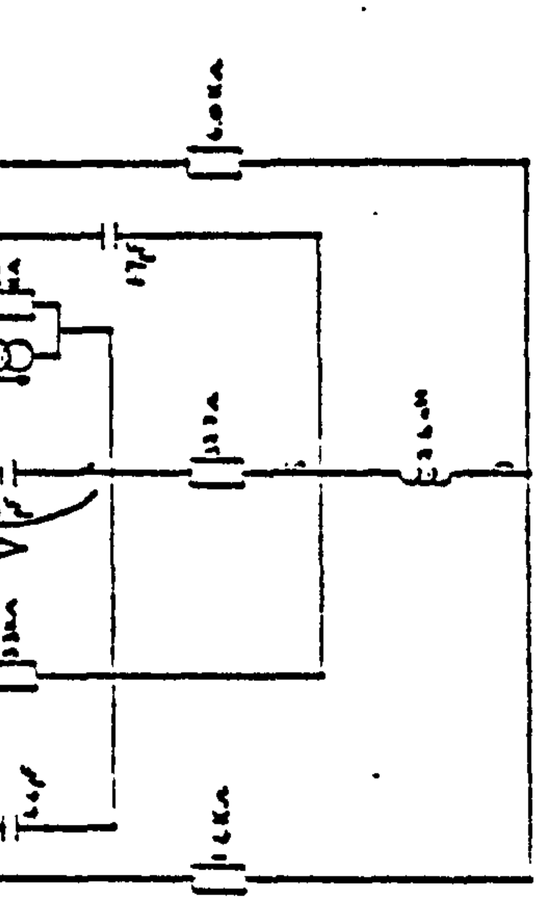

Fig 7 Measured and Calculated Values of Modulus S_{21}

EUROPEAN CONFERENCE on ELECTRONIC DESIGN AUTOMATION

1-4 September 1981

Organised by the

Electronics and Management and Design Divisions
of the Institution of Electrical Engineers

in association with the

British Computer Society (BCS)
Convention of National Societies of Electrical
Engineers of Western Europe
Institute of Electrical and Electronics Engineers Inc
(Circuits and Systems Society) (IEEE)
Institute of Electrical and Electronics Engineers Inc
(Region 8) (IEEE)
Institution of Electrical Enginers (IEE)
(Southern Centre)
Institution of Electronic and Radio Engineers (IERE)

Venue

University of Sussex,
Brighton, United Kingdom

EQUIVALENT CIRCUIT MODELLING OF A SMALL SIGNAL HIGH FREQUENCY BIPOLAR TRANSISTOR AT DIFFERENT BIAS CONDITIONS

Monica Dowson

University of Leicester, UK

INTRODUCTION

The purpose of this paper is to describe the progress made in the equivalent circuit modelling of two similar small signal high frequency bipolar transistors under different bias conditions.

The transistors being modelled were bipolar transistors designed to be used in beam lead integrated circuits. S-parameter data for the transistors was available in the frequency range 100 MHz to 2 GHz for several different emitter currents.

Using optimisation techniques, the aim was to produce accurate models simulating the measured S parameters of the transistors, with as few bias dependent elements as possible.

A brief description is given here of the optimisation techniques used and the results obtained are illustrated by diagrams of the model together with the S parameters of the model compared with those measured for the transistors.

DESCRIPTION OF THE TRANSISTORS

The transistors being modelled were isolated n-p-n transistors made in silicon with implanted arsenic emitters and diffused boron bases (Slatter (1)). The first type (A) had one emitter stripe and the second type (B) had three emitter stripes. The data for these transistors was supplied by Philips Research Laboratories (Slatter (2)) and consisted of the S parameters of the transistors in common emitter configuration at 12 frequencies in the range 100 MHz to 2 GHz at emitter currents of 0.5 mA to 10 mA for type A and of 0.5 mA to 27 mA for type B.

From the graphs in Fig.1 it can be deduced that the normal operating range of type A up to 1 GHz was 0.5 mA to 2 mA and of type B was 1 mA to 8 mA .

MODELLING TECHNIQUE

The modelling process was started by working on type A only. Using an initial model as shown in Fig.2, an optimised model was obtained for the whole of the given range of frequencies at a single value of emitter current within the normal operating region of the device. This optimised model, shown in Fig.3, was obtained by using successive applications of Gauss Newton to minimise the weighted errors between both the calculated modulus and phase of each of the S parameters of the model and the given measurements of the device. The correction terms calculated by Gauss Newton were used to indicate where topology changes were required, convergence in Gauss Newton being required at each stage in the development of the model.

Details of this modelling technique have been given previously by Cutteridge and Dowson (3) and Dowson (4).

The optimised model was then used as the initial model for type B and gave good results without any further topology changes.

Thus, taking the model as the basis of a bias dependent model, the optimisation algorithm described above was then used to obtain suitable element values at different values of emitter current.

BIAS DEPENDENT MODEL

The model shown in Fig.3 gave good results for both type A and type B transistors over the entire range of frequencies at emitter currents within the normal operating regions described above. However, at currents in excess of the maxima stated further changes in the topology of the model were required.

The original hypothesis was that there would be a small number of linearly varying elements in the model that would describe the bias variation. Within the normal operating regions this was found to be a valid assumption for this particular model. For example, as is suggested by the graphs in Fig.4, R_1 is inversely proportional to the emitter current and C_1 can be approximated by a function of the form

$$C_1 = a - \frac{b}{I_e}$$

where a and b are constants.

Taking the model beyond the normal operating regions, evidence of the type of topology changes required is given by C_2, which in Fig.4 shows a rapid increase in value as the emitter current rises and which the optimisation algorithm deletes open circuit at higher values of current, and by R_2 which is later deleted short circuit.

RESULTS

Examples of the S parameters calculated for the model compared with the measured parameters of type A and type B transistors are given in Figs.5 and 6. As can be seen these give good agreement over the entire frequency range 100 MHz to 2 GHz and there is a smoothing effect in cases where there appear to be measurement errors.

CONCLUSIONS

The bias dependent model obtained shows several similarities to the one described by Slatter (1) which was produced by a different approach to the problem.

The model described here simulates the transistors being modelled over a wide range of

frequencies and emitter currents and with topology changes gives good results at even larger values of emitter current.

ACKNOWLEDGEMENT

The author would like to thank K.W. Moulding and P.J. Rankin of Philips Research Laboratories for providing the necessary data.

REFERENCES

1. Slatter, 1977, "Optimisation of a Small Signal High Frequency Bipolar Transistor Model Using S Parameter Measurements at Different Bias Conditions", Conference on Modelling Semiconductor Devices, Ecole Polytechnic de Lausanne, October 1977.

2. Slatter, J.A.G., Internal Publication, Philips Research Laboratories, 1977.

3. Cutteridge, O.P.D. and Dowson, M., "Experience in Modelling Integrated Circuit Transistors", I.E.E. Conference on Computer Aided Design and Manufacture of Electronic Components, Circuits and Systems, July 1979.

4. Dowson, M., "Considerations on Model Modification", I.E.E. Colloquium on Model Parameters for Circuit Analysis, March 1981.

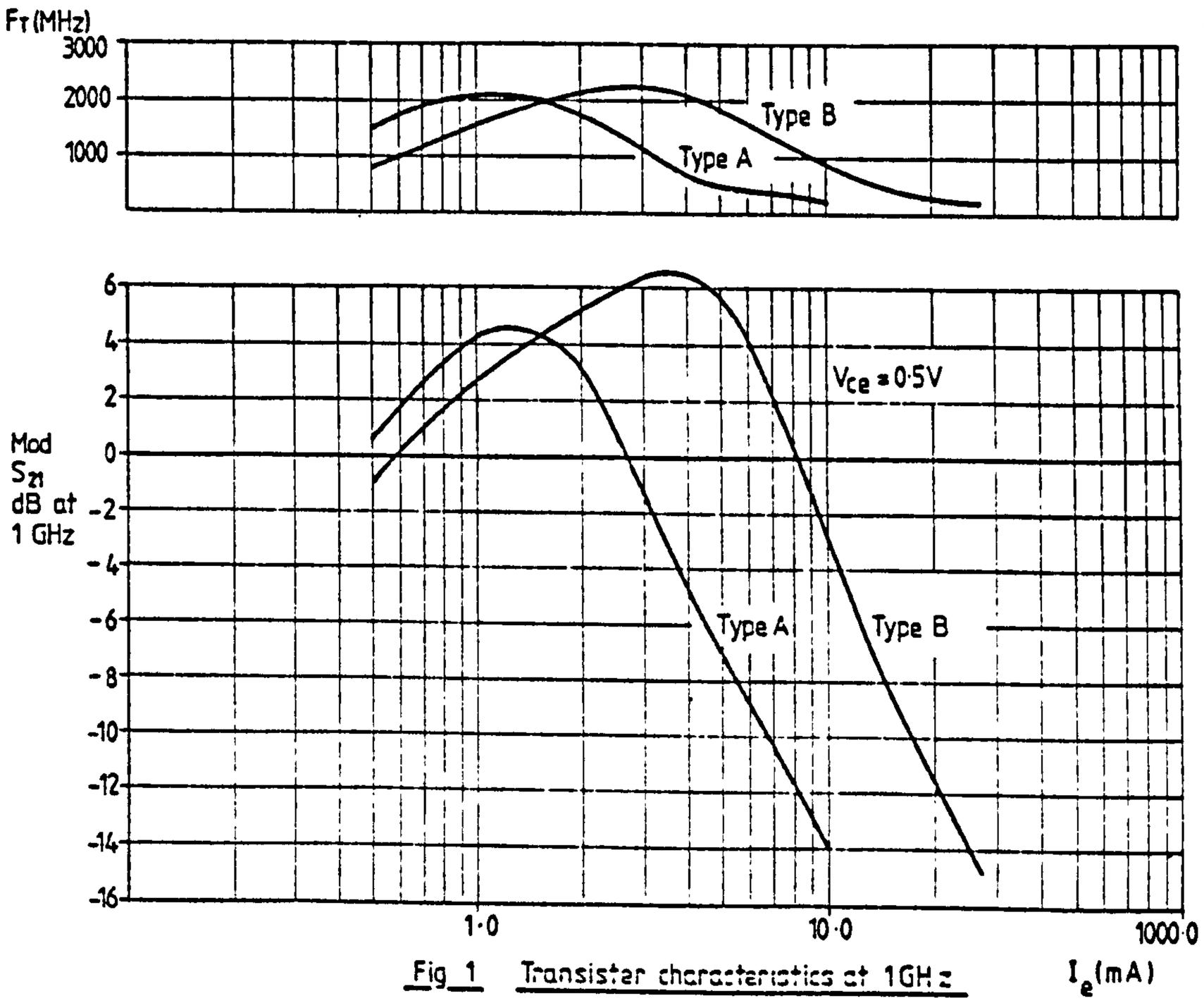

Fig 1 Transistor characteristics at 1GHz

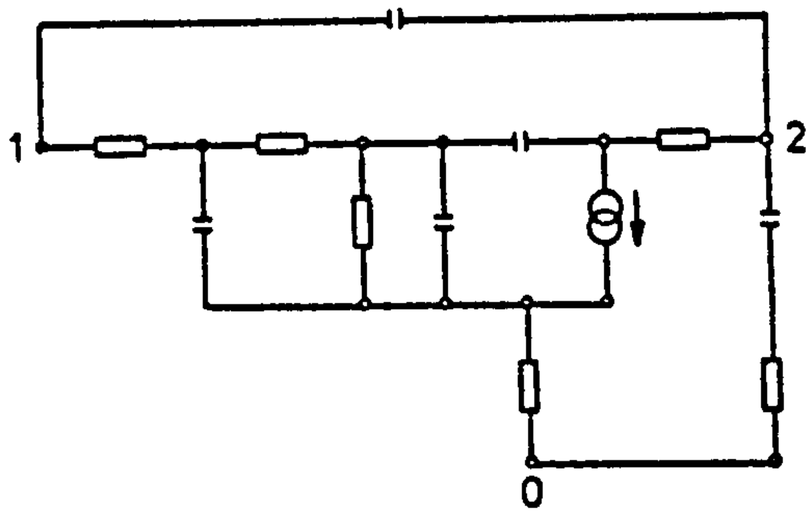

Fig. 2 Initial Model

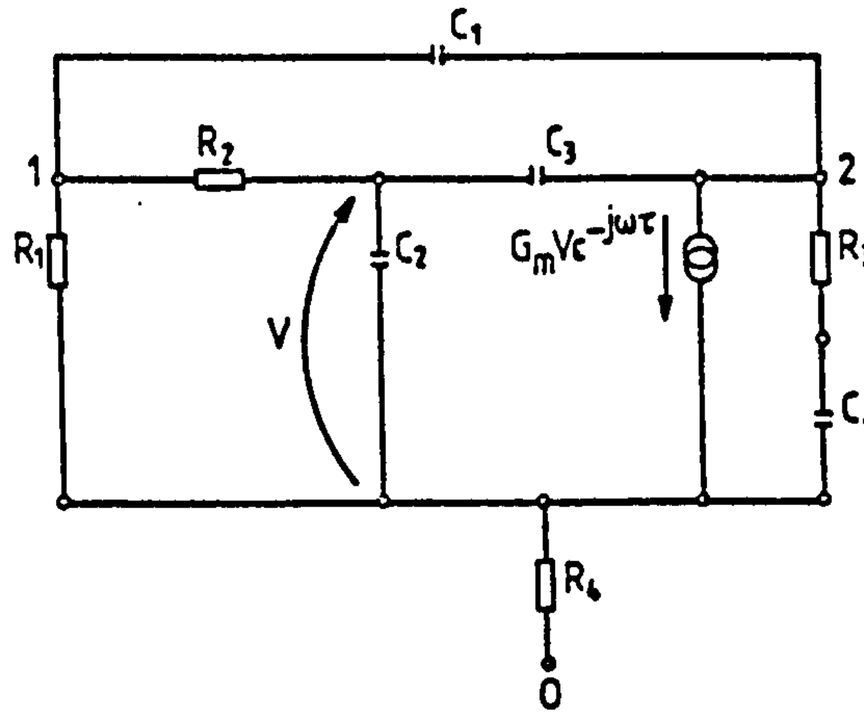

Fig. 3 Optimised Model

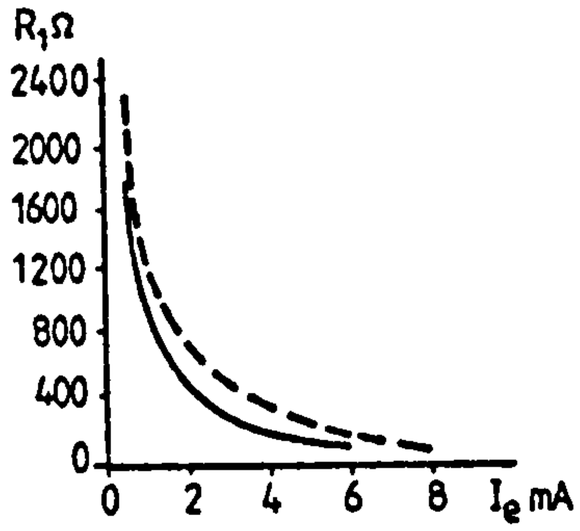

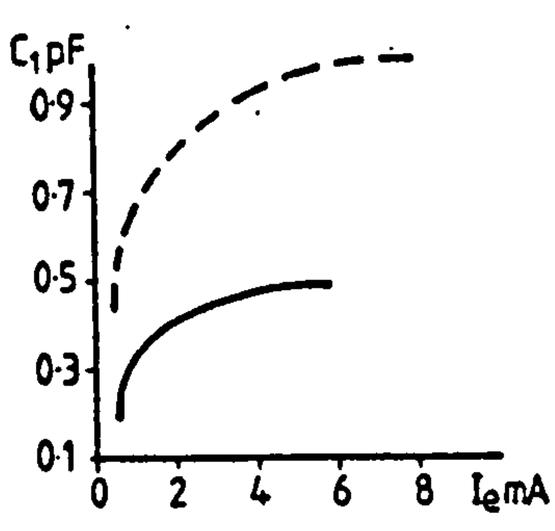

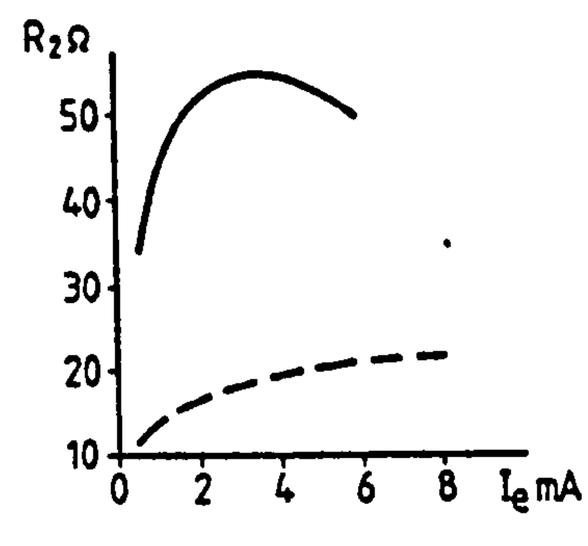

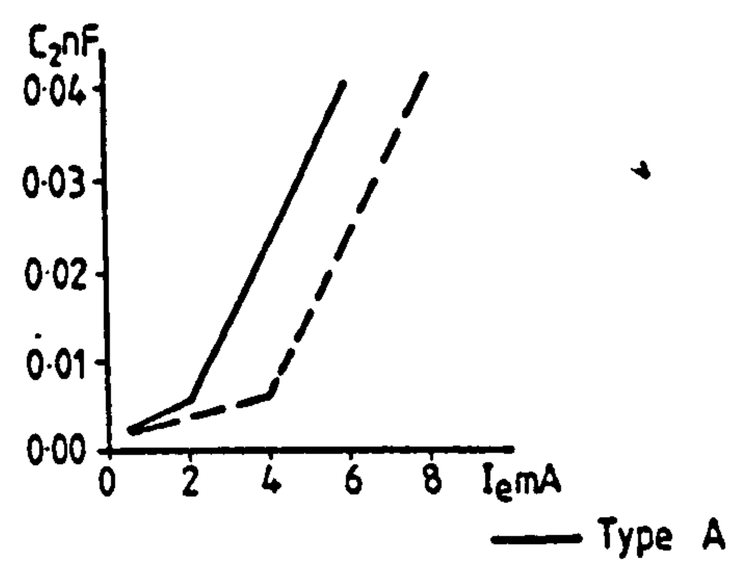

Fig. 4 Examples of bias dependent element values

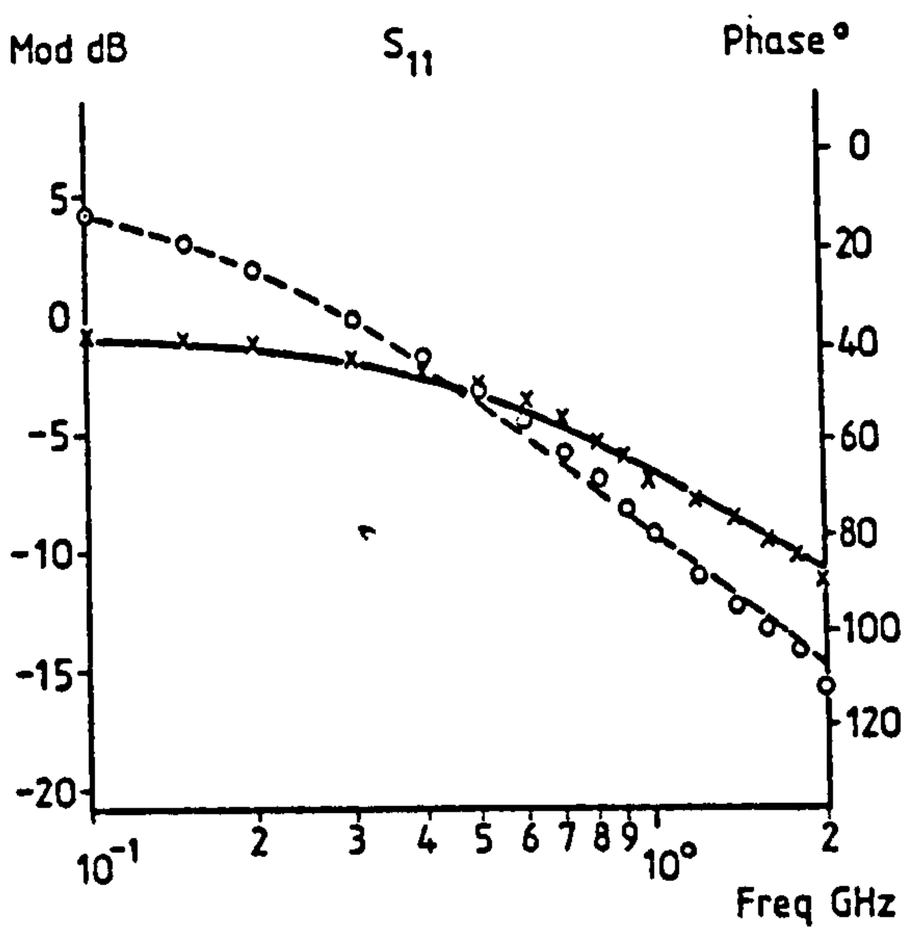

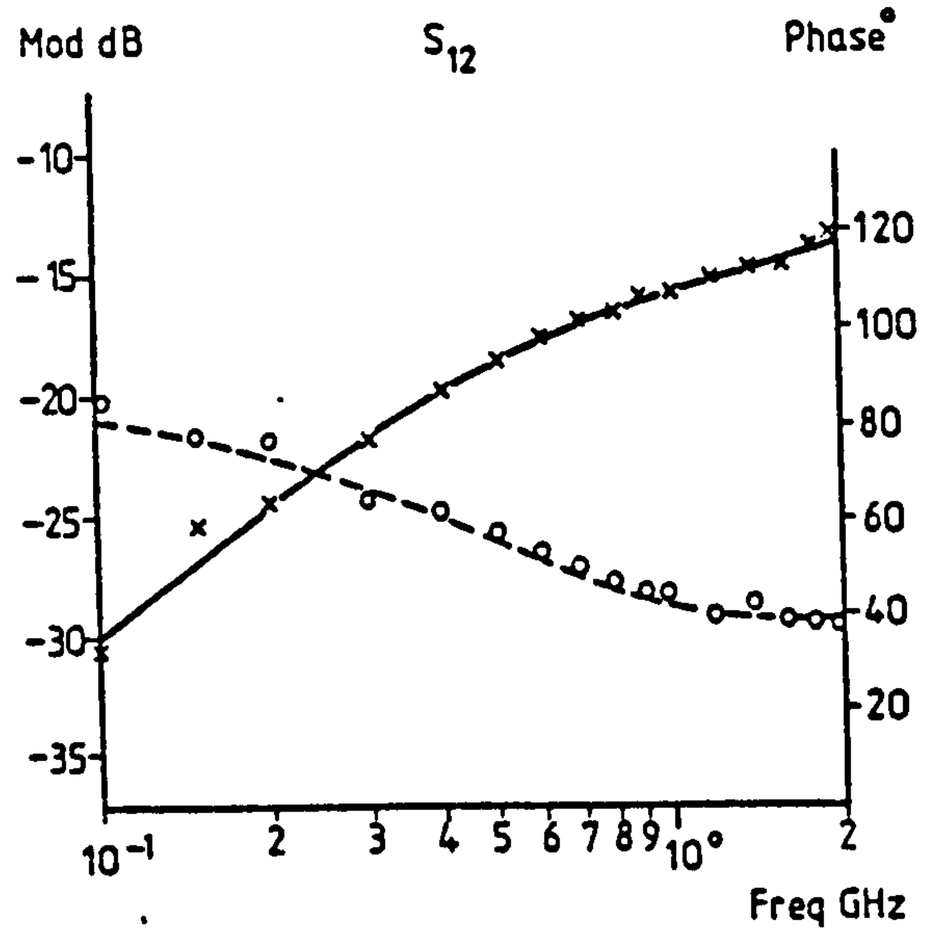

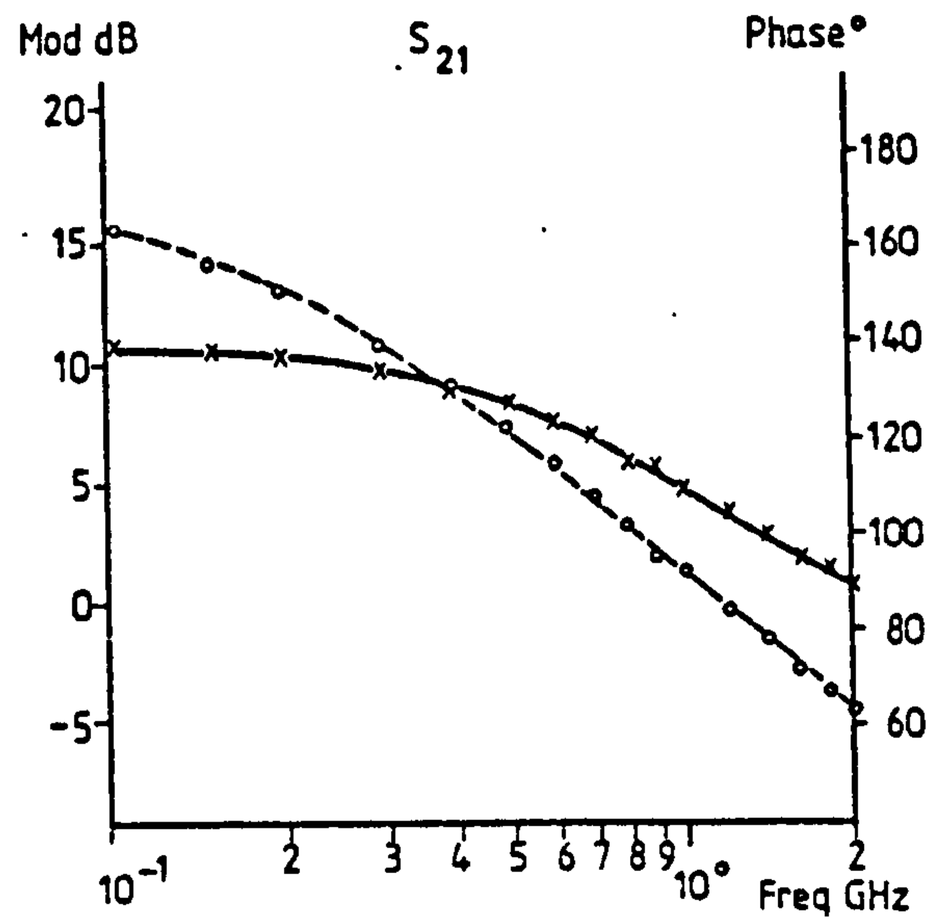

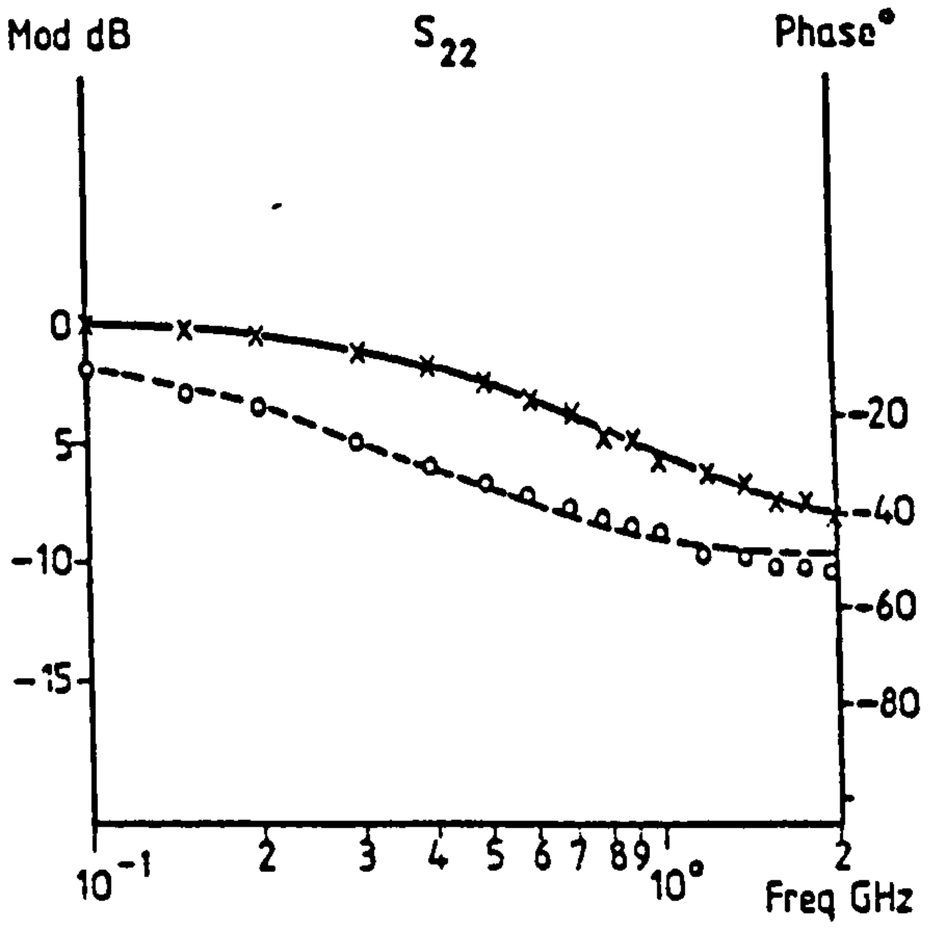

Modulus S ——— model x measured
Phase S ——— model o measured

I_e = 1mA
V_{ce} = 0·5V

Fig 5 Measured and model S parameters – Type A

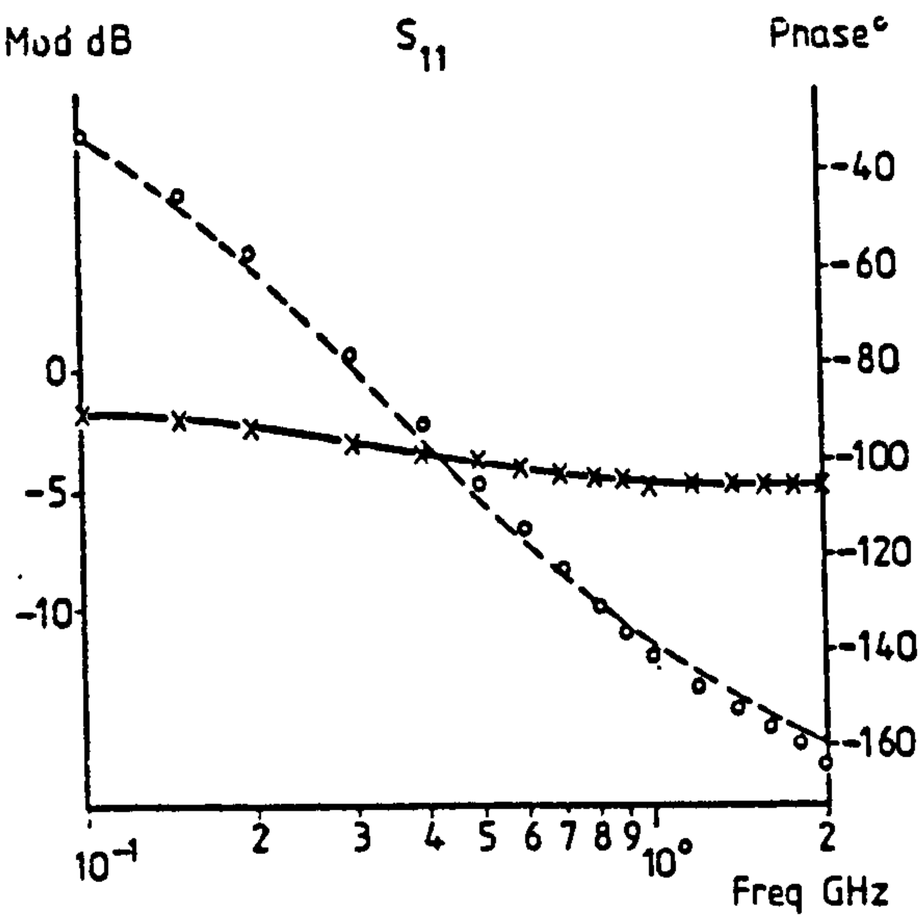

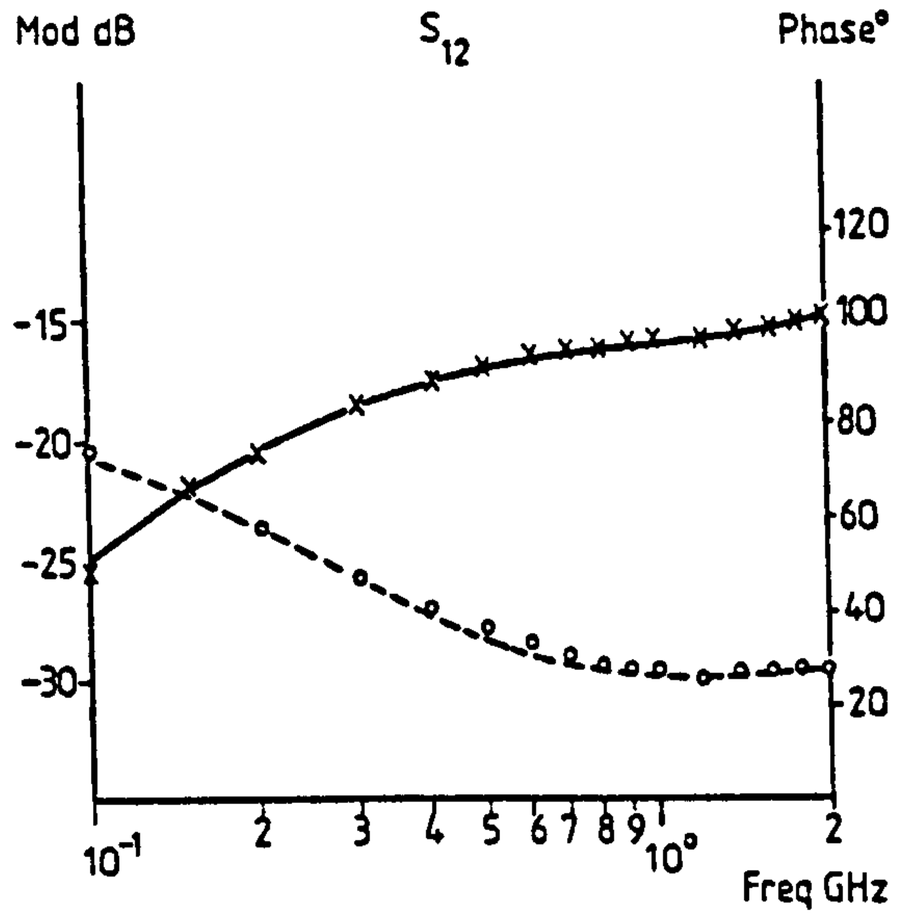

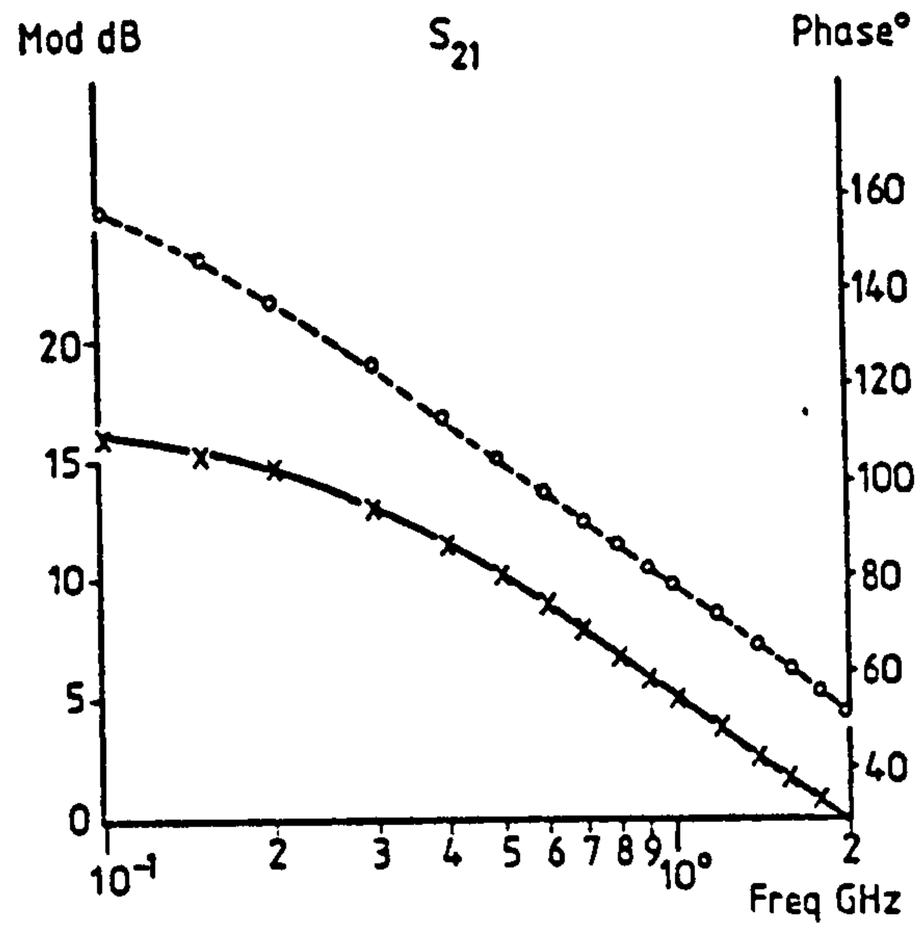

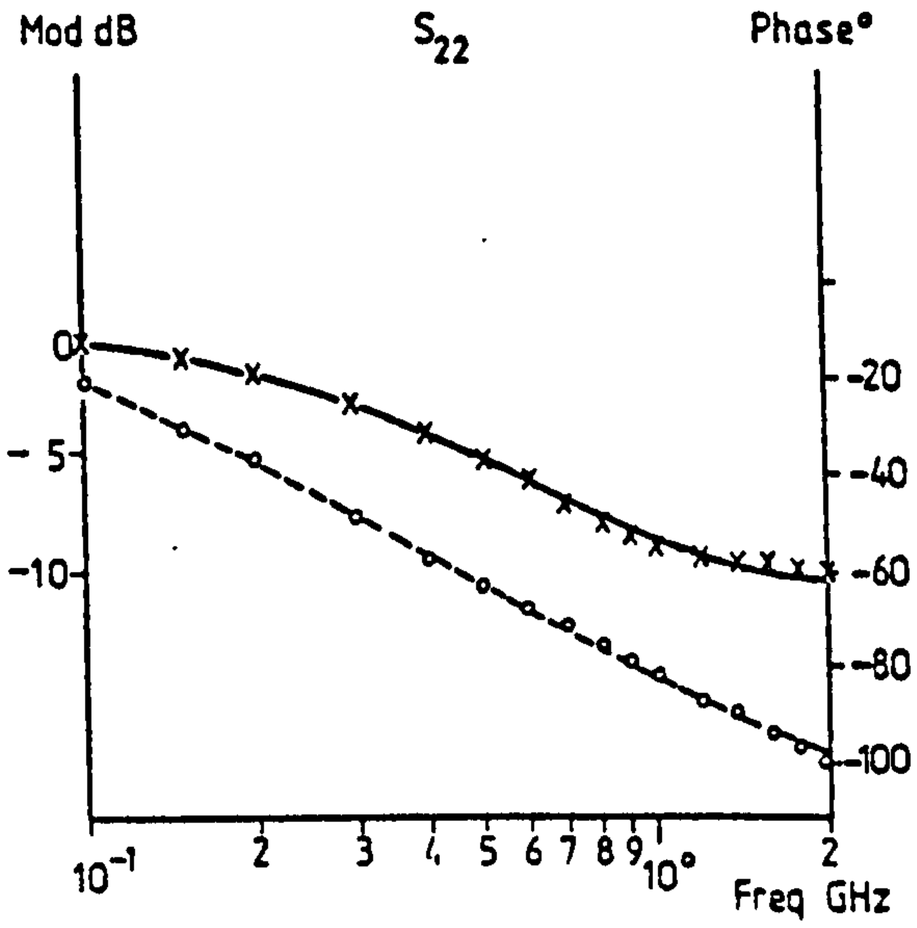

Modulus S ——— model x measured
Phase S - - - - model o measured

I_e = 2mA
V_{ce} = 0·5V

Fig 6 Measured and model S parameters –Type B

REFERENCES

1. MacLean, D.J. (1977), "Problem 2", Electronics Circuits and Systems, Vol.1, No.2, p.84.

2. Mathews, N.A. and Ajose, S.O. (1977), "Modelling Technique for Microwave FETs and Bipolar Transistors", Conf. proc. 'Computer-Aided-Design of Electronic and Microwave Circuits and Systems', University of Hull, 12-14 July 1977.

3. diMambro, P.H. (1970), "An Investigation into the Uses of Coefficient Matching in Network Synthesis", M.Sc. Thesis, University of Leicester.

4. diMambro, P.H. (1974), "A Study of the Evolutionary Approach to Network Synthesis Using Coefficient Matching", Ph.D. Thesis, University of Leicester.

5. Wright, D.J. (1974), "Studies in Optimisation as an Aid to Circuit Synthesis and Design", Ph.D. Thesis, University of Leicester.

6. Krzeczkowski, A.J. (1976), "Theory and Design of Lumped Linear Three-Terminal RC Networks", Ph.D. Thesis, University of Leicester.

7. Hegazi, O.M.H.O. (1977), "An Investigation into Current Possibilities in Automated Network Design", Ph.D. Thesis, University of Leicester.

8. Savage, W.H. (1979), "Automated Synthesis of Lumped Linear Three-Terminal Networks", Ph.D. Thesis, University of Leicester.

9. Dowson, M. (1976), "Multimodal Univariate Search Techniques and their Application to Optimisation Problems", M. Phil. Thesis, University of Leicester.

10. Henderson, J.T. (1978), "Optimization Techniques and their Application", Ph.D. Thesis, University of Leicester.

11. Dimmer, P.R. (1979), "The Use of Second Derivatives in Applied Optimisation", Ph.D. Thesis, University of Leicester.

12. Cutteridge, O.P.D. and diMambro, P.H. (1970), "Simultaneous Generation of the Coefficients of Network Polynomials and their Partial Derivatives from the Nodal Admittance Matrix", Electron. Lett., Vol. 6, No. 10, pp. 308-310.

13. Rankin, P.J. and Moulding, K.W. (1977), Private communication with Dr. O.P.D. Cutteridge, 17 June 1977.

14. Rankin, P.J. and Moulding, K.W. (1977), Private communication with Dr. O.P.D. Cutteridge, 25 July 1977.

15. Rankin, P.J. (1979), Private communication with Dr. O.P.D. Cutteridge including extracts from Ref.(16), 24 July 1979.

16. Slatter, J.A.G. (1979), Internal Report, Philips Research Laboratories, Redhill.

17. Slatter, J.A.G. (1977), "Optimisation of a Small Signal High Frequency Bipolar Transistor Using S Parameter Measurements at Different Bias Conditions", Conf. proc., 'Modelling Semiconductor Devices!' Ecole Polytechnique Federale de Lausanne, 18-20 October 1977, Journées d'Electronique, pp. 183-193.

18. Barson, R.J., Bradly, D.P., Dimmer, P.R. and Young, A.G. (1977), "Engineering Applications", course notes for "Interactive Computer Graphics for Engineers", University of Leicester, pp.H1-H20.

19. Electronics (1968), "The Transistor: Two Decades of Progress", Electronics, Vol. 41, 19 February 1968, pp.77-130.

20. Getreu, I.E. (1978), "Modeling the Bipolar Transistor", Elsevier.

21. Navon, D.H. (1975), "Electronic Materials and Devices", Houghton Mifflin Company.

22. U.S. Department of the Army (1963), "Basic Theory and Application of Transistors", Dover Publications Inc.

23. Hamilton, D.J. and Howard, W.G. (1975), "Basic Integrated Circuit Engineering", McGraw-Hill Inc.

24. Chua, L.O. and Lin, P.-M. (1975), "Computer Aided Analysis of Electronic Circuits", Prentice-Hall Inc.

25. Brown, R.W. (1969), "Device Models for Circuit Analysis Programs", Computer Aided Design, Vol. 1, No. 2, pp. 33-42.

26. Brown, R.W. (1970), "Device Modelling" in "Computer Aided Design Techniques", ed. E. Wolfendale, Butterworths.

27. Gray, P.E. and Searle, C.L. (1969), "Electronic Principles - Physics, Models and Circuits", John Wiley & Sons Inc.

28. Brayden, R.L. (1967), "Simplified Characterisation of H.F. Transistors", Electro-Technology, May, pp. 42-45.

29. Ebers, J.J. and Moll, J.L. (1954), "Large Signal Behaviour of Junction Transistors", Proc. I.R.E., December, pp. 1761-1772.

30. Linvill, J.G. (1958), "Lumped Models of Transistors and Diodes", Proc. I.R.E., Vol. 46, pp. 1141-1152.

31. Beaufoy, R. and Sparkes, J.J. (1957), "The Junction Transistor as a Charge-Controlled Device", ATE Journal, Vol. 13, pp. 310-324.

32. Hamilton, D.J., Lindholm, F.A. and Narud, J.A. (1964), "Comparison of Large Signal Models of Junction Transistors", Proc. I.E.E.E., Vol. 52, No. 3, pp. 239-249.

33. Ruch, J.G. (1977), "Modelling Bipolar Transistors", Conf. proc. "Modelling Semiconductor Devices", Ecole Polytechnique Federale de Lausanne, 18-20 October, Journées d'Electronique, pp. 89-118.

34. Agajanian, A.H. (1975), "A Bibliography on Semiconductor Device Modelling", Solid State Electron., Vol. 18, pp. 917-929.

35. Orlik, A. (1979), "Parameters Identification Method for I.C. Bipolar Transistor Charge Control Model", I.E.E. Conf. proc. "Computer Aided Design and Manufacture of Electronic Components, Circuits and Systems", University of Sussex, 3-6 July, pp. 145-149.

36. Roulston, D.J. (1981), "Determination of CAD Model Parameters for Bipolar Transistors from Fabrication Data Using the Bipole Numerical Program", I.E.E. Colloquium "Model Parameters for Circuit Analysis", 27 March, Digest No. 1981/25, pp. 4.1 - 4.5.

37. Bassett, H.G. (1966), "The Derivation of Equivalent Circuits for Transistors by Optimization Methods, Using a General Purpose Computer Programme", Symposium "The Use of Computers as an Aid to Circuit Design and Analysis", R.A.E. Farnborough, October, Tech. Memo. RAD759, pp. 53-65.

38. Lucal, H.M. (1955), "Synthesis of Three-Terminal RC Networks", I.E.E. Trans. Circuit Theory, Vol. CT-2, pp. 308-316.

39. diMambro, P.H. (1977), Private communication with O.P.D. Cutteridge, 6 November 1977.

40. Enden, A.W.M. v.d. and Groenendaal, G.C. (1977), "An Improved Complex-Curve Fitting Method", Conf. proc. "Computer-Aided-Design of Electronic and Microwave Circuits and Systems", University of Hull, 12-14 July 1977, pp. 53-58.

41. Calahan, D.A. (1965), "Computer Design of Linear Frequency Selective Networks", Proc. I.E.E.E., 53, No. 11, pp. 1701-1706.

42. Spence, R. (1970), "Linear Active Networks", Wiley-Interscience.

43. Aitken, A.C. (1956), "Determinants and Matrices", University Mathematical Texts, 9th ed.

44. Traub, J.R. (1966), "Associated Polynomials and Uniform Methods for the Solution of Linear Problems", SIAM Rev.,8, pp. 277-301.

45. Cutteridge, O.P.D., and diMambro, P.H. (1971), "Simultaneous Generation of the Partial Derivatives of Network Polynomial Coefficients: Further Details and Results", Electron. Lett., Vol. 7, No. 1, pp.3-4.

46. Fairbrother, L.R. and Bassett, H.G. (1965), "A Computer Program for Analysing Networks Containing Three-Terminal Active Devices Characterised by their Two-Port Parameters", Radio and Electron. Eng., Vol. 29, pp. 85-92.

47. Weinert, F. (1966), "Scattering Parameters Speed Design of High-Frequency Transistor Circuits", Electronics, 5 September 1966, pp. 78-88.

48. Hewlett Packard (1968), "S-Parameters - Circuit Analysis and Design", Hewlett Packard Application Note 95, September 1968.

49. Hewlett Packard (1967), "Transistor Parameter Measurements", Hewlett Packard Application Note 77-1, February 1967.

50. Dixon, L.C.W., Gomulka, J. and Szegö, G.P. (1975), "Towards a Global Optimisation Technique" in "Towards Global Optimisation", eds. Dixon, L.C.W. and Szegö, G.P., North Holland/American Elsevier, pp. 29-54.

51. Price, W.L. (1977), "A Controlled Random Search Procedure for Global Optimisation", Computer J., Vol. 20, pp. 367-370.

52. Price, W.L. (1978), "A Controlled Random Search Procedure for Global Optimisation", in "Towards Global Optimisation 2", eds. Dixon, L.C.W. and Szegö, G.P., North Holland/American Elsevier, pp. 71-84.

53. Box, M.J. (1966), "A Comparison of Several Current Optimization Methods and the Use of Transformations in Constrained Problems". Computer J., Vol. 9, pp. 67-77.

54. Lootsma, F.A. (1972), "A Survey of Methods for Solving Constrained Minimization Problems via Unconstrained Minimization", in "Numerical Methods for Non-Linear Optimization", edited by Lootsma, F.A., Academic Press, pp. 313-348.

55. Knudsen, M.S. (1981), "Optimization Procedure for MOS - Transistor Parameter Determination", I.E.E. Conf. proc., "Electronic Design Automation", University of Sussex, 1-4 September 1981, pp. 34-38.

56. Nelder, J.A. and Mead, R. (1965), "A Simplex Method for Function Minimisation", Computer J., Vol. 7, pp. 308-313.

57. Price, W.L. (1979), "A Weighted Simplex Procedure for the Solution of Simultaneous Non-Linear Equations", J. Inst. Maths. Applics. Vol. 24, pp. 1-8.

58. Price, W.L. and Dowson, M. (1979), "Algorithm 107 - A Weighted Simplex Procedure for the Solution of Simultaneous Nonlinear Equations", Computer J., Vol. 22, pp. 282-283.

59. Durbin, F., Montaron, J. and Heydemann, M.H. (1981), "A Tentative Approach towards the Global Optimization of Electrical Circuits", I.E.E. Conf. Proc., "Electronic Design Automation", University of Sussex, 1-4 September 1981. pp. 127-130.

60. Cutteridge, O.P.D..and Dowson, M. (1979), "Experience in Modelling Integrated Circuit Transistors", I.E.E. Conf.Proc., "Computer Aided Design and Manufacture of Electronic Components, Circuits and Systems", University of Sussex, 3-6 July 1979, pp. 138-140.

61. Agnew, D.G. (1979), "Minimax Optimization Techniques for Electronic Circuits", ibid., pp. 12-14.

62. Cutteridge, O.P.D. (1974), "Powerful 2-Part Program for Solution of Nonlinear Simultaneous Equations", Electron. Lett., Vol.10, No.10, pp. 182-184.

63. Fletcher, R. and Reeves, C.M. (1964), "Function Minimisation by Conjugate Gradients", Computer J., Vol. 7, pp. 149-154.

64. Davidon, W.C. (1959), "Variable Metric Method for Minimization", A.E.C. Research and Development Report No. ANL-5990.

65. Fletcher, R. and Powell, M.J.D. (1963), "A Rapidly Convergent Descent Method for Minimization", Computer J., Vol. 6, pp. 163-168.

66. Lanca, M.J.A. and Nichols, K.G. (1981), "Interactive Design to Time-Domain Specifications", I.E.E. Conf. Proc., "Electronic Design Automation", University of Sussex, 1-4 September 1981, pp. 122-126.

67. Levenberg, K. (1944), "A Method for the Solution of Certain Non-Linear Problems in Least Squares", Quart. Appl. Math., Vol. 2, pp. 164-168.

68. Marquardt, D.W. (1963), "An Algorithm for Least Squares Estimation of Non-Linear Parameters", S.I.A.M.J., Vol. 11, pp. 431-441

69. Broyden, C.G. (1965), "A Class of Methods for Solving Non-Linear Simultaneous Equations", Math. Comp. Vol. 19, pp. 577-593.

70. Gill, P.E. and Murray, W. (1972), "Quasi-Newton Methods for Unconstrained Optimisation", JIMA, Vol. 9, pp. 91-108.

71. Brown, K.M. and Dennis Jr., J.R. (1972), "Derivative Free Analogues of the Levenberg-Marquardt and Gauss Algorithms for Nonlinear Least Squares Approximation", Num. Math., Vol. 18, pp. 289-297.

72. Nabawi, A.A.-F. and Nichols, K.G. (1979), "Optimisation and Design of Linear Networks, Including Nested Subnetworks to Some Frequency-Domain Specifications", I.E.E. Conf. Proc. "Computer Aided Design and Manufacture of Electronic Components, Circuits and Systems", University of Sussex, 3-6 July 1979, pp. 7-11.

73. Dowson, M. (1981), "Considerations on Model Modification", I.E.E. Colloquium on "Model Parameters for Circuit Analysis", 27 March 1981, Digest No. 1981/25, pp.2.1 - 2.4.

74. Cutteridge, O.P.D. (1978), "Expressions for Optimum Values to Grow Virtual Elements", I.E.E. J. on Electronic Circuits and Systems, Vol. 2, No. 1, pp. 29-30.

75. Callahan, M.J.Jr. (1972), "Models for the Lateral P-N-P Transistor Including Substrate Interaction", I.E.E.E. Trans.on Electron. Devices, pp. 122-123.

76. Dowson, M. (1981), "Equivalent Circuit Modelling of a Small Signal High Frequency Bipolar Transistor at Different Bias Conditions", I.E.E. Conf. Proc., "Electronic Design Automation", University of Sussex, 1-4 September 1981, pp. 24-28.

77. Weinberg, L. (1962), "Network Analysis and Synthesis", McGraw-Hill Inc.

78. Numerical Algorithms Group (1976), "E02ADF", NAG Fortran Library Mark 5.